DEGRADATION OF ADDITION POLYMERS BY

ULTRASONIC WAVES

&

THE ROLE OF CAVITATION

ERRATUM.

In captions of Figures (53), (54) and (58)

Case 1 should read Case (i)
Case 2 should read Case (ii)

A THESIS

Submitted to the University of Glasgow

for

The Degree of Doctor of Philosophy

in

The Faculty of Science

By

M. A. K. Mostafa

Department of Natural Philosophy

Royal College of Science & Technology

Glasgow.

1957

ProQuest Number: 13849106

ProQuest 13849106

ACKNOWLEDGEMENT.

C O N T E N T S.

CHAPTER I.

CRITICAL SURVEY.

CRITICAL SURVEY:

Early experiments on the degradation of high polymer solutions showed that violent mechanical shaking of the sol= :ution for a period of a few hours resulted in a decrease in its molecular weight. The fact that this degraded polymer showed no tendency to revert to its original molecular weight, on precipitation and redissolution without shaking, provided strong evidence that true chain scission was involved.

Early experiments in 1934 by Staudinger and Heuer[1] on solid polymers showed that grinding polystyrene in a ball mill for a period of 40 hours resulted in a fall in molecular weight from an initial value of about 450,000 to a limiting value of about 10,000. It is almost beyond doubt that the considerable amount of heat developed during that process was the main factor causing this degradation, although mech= :anical degradation is not completely excluded.

Their experiments on a solution of the same polystyrene sample in tetraline, on the other hand, showed that by creat= :ing a turbulent flow by forcing the solution through fine nozzles where cavitation undoubtedly occurs, the polymer was degraded. The fall in molecular weight was not so marked and the limiting value of the molecular weight was found to be 380,000

Although these workers concluded that the breakdown was caused by the shearing forces produced by the turbulent flow, yet one can infer from their experiments that:

1. Thermal degradation plays a less important role, and

2. Cavitation produced by the turbulent flow is likely to be playing the main role in causing degradation. Never- :theless mechanical degradation cannot be ruled out.

Almost at the same time in 1933, Szalay[2] on the one hand and Flosdorf and Chambers[3] on the other, reported that it is possible to break down large molecules into smaller molecules by the use of ultrasonics or intense sound waves. They had observed that the viscosity of different solutions of starch, gelatin, rubber, agar-agar, formaldehyde polymerisates, etc., decreased gradually during strong sound treatment (10-15 Kc/sec.). They explained this decrease of viscosity as depolymerisation.

These observations have been confirmed several times in the following years and have also been extended. In 1937 Freundlich and Gilling[4] showed, by detailed experiments, that the simple explanation of the decrease of viscosity as a depolymerisation effect is doubtful and that it cannot be applied in some cases. It became evident, by that time, that the decrease of viscosity in some solutions (mostly in gelatines) was entirely recovered after having been left

alone for several hours at the end of the sonic treatment.
Furthermore, since it had become known from earlier experi=
:ments that thixotropic gels could be liquified by ultrasonics,
apart from depolymerisation, Freundlich and Gilling got the
impression that the decrease in viscosity could not be inter=
:preted wholly as depolymerisation but could be either a change
in the structure of the solution or attributed to the thixo=
:tropic characteristics of the solution.

On the other hand, there were cases where the tearing
of macromolecules by ultrasonics could be proved beyond doubt.
Brohult[5] for instance, using a frequency of 250 Kc/sec.,
proved by measurements with the ultracentrifuge that the hae=
:mocyanin molecules were split by ultrasonics into fractions
of 1/2 to 1/8 of their original size.   No tendency to recom=
:bine was observed in this case.   It was concluded that an
actual break down of the molecule had taken place.   Whether
this breakdown was due to the ultrasonic waves directly or
could be attributed to the cavitation mechanism cannot be
stated from the data available.   In fact, Freundlich and
Gilling found that by applying a pressure of 10 atmospheres
above the solution - presumably to inhibit cavitation the
decrease in viscosity failed completely to appear in four out
of six solutions while they observed a slight reduction in
the viscosity of the remaining two which were gelatine and

agar-agar. The question whether you can tear big molecules into smaller ones, purely by the ultrasonic vibrations alone, remained unanswered.

In 1938, Thieme(6) obtained a similar fall in viscosity with solutions of gelatine, agar-agar and gum arabic. Thieme's work was based on measuring the change in the relative viscosity η_r of the polymer solution. Thieme also tried to discover an empirical relation to fit his degradation results. His interpretation of the results were not altogether correct and it was shown later by Schmid that this was due to Thieme's graphical representation of his results.

The polymers used by the majority of the above workers were all natural products of ill-defined chemical composition. Schmid and Rommel[7] realising this fact, used solutions of various synthetic polymers. These synthetic polymers which, according to Staudinger are chain threads held together by primary bonds, have the advantage that only one main bond has to be dissolved in order to split the molecule into two parts, while in natural polymer molecules (branched), more than one bond would have to be dissolved. Another advantage is the accepted relation found by Staudinger between viscosity and chain length of the molecule which helps to follow with a higher degree of certainty the process of degradation of these synthetic polymers.
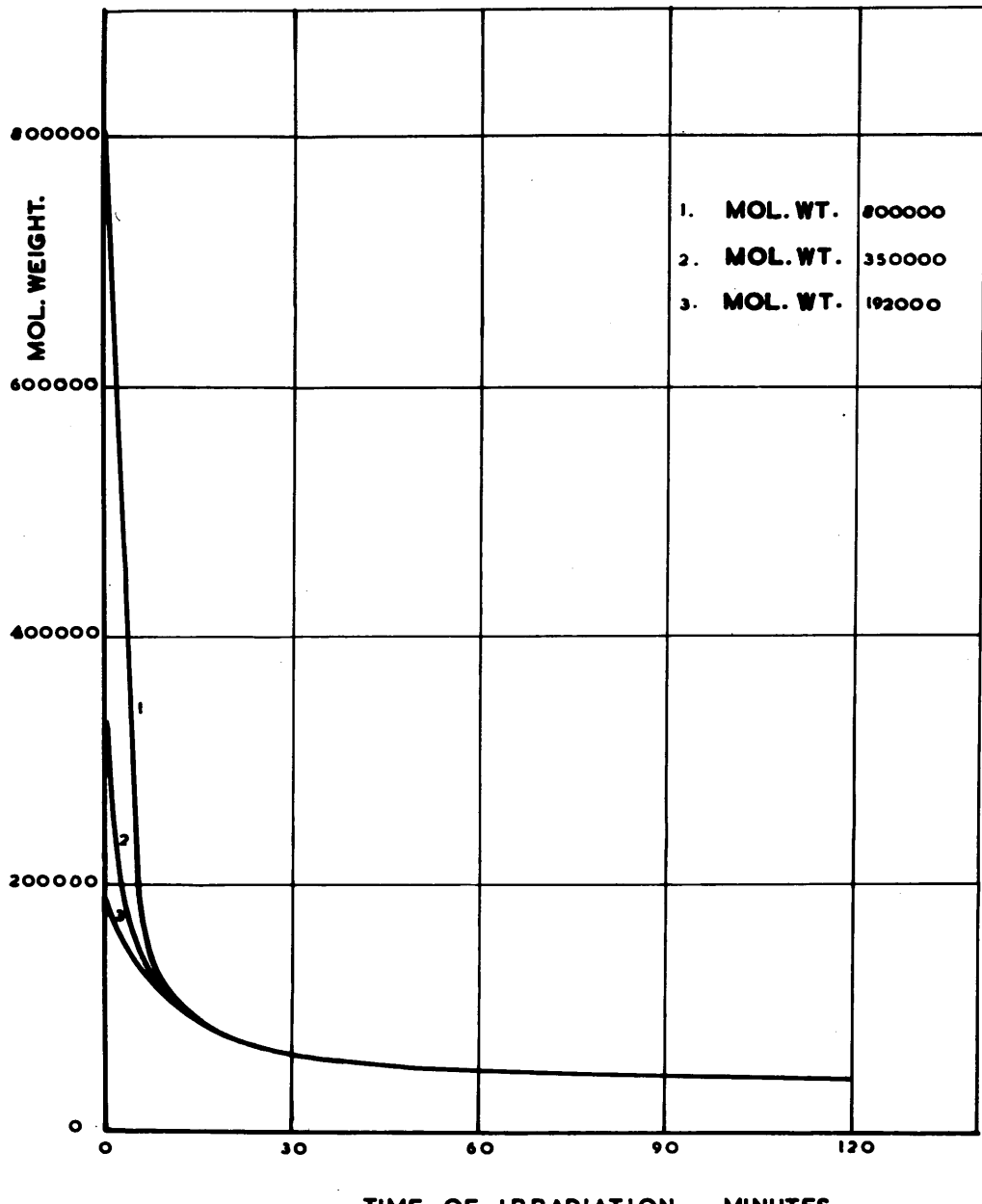
FIG.1   DEGRADATION OF POLYSTYRENE
IN TOLUENE.   G. SCHMID & O. ROMMEL.

Schmid and his co-workers carried out extensive tests on synthetic polymers such as polystyrene, polymethylacrylate, polyethylacrylate and polyvinylacetate. The results of these experiments are given below in a classified form:

1.   Polymers do not degrade to the monomer but only to an intermediate chain length, independent of the initial chain length but dependent on the power output of the ultrasonic source, the solvent, and the concentration of the polymer solutions. Fig.1, which is taken from Schmid's results, illustrates the above statement and represents the degrada- :tion curves of three samples of polystyrene in toluene of different initial molecular weight.

2.   Schmid[8] assumed that the rate of breakdown is propor- :tional to the difference $P-P_e$ and gave his initial express- :ion in the form:

$$\frac{dX}{dt} = K(P-P_e)$$

where $\frac{dX}{dt}$ is the average number of broken molecules per litre per min., i.e., the rate of degradation;

   P   is the average chain length at time t;

   P_e is the average chain length at the end of degradation;

   K   is a constant usually known as the rate constant.
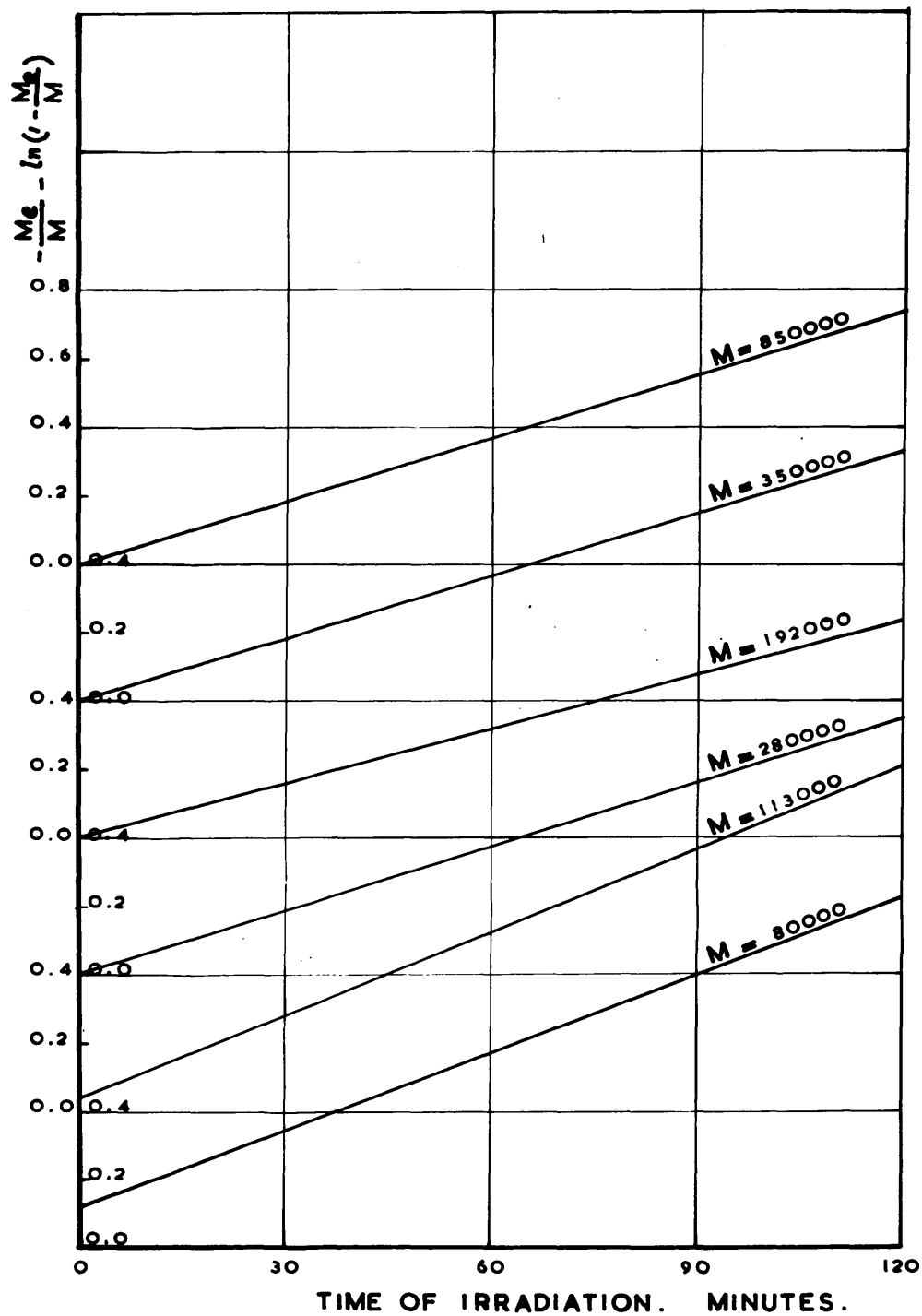
FIG.2. POLYSTYRENE IN TOLUENE.

G.SCHMID & O.ROMMEL.

He then proceeded to develop a theory to account for the ultra-
:sonic degradation of long-chain molecules, which is repre-
:sented by:

$$-\frac{M_e}{M_t} - \log(1-\frac{M_e}{M_t}) = \frac{K}{C_m}(\frac{M_e}{M_m})^2 \cdot t - \frac{M_e}{M_o} - \log(1-\frac{M_e}{M_o})$$

where M_e is the molecular weight corresponding to the average
chain length at the end of degradation;

M_t is the average molecular weight at time t;

C_m is the concentration in base moles per litre,

and M_o is the initial average molecular weight, i.e.,
at $t = o$.

Schmid did not take account of the size distributions
obtained during the degradation process nor did he make clear
distinctions between number and weight average molecular weights.
Although by inspecting his derived formula M_o should be, cate-
:gorically, a number average molecular weight, yet in verify-
:ing his equation he plotted $\frac{M_e}{M_t} + \log(1-\frac{M_e}{M_t})$ against t, taking
M_t as the weight average molecular weight obtained from vis-
:cosity measurements. Nevertheless he obtained straight lines
as required by the above equation and as shown in Fig. 2 for
a sample of polystyrene in toluene. Schmid's theory will be
discussed in more detail in Chapter V.

3. Schmid[8] investigated theoretically the possibility
that the macromolecules are broken by frictional forces. A

frictional force can exist if there is a relative motion between the solvent molecules and the macromolecules. The relative motion can be set up as the result of the propagation of the ultrasonic waves. He assumed that a polymer molecule can be represented by a frictionless thread to which are attached, at regular intervals along its axis, spheres of radius equal to the radius of the benzene ring '3 A.U.' (case of polystyrene). Schmid, then applied Stokes formula :

$f_o = P.6 \pi \eta r V_r$ to estimate the frictional force that may be developed if V_r is the relative velocity. He found that the frictional force is of the same order of magnitude as the force required to dissolve a C-C bond. The relative motion developed between solvent molecules and polymer mole-:cules can be due to either the inertia or the rigidity of the macromolecules. Schmid therefore, conducted a series of experiments with a view to throw more light on the effect of these two factors. Unfortunately his interpretation of the results of these experiments did not take into account the effect of mixing solvents on producing nuclei for the inception of cavitation. Of all of Schmid's experiments those contem-:plated to show the effect of inertia failed to provide con-:clusive evidence. Nevertheless Schmid attributed the exis-:tence of relative motion to the rigidity of macromolecules in solution, and explained most of his results on the basis of that conception.
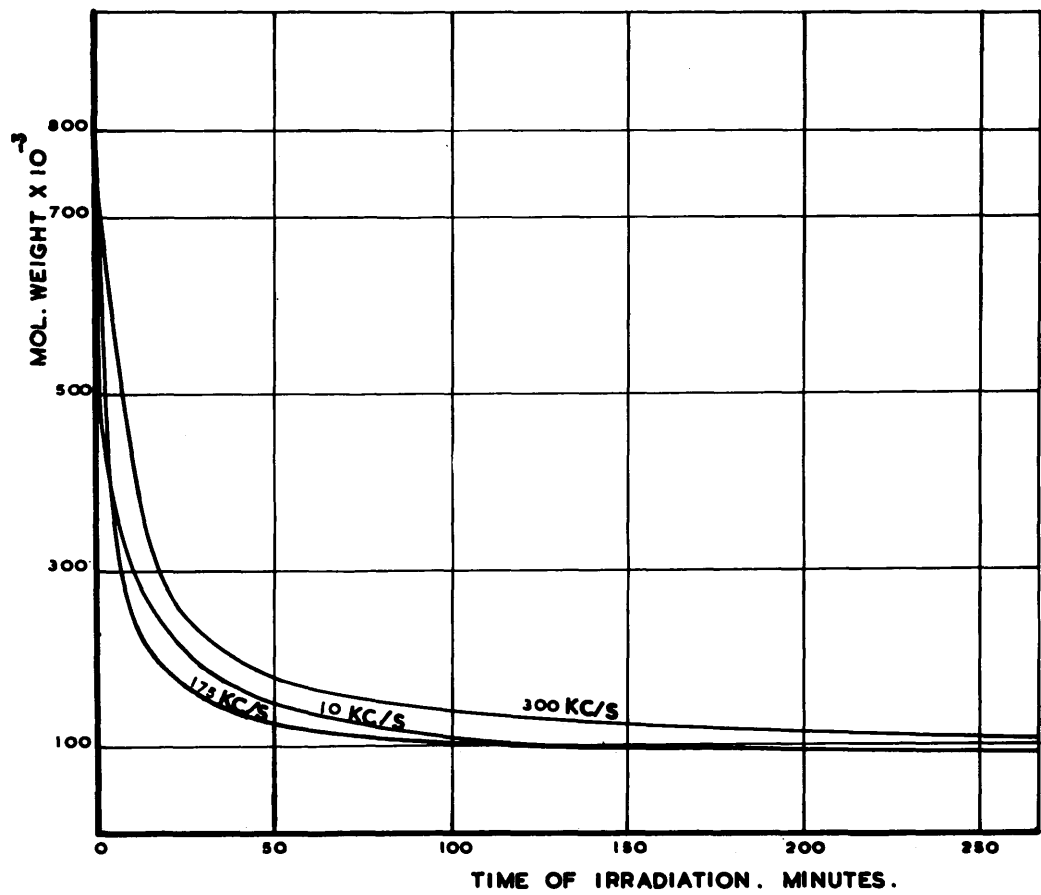
FIG.3. FREQUENCY EFFECT ON ULTRASONIC
DEPOLYMERIZATION. SCHMID & POPPE

4. Schmid's[9] experiment on the dependence of degradation of polymers on the frequency of ultrasonic waves showed that within the range 10-300 Kc/sec., the degradation is independ- :ent of frequency. According to his mechanism for degrada- :tion, the rate of degradation is anticipated to decrease with the decrease in frequency as the rigidity of the macro- :molecules becomes less. Again since all his experiments on that aspect were carried out in air under atmospheric condit- :ions cavitation taking place is more than likely to play a major role in the degradation process. Since frequency dependence of cavitation is likely to exist in such a way as to offset the effect of the rigidity of macromolecules, this series of experiments failed again to add any conclusive evidence to support his hypothesis. A copy of his results is given in Fig. 3. which showsthe degradation curves for a 0.3% solution of polymethyl methacrylate in benzene.

5. Schmid[10] carried out another series of experiments on the degradation by ultrasonics of nitrocellulose in n-butylac- :etate and of polystyrene in toluene at temperatures of 40°, 60°, 80°, 100° and 120^oC. At the same time he examined their pure thermal degradation at the same temperatures. In inter- :preting his results, he considered the two types of degra- :dation, i.e., thermal and ultrasonic to be additive and by

subtracting the thermal effect from the combined degradation he obtained the degradation due to ultrasonic waves alone. This was shown to decrease quickly at higher temperatures and to stop completely at a remarkably higher molecular weight. In trying to explain his observations according to the con-:ception of rigidity of macromolecules he atrributed the decrease in degradation to a decrease in viscosity of the solution at higher temperatures, but he admitted the difficulty of giving a correct explanation of the main reason for the decrease of degradation at increasing temperatures.   Once again, it seems feasible to assume that cavitation is the reason.   The severity of cavitation is known to decrease with increasing temperature.   This fact is a consequence of the effect of temperature on the vapour pressure of the solvents. Vapour pressure increases as the temperature increases and the collapse of the cavitation bubbles will be less violent.   This results in a great reduction in the severity of cavitation if not a complete change from destructive to non-destructive cavitation.

6.   In order to suppress cavitation, Schmid[7] conducted several experiments under high external pressure in a Berthelot steel Bomb at a temperature of $65^{\circ}C$.   The external pressure above the free surface of the solution was applied from
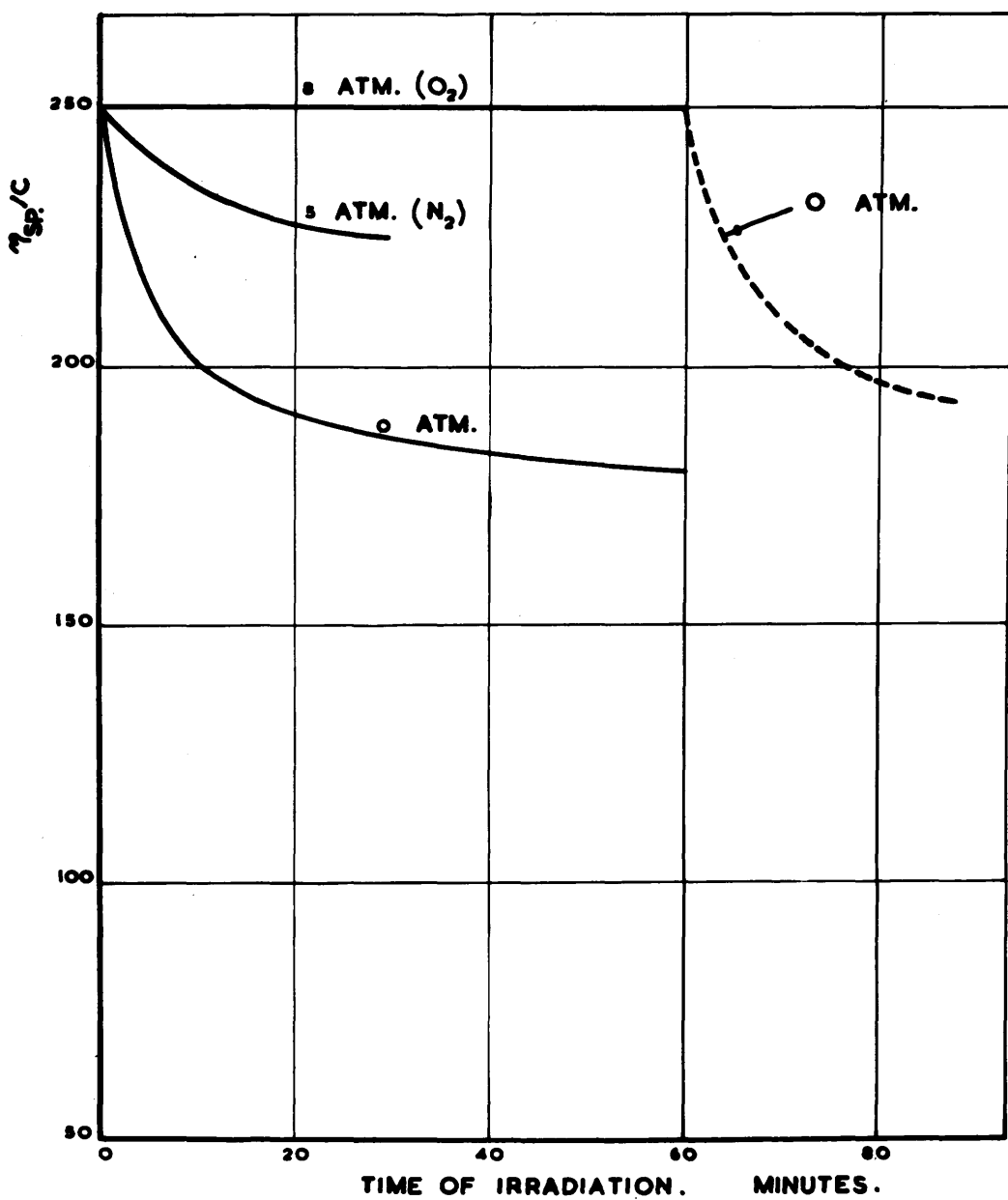
FIG.4. DEGRADATION OF GUN-COTTON
UNDER EXTERNAL PRESSURE.
G. SCHMID & O. ROMMEL
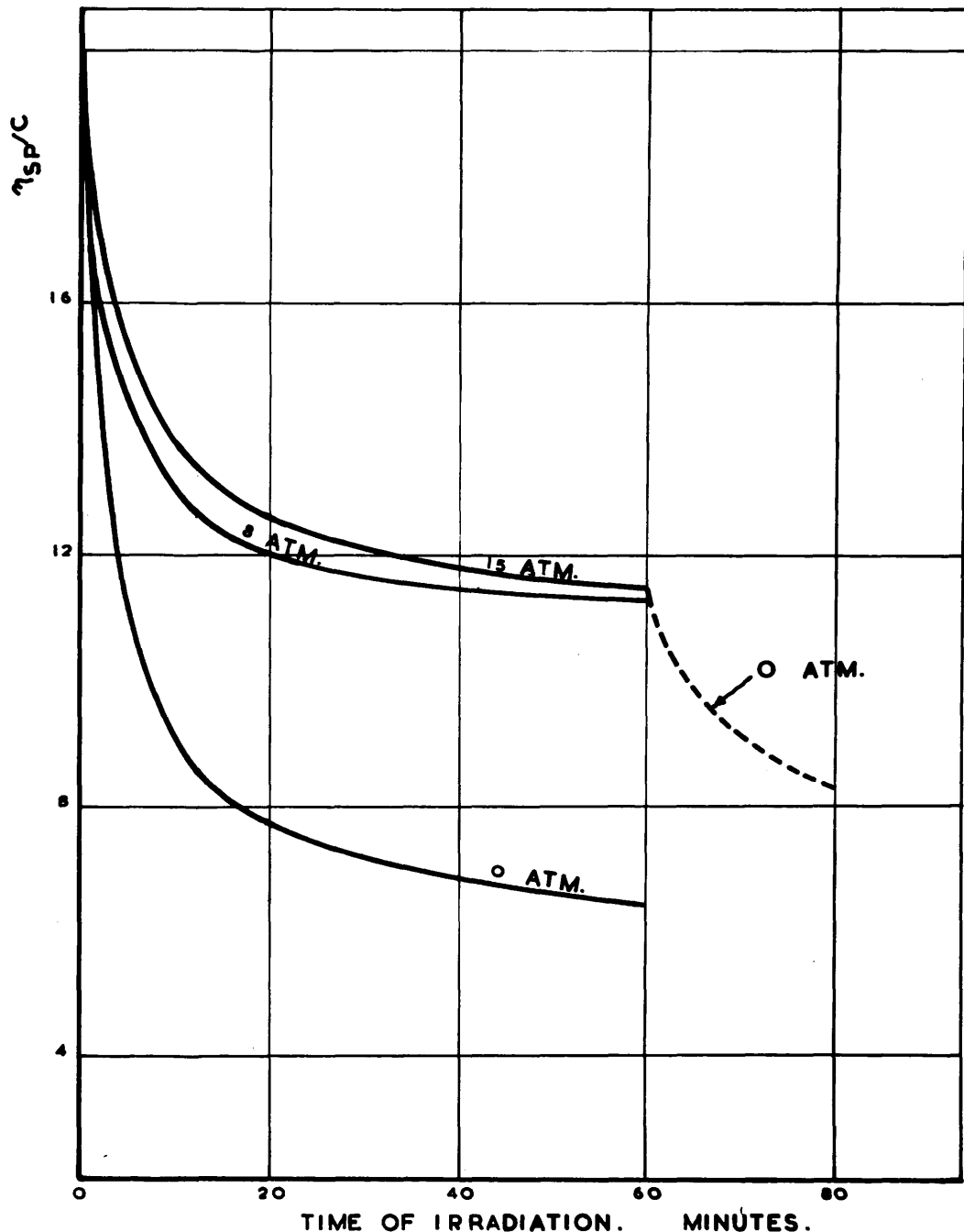
FIG.5.   DEGRADATION OF POLYSTYRENE
UNDER EXTERNAL PRESSURE.
G. SCHMID   &   O. ROMMEL.

compressed oxygen cylinders in some experiments and oxygen=
free nitrogen cylinders in others.

In one of his experiments on nitrocellulose the degra=
:dation was inhibited completely by applying a pressure of
8 atmospheres while in the other two experiments on polystyrene
the application of 15 atmospheres resulted only in reducing
the degradation as shown in Figures 4 and 5.

Weissler[11] questioned the findings of Schmid and his
claim of suppressing cavitation by applying a pressure of 15
atmospheres on the free surface of the solution. He indicated,
however, that under the experimental conditions used by Schmid
the pressurized oxygen will be forced into solution according
to Henry's Law. Therefore, when the instantaneous pressure
is reduced by a few atmospheres during the negative part of
the sound wave cycle, oxygen will come out of solution and
bubbles will be formed in the liquid. Weissler's statement
is most likely to be true, although there is no reason to
expect this degassing to be true cavitation.

In a later contribution by Schmid[12] he examined the
products of degradation of two similar unfractionated samples
one under thermal and the other under ultrasonic conditions.
By fractionating the resulting polymer at the end of degra=
:dation in the two cases and plotting their distribution
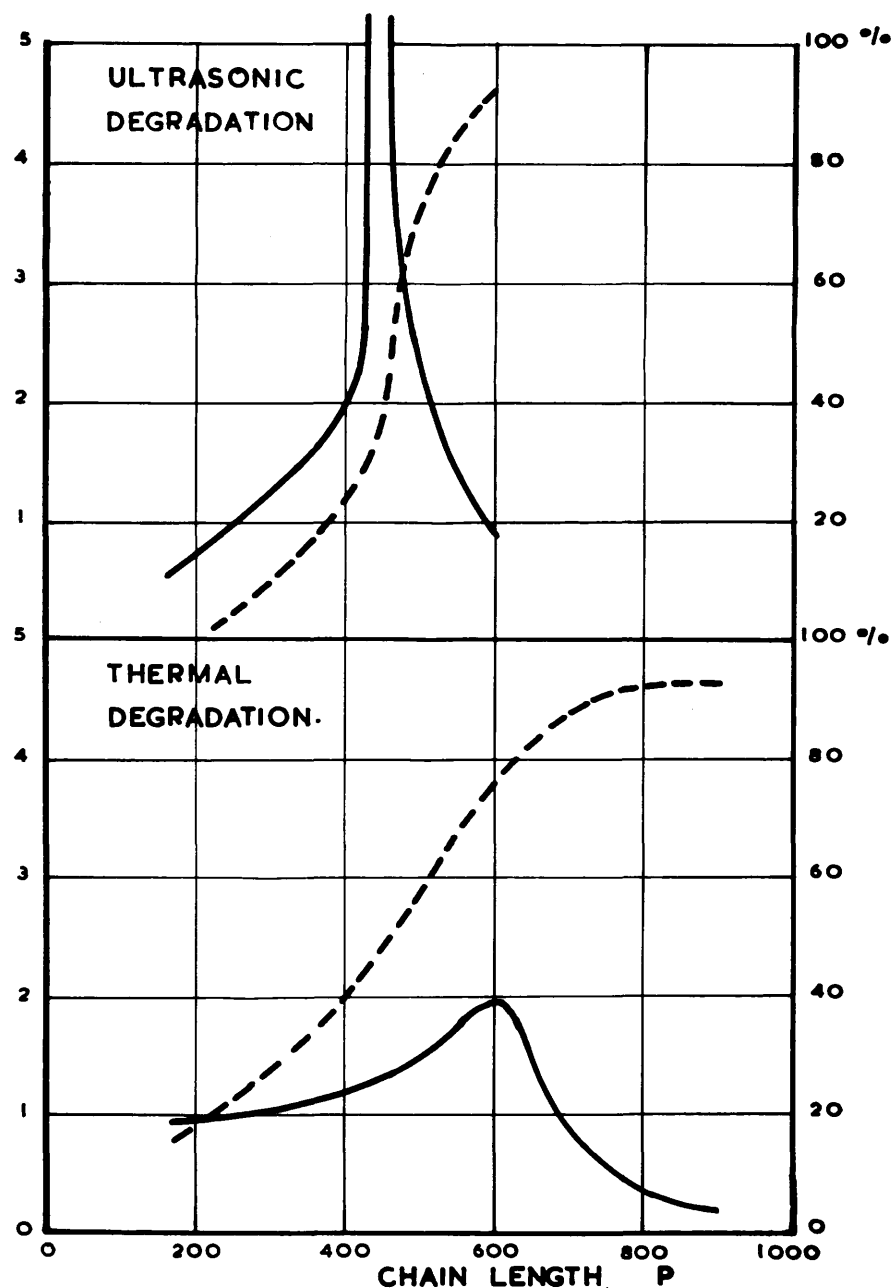
FIG. 6.   DISTRIBUTION CURVES OF STRONGLY
            DEGRADED POLYMETYYL METHACRYLATE

SCHMID , PARRET & PFLEIDERER.

curves which showed a marked difference, as shown in Fig. 6, he concluded that the degradation produced by ultrasonic waves could not possibly be considered to be due to thermal effects.

So far, it would appear that degradation of macromole-:cules by ultrasonic waves is mainly a result of cavitation inception in the solution. although frictional forces may be playing a minor role. This view point is confirmed by Prudhomme[13] who has been convinced that together with the strong action of cavitation there also exists a weaker effect of the so-called 'frictional forces'.

Another interesting contribution is the work of H. W. Melville and A. J. R. Murray[14] which proved that, apart from the strong action of cavitation, a strong degradation of long chain polystyrene molecules was detected by irradiating the solutions in an evacuated reaction vessel, after suppressing cavitation. Furthermore, it is quite possible that cavitation can lead to oxidation processes, even in the presence of nitrogen or an inert gas, after eliminating any traces of oxygen. R. O. Prudhomme and P. Grabar[15] in France and P. Gunther[16] in Germany have found that the oxidation effect is not due to activated oxygen, but probably to the liberation of O. H. radicals as an effect of cavitation. The chemical action was always closely related to a weak luminescence resulting from

the collapse of bubbles, probably either due to the adiabatic compression of the gas inside the bubble or due to some electrical phenomenon. Electrical discharges do occur as a result of the electrical potential built up between oppos-:ite walls of the cavity. Furthermore, the addition of a few drops of liquids of high vapour pressure such as ether or acetone usually inhibits luminescence or reduces it to a great extent with a consequently similar effect on the chem-:ical action. Under these circumstances it becomes doubtful again whether degradation of macromolecules is basically due to mechanical friction or simply due to cavitation and its associated effects.

Wiessler[17] added a little more to the perplexity of the problem by reporting that no degradation took place when he irradiated a 1% solution of polystyrene in toluene which was given a preliminary treatment of degassing by boiling under vacuum. He concluded, emphatically, that cavitation is the only cause of degradation, and that the opposite con-:clusion arrived at by earlier investigators is attributed to their inadequate methods for eliminating cavitation. He also inferred that oxidants, known to be produced by ultra-:sonic waves in solutions containing dissolved oxygen or nitrogen, cannot be responsible for the degradation because substantially the same amount of depolymerisation occurs

even when helium is the only gas present.

Based on the findings of Schmid, Jellinek and his co-
:workers[18] developed a theory of the degradation process
of long-chain molecules by ultrasonic waves. His theory
applies only to a homogeneous polymer. It gives the size
distributions at various stages of the degradation from which
the average chain lengths and molecular weights at definite
stages of the degradation can be calculated. He found
satisfactory agreement between experiment and theory for the
main features of degradation.

Furthermore, Jellinek[19] pointed out the fact that
neither the frictional forces as suggested by Schmid, nor
the impact forces as an alternative mechanism for breaking
the macromolecules, can explain his results. An adequate
theory of the mechanism of breakdown ought really to take
into account the many entanglements which must occur in the
solution and closely affect the viscosity of the solution
which depends, besides other factors, on the concentration of
the sample.

Jellinek[20] discussed the possibility of the ultra-
:sonic degradation being thermal in origin. Knapp and
Hollander[21] showed experimentally with the aid of a high
speed camera that the collapse of a bubble is very rapid
indeed, of the order of a microsecond. This experimental

observation was confirmed later by Noltingk and Neppiras[22] in their theoretical analysis of cavitation produced by ultrasonics. The collapse of a cavity was considered as an adiabatic compression and the gas temperatures inside the collapsing cavity can reach very high values ($10,000^{\circ}K$) depending on the compression ratio of the collapsing cavity and on the nature of the gas. Consideration of this aspect indicates that, if ultrasonic degradation is thermal in origin, the rate of degradation of a solution saturated with monatomic gas should differ appreciably from a solution saturated with a diatomic gas provided that both gases have similar solubilities in the solvent.

The experiments conducted by Jellinek[20] on 1% sol=:utions of fractionated polystyrene in benzene, after bubbling different gases in solutions for 20 minutes, and those con=:ducted by Melville and Murray[14] on two samples of copolymer of polymethyl methacrylate-acrylonitrile, proved that ultra=:sonic degradation is not thermal in its origin.

Jellinek, following Noltingk and Neppiras theoretical treatment, worked out the velocity developed in the solution in the neighbourhood of a collapsing cavity and then applied Stokes' law to calculate the frictional forces acting on a chain molecule touching the wall of the collapsing cavity. He found that this frictional force is sufficient to rupture

a C=C bond.   The observed rates of degradation for solutions
saturated with monatomic and diatomic gases were in agreement
with the conception that degradation is effected by cavitation.

....   It can be concluded from Jellinek's work that although
he was in favour of accepting cavitation to be the cause of
degradation, yet he was not entirely convinced that pure
ultrasonic waves do not produce degradation in the absence of
cavitation.   Furthermore, he seemed to agree that mechanical
forces and not the heat associated with cavitation, are the
origin of ultrasonic degradation.

It is worth mentioning at this stage that the role of
pure ultrasonic waves in the degradation of long chain mole-
:cules is far from being clearly defined.

It even becomes more ill-defined when the results of
the experiments of Alexander and Fox[23] on polymethacrylic
acid are considered.   No degradation under vacuum was observed,
indicating that ultrasonic waves alone are incapable of rup-
:turing the polymer chain and that cavitation is essential
for any process of degradation.   Their experiments on solu-
:tions of molecules of different shapes showed that the more
coiled the molecules the less is the resulting degradation.
This seems to indicate that the degradation is of a mechan-
:ical origin as the frictional forces are dependent on the
shape of the molecule.
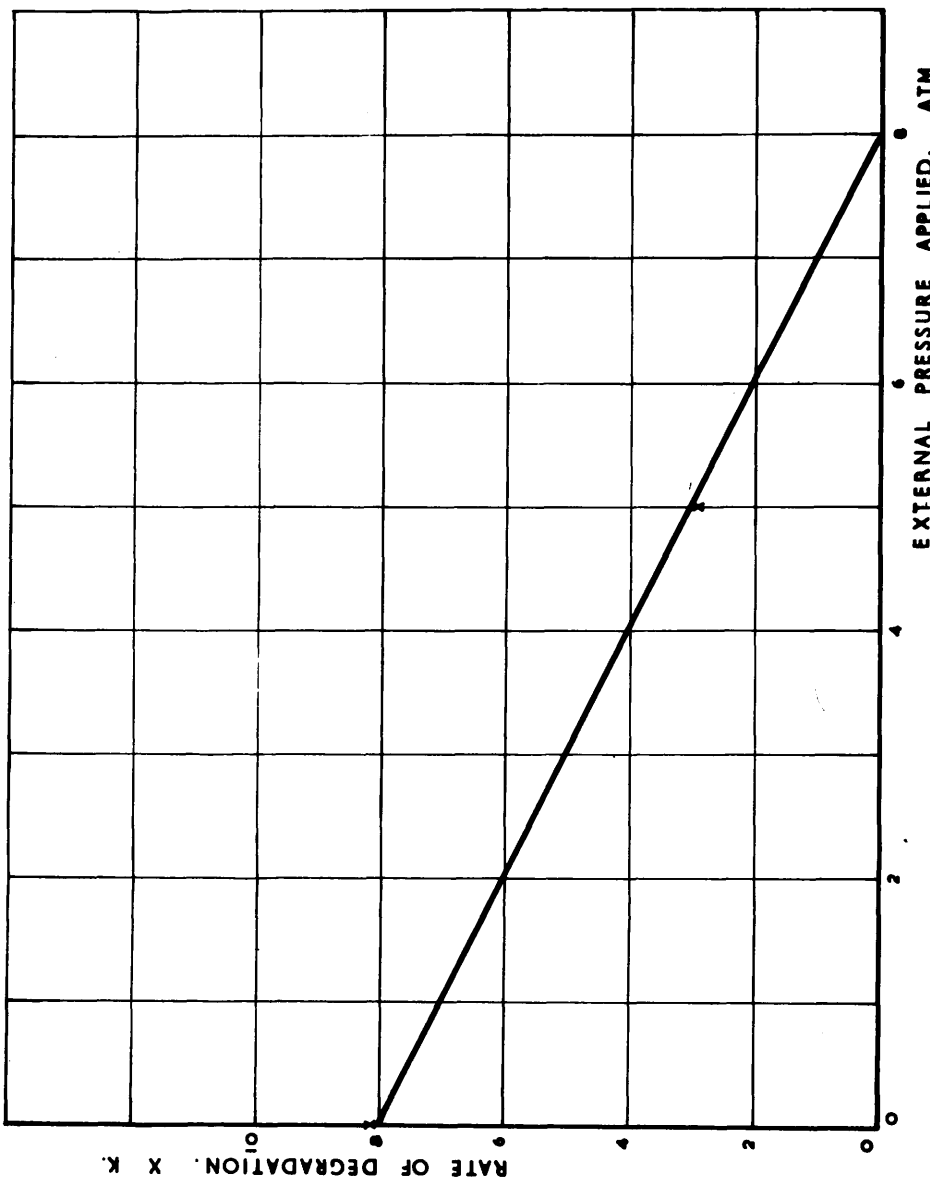
RATE OF DEGRADATION. X K.

EXTERNAL PRESSURE APPLIED.   ATM.

FIG. 7A.   RELATION BETWEEN RATE OF DEGRADATION &
APPLIED PRESSURE.   DEDUCED FROM SCHMID & ROMMEL.

RATE OF DEGRADATION.

EXTERNAL PRESSURE APPLIED.   ATM.
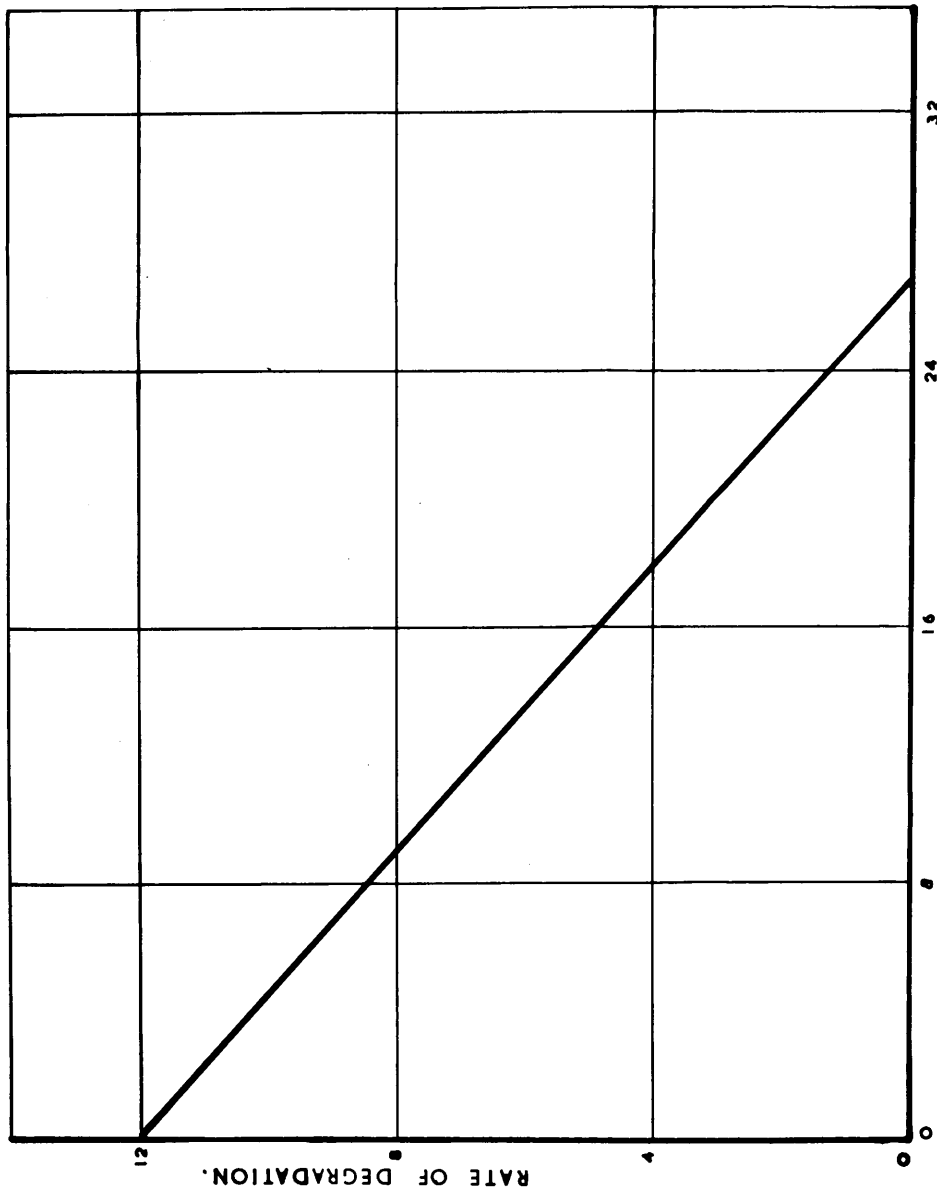
FIG. 7ᴮ   RELATION BETWEEN RATE OF DEGRADATION &
APPLIED PRESSURE.   DEDUCED FROM SCHMID & ROMMEL.

Summing up, it is generally agreed that chain sciss-
:ion is a consequence of the strain placed on the polymer
molecules either by frictional or impact forces.   These
forces can be a direct effect of the ultrasonic waves or due
to cavitation which is initiated by intense ultrasonic waves.
As the external pressure is increased, the rate of degradation
gradually decreases as a result of the smaller tendency to
cavity formation.   Even at pressures as high as 15 atmos-
:pheres, however, a residual rate of degradation remains.
Many earlier workers (Schmid and co-workers, Melville and
Murray), seem to have accepted this result as sufficient evid-
:ence of degradation in the absence of cavitation, most pro-
:bably as a result of frictional forces between solvent and
solute molecules.   But, if Schmid's results are considered
from a different angle and the rate of degradation is plotted
as a function of the applied external pressure it can be
noticed from Fig.7A that the rate of degradation of gun
cotton at the beginning of degradation (i.e., at t = 0)
decreases linearly as the pressure increases.   Furthermore,
the degradation ceases completely at a pressure of 8 atmos-
:pheres.   The same linear relation appears, from Fig.7B, to
exist in the degradation of polystyrene.   The value of exter-
:nal pressure at which the degradation ceases is found by
extrapolation to be somewhat higher and, in fact, it is
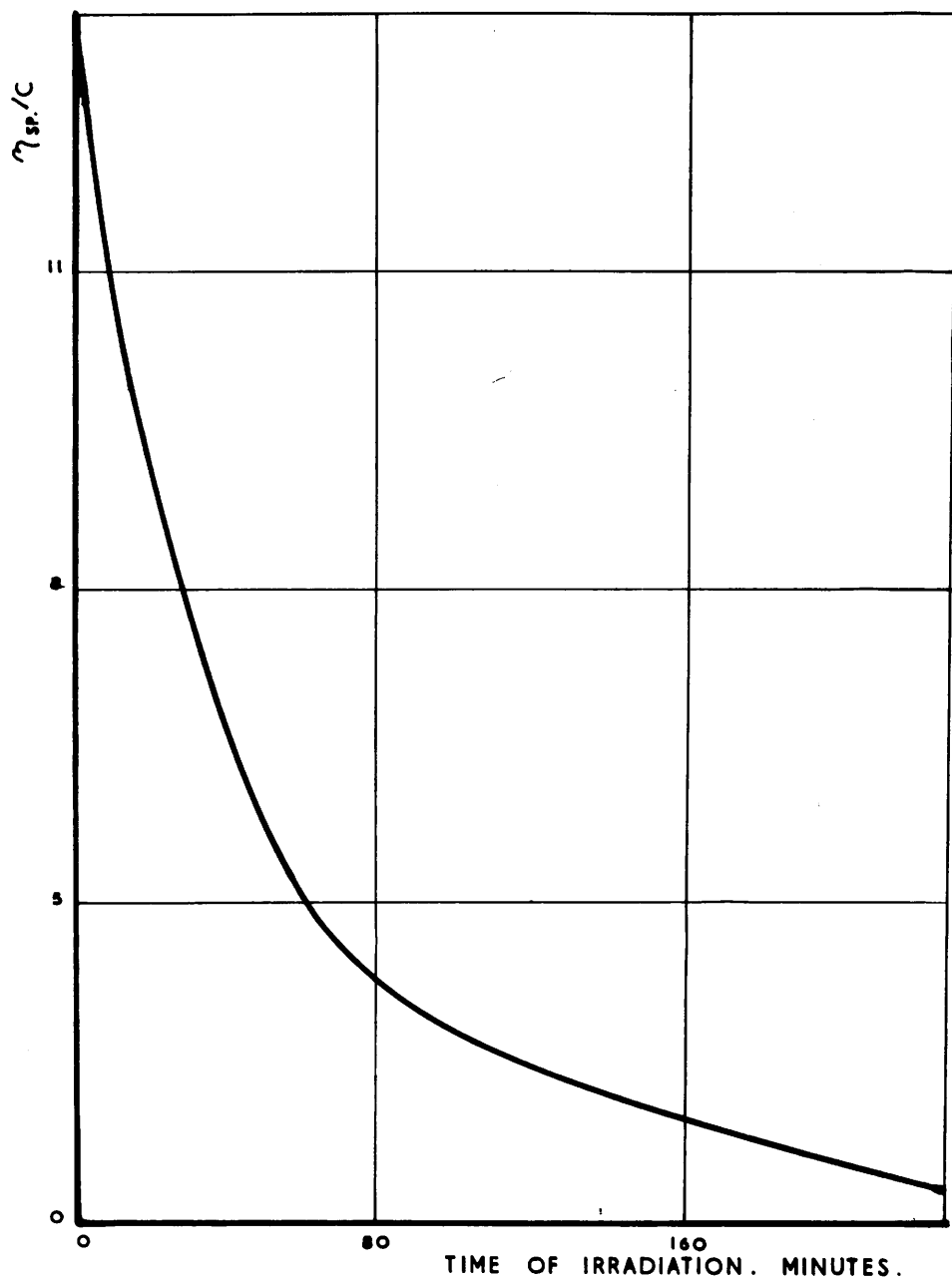
FIG.8.   DEGRADATION OF HIGH MOL. WT. POLYMETHYL METHACRYLATE IN VACUO.   MELVILLE & MURRAY.

almost three times (24 atmospheres) its value in the case of gun cotton.   This result indicates that there seems to exist a critical external pressure beyond which no degradation takes place.   This can be interpreted in two ways.   On one hand, it can be said that cavitation is completely suppressed and from this it follows that cavitation is the principal and only factor causing the degradation.   On the other hand, since cavitation can be suppressed, at least theoretically, by the application of much smaller pressures than those applied during the experiments, it may be inferred that the excess pressure is, presumably, needed to increase the rigidity of the solvent molecules and thus the relative motion between solvent and solute will decrease resulting in reducing the frictional forces below the minimum value required for effect-:ing degradation.   This implies that degradation produced purely by ultrasonic vibrations cannot be completely excluded.

As mentioned before attempts have been made by Melville and Murray to eliminate cavitation in a polymethyl methacryl-:ate solution in benzene by evacuating the system of permanent gases on the principle that the cavities once formed, would not collapse.   Their results, shown in Fig.8, indicate that the rate of degradation is only reduced but degradation still continues.   On the other hand, Weissler carried out experi-:ments under similar conditions of vacuum with polystyrene
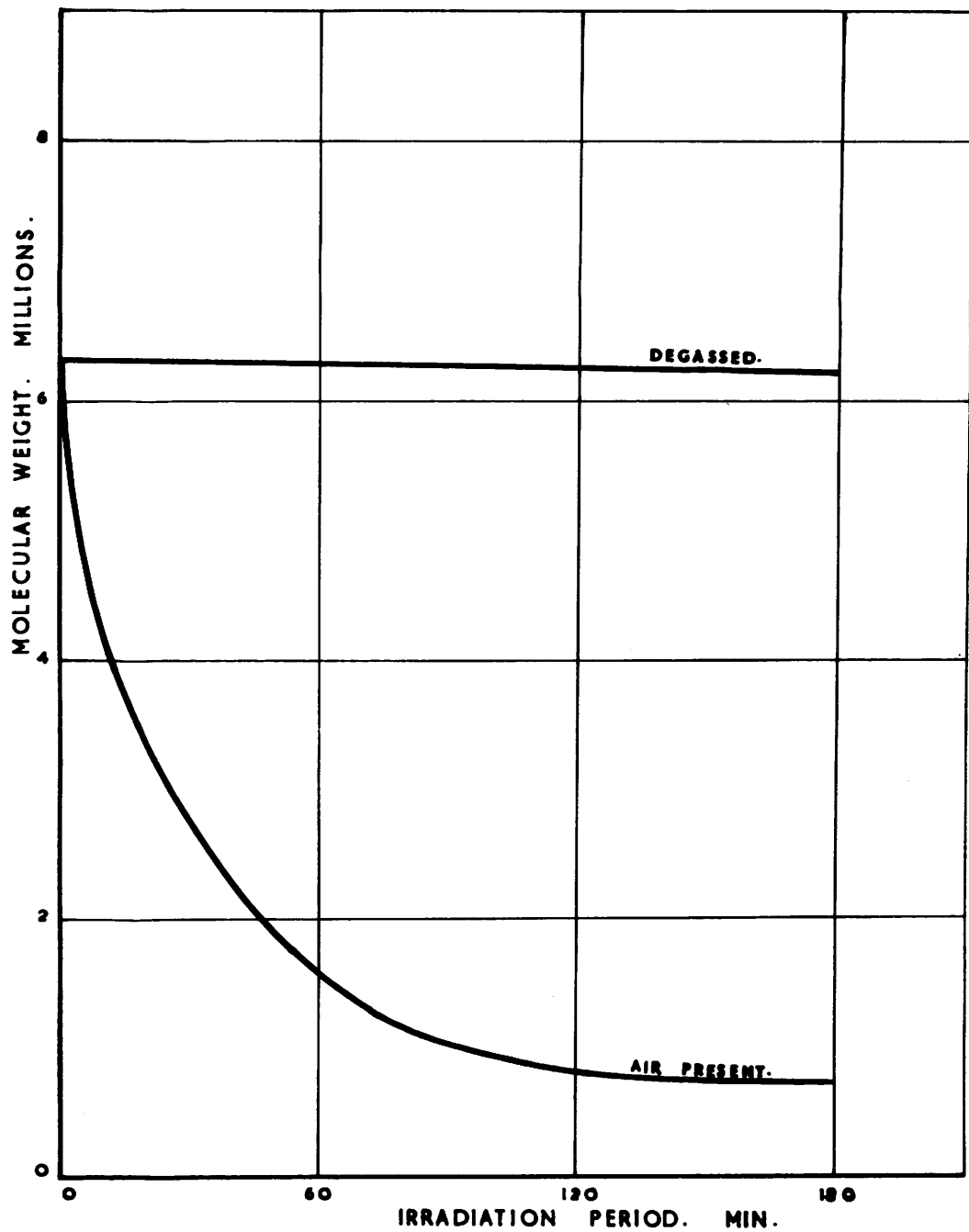
FIG. 9.   ULTRASONIC DEPOLYMERIZATION OF POLYSTYRENE
IN TOLUENE.   A. WEISSLER.

in toluene and found no degradation, as shown in Fig. 9.
Similarly, Alexander and Fox could detect no degradation on
irradiating evacuated aqueous polymethacrylic acid solutions.
Hence, it can be stated that despite the various claims, there
is no real evidence that degradation can take place in the
absence of cavitation.

Furthermore, the only detailed theoretical treatment
expressing the degradation of polymers by ultrasonic waves is
that given by Jellinek and it is only limited to homogeneous
polymer samples. Obviously this limitation is a serious
drawback in the study of ultrasonic degradation of polymers.
This is mainly due to the fact that proper fractionation is
a very complex process, which inspite of all precautions
results in a heterodisperse fractions.

Up to the time this work had been undertaken, no
general solution expressing the kinetics of random degradation
of heterogeneous polymer samples had been developed. However,
in view of the fact that the most commonly used polymers are
heterogeneous usually prepared thermally, this work has been
contemplated mainly to develop a complete theoretical solution
of the problem of degradation of heterogeneous polymers. The
general solution can be applied to express any type of random
degradation. In the course of this work this general solution
will only be applied to the case of addition polymers (prepared

thermally) and their degradation by ultrasonic waves.

Factors Controlling Cavitation.

In 1917, Rayleigh[24] examined theoretically the behaviour of an incompressible fluid in which he imagined a spherical void to be suddenly formed. Later, in 1942, Beeching[25] extended Rayleigh's analysis by taking into account surface tension effects, and the pressure of the liquid vapour in the bubble. At the same time, Silver[26] introduced thermodynamic considerations, but several question- :able assumptions in his treatment render his results doubt- :ful. The experimental results of Knapp and Hollander(1948), using high speed cinematography, confirmed the existence of very large radial velocities and accelerations during the collapse period of a cavity, and consequently agreed closely with Rayleigh's predictions. Further, in 1949, Plesset[27] developed an equation for the motion of a vapour-filled bubble in a changing pressure field.

An attempt, to define theoretically the conditions for the appearance of cavitation in liquids subjected to alter- :nating pressure changes, was made by Noltingk and Neppiras[28]. They found that the occurrence of cavitation is restricted to a definite range of variations of the following parameters:

1. The alternating pressure amplitude of
   ultrasonic waves, P_O

2. The frequency of ultrasonic wave, ω

3. The radius of the bubble nucleus, R_O

4. The hydrostatic pressure applied to
   the liquid, P_A

Furthermore, they predicted that under certain condit-:ions, the change from non-cavitating to cavitating conditions is found to be exceedingly sharp. This enabled them to express accurately and in simple terms the threshold for cavitation inception.

In order to get a clearer picture of the effect of each of these factors on the inception of cavitation and the role played by each in suppressing cavitation, a discussion of each factor separately seems justifiable.

Thresholds for R_O.

Assuming that all the other factors are kept constant, it is predicted that as R_O is increased from indefinitely small values, the changes in radius are at first small and the bubble motion is truly sinusoidal but 180° out of phase with the impressed alternating pressure. From the energy equation given by Noltingk and Neppiras, for which a number of solutions were found using a differential analyser, the
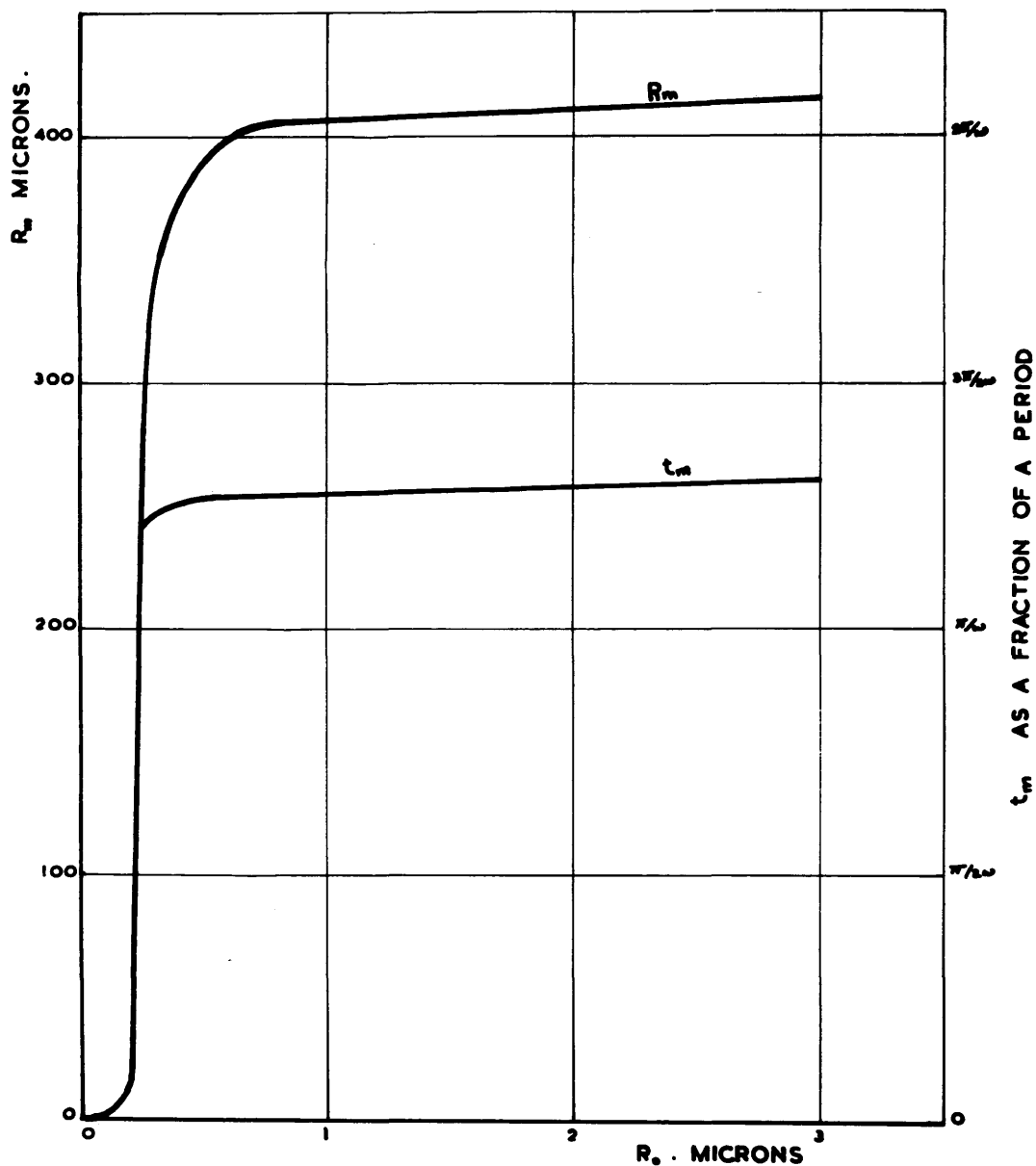
FIG. 10. R_m & t_m AS FUNCTIONS OF R_o

FOR $P_o = 4 \times 10^6$ $\omega = 9 \times 10^4$ $P_4 = 10^6$

NOLTINGK & NEPPIRAS.

radius-time curves (Fig. 10) show that as the lower threshold of R_0 is approached the curves become distorted. Furthermore at the critical value of R_0 (depending on the frequency, hydrostatic pressure and pressure amplitude considered), a sudden expansion occurs resulting in a sharp rise in the value of the bubbles maximum radius R_m indicating the inception of true cavitation. Cavitation conditions continue, presumably with increased intensity, as R_0 increases. On further increase in R_0, the intensity of cavitation reaches a peak and then starts to decrease until R_0 reaches and passes its resonant value corresponding to the frequency of the ultrasonic waves. This critical frequency '$\frac{\omega}{2\pi}$' has been expressed by the following equation:

$$\omega^2 R_0^2 = 3\gamma \left(p_A + \frac{2S}{R_0}\right) - 2S/R_0$$

where γ = ratio of sp. heats of gas

inside the bubble;

and S = surface tension of liquid;

After passing through this threshold, no true cavit-:ation takes place. The bubble motion again becomes sinusoidal and can be represented by the equation:

$$R = R_0 - \frac{R_0 p_0 \sin wt.}{3\left(p_A + \frac{4S}{3R_0}\right)}$$

Threshold of ω.

From the analysis of the effect of varying R_O, and considering the equation of bubble motion at the upper threshold of R_O, it is apparent that any increase in frequency results in a lowering of this upper threshold. Naturally, if the frequency continues to increase, a value will be reached where the upper threshold of R_O coincides with the lower limit. Beyond that frequency true cavitation can never occur, theor= :etically, whatever the distribution of nuclei.

However, cavitation effects are expected to fall off with increasing frequency, and to disappear completely in the region of frequency given by:

$$\omega = \frac{1}{2\pi R_O} \left[3\gamma \left(p_A + \frac{2S}{R_O} \right) \right]^{\frac{1}{2}}$$

Noltingk and Neppiras' theory indicates no lower threshold for ω, implying that the cavitation intensity would increase as ω is decreased. However, since at low frequencies the liquid will have time to follow the impressed pressure variations, no sufficient tensions in the liquid will develop and no cavitation will occur.

This frequency dependence of cavitation was later illus= :trated by Gaertner W.,[29] after introducing some simplifying assumptions which seem justifiable. He emphasised the fact that the effects of ultrasonic cavitation will cease above

a certain frequency range as a consequence of the limitations
on the expansion of the nucleus.   His discussion gives a
strong indication that the optimum frequency for applications
of ultrasonics utilising cavitation effects lies below 2 Mc
and most likely below 1 Mc at the intensities reached with
ordinary transducers.

Although Schmid and his co-workers found that depoly-
:merisation of long chain molecules is independent of frequency
in the range 10-300 Kc/sec., yet, in view of the practical
importance of finding an optimum frequency for cavitation
effects, an experimental investigation of the problem seems
highly desirable in the range of frequencies 0.5 - 2 MC./sec .

Thresholds of p_A and p_o.

Changes in the hydrostatic pressure p_A affects the
rapidity of the collapse of a cavitation bubble.   If p_A is
decreased the bubble will grow larger.   If the bubbles become
very large the time required for their collapse may be so
great that the pressure begins to go negative before the
completion of the collapse.   The collapse will tend to be less
violent.   Obviously a lower threshold must exist below which
no destructive cavitation will occur, as the bubbles will not
have time to collapse completely.   Any further reduction in
p_A below this threshold will result in slower changes in the

MAX. FLUID PRESSURE P_m (ATM. $\times 10^6$)

P_A. ATM.

$R_o = 1.6 \times 10^{-4}$

$\omega = 9 \times 10^4$

$P_o = 4 \times 10^6$

R_m MICRONS
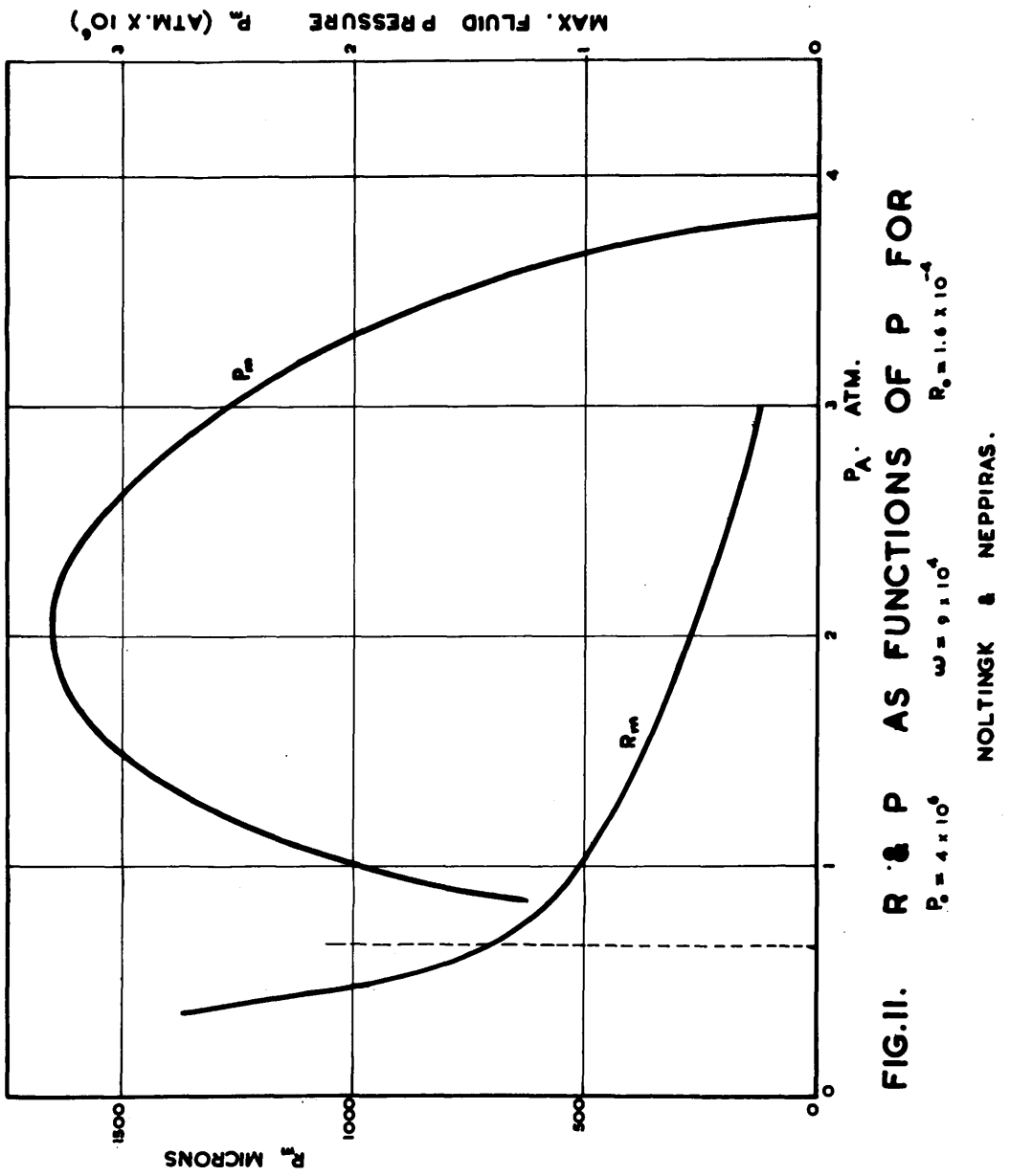
FIG. II.   R & P AS FUNCTIONS OF P FOR

NOLTINGK & NEPPIRAS.

t_m AS FRACTION OF A PERIOD.

P_o ATMOSPHERES.

FIG.12. R_m & t_m AS FUNCTIONS OF P_o.

FOR $R_m = 2 \times 10^4$ $w = 9 \times 10^4$ $P = 10^6$

NOLTINGK & NEPPIRAS.

R_m MICRONS.
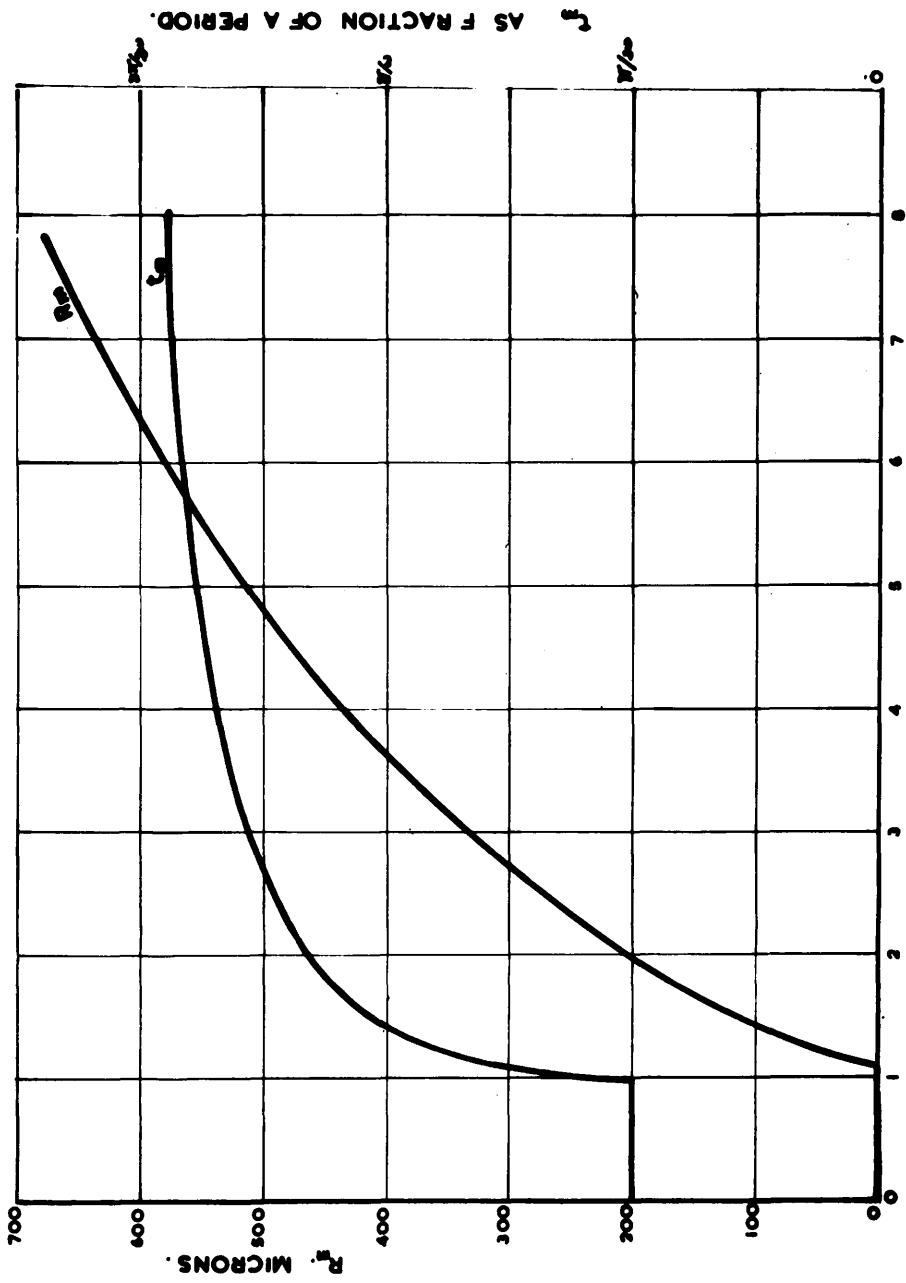
bubble radius.   A typical illustration of the effect of

varying p_A is shown in Fig.11 given by Noltingk and Neppiras

in which the broken line shows the lower limit of p_A below

which the collapse will not be completed before the end of

the positive half-cycle of the pressure wave.   In addition

the figure shows that with increasing p_A an upper limit will

be reached beyond which cavitation never occurs.   Further-

:more, on considering the maximum fluid pressure p_m produced

by the bubble's collapse, the steep front of its curve implies

a rapid change from cavitating to non-cavitating conditions.

The effect of varying the amplitude of the impressed

pressure waves p_o is best illustrated by Fig.12, which shows

a sudden expansion of the bubble when the value of p_o is

nearly equal to p_A.

Although the graphs illustrate specific cases for

selected values of parameters, and cannot be braodly inter-

:preted, yet it can be safely concluded within the limitations

of the theory that cavitation can be suppressed either by

reducing p_o to be less than p_A, or by increasing p_A to be

greater than p_o, even in ordinary 'gassy' liquids containing

comparatively large bubbles.

It is worth mentioning in this respect that for the

above conclusion to prove valid the pressure should be applied

directly to the liquid in the absence of any air or gas above

the free surface of the liquid.

Object of Investigation.

From the critical survey of past work on degradation of long chain molecules by ultrasonic waves, it is quite clear that in many of the published work the type of polymer samples used in the investigations was not clearly defined, i.e., whether fractionated or unfractionated polymers were used. Obviously, fractionation of a polymer sample is a troublesome task, and it would be much better if unfraction-:ated samples could be used, provided their degradation characteristics can be predicted at the different stages of degradation.

Furthermore the ultrasonic intensities in the polymer solutions proper were more or less a matter of conjecture than truly measured values.

The role played by cavitation in the process of degra-:dation by ultrasonic waves is still, however, as it was before, subject to controversy. In this respect it seems possible to conclude that more experimental work under more controlled conditions than had been hitherto the case is needed on this aspect. An investigation which can throw more light on the problem is, beyond doubt, relevant to the complete understanding of the mechanism of degradation of long chain molecules by ultrasonic waves.

Finally, from a practical point of view, it seems desirable to investigate the existence of an optimum frequency for the process of degradation as suggested by Gaertner.

With an aim to contribute to the clarification of the above mentioned points a programme for this work was contem=plated to include the following:

1. To design, construct and put into use an ultrasonic generator of 1 KW. output covering a frequency range 0.5 to 2 MC/sec.

2. To construct, calibrate and put into use a simple and reliable device for measuring ultrasonic intensity and viscosity.

3. To develop a general solution for the random degradation of long chain molecules and to apply the theory to express the degradation of addition polymers by ultrasonic waves.

4. To carry out experiments on the degradation of addition polymers with the purpose of verifying the theory and check=:ing the limitations of its validity.

5. To investigate the possibility of using D.P.P.H. to detect any free radicals that may have been produced in the solution during the process of degradation and also to supply further evidence on the validity of the theory developed.

6.　To investigate the effects of intensity and initial chain length on the degradation process.

7.　To investigate the frequency dependence of the ultra-:sonic degradation of addition polymers in the 0.5 - 2 Mc/sec. frequency range.

8.　To suppress cavitation at least by one method in order to determine the role of cavitation in the degradation of polymers by ultrasonic waves.

BIBLIOGRAPHY.

1. Staudinger, H. and Heuer, W.
   Ber. 67, 1159 (1934).

2. Szalay, A.
   Z. Phys.Chem. A164, 234 (1933).

3. Flosdorf, H.W. and Chambers, L.A.
   J.Amer.Chem.Soc. 55, 3051 (1935).

4. Freundlich, H. and Gilling, D.W.
   Trans. Far. Soc. 34, 649 (1938).

5. Brohult, S.
   Nature, 140, 805 (1937).

6. Thieme, E.
   Phys. Zeit. 39, 384 (1933).

7. Schmid, G. and Rommel, O.
   Z.Phys.Chem. 185A, 98 (1940).

8. Schmid, G.
   Z. Phys.Chem. 186A, 113 (1940).

9. Schmid, G. and Poppe, W.
   Z. Elektrochem. 53, 28 (1949).

10. Schmid, G. and Buttenmuller, E.
    Z. Elektrochem. 50. 209 (1944).

11. Weissler, A.
    J. Applied Physics. 21, 171 (1950).

12. Schmid, G. Paret, G. and Pfleiderer. H.
    Kolloid Z. 124, 150 (1951).

13. Prudhomme, R.O.
    J. Chem.Phys. 46, 318 (1949).
    ibid. 47, 795 (1950).

14. Melville, H.W. and Murray, A.J.R.
     Trans. Farad. Soc.   46, 996 (1950)

15. Prudhomme, R.O. and Grabar, P.
     J. Chim. Phys.   46, 323 (1949).
     ibid.   46, 667 (1949).

16. Gunther, P. and Theobald, H.
     Zeit. Phys. Chem. 40B, 1 (1938).

    Gunther, P. and Holzapfel, L.
     Zeit. Phys. Chem.   42B, 346 (1939).

17. Weissler, A.
     J. Acoust. Soc. Amer.   23, 370 (1951).

18. Jellinek, H.H.G. and White, G.
     J. Pol. Sci.   6, 745 (1951).

19. Jellinek, H.H.G. and White, G.
     J. Pol. Sci.   7, 21 (1951).

20. Brett, H.W.W. and Jellinek, H.H.G.
     J. Pol. Sci.   13. 441 (1954).

21. Knapp, R.T. and Hollander, A.
     Trans. Am. Soc. Mech. Eng.   70, 419 (1948).

22. Noltingk, B.E. and Neppiras, E.A.
     Proc. Phys. Soc.   B63, 674 (1950).

23. Alexander, P. and Fox, M.
     J. Pol. Sci.   12, 533 (1954).

24. Lord Rayleigh,
     Phil. Mag.   34, 94 (1917).

25. Beeching, R.
     Trans. Instn. Engrs. and Shipb.   85, 210 (1942).

26.   Silver, R.S.

        Engineering, 154, 501 (1942).

27.   Plesset, M.S.

        J. Appl. Mech.   16, 277 (1949).

28.   Noltingk, B.E. and Neppiras, E.A.

        Proc.Phys.Soc.   B64, 1032 (1951).

29.   Gaertner, W.

        J.Acous.Soc.Amer.   26, 977 (1953).

CHAPTER II.

1. ULTRASONIC GENERATOR.
2. CRYSTAL TRANSDUCERS.

1. ULTRASONIC GENERATOR.

A. Introduction.

It was necessary, for carrying out this investigation, to build a powerful ultrasonic generator. The power rating of the ultrasonic generator was estimated to be about 1 KW. Many types of oscillators were studied among which are the following:

(a) resonant drive type (Hartley);

(b) self-maintaining type (Pierce);

(c) push-pull type.

From the above mentioned three types, the push-pull oscillator cricuit was accepted as the most convenient type of ultrasonic generator. Some of the salient features of a push-pull operation, which favoured its selection, are summar-:ised below:

1. The effective plate resistance is twice that of a single valve.

2. The power output is twice that of a single valve oper-:ating under the same conditions as either of the push-:pull pair.

3. The fundamental component of plate-current is that of a single valve; the corresponding tank-voltage is twice that for a single valve.
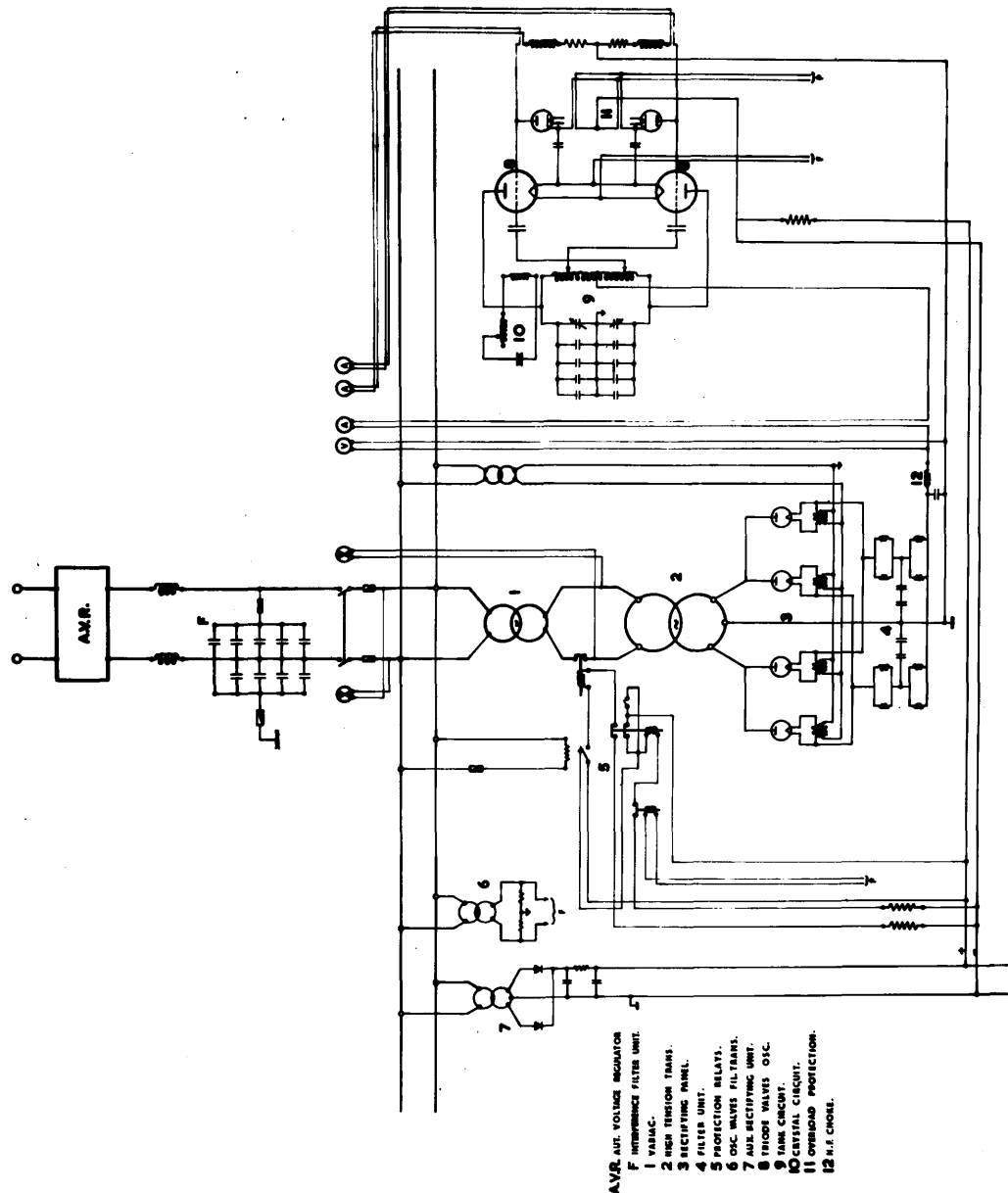
FIG. 13. ULTRASONIC GENERATOR CIRCUIT DIAGRAM.

A.V.R. AUT. VOLTAGE REGULATOR
F INTERFERENCE FILTER UNIT.
1 VARIAC.
2 HIGH TENSION TRANS.
3 RECTIFYING PANEL.
4 FILTER UNIT.
5 PROTECTION RELAYS.
6 OSC. VALVES FIL.TRANS.
7 AUX. RECTIFYING UNIT.
8 TRIODE VALVES OSC.
9 TANK CIRCUIT.
10 CRYSTAL CIRCUIT.
11 OVERLOAD PROTECTION.
12 H.F. CHOKE.

4. The correct load impedance (plate to plate) is twice
    that of a single valve.

5. The total drive voltage (grid to grid) is twice that of
    a single valve; drive power is also doubled.

    These features provide certain advantages of the push-
pull type of oscillator over other types of oscillators.
Some of these advantages are:

1. Increased power and frequency stability.

2. All oscillatory voltages and currents, with the exception
    of even harmonics, are symmetrical with respect to earth
    and to the D.C. supply.   There are no A.C. components
    in the D.C. supply, other than even harmonics.   With
    exactly similar valves there are no even-harmonic
    components in the tank-circuit.

3. Valve inter-electrode capacities (grid to cathode, and
    plate to cathode) are effectively halved, since they
    are in series.   This is a useful property when working
    at very high frequencies, since valve capacities set
    a limit to the frequency at which satisfactory oper-
    :ation is obtained.

B. Circuit Diagram.

    The circuit diagram of the push-pull ultrasonic gener-
:ator is shown in Fig.13.   The design, construction, mounting,

connections, earthing and screening are all in accordance with the conventional methods recommended in building such high frequency oscillators[1,2].

The impossibility of obtaining exactly similar character= :istics for two valves, and the difficulty of determining the exact electrical centre of the tank-coil both make it desir= :able to include a H.F. choke(12) in the plate supply lead. This choke allows the H.F. potential of the feed-point to vary somewhat, according to the degree of asymmetry of the valves and circuit.

C. Protection Systems and Relays.

i. Protection against sudden loading at switching on.

It is essential for the long life operation of the oscillator that the filaments currents should be allowed at least a minute to heat up the filaments before the anode volt= :age is switched on. A thermal bimetallic relay, a mercury switch and a group of post office relays were connected, as shown in Figure 13 (5), to cause a delay of approximately two minutes before the anode voltage could be switched on.

ii. Automatic no-load protection.

A reduction in loading of an oscillator delivering its rated power output is usually accompanied by:

a.   a rise in tank circuit Q, voltage, current, and KVA.

b.   an increased H.F. drive-voltage between grid and

      cathode, since it is obtained from the tank.

c.   a decrease in peak and average values of plate-current.

d.   an increase in grid current.

e.   an increase in grid-bias voltage consequent upon the

      increase in grid-current.

With the drive correctly adjusted for full load con-:ditions, the accidental removal of load might result in excessive grid-current. This in turn might lead to blocking of the oscillator, and perhaps even melting of the grid wires. As shown in the circuit diagram a post office relay was used in conjunction with a high vacuum double diode (11) giving protection against serious over-driving. The diode is biased so that it passes no current unless the drive voltage exceeds a predetermined value; above this value the diode load damps the drive circuit and minimises the increase in grid-current. The relay operates and interrupts the H.T. supply if the diode current exceeds a certain amount.

D. Interference Suppression.

To suppress interference, which may be caused by the H.F. power being fed into the supply mains from the oscill::ator and transmitted through the mains to other apparatus

in the neighbourhood, an electric filter was built and placed
in the supply mains, at the nearest point to the oscillator.
This arrangement is shown in the circuit diagram under
symbol F.

E. <u>Voltage Stabiliser.</u> (ASR).

An ASR-1150 automatic voltage regulator was connected
on the input side of the ultrasonic generator to maintain
the voltage from the supply mains constant within $\pm$ 2.5% .
This was found essential due to the fluctuating character
of the supply voltage available.   The stabiliser consists
of an autotransformer, which is provided with one input tapping
and three output tappings.   Relative to the input voltage,
the output tappings provide voltages which are respectively
'7.5%' above the input, '2.5%' above, and 2.5% below.   The
tap changes are performed by means of microswitches, operated
by quick-acting relay movements, which are controlled by an
electronic 'sensor' unit.

The actual time lag of switching is of the order of
only two milliseconds, so that the voltage stabiliser is
ideally suited to the existing conditions where sudden voltage
surges or drops are quite frequent.

Furthermore, during the brief period of tap changing,
a resistance-condenser network, which is bridged across the

micro-switch contacts, is employed to eliminate surges and contact arcing.

F. Power Control.

The R.F. output from an ultrasonic generator is usually controlled by either of the following methods:

(i)   variations in grid drive;

or   (ii)   variation in load matching;

or   (iii)   variation in filament emission;

or   (iv)   variation in H.T. voltage.

The first of these methods, as a means of varying the output from an R.F. generator, is beset with severe limita-:tions.   Load matching on the other hand relies upon reson-:ance effects in tuned circuits and consequently depends on critical adjustment.   Furthermore, it can easily permit over-:load conditions to prevail.

It is not an uncommon method to control the power output by varying the voltage applied to the filaments.   This method, however attractive it may look, is not altogether satisfactory, since it is inclined to overload the generator with a bigger proportion of the power input dissipated at the anodes.

In the ultrasonic generator built as part of this work, the fourth method of power control was adopted.   From an electrical point of view variations in the H.T. voltage

offer the most ideal method of power control.   From an
acoustic point of view since the power input to the quartz
transducer to a first approximation is proportional to the
square of the H.T. voltage, this method provides a rough
estimateof the power input to the quartz transducer.

A variac (1) in the circuit diagram was used for that
purpose.

G. Metering.

In a push-pull circuit, where it is required that the
two similar valves should be equally loaded, it is necessary
to introduce two meters either to measure the grid currents
or the anode currents.   Two ammeters were used to measure
the grid currents of the two valves thus providing a contin-
:uous check on the performance of the R.F. generator.   An
electrostatic voltmeter and a D.C. ammeter which measures the
total anode current, were also connected.   This provides a
rough estimation of the power input to the generator.   Further-
:more, the ammeter helps to indicate whether the generator
is tuned to the required frequency.

A hot wire ammeter was used in the load circuit which
assists in the proper tuning of the generator.
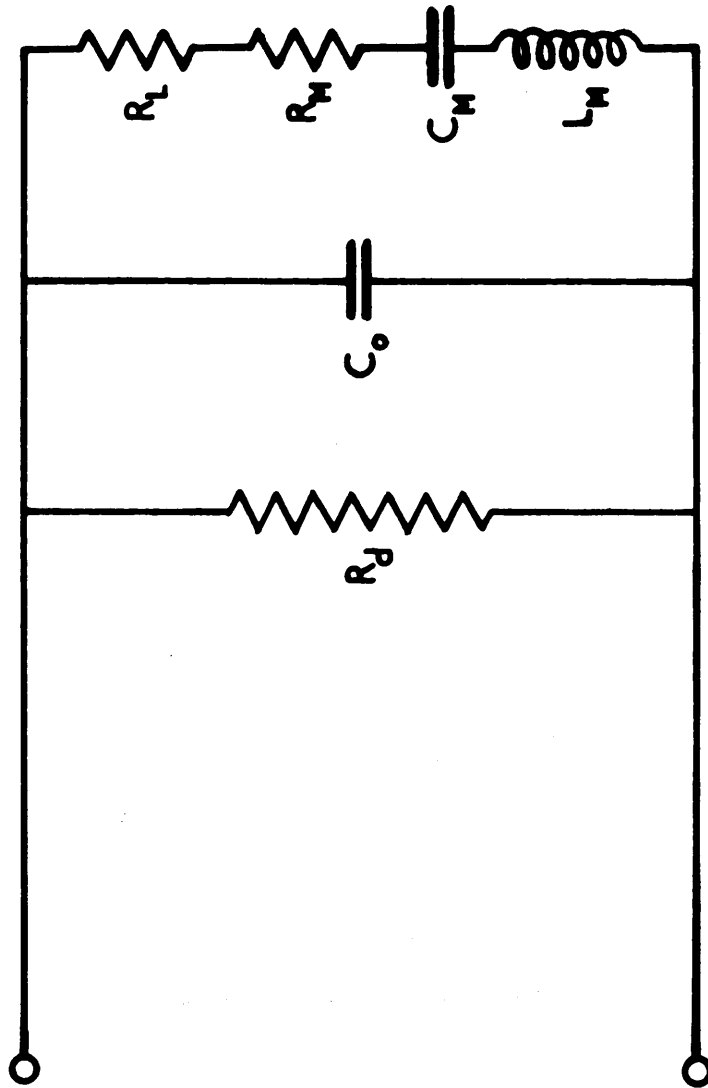
FIG. 14. EQUIVALENT ELECTRICAL CIRCUIT FOR A LOADED PIEZOELECTRIC ELEMENT.

H. Efficiency.

A loaded piezoelectric quartz crystal can be repre-
:sented by its equivalent electrical circuit shown in Fig.
14, where

R_d represents the load imposed by dielectric
      losses in the crystal and its holder;

C_o is the simple capacitance between the two
      electrodes;

R_m represents the mechanical frictional resistance
      in the crystal and holder;

R_L is the acoustic load to which the crystal
      is coupled;

C_m and L_m represent with R_m the motional properties
      of the transducer.

Provided the transverse dimensions of a crystal plate
are larger than one wave length, the effective motional imped-
:ance at resonance

R_L ($= Z_L$) is given by

$$R_L = a^2 t^2 \rho_o v_o / 4 \delta^2 S$$

where a is the compressibility of the crystal,

   t is the thickness of the plate,

ρ_o is the density of the medium irradiated,

v_o is the velocity of sound waves in the medium
      irradiated,

δ is the piezoelectric constant of the crystal,

S is the radiating area.

Since the resonance frequency for a quartz plate is given by $t = \dfrac{2780}{f_R}$ KC/sec. where t is measured in millimeters, therefore, the motional resistance falls off rapidly as the frequency is raised. Consequently the same power can be obtained from crystals with lower applied voltages.

For X-cut quartz plates in thickness vibration the radiation resistance, at resonance, is given by

$$R_L = \frac{9.69 \times 10^{17}}{S. \; f_R^{\;2}} \quad \text{ohms.}$$

where S is the effective area of the radiating surface

      of the quartz crystals,

and f_R is the resonant frequency of the crystal.

This radiation resistance will be shunted by the reactance of the condenser C_o which will be considerably lower in value. This reactance is given by

$$X_c = \frac{1}{2\pi \; f_R \; C_o} = \frac{1.12 \times 10^{17}}{S \; f_R^{\;2}}$$

Hence the radiation resistance of the crystal is about 8.65 times as large as the reactance of the crystal, and if the crystal alone is connected to the oscillator it is impossible to get all of the electrical energy into acoustic energy.

Furthermore, the efficiency drops off rapidly for a 5 per cent change in frequency away from the resonant frequency.

By using a coil to neutralise the static capacitance of the crystal, the region of high efficiency can be extended over a wider frequency range, and the absolute efficiency of conversion can be made considerably higher. This can be done by using either a series coil or a shunt coil [3]. The series coil gives a low impedance circuit while the shunt coil gives a high impedance cricuit.

It was found more convenient for matching purposes to use a series coil in the crystal circuit. The introduction of this coil showed a marked difference in the acoustic out-
:put of the crystal. The crystal, after inserting the series coil became a much more efficient radiator transferring at least least 70 per cent of the electrical energy into acoustic energy over a wider frequency band centred around the resonant frequency of the crystal, compared to 10% energy transferred without the use of the coil. Outside this frequency band the amount radiated falls off more rapidly than for the crystal alone.

I. Design Data and Operating Conditions.

Valves used - 2 Mullard V.H.F. power triodes

type TY3 - 250.

Valve ratings – limiting values – V_a 1.5   KV.

V_g -120   V.

$I_{a_{d.c.}}$ 400   m.A.

$I_{g_{d.c.}}$ 80   m.A.

$V_{in(pk)}$ 295   V.

P_{drive} 22   watts.

P_a 175   watts.

P_{output} 425   watts.

η 71   %

With a circuit transfer efficiency of 80%. P_{load} 340   watts.

Operating Conditions.

A sample of the calculations for designing the push-:pull oscillator, shown in Fig.13, is summarised below:

Duration of anode current $= 2\theta_a$ $= 140^{\circ}$

$i_{a_{pk.}}$ $= 3.9 \times 400 = 1560$ m.A.

From valve characteristics $v_{g_{max.}} = 175$ V.

$v_{a_{min.}} = 230$ V.

$i_{g_{pk}}$ $= 400$ m.A.

$I_{g_{d.c.}}$ $= 80$ m.A.

$$\alpha = \frac{\mu V_{g\ max.}}{E_b} = 1.9$$

$$\beta = 3.0$$

$$V_g = -120\ V.$$

$$R_g = 2.0\ K\Omega$$

For Tank Circuit Components.

$$Q\ \omega L = \frac{1370 \times 2}{678} = 4040\ ohms.$$

For a frequency 0.5 MC/sec. and Q = 12, tank coil inductance

is given by $L = \dfrac{4040}{12 \times \pi} = 107\ \mu.H.$

Required tank circuit capacitance at resonance = 935 p.F.

2. CRYSTAL TRANSDUCERS.

A. Introduction.

Quartz was used for producing the high intensity ultra-:sonic waves required for this investigation. Quartz was selected because it is physically robust, non-hygroscopic and capable of withstanding reasonably high temperatures. Although it has a relatively small piezoelectric constant, it can be effectively employed as a powerful generator at resonant frequencies.

Crystals of 1" diameter were obtained from the quartz crystal company. Both faces of the crystals were silver plated, leaving an annular ring 1/16" wide at the circum-:ference unsilvered. The crystals were X-cut for thickness vibration having resonant frequencies of 0.75, 1, 1.25, 1.5 and 2 Mc/sec.

The crystal was usually mounted in such a way that it could be immersed in a liquid medium which represents the acoustic load. It was usually excited to vibrate at its mechanical resonant frequency in order to secure the maximum acoustic output. The generated acoustic intensity is pro-:portional to the square of the product of applied voltage and operating frequency. High intensities are usually limited by an upper frequency limit of about 2 Mc/sec. Above that limit the quartz plate is liable to mechanical fracture due

to its decreased thickness. At the same time the tendency for a voltage break down increases imposing an upper limit on the maximum voltage which can be applied safely to the crystal immersed in the medium without a break down taking place.

In view of these limitations the highest possible efficiency must be obtained from the crystal transducer. This implies that the mounting of the crystal must secure the min-:imum damping of the crystal at its support. Furthermore, the acousting loading on the radiator should be concentrated on one face only. In other words, the other face of the crystal has to be coupled to a medium of very high or very low acoustic impedance. This was accomplished by immersing the crystal so that its upper surface is in direct contact with the liquid medium while the bottom surface is backed with air.

B. Matching of Transducer.

In order to ultimately obtain large intensities such as required for the process of degradation of high polymer solutions, the matching of acoustic impedances is a necessity. The specific acoustical resistance 'ρc' for quartz is 146×10^4 while that for a polymer solution in benzene is about 11.6×10^4 giving an acoustical resistance ratio of 12.5. For such a ratio only 29% of the mechanical acoustical energy will be

POLYMER SOLUTION

EARTH
ELECTRODE

MAGNESIUM WAVE PLATE

CRYSTAL

H.T. ELECTRODE

AIR SPACE
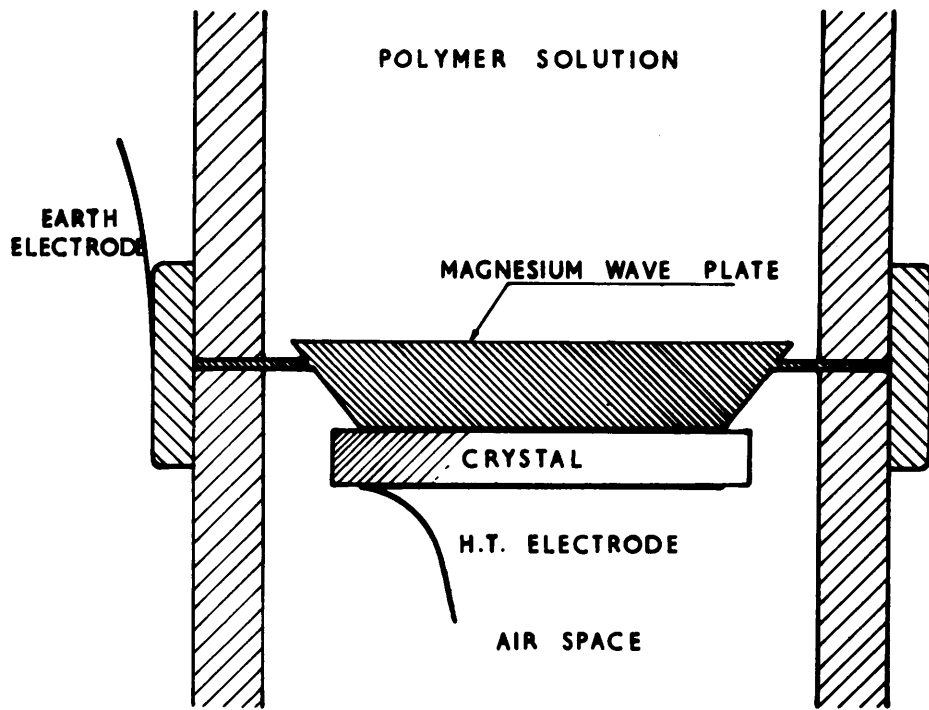
FIG. 15.   QUARTZ_MAGNESIUM WAVE_PLATE
TRANSDUCER.

transmitted through the polymer solution if it is directly irradiated by the quartz transducer.

A medium having a specific acoustical resistance equal to the geometric mean of the above mentioned specific acoust= :ical resistances is ideal as a matching medium. Magnesium is the nearest substance to suit this requirement. Using magnesium as an intermediate medium between quartz and polymer solution in benzene, 40% of acoustical energy will be trans= :mitted through the polymer solution provided that the thick= :ness of the magnesium plate is a multiple of a halfwave length.

An arrangement using magnesium as an intermediate medium is shown in Fig.15. Since magnesium cannot be soldered, it was first fixed to the quartz using silver cement LGR.72. This method resulted in a discontinuous monomolecular layer of air at the magnesium-quartz interface which expanded by the heat developed during irradiation, and caused a marked reduct= :ion in the acoustical output on increasing the applied voltage. Magnesium was then fixed to quartz using cold setting Araldite type 101. No diminution in acoustical output occurred but arcing across the quartz crystal took place when high voltage was applied to the crystal. Furthermore, when the transducer flange was clamped in position so as to enable its use under applied hydrostatic pressure the acoustical output from the
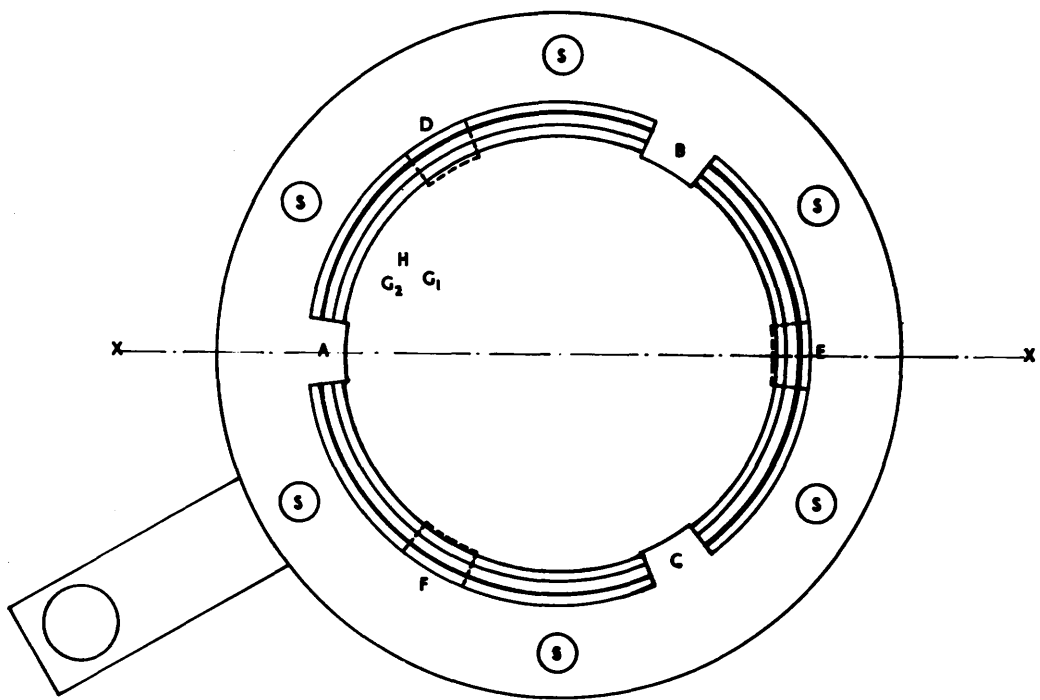
PLAN VIEW OF THE CRYSTAL HOLDER.
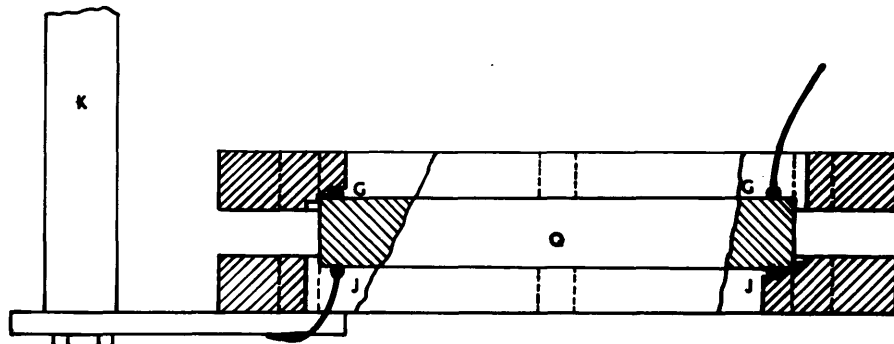
PARTIAL SECTION THROUGH XX.

FIG.16.   CRYSTAL HOLDER AFTER MELVILLE & MURRAY.

transducer decreased markedly. After many trials it proved exceedingly difficult to locate the nodal plane in the magnes- :ium wave plate. It was also found difficult to machine the nodal flange thin enough in order not to affect output when it is clamped. However, it appeared from many trials with different kinds of mounting that the main difficulty would be th~ suppression of arcing across the crystal on applying the high frequency A.C. voltage to its faces. Methods suggested by Noltingk[4], Gutmann[5] and Crawford[6] were tried, but these all failed to give satisfactory results. These results left no option but to use transformer oil as a matching medium, and to serve as an insulator for the crystal due to its good dielectric properties.

C. Crystal Holders.

A holder recommended by Melville and Murray to provide the maximum circulation of oil at the edges of the crystal was tried out. The crystal, as shown in Fig.16, is held by lugs projecting from the main holder. The lugs, A, B, and C, are those on the upper half of the perspex holder, the lugs D, E, and F, shown by dotted lines are those protruding from the lower half of the holder. The lugs in each half of the holder are placed 120° to each other, and the two halves are assembled to give a 60° spacing between any two lugs. This

arrangement provides a secure support to the crystal and at no point are both faces of the crystal in contact with the holder. Two grooves are cut, the first to locate the electrode and the second to locate the crystal. The depth of the electrode groove is arranged to ensure that the crystal would rest on the ring electrode and not on the base of the crystal groove.

In use the crystal holder was supported by a bakelite rod. The holder was immersed to a depth of a few inches in a bath of transformer oil. When the crystal was oscillating cavitation took place at both faces of the crystal. Only those bubbles liberated at the lower face were trapped below it, within the lower ring. This is due to the fact that the lower ring electrode fits tightly against the crystal face and prevents the bubbles formed from escaping. The output from the crystal was noticed to increase continuously as a conse-:quence of the accumulation of air under the crystal. The continuous increase in output reaches a steady maximum as the air layer covers the whole effective area of the bottom face of the crystal. The air layer would be reflecting the down-:ward radiation and almost doubling the intensity in the upward direction.

This holder proved quite satisfactory at lower applied voltages but it failed at higher voltages. Arcing started

Q   QUARTZ CRYSTAL
H   HOLDER
L   LEADS
B   BREATHING TUBE
W   WOODS METAL SEAL.
A   ARALDITE 101 SEAL
S   SILVER PLATED
    SURFACES.
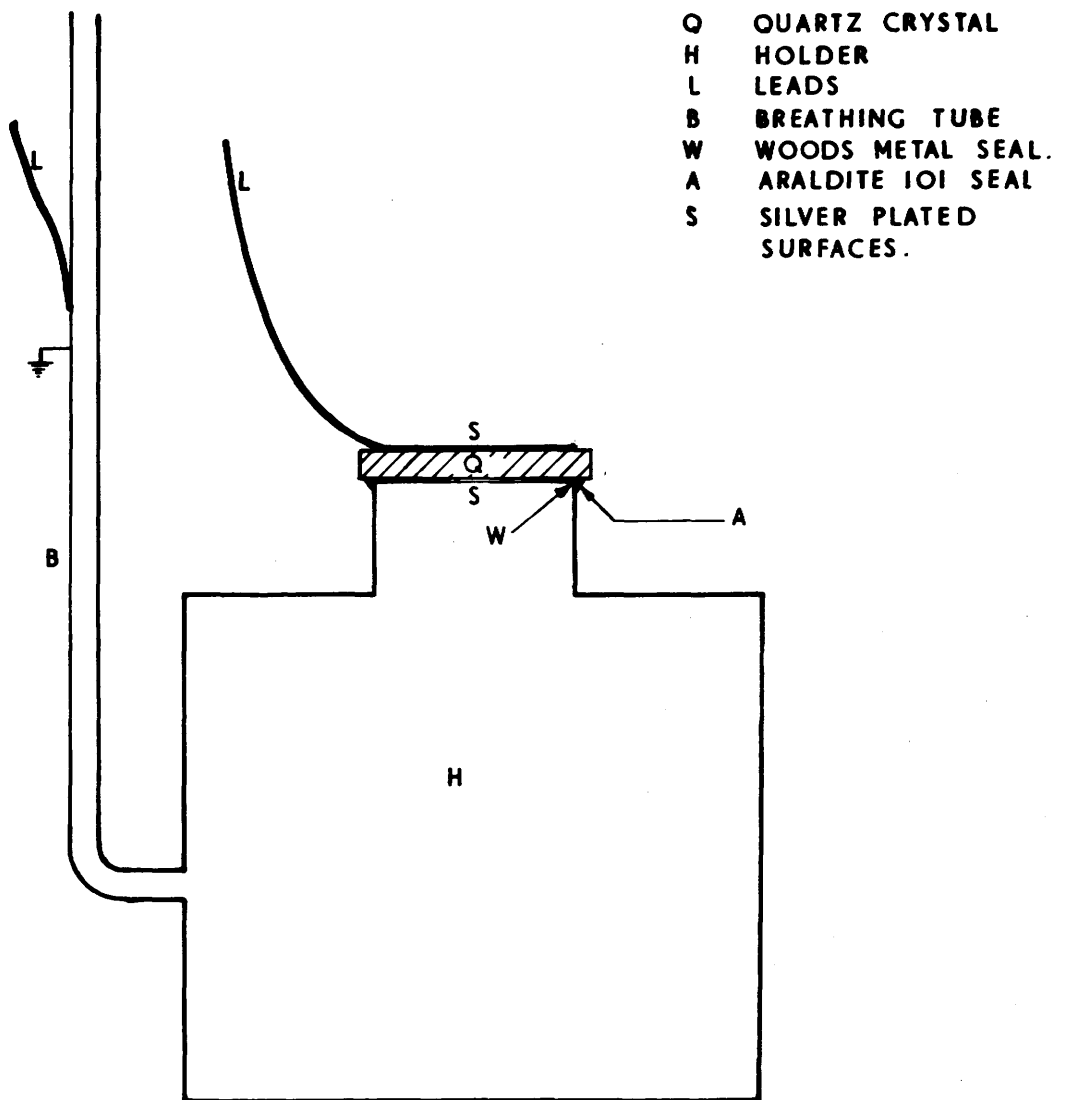
FIG. 17.   SIMPLIFIED CRYSTAL
            HOLDER.

between the brass ring (upper electrode) and the silvered face
of the crystal in contact.   Once the arcing started at any
point it spread all round the annular area of contact, thus
stripping and destroying the silver coating on the face of
the crystal, if not chipping or damaging the crystal.
Obviously this holder had the inherent disadvantage that the
maximum acoustic output cannot be immediately obtained on
applying the voltage to the crystal.

Finally a simple crystal mounting was used.   This type
of crystal holder is a simplified version of the holder devel-
:oped by Stumf[8].   Its simple design made it possible to
use the crystal under different experimental conditions.   The
holder in its simplest form is illustrated in Fig.17.   The
circumference of the silvered bottom face of the crystal was
soldered to an air compartment with wood's metal and then
covered by a layer of araldite type 101 to improve the
strength of the joint and to avoid air leakage.   For experi-
:ments conducted under atmospheric conditions, the air com-
:partment is simply connected to a breathing tube open to the
atmosphere.   The purpose of this breathing tube is to provide
direct communication with the atmosphere, thus avoiding any
pressure rise in the air compartment which may cause a break
in the seal at the crystal-compartment interface.   Such a

break will allow hot air to leak outside the compartment when the crystal is vibrating. When the crystal is switched off air in the compartment will create partial vacuum as it cools down and thus forces the transformer oil to leak inside the compartment. This leakage, after a few runs, will affect the acoustical output of the crystal due to incomplete reflect-:ion from its bottom surface. A thin copper wire is soldered on the upper face of the crystal near the periphery, using low melting point solder, provides the H.T. lead while the earth lead is connected to the breathing tube.

During the experiments the holder was fixed to the base of a travelling microscope while the reaction vessel was mounted on a platform fitted to its moving arm. This arrangement proved very satisfactory in repeating tests whenever required, since the relative positions of crystal and reaction vessel were completely under control. Furthermore, with such an arrangement there was no need to worry about the position of the reaction vessel with respect to the surface of the trans-:former oil in which the crystal holder and base were immersed.

This simple type of crystal holder with the above men-:tioned arrangement was used in all the experiments which were carried out either at atmospheric pressure or under vacuum.

It should be pointed out at this stage that the pro-:gramme originally set for this work included some degradation

experiments under applied external pressure. The main purpose of these experiments was to determine whether ultrasonic waves are by themselves sufficient to cause degradation of long chain molecules or that cavitation is essential in order to effect any degradation. As mentioned in Chapter I, such experiments were carried out by previous workers, each conduct-:ing his experiments with a different type of apparatus.

The apparatus built up for conducting the experiments contemplated in the course of this work was designed to secure flexibility of operation under conditions which would not raise any doubt about the significance of the results obtained, as was the case with previous investigations. After completing the apparatus preliminary experiments were condcuted to ensure that each part was functioning properly. The incorporated rolling sphere viscometer was calibrated as reported in Chapter III. By that time the experiments on the verification of the theory reported in Chapter IV had reached a stage where it was decided, for the time being, to dispense with these experiments contemplated to investigate the role of cavitation in the degradation of long chain polymers, as mentioned above.

The new approach to the problem was to investigate the frequency dependance of the degradation of addition polymers. It was thought that this approach would ultimately lead to the estimation of the role of cavitation in the process of degra=

:dation of long chain molecules by ultrasonic waves, and that the results obtained from these experiments would be more significant since they were not dependent on the effectiveness of suppressing cavitation; a condition which cannot be fully guaranteed due to the incomplete theoretical treatment of cavitation. Furthermore, it was hoped that this approach would throw more light on all aspects of ultrasonic degrada-:tion of long chain molecules, including the mechanism of degradation. However, since much time was devoted to the building and testing of the apparatus a brief description (see Appendix V), of it does not seem to be irrelevant, if only because it includes some features which may be of general interest to any person working along similar lines.

BIBLIOGRAPHY.

1. Langton, L.L. 'Radio-Frequency Heating Equipment'
Pitman and Sons Ltd., London 1948.

2. May, E. 'Industrial High Frequency Electric Power'
Chapman and Hall Ltd., London 1949.

3. Mason, P. 'Electromechanical Transducers and Wave Filters'
p.235. D. Van Nostrand, New York, 1942.

4. Noltingk, B.E. J. Brit. Inst.Radio Engrs. 11, 1 (1951).

5. Gutmann, F. J. Sci. Instrum. 24, 276 (1947).

6. Crawford, A.E. 'Ultrasonic Engineering' Chapter 3.
Butterworths Scientific Publications, London 1955.

7. Melville, H.W. and Murray, A.J.R.
Trans.Farad.Soc. 46, 996 (1950).

8. Smith, F.W. and Stumpf, P.K.
Electronics, 19, 116 (1946).

CHAPTER III.

MEASUREMENTS TECHNIQUES AND APPARATUS.

1. INTENSITY MEASUREMENT.

A. Energy Measurement.

The measurement of ultrasonic energy is an essential factor in assessing quantitatively the results obtained when applying ultrasonics to a specific process. Fundamentally it is possible to estimate the power output of a crystal transducer from the electrical energy input and the electro-:mechanical conversion factor. With a known conversion efficiency the intensity of ultrasonic radiation at the rad-:iating face of the transducer can be calculated. This value, however, is of little significance since attenuation and beam divergence can appreciably decrease the power intensity at the point of application of the wave energy. In most of the previous work done on the degradation of high polymers by ultrasonic waves, a calorimetric method was usually applied. The method measures the overall power dissipated, since theo-:retically all sonic energy propagated into a liquid system must be converted into heat as a result of the total reflect-:ion occurring at the liquid/air interface. This method, frequently used in previous works was, therefore, employed for absolute measurements, and was accepted by most investi-:gators as a rough estimation of the radiated power.

The sound intensity I (either in $ergs/cm^2$ or in mW/cm^2) for progressive plane sound waves can be represented

by either of the following relations:-

$$I = \frac{\rho C}{2}(\omega A)^2 = \frac{\rho C}{2} u^2 = \frac{p^2}{2\rho C} = \frac{pu}{2} \quad \ldots\ldots\ldots\ldots (1)$$

where A is the amplitude of particle vibration in cms.

ρ is the density of medium in gm. per cm^3.

ω is the angular velocity of the particle and $= 2\pi f$.

C is the velocity of sound waves in the medium in cm. per sec.

p is the pressure amplitude of the sound waves in dynes/cm^2.

u is the particle velocity in cm. per sec.

Obviously sound intensities can be measured by measur= :ing any of the involved quantities, A, u, or p.

The mechanical elongation produced in thickness vibra= :tion when a potential difference V e.s.u. is applied to an X-cut quartz plate having a thickness t cms. parallel to the X axis is given by Voigt[1] to be:

$$e = d_{11} V \quad \text{for the longitudinal effect.}$$

where e is the elongation produced,

V is the applied potential across the faces of the crystal in e.s.u.

and d_{11} is the piezoelectric modulus for this mode of vibration.

For an X-cut, thickness vibration, crystal

$$d_{11} = +6.9 \times 10^{-8} \text{ e.s.u.} = \frac{6.9 \times 10^{-8}}{300} \text{ cm/volt.}$$

as recommended by Cady[2]. For a quartz crystal vibrating in a liquid medium the particles of the medium at the liquid quartz interface have the same amplitude as that of quartz, i.e., A = e. Thus the equation for intensity can be rewritten as:

$$I \;=\; \frac{\rho C}{2} \, \omega^2 \, d_{11}^2 \; V^2/9x10^4 \text{ ergs./cm}^2.$$

The density of transformer oil used is ρ_{20} = 0.85
Velocity of sound in transformer oil is C = 1420 metres/sec.
Substituting in the above equation for intensity we get the relation:

$$I \;=\; 126 \times f^2 E^2. \times 10^{-15} \text{ ergs./sec/cm}^2. \quad \ldots\ldots\ldots(2)$$

which gives the acoustic intensity as a function of the applied voltage and frequency.

An approximate value of the maximum output voltage of the oscillator can be obtained using a valve-voltmeter con-:nected to a known non-inductive resistance which is connected in series with a known high-non-inductive resistance across the terminals of the oscillator. The maximum output voltage measured by this method was found to be 30 KV across the crystal at a frequency of 1 Mc/sec.

Substituting the appropriate values in equation (2), the sound output was found to be:

$$I = 11.34 \text{ watts/cm}^2. \text{ at a frequency of 1.0 Mc/sec.}$$

Since the crystal is mounted with one face coupled to air,

GLYCERINE

TRANSFORMER
OIL

TERYLENE MEMBRANE

CRYSTAL HOLDER.
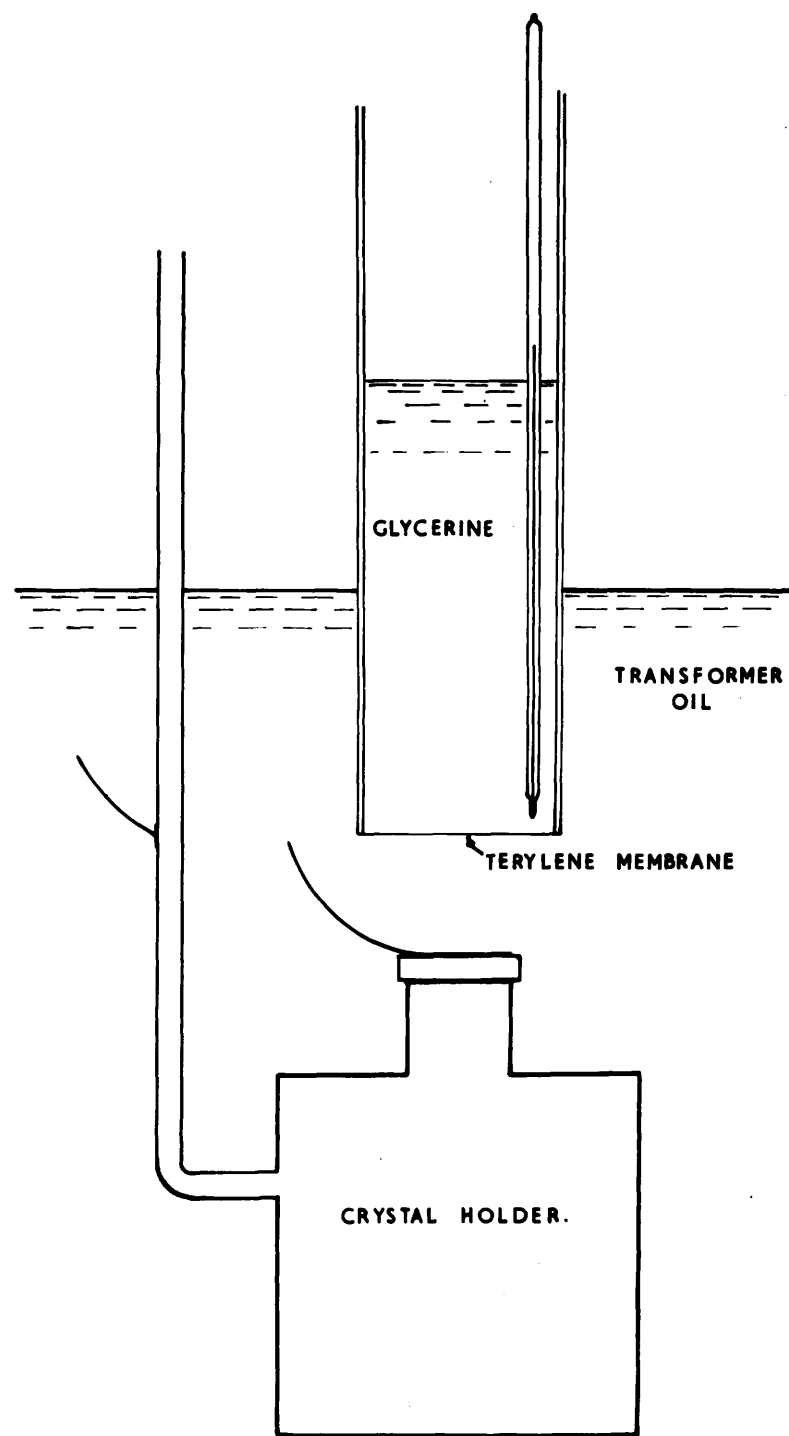
FIG.18.   CALORIMETRIC METHOD OF
FOR MEASURING SONIC INTENSITY.

all the energy from this face will be reflected and the total intensity from the radiating face will be doubled, i.e.,

acoustic intensity in transformer oil = 2 x 11.34 = 22.68 watts/cm^2.

The effective area of the crystal (i.e., the area of the silvered faces) is 3.88 cm^2. per face, so that the maximum acoustic power radiated from the crystal into the liquid should be about 88.3 watts.

This calculation is based on the assumption that the amplitude of the liquid particles is the same as that of the quartz at the liquid-quartz interface. In addition, it is assumed that Voigt's formula $e = d_{11}.V$ can be applied to a vibrating quartz. This assumption, however, is justified in the case of a piezo-electric crystal vibrating at its resonant frequency. At resonant frequency the mechanical strain is in phase with the applied electric stress.

However, this method provides only an approximate esti=:mate of the acoustic energy output from the crystal. A calorimetric method was used to measure the output acoustic intensity from the crystal as a guiding estimate. The arrange=:ment used is shown schematically in Fig.18. The glass tube is filled with glycerine which practically absorbs all the ultrasonic energy radiated. The output power from the crystal, as a function of the heat developed due to absorption, was

measured calorimetrically from the equation:

$$P = \rho V s J \left(\frac{dT}{dt}\right)_{t=o} \text{ watts.} \qquad (3)$$

where ρ = density of the glycerine;

V = volume of the glycerine;

s = specific heat of glycerine;

J = Joule's equivalent;

$\left(\frac{dT}{dt}\right)_{t=o}$ = Temperature time gradient at time t=o.

B. Radiation Pressure.

It is known that the propagation of plane sound waves is always accompanied by a direct, unidirectional pressure component due to radiation. This sound radiation pressure is, theoretically, a consequence of the quadratic terms in the wave equation. There is also a hydrodynamic streaming, associated with the propagation of sound waves in liquids, which causes a movement of the liquid away from the transducer.

The radiation pressure, therefore, provides a steady force against a body immersed in the liquid and is given by the relation:

$$S = \frac{1}{2}(\gamma + 1)\frac{I}{C} = \frac{1}{2}(\gamma + 1)E = KE \qquad (4)$$

where γ is the ratio of specific heats;

E is the sound energy density;

K is a constant.

From equation (4) the radiation pressure 's' is proportional to the sound energy density E. The value of the constant

'K' is equal to 1 for liquids under normal operating con-
:ditions.

However, in the course of this work five methods for
the direct measurement of intensities were tried.   The dev-
:ices used in these attempts which will be discussed in
detail below are:

(i)   A 'point source' probe.

(ii)   A radiation balance.

(iii) An inverted funnel.

(iv)   A condenser microphone (capacity gauge).

(v)   A thermo-element.

(i) The 'point source' probe.

The probe built was almost similar to the 'point source'
probe devised by Fein[3].   In agreement with Fein the perfor-
:mance of the probe proved that:

a. It offered minimum distortion of the acoustic field.

b. It has good non-directional characteristics accompan-
    :ied by a minimum integrating effect of the acoustical
    signal intercepted by the probe.

c. It has a low electrical impedance, which was a desir-
    :able characteristic when the probe was connected
    to the measuring electrical circuit.

d. The ammonium dihydrogen phosphate (ADP) temperature
    :characteristics in the temperature range of the exper-
    :iments was less erratic than other types of sensitive
    piezoelectric materials, namely barium titanate.

A. ARALDITE 101 COATING.
A.D.P. AMMONIUM DIHYDROGEN PHOSPHATE CRYSTAL.
B.P. BRASS PIN.
B.PL. BRASS PLATE.
C. CONNECTOR.
P.D. POLYTHENE DISC.
P.T. POLYTHENE TUBE
M.H. METAL HOUSING.
S.P. SILVER PASTE
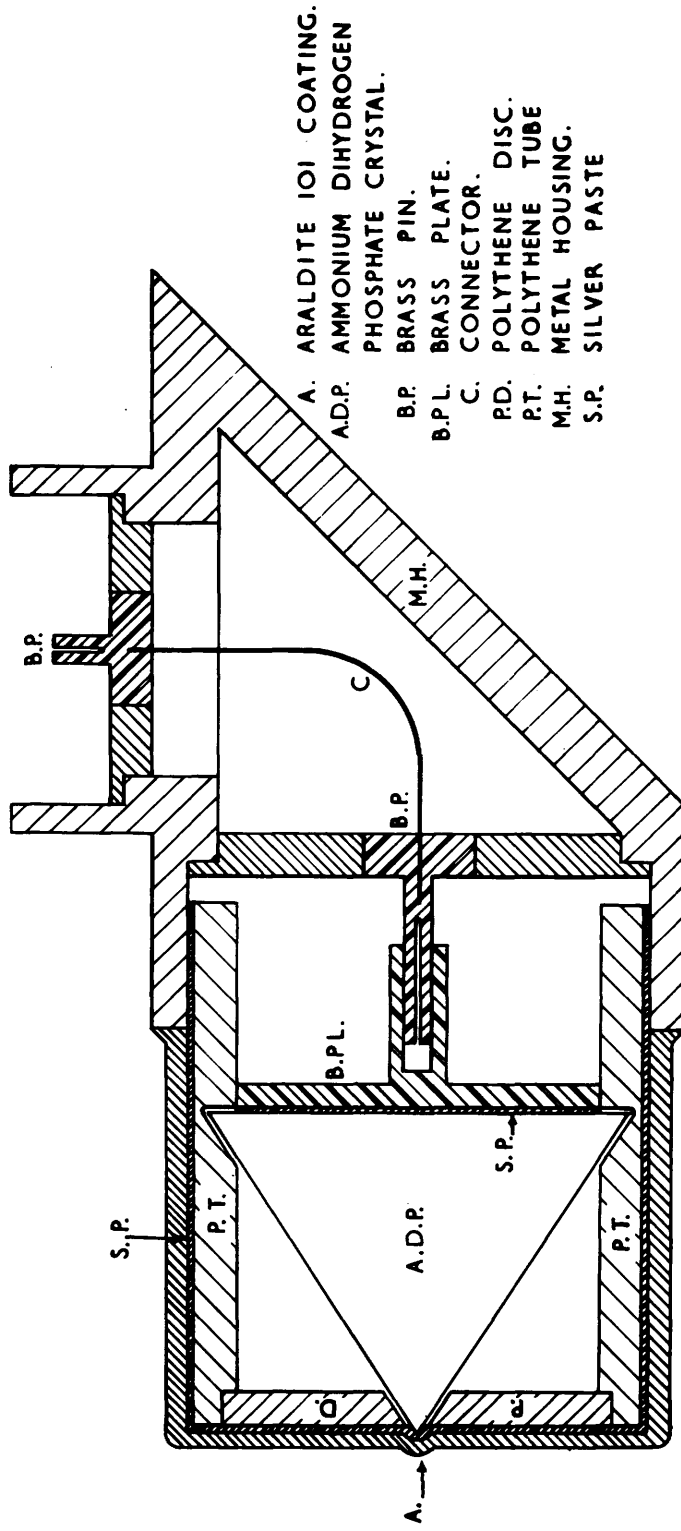
FIG.19.   SECTION OF CRYSTAL ASSEMBLY & LIQUID–TIGHT HOUSING.

This probe was built from a piece of ADP crystal. As shown in Fig.19 it is in the form of a truncated right cir- :cular cone with its apex intercepting the sound field. The axis of the cone is parallel to the 45° line between the X and Y axes of the crystal.

The probe was calibrated by the reciprocity method. The calibration was carried out in transformer oil at one frequency only. The length of the axis of the cone was such that the resonant frequency of the probe was about 1 Mc. The speaker and transducer were two 1 Mc/sec. X-cut quartz crystals suitably mounted to suit the specific purpose of calibrating the probe. A sensitive valve voltmeter was used to measure the microphone output voltage and a thermojunction R.F. ammeter was used to measure the input current to the transducer when used as a speaker.

Great troubles were encountered in screening the elect- :rical components of the receiver circuit to eliminate the electromagnetic pick-up from the oscillator and the high tension lead to the speaker. Every instrument and every component was externally earthed. Earthed brass gauge screen, with a hole in it to permit a free undiffracted passage of the acoustic beam, served as an efficient under-liquid screen. An earthed aluminium sheet across the top of the tank produced effective screening of the receiver's side from the H.T. lead to the

QUARTZ CRYSTAL.

REFLECTOR
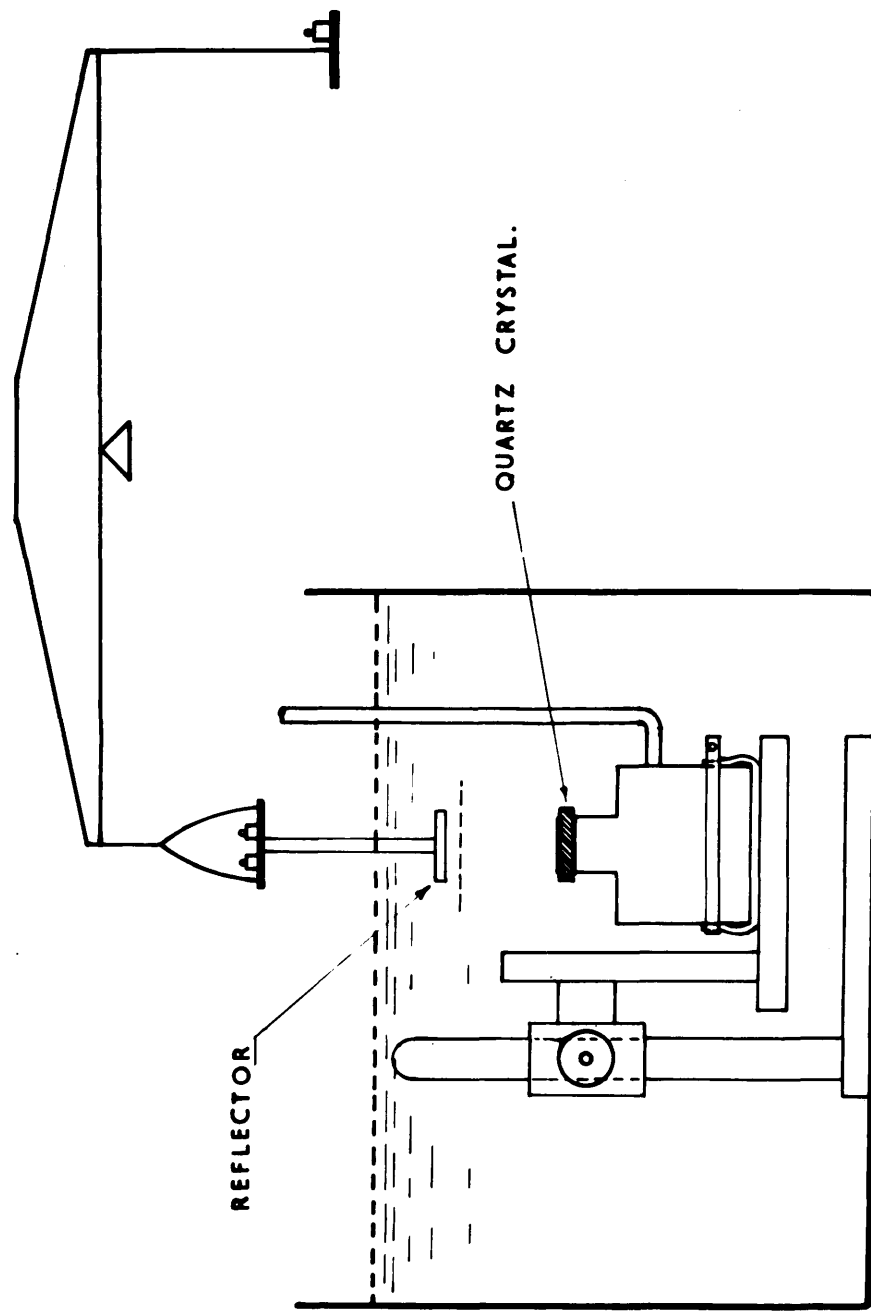
FIG.20. BALANCE METHOD FOR MEASURING THE RADIATION PRESSURE IN OIL.

crystal. This screening when carried out was found to cut almost 90% of the signal originally received by the probe before the screening was undertaken.

Results of the calibration of the probe gave a value of the sensitivity of 4.19×10^{-8} volts/dyne/cm^2, at a fre= :quency of 1 Mc/sec. This probe was used in some experiments on cavitation nuclei which are not included in this work.

(ii) The radiation balance.

Owing to the great difficulties in screening the piezo= :electric probe and the receiver circuit it was thought advisable to try some other device which provides less complications and enables direct measurement of the intensity, independent of the frequency of the ultrasonic waves. By this method screening troubles would be avoided.

The radiation balance method was employed for the measurement of energy at any given area within the beam. The radiation pressure provides a steady force against a body immersed in the liquid and its value is a measure of the intensity as mentioned before.

Fig.20 shows the general arrangement of the system. The intercepting body acts as a perfect reflector for the ultrasonic waves. One factor must not be overlooked; the intercepting body must be completely immersed in the liquid,
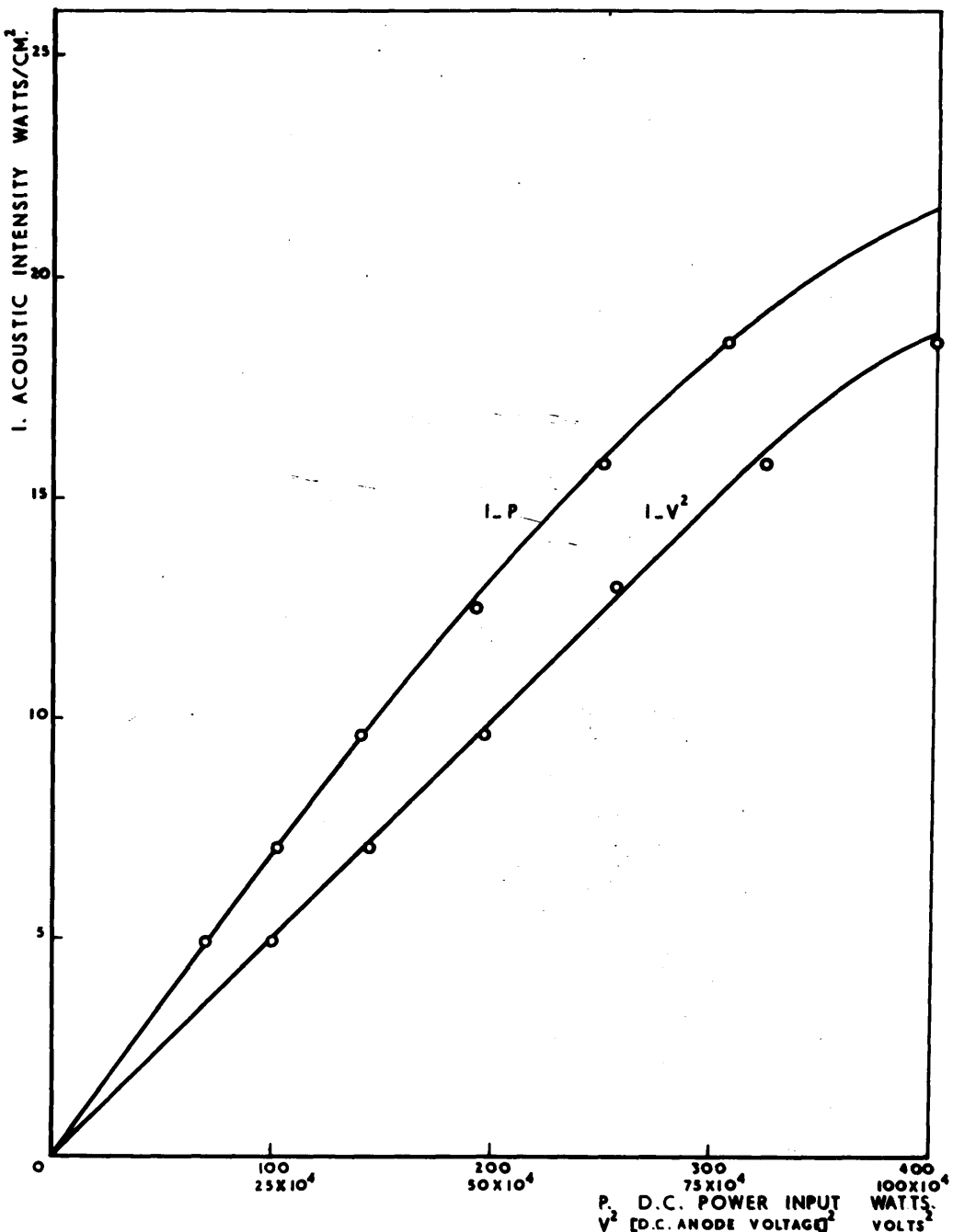
FIG. 21. INTENSITY MEASUREMENT BY RADIATION
BALANCE METHOD.

otherwise the surface tension forces round its cylindrical surface - which are comparable in magnitude with the radiation pressure - may render any results obtained highly erratic. The terylene membrane just below the reflector acts as a shield preventing the hydrodynamic forces, set up by the stream=:ing of the liquid, from affecting the deflection of the rad=:iation balance [Cady and Gittings[4]].

A typical sample of the values of ultrasonic intensities as obtained by the radiation balance method are shown in Fig.21 as a function of the D.C. power input to the push-pull oscill=:ator and also as a function of the square of the D.C. anode voltage.

Theoretically, the radiation pressure is proportional to the intensity of ultrasonic waves, i.e., proportional to the square of the D.C. anode voltage. This seems to be rea=:sonably the case, up to the highest values of intensities needed for this work. For higher intensities, however, the linear relation between radiation pressure and the square of anode voltage will not be maintained due to the occurrence of cavi=:tation.

(iii) <u>The inverted funnel.</u>

This method wasoriginally suggested by Richards(5). Its operation depends on the ear trumpet principle, i.e.,

concentrated sound energy provides a more sensitive means of estimating the radiation pressure measured as hydrostatic pre-:ssure. The possibility of using this method as a means of measuring intensities was investigated by Murray[6]. A small funnel was blown on the end of a fine capillary tube and immer-:sed in the liquid irradiated. Murray encountered some troubles due to cavitation taking place in the liquid column in the capillary. As indicated by Richards, enormous differences in the height of the liquid column in the capillary tube were due to small changes in the position of the funnel in the sound field. The mouth of the funnel should always be placed in the standing wave field in a position which would produce maximum height of the liquid column, in order to secure comparable results for different intensities.

Richards pointed out that with fine capillaries used, the liquid should be wholly air free. In general the capill-:aries should be perfectly clean and completely free from grease. Capillaries used must have a bore not less than $0.5 \, ^m/_m$. to avoid increasing the resistance to the flow of liquid, thus decreasing the sensitivity of the instrument.

This device, as it stands, however, can give only a relative and not an absolute measure of sound intensity unless reflections from funnel walls are perfect, and no interference takes place during the concentration of sonic waves.
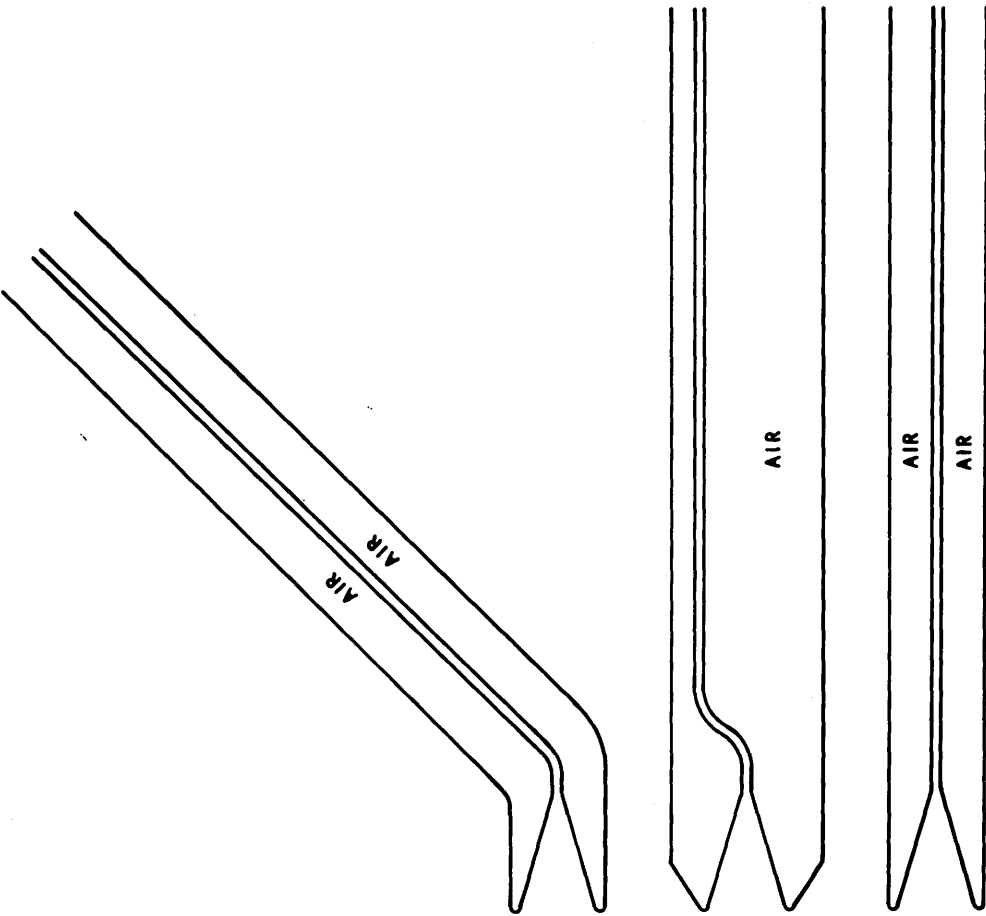
FIG. 22. INVERTED FUNNEL CONFIGURATIONS FOR ACOUSTIC INTENSITY MEASUREMENTS.

In the course of this work the design of the funnel was modified, to secure (1) no loss of acoustic energy from the walls of the funnel; (2) minimum interference during the propagation of sound waves in the funnel. The different configurations shown in Fig. 22 were tried, which gave incon-:sistent results. The results obtained were not reproducible. It is worth mentioning in this respect that there is an inher=:ent defect in this method. Awareness of this defect from the beginning urged the configurations in the shape of the funnel to be considered. Since the amount of upward displace=:ment for a given intensity is roughly in inverse proportion to the square of the radius of the capillary tube it became apparent that there is an upper limit of the intensities which could be reliably measured. This limit is controlled by two factors:- (1) the ratio between the area of the mouth to that of the throat of the funnel; (2) the threshold of cavitation inception in the irradiated liquid.

However, high intensities of ultrasonic waves, of the order of magnitude usually used in degradation processes, are very difficult to measure due to the occurrence of cavitation, and this method was tried with the hope that it would prove amenable to absolute calibration. Due to unreliable perfor=:mance it was rejected as a method for measuring the intensity in the course of this work.

(iv) The condenser microphone.

Since degradation experiments can be carried out under different operational conditions, a type of condenser micro-:phone was developed which is suitable for operation under varied conditions. Although, fundamentally its calibration is straightforward, yet due to the implications of the very high sensitivity required for the successful operation of such a microphone it involved many unforseen difficulties.

Many types of microphones, serving different purposes, have been described in literature[7]. At the time when this condenser microphone was designed in 1953 none of these micro-:phones was operated to measure the radiation pressure assoc-:iated with propagated sound waves. Nevertheless in 1953, a condenser microphone was developed by McNamara and Beyer[8], to measure the modulated pressure amplitude in liquids, which was produced by a modulated input voltage applied to the crystal. The condenser microphone, described below, operates in a slightly different way. The radiation pressure itself intercepted by the microphone causes a change in its capacitance. This change in capacity offsets the balance of a very sensitive capacity bridge. The out-of-balance signal having a frequency of 3000 cycles per second is then modulated by a carrier wave of ~500 KC/sec. The resultant modulated signal is there-

A   NILO 36 MEMBRANE   EARTHED
B   ADJUSTABLE ELECTRODE   LIVE
C   SPARKING PLUG TERMINAL   LIVE
D   CYLINDERICAL BRASS CASING   EARTHED
E   BRASS TUBE FOR NEUTRALISING HYDROSTATIC PRESSURE
F   EARTHED BRASS SHIELD
G   PERSPEX TUBE
H   SLIDING CONTACT
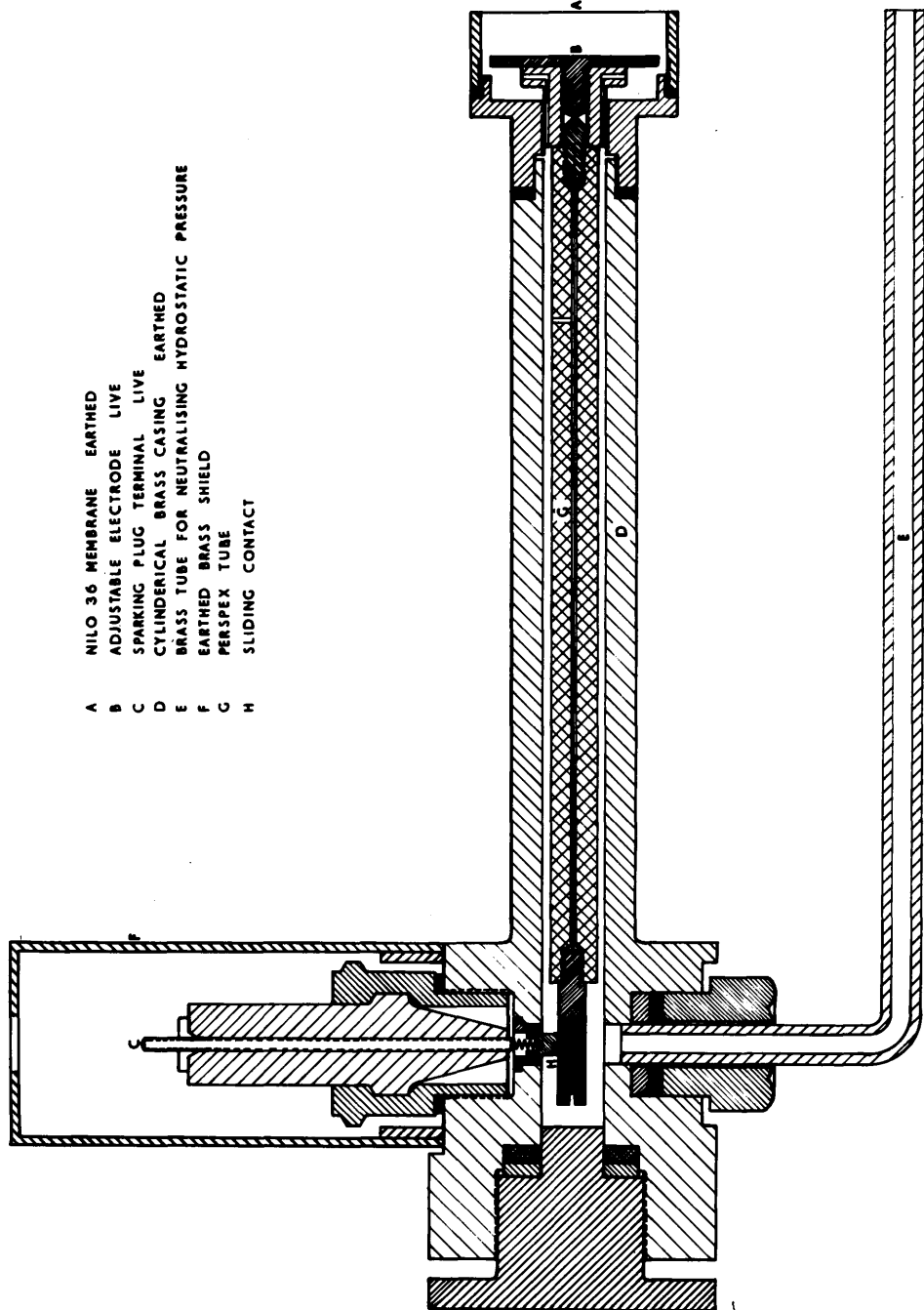
FIG.23.   CAPACITY GAUGE FOR ULTRASONIC INTENSITY MEASUREMENT

:after amplified, then demodulated and then fed to a sensitive galvanometer, the reading of which is directly proportional to the change in capacity.

The gauge, by its design, can be used to measure the radiation pressure and consequently the intensity of ultra-:sonic waves in a liquid. The liquid may be under normal atmospheric pressure, any applied pressure, or any maintained negative pressure (vacuum).

Fig.23 shows the details of construction of the gauge. Its dimensions are governed by the small size of the crystal transducer and the large size of the gauge required for a high degree of sensitivity.

The capacity bridge of the proximity metre used in con-:junction with the gauge is extremely sensitive. In that respect the gauge, by its design, provides an earthed 'shell' which shields the live electrode of the gauge effectively from any external interference. The adjustable live (inner) elect-:rode provides one way of controlling the sensitivity of the measuring circuit by adjusting the initial capacity of the gauge head. The sensitivity is further controlled by ccarse and fine sensitivity controls of the proximity metre.

Air is allowed to reach the interior of the gauge head at the back of the diaphragm. As this air is automatically

kept at the same pressure applied to the liquid, it follows
that the net differential static pressure acting on the dia-
:phragm is very nearly equal to zero.   Consequently, the gauge
can be rendered sensitive only to the radiation pressure, irr-
:espective of whether the applied external pressure is positive
or negative.

At maximum sensitivity the measuring circuit gives a
full scale deflection of the meter for a pressure of less than
1 cm. of water.   Many difficulties arose due to such high
sensitivity.   It was found for instance that the successful
performance of the gauge depends upon the dielectric properties
of the material used to insulate the live (inner) electrode
from the outer earthed casing.   Poor insulators caused a creep
in the meter to take place which was interpreted as a polar-
:ization effect in the dielectric.   The continuously increasing
deflection of the meter due to this creep can reach values far
in excess to those produced by the radiation pressure.

However, it is surprising to notice that McNamara and
Beyer in describing their capacity gauge forgot to mention any
of the limitations of its use in measuring large acoustic in-
:tensities.

In developing this gauge, diaphragms made of different
materials were tried.   These diaphragms could be classified
in two groups.

(a) Non-metallic diaphragms.

(b) Metallic diaphragms.

(a) Non-metallic diaphragms.

Mica diaphragms 0.0015" thick.

Terylene " 0.0005" thick.

In both cases a thin film of chromium (50 A.U.) was evaporated on the diaphragm as a first coating. This coating served as a backing for a thin film of silver (～100 A.U.) evaporated on top of the chromium. Furthermore, this pro-:cedure is known to improve the adhesion of the metallic film to the non-metallic diaphragm.

This arrangement gave satisfactory results at acoustic intensities less than 1 watt/cm^2. However, at higher inten-:sities the pointer of the meter started creeping. This was found to be due to the destructive effect of cavitation. Cavitation occurred in the vicinity of the diaphragm. Either the bubbles collapsing directly on the membrane or the shock waves associated with cavitation caused a continuous disinte-:gration of the evaporated film. This effect caused a contin-:uous decrease in capacity which was noticed as a creep on the metre.

Another possible reason for this creep is the acoustic energy absorbed by the membrane. This absorbed energy will effect a continuous increase in the temperature of the conduct-

:ing membrane. This rise in temperature will cause a contin-
:uous expansion of the membrane which results in a continuously
changing capacity indicated by the creep observed.

Under these conditions it was difficult to say if the
creep was a result of one factor or the other, or both.

(b) Metallic diaphragms.

0.0015" Brass diaphragms.

0.002" Berillium Copper diaphragms

Since evaporated films on non-metallic diaphragms showed
signs of disintegration with the inception of cavitation,
metallic diaphragms were tried since any erosion resulting
from cavitation will not affect the capacity of the gauge.

Although calibration of the gauge with a static pressure
proved to be successful, yet when the gauge was used to measure
the acoustic intensity an anomalous behaviour of the metre was
observed. These metal diaphragms showed to be temperature
dependent and deflections several times that corresponding to
the true intensity were produced. This fact was further
confirmed by the gauge showing similar behaviour when exposed
to a slow stream of hot air in a closed compartment. Temper-
:ature compensation devices including a water jacket were tried
without any positive result. It was concluded that capacity
gauges could not be used to measure high ultrasonic intensities
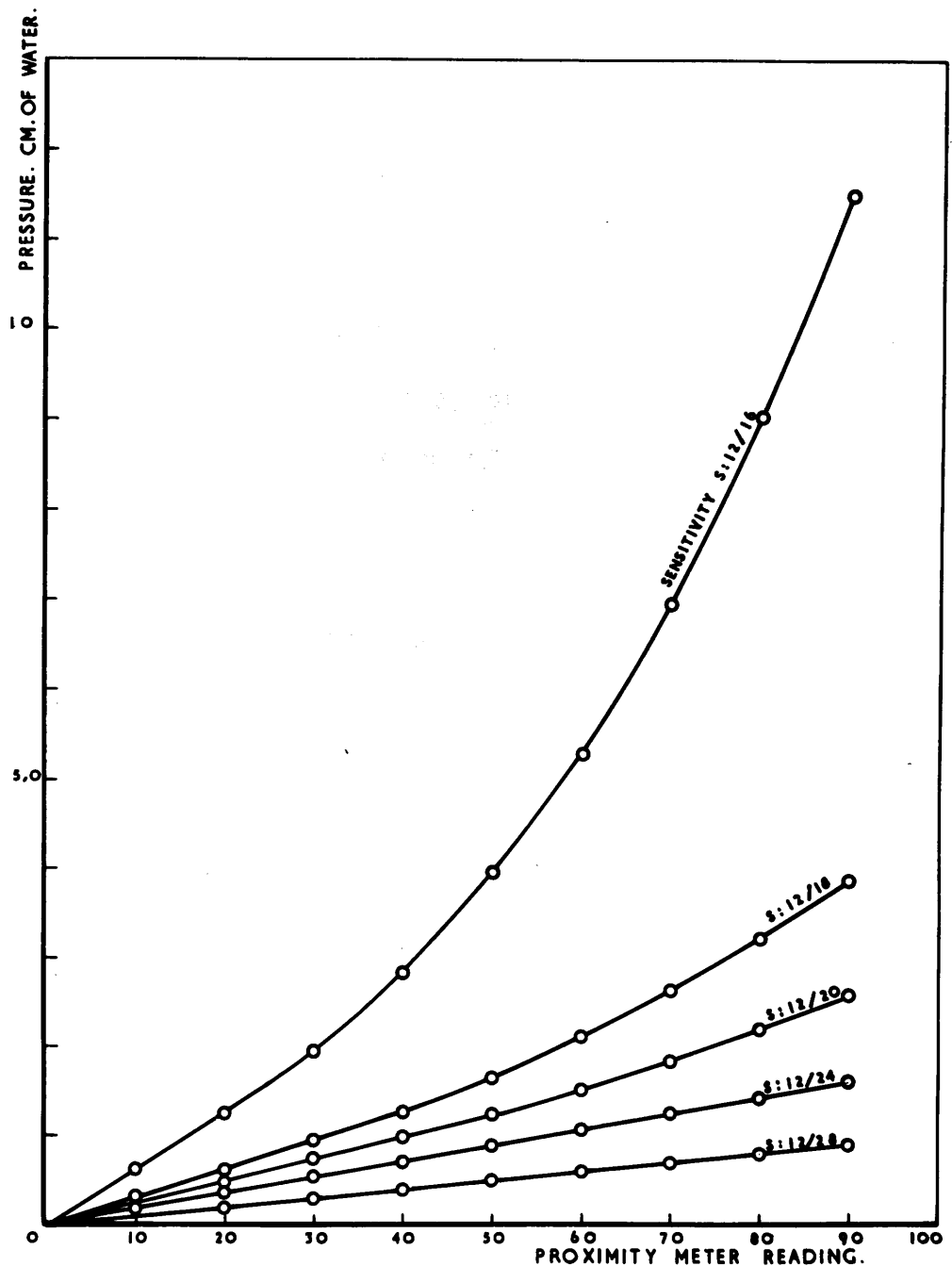
FIG.24. CALIBRATION OF CAPACITY GAUGE FOR
INTENSITY MEASUREMENTS.

unless the diaphragm is made of a metal which has almost zero coefficient of expansion. It was, therefore, decided to use a diaphragm made of a nickel alloy known commercially as 'Nilo 36' which has a coefficient of expansion 1.8×10^{-6} per $^{\circ}C$. The diaphragm used was $0.003"$ thick.

Using the $0.003"$ Nilo 36 diaphragm, the capacity pressure gauge did not show any creep provided that the temperature of the surrounding medium (transformer oil or polymer solution) was thermostatically controlled and kept constant within $\pm 0.2^{\circ}C$.

A typical set of calibration curves of the gauge is shown in Fig. 24 in which the sensitivity is given by the setting of the sensitivity coarse control followed by the setting of the fine control. It can be noticed from the curves that the metre reading of the P.M.4 is directly proportional to the applied pressure below 2 cms. of water. For pressure exceed-:ing this limit the linear relation is no longer maintained. This is attributed to the non-linear change in capacity due to the curvature of the diaphragm.

v. The Thermoelement.

Two pairs of thermojunctions were made of 40 s.w.g. Copper and constantan wire and were supported in two silicon tubes so that the junctions were protruding from the end of each silicon tube. The silicon tubes were supported 10 cms.
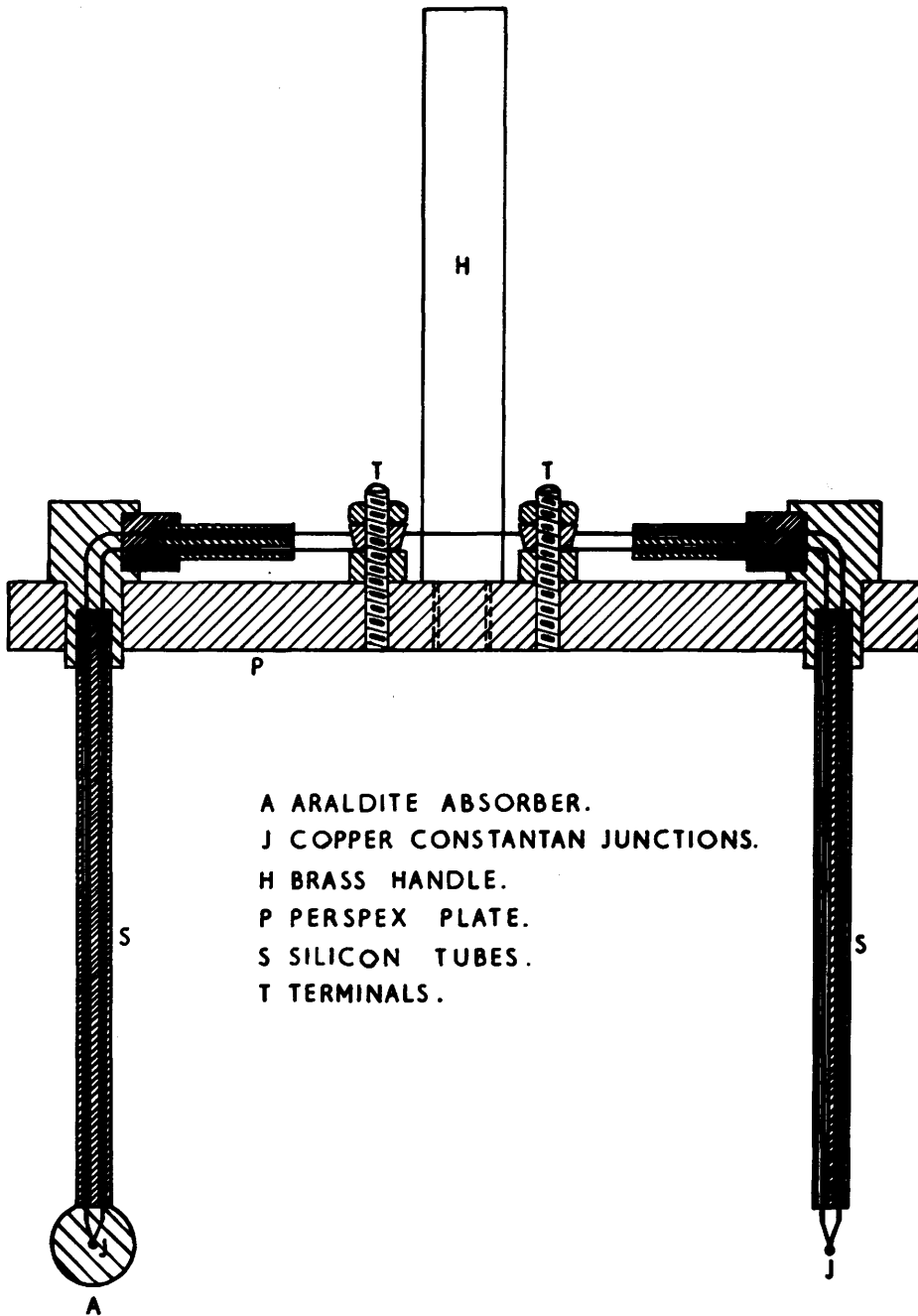
FIG. 25. THERMOCOUPLE ELEMENT FOR COMPARING INTENSITIES. SECT. ELEV.

A ARALDITE ABSORBER.
J COPPER CONSTANTAN JUNCTIONS.
H BRASS HANDLE.
P PERSPEX PLATE.
S SILICON TUBES.
T TERMINALS.

apart in a perspex block which could be mounted on a probing rack. Leads from the thermocouples were brought to terminals on the perspex block which could be connected to a sensitive galvanmeter and series resistance.

One pair of thermocouples were left bare, while the other was coated by a cold setting resin Araldite D as an absorbing substance. When this device - shown in Fig.25 - was used for comparing intensities, the coated junction was situated along the line of propagation of the ultrasonic beam. This device proved quite useful and was used as a check on the radiation balance method.

The size and sensitivity of this thermoelement can be easily controlled, yet with the number of pairs mentioned above it proved to be working satisfactorily. The instrument can be calibrated to a standard if it is required for absolute measurements. In both cases it is important, however, to remove all air films and bubbles adhering to the absorbing sphere before taking readings.

2. VISCOSITY MEASUREMENTS.

A. Referee Viscosity.

The degradation process of high polymeric solutions is better followed by observing changes in the molecular weight of polymer or changes in intrinsic viscosities, without apply-:ing the Staudinger equation, than absolute viscosities. Obviously both methods involve measuring the viscosity of the solution at different concentrations, a process which necessi-:tates disturbing the conditions inside the irradiated chamber of the viscometer. To avoid altering the conditions inside the chamber a single measurement of specific viscosity was sought from which the intrinsic viscosity could be deduced.

Martin[9] suggested a technique for measuring viscosities of cellulose under conditions such that a constant viscosity was obtained and the velocity gradient was held at a selected value. An automatic compensation for chain length of cell-:ulose was made by changing the concentration of the solution. However, it was extremely important to choose a solvent with uniform viscosity and with uniform solvent power at the constant $[\eta] C$ value chosen in his equation:

$$\eta_{sp} = [\eta] c \, e^{k[\eta] c} \qquad \ldots\ldots\ldots\ldots (5)$$

Lindsley[10] pointed out that this method was not suitable for calculating the intrinsic viscosity $[\eta]$ from a single viscosity measurement. Lindsley modified the following two

equations given by Huggins and Baker respectively:

$$\eta_{sp}/C = [\eta](1 + k \, \eta_{sp}) \quad \ldots\ldots\ldots\ldots(6)$$

$$[\eta] = \frac{a}{c}(\eta_r - 1) \quad \ldots\ldots\ldots\ldots(7)$$

By rearranging and expanding in power series, and discarding higher powers of the product $[\eta]$ C, which is legitimate at sufficiently low concentrations, the equations can be put in the following respective forms:

$$\log(\frac{\eta_{sp}}{C}) = \log[\eta] + \frac{K'}{m}[\eta] C \quad \ldots\ldots\ldots\ldots(8)$$

and

$$\log(\frac{\eta_{sp}}{C}) = \log[\eta] + \frac{a-1}{2am}[\eta]C \quad \ldots\ldots\ldots\ldots(9)$$

where 'K"' in the modified form of Huggins equation == 0.35 and 'a' in the modified form of Baker's equation == 8

Substituting these values in the above two equations gives the following relations:

$$\log(\frac{\eta_{sp}}{C}) = \log[\eta] + 0.15[\eta]C \quad \text{Huggins}\ldots(10)$$

and

$$\log(\frac{\eta_{sp}}{C}) = \log[\eta] + 0.19[\eta]C \quad \text{Baker}\ldots\ldots(11)$$

The value $[\eta]$ C must be kept sufficiently low so that the above two equations could be valid. At low concentrations (0.22-0.1%) both Baker and Huggins equations were found to be in good agreement with the values of $[\eta]$ obtained using viscosity measurements at several concentrations. At high concentrations, Baker's equation only is valid. However, both modified forms mentioned above are similar to the

representation proposed by Martin, i.e.,

$$\frac{\eta_{sp}}{C} = [\eta] e^{k[\eta]C}$$

or $$\log\left(\frac{\eta_{sp}}{C}\right) = \log[\eta] + k[\eta]C \qquad \ldots\ldots\ldots\ldots(12)$$

where $\eta_{sp} = \eta_r - 1 =$ specific viscosity

   C = concentration of solution in gms/100 c.c. of solvent;

and   K = a constant which depends on the polymer solvent combination and on temperature.

Roseveare and Poore[11] suggested a simpler mathematical interpretation of Martin's equation. This method was adopted in this work as any error in estimating the intrinsic viscosity would be the same for all polymer solutions regardless of chain length and concentration.

Considering Martin's equation (12) which holds good for high concentrations, it can be rewritten in the parametric form:

$$[\eta] = X/kC \qquad \ldots\ldots\ldots\ldots\ldots\ldots(13)$$
$$Xe^X = k\eta_{sp} \qquad \ldots\ldots\ldots\ldots\ldots\ldots(14)$$

where X is a variable parameter. To carry out any referee viscosity measurement the value of the constant 'k' must be determined in advance, for the polymer-solvent combination at the specified temperature required; and for the specific vis-:cometer used, in the conventional way.
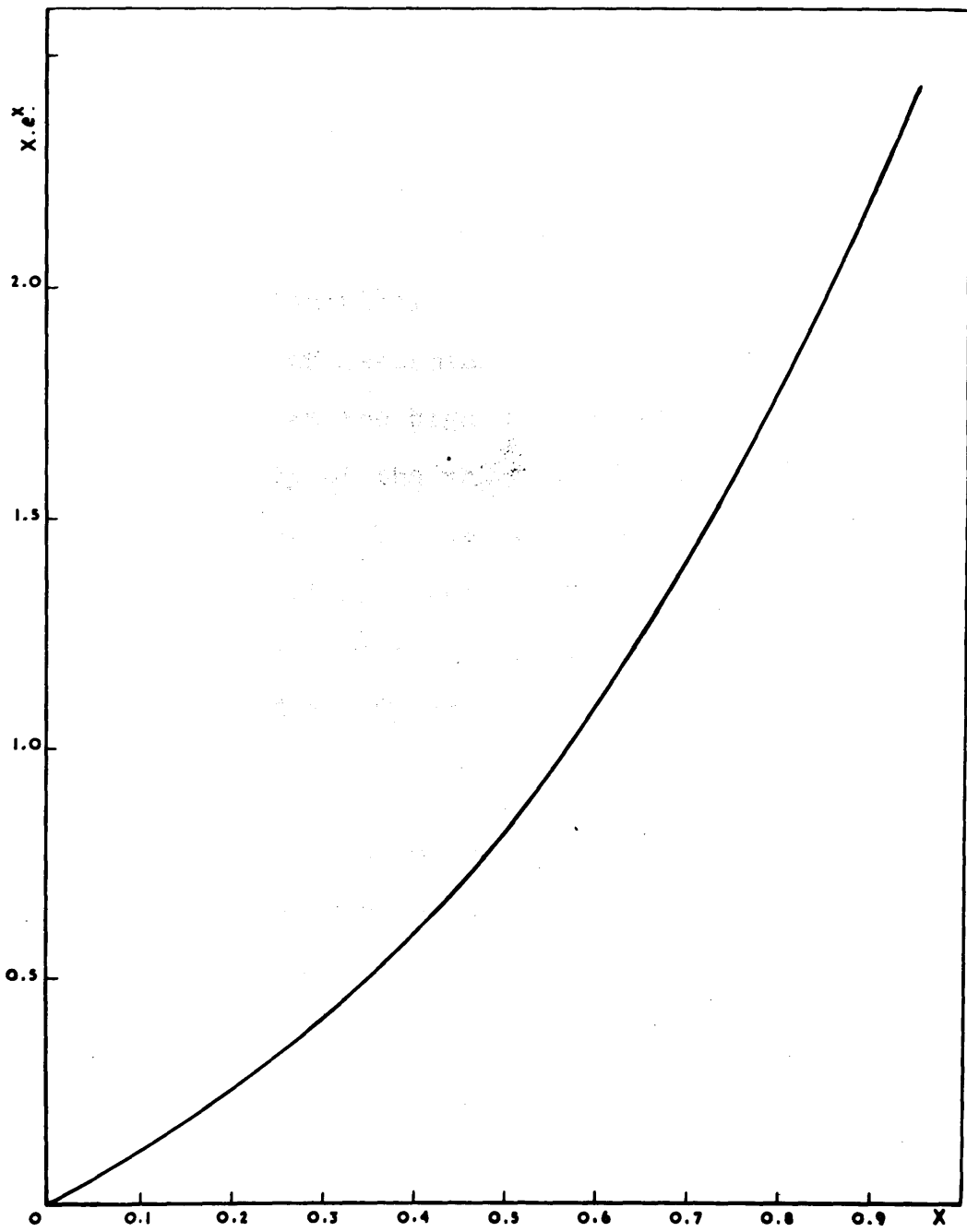
FIG. 26. X.e^X. VERSUS X

The first step in obtaining the intrinsic viscosity is to determine the value of Xe^X by substituting k and η_{sp} in equation (14), then the value of X for this value of Xe^X is read from a graph plotted for Xe^X against X (Fig.26). This value of X divided by kC is the intrinsic viscosity, as indicated by equation (13).

This method of determining the intrinsic viscosity should not be used at too high a concentration because of possible uncertainty of the value of the constant 'k' or at too low a concentration because of increased errors in specific viscosity determination. However, it was found quite satis-:factory for most of the range of concentrations envisaged in this work, viz., 0.5 - 2% wt./vol.

B. <u>Viscometers.</u>

Since it is always preferable to measure the viscosity of the irradiated polymer solution without removing it from the irradiation chamber, to secure that the conditions during the degradation process do not alter and to avoid any change in the concentration of the polymer solution, it was decided to use the following two types of viscometers for viscosity measurements.

(a) A rolling sphere viscometer which may be incorporated with a high pressure chamber for experiments conducted

under non-atmospheric conditions.

(b)   A modified Ostwald viscometer, for experiments on the degradation of high polymer solutions conducted under vacuum as well as under normal atmospheric pressure.

    (a) The Rolling Sphere Viscometer.

    i. General.   It was apparent from a brief survey of the literature that the most suitable type of viscometer for measuring viscosities of liquids under varied operating con=:ditions is the rolling sphere viscometer. It was first con=:structed by Flowers[12] and he calculated the viscosity from the expression:

$$\eta v = C(\sigma - \rho) \quad \ldots\ldots\ldots\ldots\ldots\ldots\ldots (15)$$

in which v is the velocity and σ the density of the sphere; the 'constant' C of the instrument was found by calibration with liquids of known viscosity. His calibration showed that the value of 'C' varied slightly with the viscosity.

    Hersey[13], on the other hand, preferred in calibrating the viscometer to plot the function S.T against ν/S obtained from a dimensional analysis of the probelm; where

        T is the roll time;

        $\nu = \dfrac{\eta}{\rho}$ is the kinematic viscosity;

and   S is a function of the density $= (\dfrac{\sigma}{\rho} - 1)^{\frac{1}{2}}$.

The relation between these two functions was found to be linear except at high velocities when flow became turbulent, as will

be discussed in more detail later.

Many such viscometers were constructed, mostly for tests on oils at high pressures and both methods of calibra-:tion were adopted. Sage[14] for example, described an apparatus for studying the effect of dissolved gas on the viscosity of crude oils at pressures up to 200 atms.

A theoretical and practical investigation of the system has been made by Hubbard and Brown[15] who deduced a general equation for the motion of the sphere, valid only for the streamline region of fluid flow,

$$\eta = \frac{5}{42} \, g. \, \sin \theta. \, K.d.(D + d) \, \frac{\sigma - \rho}{V} \qquad \ldots\ldots\ldots (16)$$

where η = fluid viscosity in gm/cm/sec.

D, d = tube and sphere diameters in cms.

σ, ρ = densities of metal of the sphere and fluid.

V = Ball velocity in cms/sec.

K = Constant.

θ = The angle of inclination of the tube to the horizontal.

This equation can be simplified for any one instrument used under constant conditions to:

$$\eta = C \, \frac{\sigma - \rho}{V} \qquad \ldots\ldots\ldots\ldots\ldots\ldots\ldots (17)$$

Calibration data can be substituted directly in Equation (17) to obtain the value of the coefficient C.
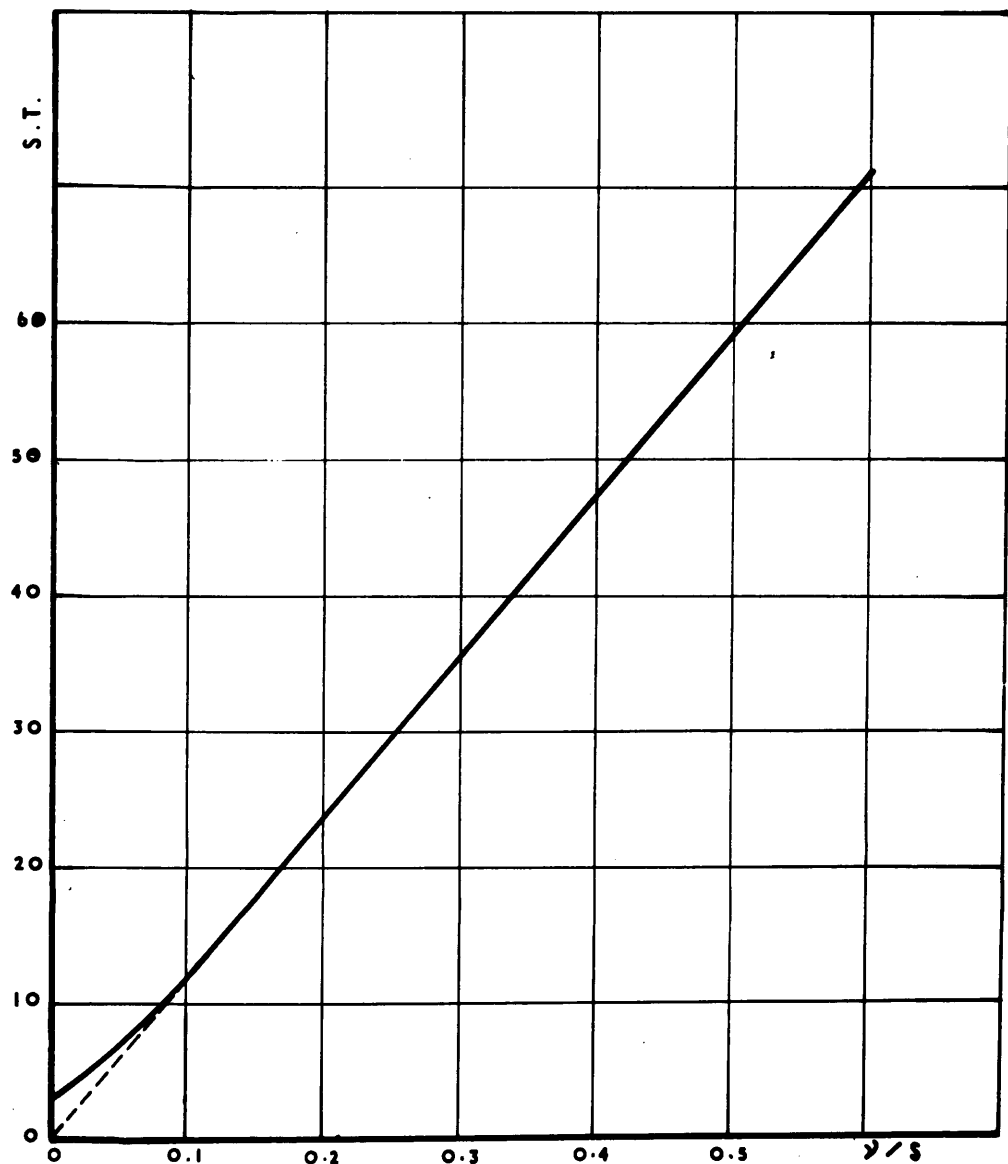
FIG.27. CALIBRATION CURVE OF ROLLING
SPHERE VISCOMETER. R.B. DOW.

In the streamline region the factor 'K' should be a
constant.   It was found to decrease slightly as the fluid
viscosity increased.   The coefficient 'C' of equation (17)
was found to be affected by changes in the temperature of the
instrument.

A viscometer having the same dimensions as those adopted
by Hersey and Shore[16] was used by Dow[17] for pressures as
high as 4,000 atms.   Dow followed Hersey's method of calibra-
:tion against liquids with known viscosities.

If ν =   kinematic viscosity

S =   a function of density $= (\frac{\sigma}{\rho} - 1)^{\frac{1}{2}}$

T =   roll time in secs.

σ =   density of the steel of the ball in gm.
   per cu. cm.

ρ =   density of the liquid in gm. per cu. cm.

$\therefore$ ST = $f \left(\frac{\nu}{S} \right)$ ....(18)

By plotting function ST against $\frac{\nu}{S}$ for the known liquids to
determine the function (f) a straight line relation, as shown
in Fig.27, was obtained from which the constant of proportion-
:ality between ST and $\frac{\nu}{S}$ could be determined:

$\therefore$ ST = $k \left(\frac{\nu}{S} \right)$ ....(19)

for long roll times.

Solving equation (18) for the viscosity $\eta = \rho\nu$

$$\nu = \frac{\eta}{\rho} = \frac{S^2 T}{k}$$

$$\eta = \frac{\rho[\frac{\sigma}{\rho} - 1] T}{K} \quad \frac{(7.36 - \rho) T}{k} \quad \ldots\ldots\ldots\ldots(20)$$

where 7.36 is the density of steel.

For a viscosity of 1 poise the time of roll was given by:

$$T_1 = \frac{K}{7.36 - \rho} \quad \text{secs.}$$

$\therefore \quad \eta = \frac{T}{T_1}$ $\quad\ldots\ldots\ldots\ldots\ldots(21)$

Thus the computation of viscosities could be done in one of two ways:

1st. If the roll time is short – region where the calibra:tion curve departs from linearity – the kinematic viscosity in equation(18) should be obtained by referring directly to the curve.

2nd. If the roll time is long, i.e., where ST varies linearly with $\frac{\nu}{s}$, equation(20) can be used directly to give η , provided the value of 'ρ' obtained by interpolating the pressure-volume-temperature data of the fluid under consideration, is substituted in the equation.

The corrections to be considered in measuring absolute viscosities at high pressures are therefore reduced to two:

1. Change in the length of the path of the ball due to pressure.

2. The initial acceleration of the ball.

The first of the two corrections involves:

1. A change in length of the viscometer.

2. A change in the diameter of the ball.

3. A change in position of the electrical contacts.

The first two effects were shown by Hersey to have almost negligible effect, while the change in position of the elect:rical contacts was appreciable.

In the design of the rolling sphere viscometer to be described later. The position of the contacts was chosen such that any error arising from change in position will have the same negligible effect as the change in length.

Correction for initial acceleration in Dow's experi:ments was computed from the equation:

$$\frac{\delta T}{T_o} = 0.21 \left[1 - (1 - \frac{8}{K T_o^2})^{\frac{1}{2}} \right] \quad \dots\dots\dots\dots\dots (22)$$

in which T_o is the observed roll time and K is a constant equal to 8.3 for liquids of specific gravity 0.8 to 1.0. This correction is negative and amounts to 16.8 percent for T_o = 1 sec., but is less than 0.5 per cent if $T_o > 5$ secs. and it is about 2 per cent for T_o = 2-3 secs.

In all the viscometers mentioned, the inclination of the tube to the horizontal was of the order of 15°, and it was noticed by Flowers that rolling of the sphere may not be uni:form at small slopes either due to roughness of the tube wall

E   ELECTRODES
E.C. EARTHING CONTACT
S.   ROLLING SPHERE
S.P. SPARKING PLUG CONTACT
T.   TEKTOR UNIT.
T.R. TIME RECORDER
V.   VARIAC
V.T. VERIDIA GLASS TUBE
W.J. WATER JACKET
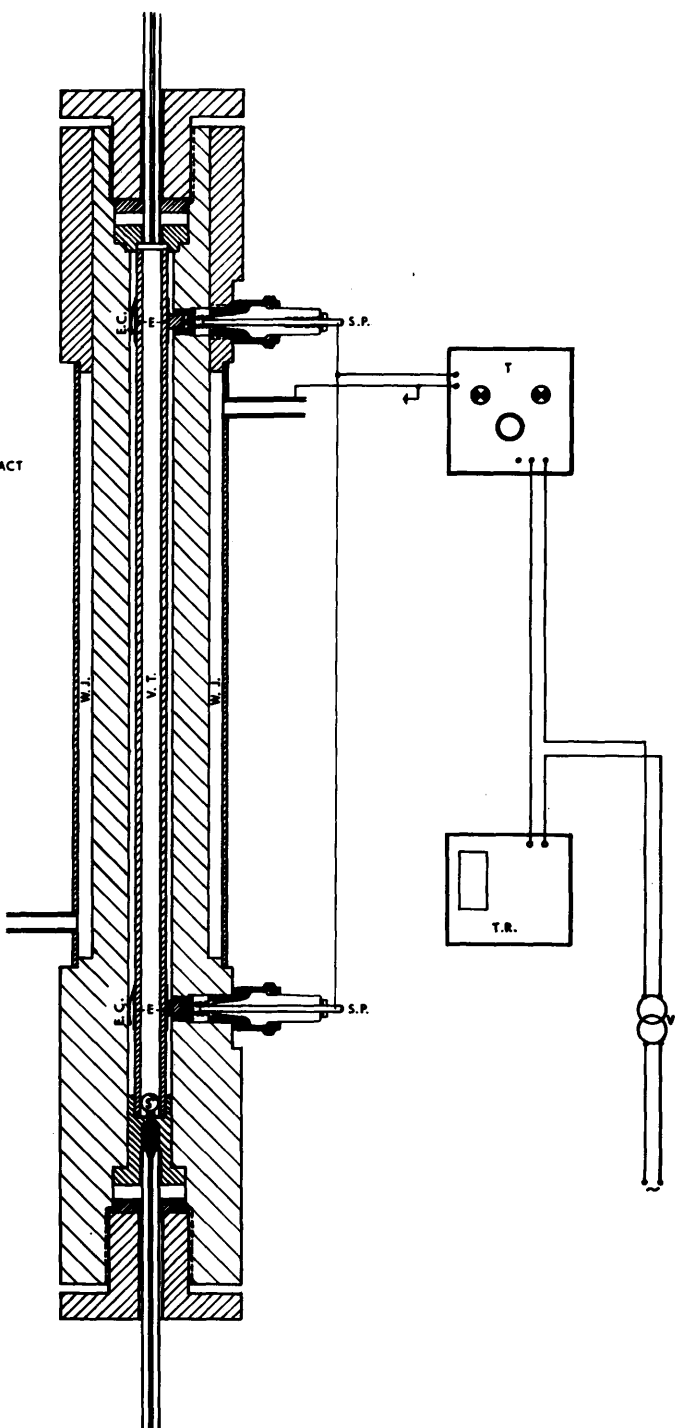
FIG.28.   ROLLING SPHERE VISCOMETER.

or irregularity of shape of the sphere. This difficulty seemed to him to disappear at higher slopes and consequently higher velocities.

Hoppler[18] used a short, nearly vertical glass tube of large diameter (11 mm.) and closely fitting balls either of glass or steel. Hisey and Brandon[19] described measurements on an instrument of this type.

For the purpose of measuring the molecular weights of high polymeric materials, one will be dealing with specific viscosities and reduced viscosities and no absolute viscosity measurements will be needed. This being the case, the errors inherent in these viscosity measurements will be minimised appreciably. The most probable error under such conditions should not exceed 1 per cent, which is nearly of the order of magnitude of the experimental error in handling the apparatus.

ii. <u>Viscometer.</u> The viscometer tube itself is of 'Veridia' glass having a bore of 6.8 m/m. ± 0.01. It is enclosed in an outer brass tube (Fig.28), so that if the chamber is pressurised, the glass tube will be under the same pressure both inside and outside and practically negligible change in its length, due to pressurization, will take place. Four electrodes on the glass tube were provided by sputtering silver on to the glass tube. The electrodes have relatively large
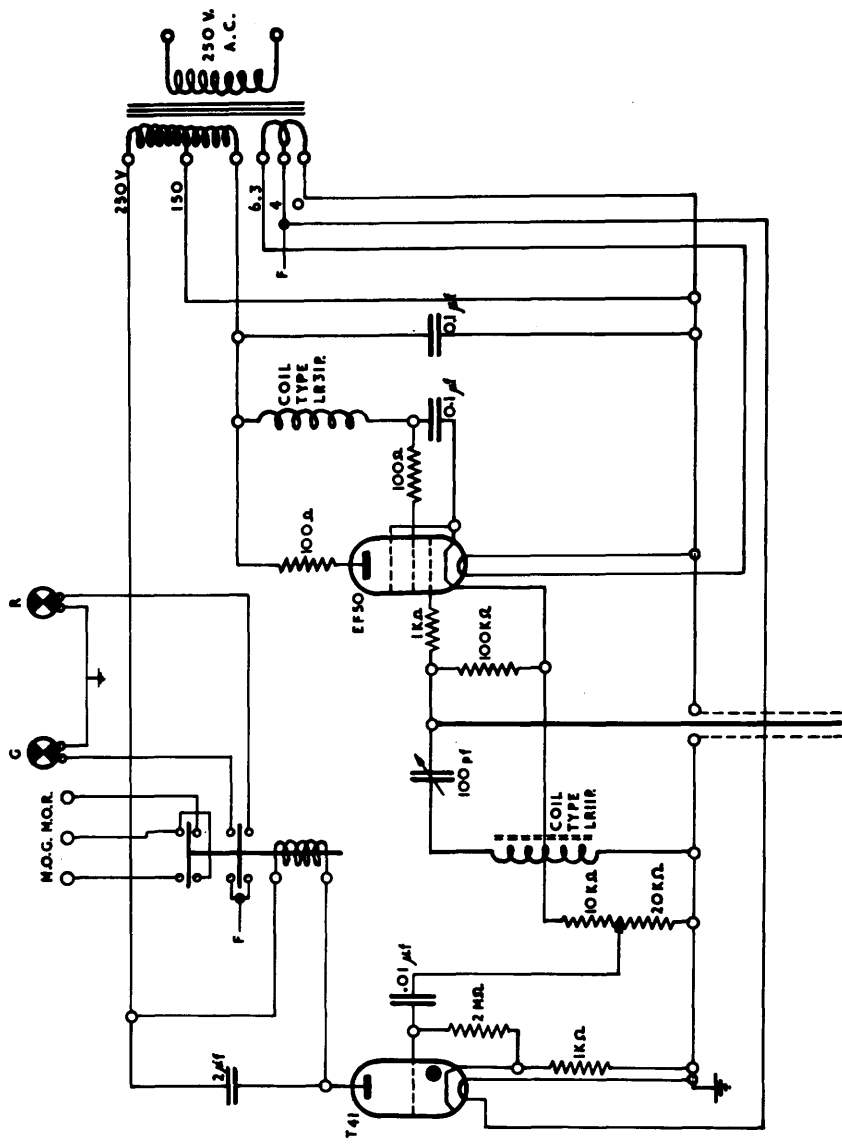
FIG. 29. TEKTOR CIRCUIT DIAGRAM.

M.O.G. MAKE ON GREEN
M.O.R. MAKE ON RED.

areas and two of them are making a sliding contact with spring
loaded brushes connected to Bosch type sparking plugs which can
stand up to a pressure of 2000 lb/sq.in.   These plugs are
fitted in the outer brass tube and are then connected to the
time recording circuit.   This sliding contact was provided so
that any change in the position of the sparking plugs due to
strain in the brass cylinder resulting from pressurization
would not affect the effective length of the tube and consequent-
:ly errors arising from a change in either the length of visco-
:meter casing or the position of the electrical contacts which
are liable to affect the operation of the viscometer were almost
eliminated.   A thermostatically controlled flow of water
through the water jacket ensures a constant temperature in the
viscometer.

    iii. Time of Roll.   In the course of these experiments
the time of roll was expected to vary from 90 secs. down to
about 3 secs. in each run, and time recording in the low range
has to be very sensitive.   For this purpose a tektor type
circuit, Fig.29, was used incorporated with a multispeed record-
:er.   The maximum speed of the recorder was 16 cm. per sec.,
and that reduced the error in time recording from 5 per cent
to 0.1 per cent.   Thus, ultimately, the rolling sphere visco-
:meter method was found to yield satisfactory results under

any restrictions which may be imposed by the experimental set up.

(b) Modified Ostwald Viscometer.

A modified Ostwald Viscometer was constructed to meet the following requirements:-

i.   The viscometer could be used as a reaction vessel with its base transparent to the ultrasonic waves; i.e., there should be no loss of ultrasonic intensity by reflection from its base.   For that purpose a terylene membrane as thin as 0.0005" under the commercial name 'Melinex' was used as a base and the dimension of the base was chosen so that the membrane could stand the highest degree of vacuum obtained.

ii.   The viscometer could be inserted in a Unicam spectro-:photometer in order to pursue the degradation process photo-:metrically by measuring the absorption of light waves by the polymer solution after adding to it a known amount of 2, 2', diphenyl-1-picryl hydrazyl (D.P.P.H.) a free radical detector.

In order to measure the viscosity from time to time during the process of degradation, either at atmospheric pressure or under vacuum, it is convenient to have a vessel in which viscosity measurements, absorption measurements and ultrasonic treatment can be carried out without opening the vessel.   One main advantage is that the concentration of the
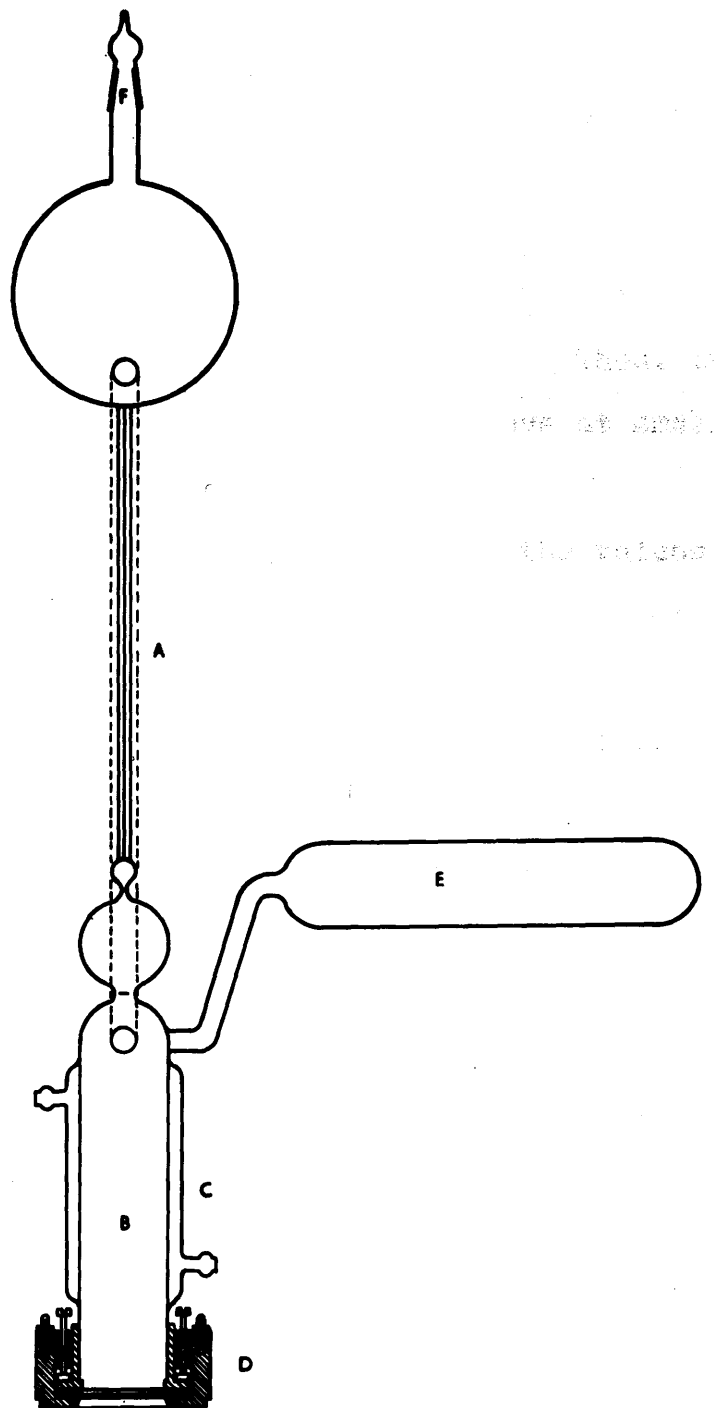
FIG. 30. REACTION VESSEL

polymer solution will not be affected by any of the above pro-
:cesses; a difficulty which was reported by many previous
workers.

The final shape of the viscometer is shown in Fig.30.
The capillary tube bore was chosen so that the time of flow of
the pure solvent is not less than 3 minutes. Thus, the errors
which may arise when using Ostwald viscometers at small times
of flow were largely reduced.

Viscosity measurements to determine the values of the
constant 'k' were also carried out by this viscometer to investi-
:gate the dependence of 'k' on the type of viscometer used.

The viscometer is a simple type of a free fall visco-
:meter A, provided with a reaction compartment B surrounded by
a cooling water jacket C. The base of the reaction compartment
is fixed with araldite adhesive type 101 to a brass arrangement
D, which enables the use of a 0.0005" terylene membrane and at
the same time secures a reliable seal. The use of the terylene
membrane was preferred to the ordinary glass bottom as the thin
terylene membrane is practically transparent to the ultrasonic
waves compared to glass which reflects a considerable part of
the ultrasonic intensity. A comparison between the results of
ultrasonic degradation obtained using terylene at the bottom of
this reaction vessel and results obtained by other investigators
showed that by applying moderate ultrasonic intensities the

weight average chain length at the end of degradation was less than what was obtained by others using higher acoustic intensit- :ies.   This proved that the arrangement chosen was superior to and more efficient than other previous arrangements used by previous workers.   The side tube is about 1" diameter, a suitable size to fit in the carriage of spectrophotometer type Unicam Sp. 360 when measuring the absorption of the D. P. P. H. in solution.

The polymer solution is introduced into the viscometer through the top tube F which is closed by a quick fit cap size B. 10.   In experiments under vacuum the reaction vessel was sealed at the top just below the B. 10 cone by a flame master while the vacuum was still maintained.

The apparatus built especially for evacuation consis- :ted of a two-stage mercury diffusion pump backed by a rotary oil pump.   The two pumps were capable of pumping down to a pressure of 10^{-5} mm. of mercury.   A liquid air trap was inserted between the main vacuum line and the mercury pump.   Taps and traps were introduced in the system to allow for flexibility of operation and any future developments.   The pressure was read on a Vacustat in the main vacuum line.

C. Calibration of the Rolling Sphere Viscometer.

As mentioned earlier the viscometer has to be calibrated against liquids of known viscosities. For this purpose 10 different samples covering a wide range of viscosities were prepared. Apart from the first sample which was pure analar benzene, each of the remaining nine samples was a solution of liquid paraffin in benzene. The ratios of benzene to liquid paraffin were chosen so as to provide a uniform increment of viscosity. One advantage of selecting these solutions is that they had the same density, which was practically the same as the density of the polymer solutions used in this work. By this choice the calibration of the rolling sphere viscometer was very much simplified, instead of plotting ST against $\frac{\nu}{S}$ as mentioned earlier, it was sufficient to plot T against ν, since $S = (\frac{\sigma}{\rho} - 1)^{\frac{1}{2}}$ was effectively constant for this series of solutions.

Furthermore, since the multispeed recorder, used to measure the time of roll is driven by a synchronous motor, i.e., constant speed, therefore the length of the trace on the recorder was taken to represent the time of roll and consequently it was plotted against ν the kinematic viscosity.

The kinematic viscosity 'ν' of the ten samples was determined using a calibrated set of Ostwald viscometers at a temperature of $25^\circ \pm 0.1$ C. These values of 'ν' were plotted
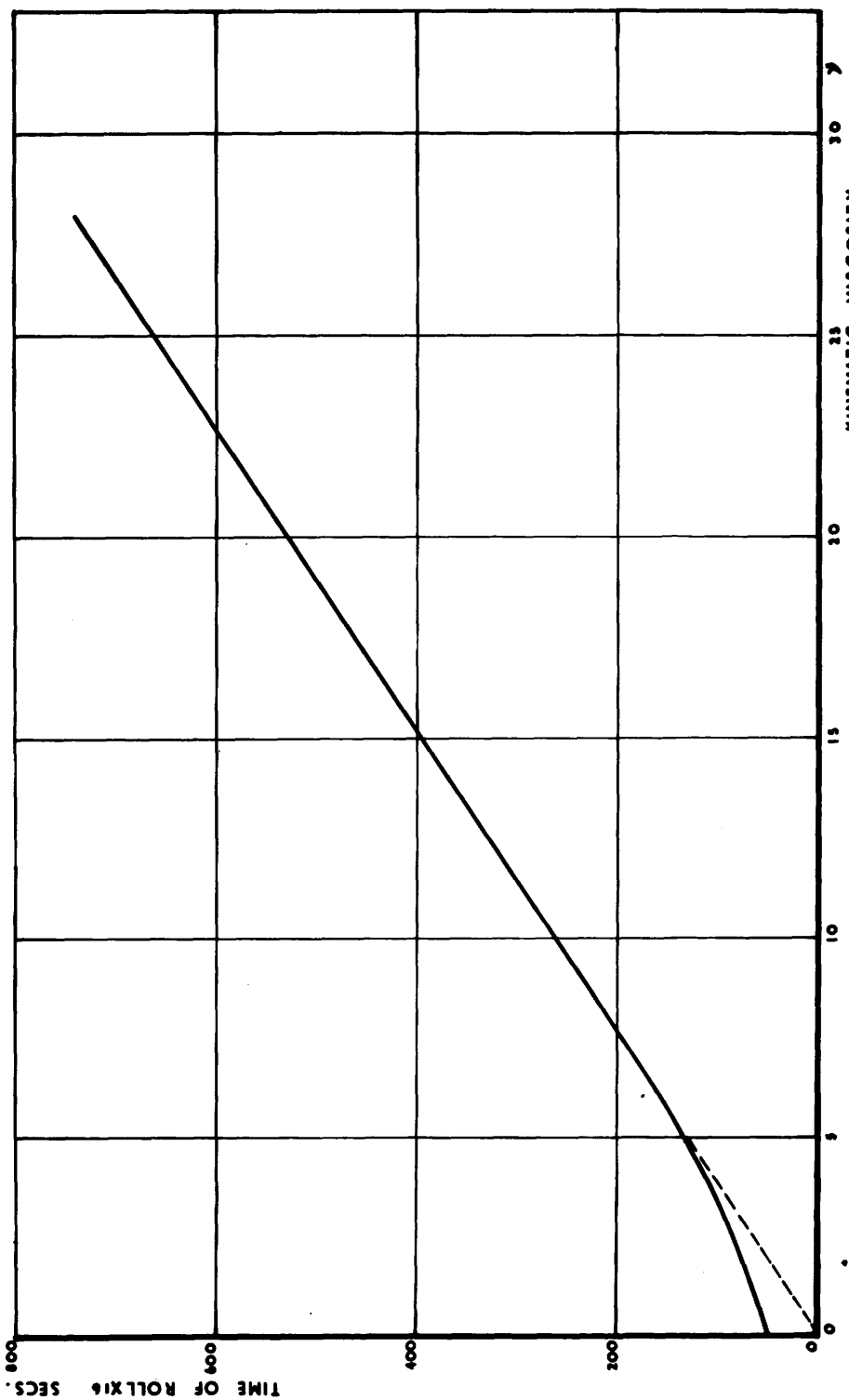
CALIBRATION CURVE OF ROLLING SPHERE
VISCOMETER. ANGLE OF INCLINATION 40°
TUBE DIAM. 6.8 ± 0.01 MM. SPHERE DIAM. ¼ INCH.

KINEMATIC VISCOSITY.

TIME OF ROLL x 10 SECS.
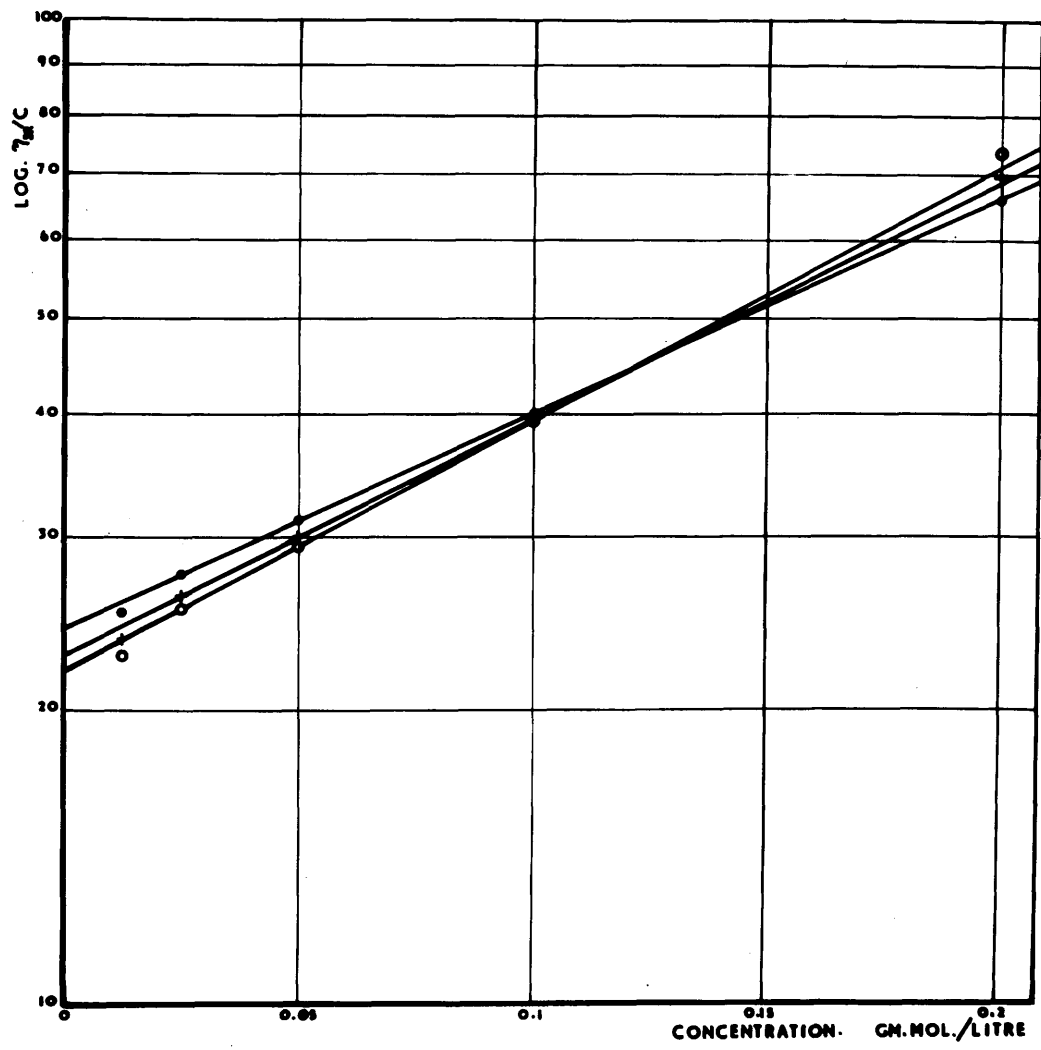
FIG. 31.

FIG. 32.   DETERMINATION OF K FOR REFEREE VISCOSITY.
• OSTWALD VISCOMETER   o ROLLING SPHERE VISCOMETER
+ REACTION VESSEL.

against their corresponding times of roll, as shown in Fig. 31. The diameter of the steel sphere used was 6.35 m/m ± 0.01 and the inclination of the axis of the viscometer to the horizontal was 40°. The distance of roll, i.e., the distance between the two pairs of electrodes was 20 cms.

The calibration curve for the devised type of rolling sphere viscometer shown in Fig. 31, is exactly similar to the calibration curve given by Dow and represented in Fig. 27.

D. Referee Viscosity Measurements.

Viscosity measurements on a 2% parent solution of poly-:styrene in benzene were carried out by three different visco-:meters, viz., an Ostwald viscometer, a modified Ostwald visco-:meter (reaction vessel) and the rolling sphere viscometer. As shown in Figure 32, the three methods yielded straight lines having different slopes, and slightly different intrinsic vis-:cosities. The value of the constant K varies from one visco-:meter to the other, as shown in Table I.

TABLE I.

Dependence of K on Viscometer shape.

Viscometer type.	Value of 'K'.
1. Ostwald Viscometer	0.198
2. Rolling Sphere Viscometer	0.279
3. Reaction Vessel	0.227

5. **MEASUREMENT OF NUMBER OF BROKEN LINKS.**

The number of broken links resulting from degradation were measured by measuring the decrease in the absorption of 2, 2', Diphenyl-1-picryl hydrazyl.

A. **2, 2' Diphenyl-1-Picryl Hydrazyl.** (D.P.P.H.)

A substance which when added to a monomer forms a non-radical product, or a radical of low reactivity incapable of adding monomer, will suppress normal polymer chain growth. Such a substance is an inhibitor if it reduces the rate of polymer growth initiation to zero. If, however, it only slows down the reaction, then it is known as a retarder. If the inhibitor is a free radical, then the reaction product with a growing polymer chain has no unpaired electron and is therefore a stable molecule incapable of adding further monomer. It should be noted, however, that the inhibitor free radical should be of low reactivity, otherwise it will initiate polymer growth, as well as terminate it. Such a compound is 2, 2' Diphenyl-1-picryl hydrazyl.

This compound is a stable free radical giving no evidence of the undesirable initiator properties; it reacts stoichiometrically with

radical chains, one inhibitor molecule being consumed by each chain radical. Similarly, during polymer degradation process,
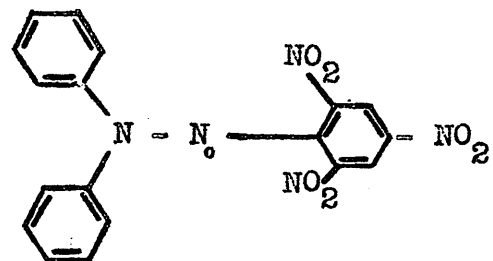
free radicals are expected to be produced whenever a scission
of a chain takes place. However, the number of free radicals
released by such scissions is equal to number of inhibitor
molecules consumed. Consequently, the number of inhibitor
molecules consumed will be equal to twice the number of sciss-
:ions (or cuts). The consumption of the inhibitor molecules
coincides with the removal of the inhibitor coloration, which
can be detected and followed by absorption measurements in the
range 4000 A.U. to 7000 A.U. in the absorptiometer.

B. PREPARATION OF D.P.P.H.

This compound was prepared according to R.H. Poirer,
E.J. Kuhler and F. Benington[20]. This method is a variation
on the original method of S.Goldschmidt and K. Renn[21].

The hydrazine was prepared first. A solution of 10
grams unsymmetrical diphenyl hydrazine hydrochloride in 125 ml.
of absolute ethyl alcohol was treated at room temperature with
9.5 gms. sodium bicarbonate and then with 11.3 grams picryl
chloride. When evolution of CO_2 was completed, the solution
was boiled under reflux for 15 minutes; an equal volume of
chloroform was then added and the solid residue filtered off
while the solution was still warm. The filterate was then
washed with two 115 ml. portions of water and was concentrated
on a steam bath to about 70 ml., then diluted with about 70 ml.

warm absolute ethanol. The solution was allowed to crystall-
:ise out overnight, when about 15 gms. of brick red hydrazine
crystals were obtained.

From this half-way product the final hydrazil was pro-
:duced. 5.1 gms. of the above substance, 5.1 gms. of anhydrous
sodium sulphate, and 31.4 gms. of lead peroxide in 100 ml. of
purified benzene were shaken together for an hour. The residue
was then filtered off through fine filter paper and the deep
violet filtrate was evaporated to dryness in vacuo. The
resultant crystals were recrystallized from a benzene-ligroin
solvent mixture (2:1 by volume) and about 3.8 gms. of violet
crystals of D.P.P.H. were formed. The overall reaction takes
place according to the following equations:-

$$\begin{array}{c} C_6H_5 \\ \diagdown \\ \diagup \\ C_6H_5 \end{array} N - NH_2 \cdot HCl \xrightarrow{\text{picryl chloride}}$$

$$\begin{array}{c} C_6H_5 \\ \diagdown \\ \diagup \\ C_6H_5 \end{array} N - NH - \underset{NO_2}{\overset{NO_2}{\bigcirc}} - NO_2 \longrightarrow D.P.P.H.$$
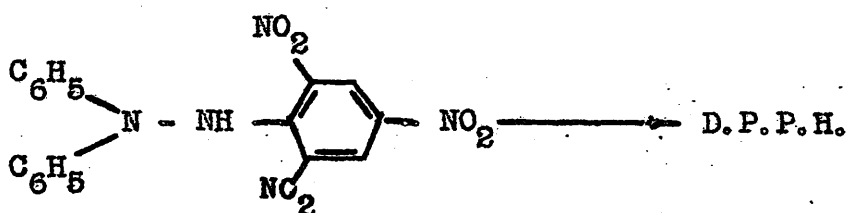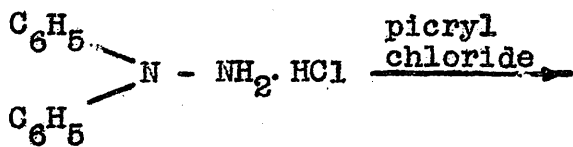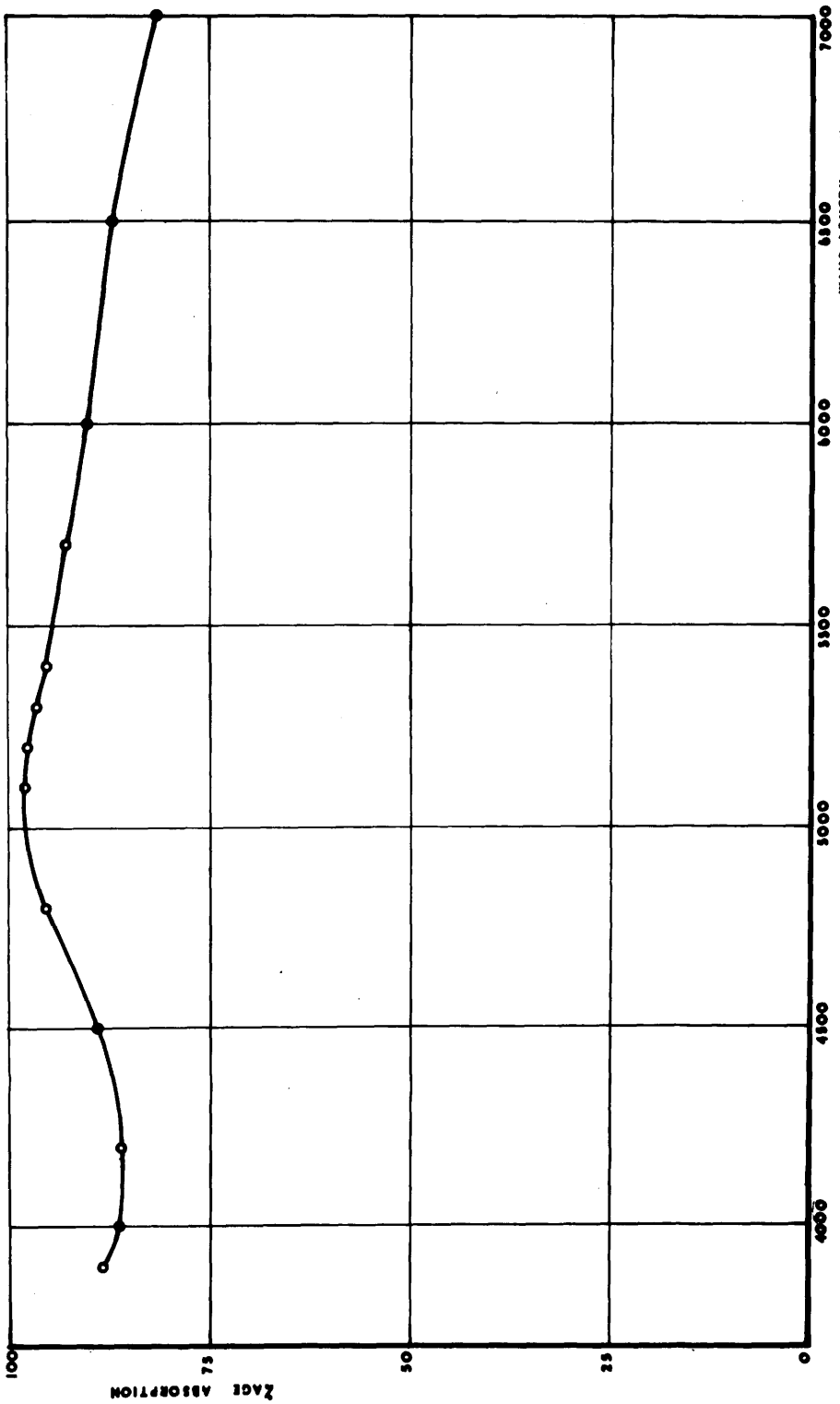
FIG. 33.   ABSORPTION CURVE FOR A D.P.P.H. IN BENZENE SAMPLE.

C. Absorption and Calibration Curves.

A solution of D.P.P.H. in moisture-sulphur-free benzene
was prepared; 0.395 gms. of D.P.P.H. were dissolved in 100 ml.
solvent. This gave a 10^{-2} M/litre solution.

1 ml. of this solution was made up to 100 ml. with
benzene to give 10^{-4} M solution. This solution was used as
the parent sample for all further test solutions.

A unicam spectrophotometer type SP.600 was used for
absorption measurements. The cell carriage was replaced by
another which was specially constructed to accommodate the
reaction vessel described in the previous section.

A preliminary test was carried out on the benzene sol-
:ution. The absorption of the solution was determined for
different wave lengths of light in the range 4000-7000 A.U.
in the absorptiometer. A maximum or peak absorption was
obtained at 5200° A.U. as shown in Fig.33. All further
investigations of the degradation process were carried out
at this wave length.

Benzene solutions with different D.P.P.H. concentrations
were prepared and a calibration curve for the absorptiometer
was constructed. The instrument was first checked for 0%
transmission and for 100% transmission through air.
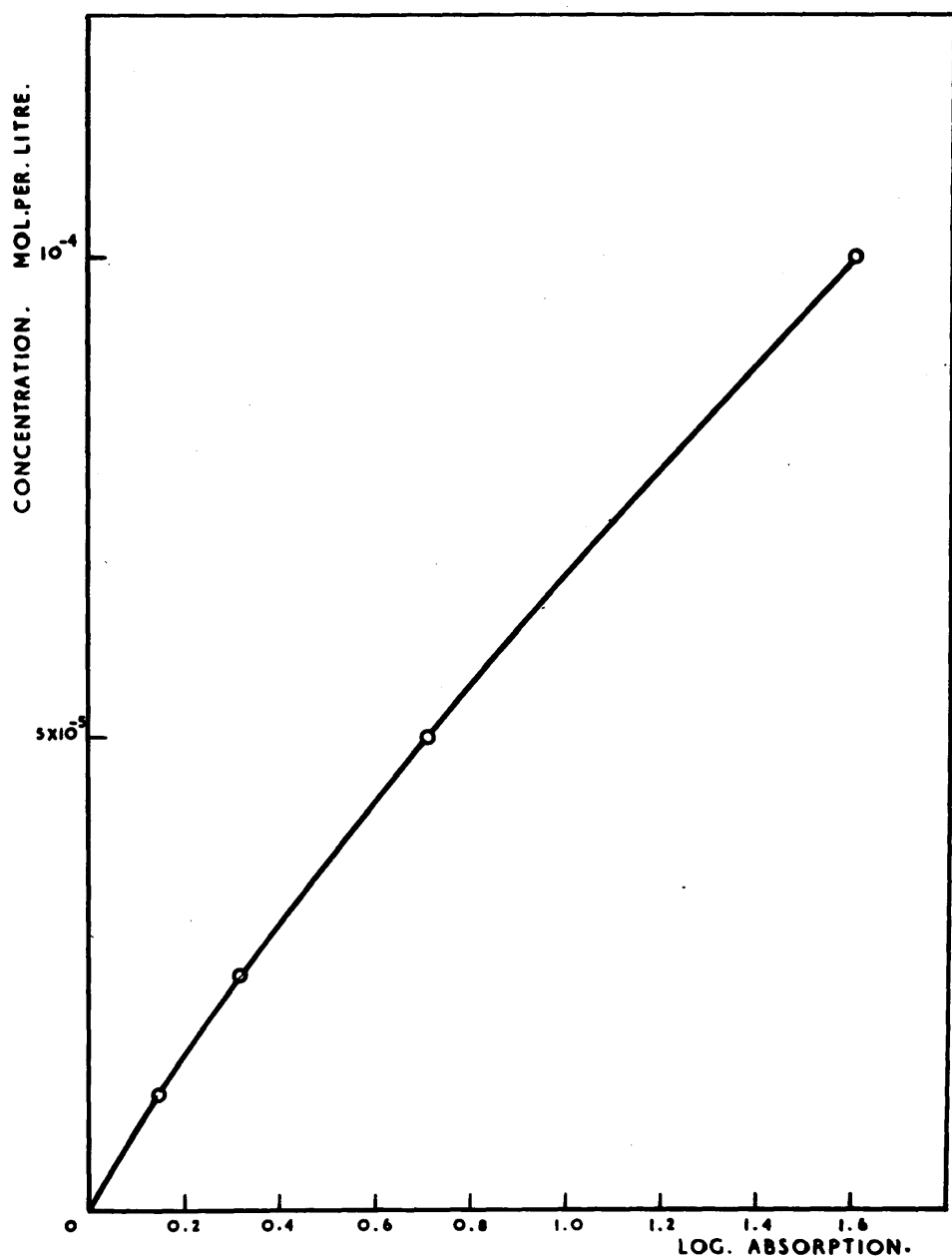
FIG. 34.   MOLAR CONCENTRATION OF D.R R H. IN
BENZENE VERSUS LOG. ABSORPTION.

An identical tube to the reaction vessel's was used for balancing.   This tube was filled with benzene alone and was used for initial adjustment of the spectrophotometer.   The reaction vessel containing the benzene + D.P.P.H. solution was then introduced.   The absorption measured was that of D.P.P.H. alone.

The absorption measurement was carried out for the above mentioned solutions, which vary in D.P.P.H. concentration from 0 Mol./litre to 10^{-4} Mol./litre.   Results of these measure=:ments are illustrated in Fig.34.

REFERENCES.

1. Voigt, W.
    Abh. Ges. Wiss Göttingen, 36, 1, (1890).

2. Cady, W.G.
    'Piezoelectricity', p.219.

3. Fein, L.
    J.A.S.A. 22, 876, (1950).

4. Cady, W.G. and Gittings, C.E.
    J.A.S.A. 25, 892, (1953).

5. Richards, W.T.
    Proc.Nat.Acad.Sci.N.Y., 15, 310 (1929).

6. Murray, A.J.R., Ph.D. Thesis.

7. Hall, W.M.,
    J.A.S.A. 4, 83, (1932-1933).

8. McNamara, F.L. and Beyer, R.T.
    J.Acoust.Soc.Amer. 25, 259 (1953).

9. Martin, A.F.
    Tappi, 34, 363 (1951).

10. Lindsley, C.H.
    J.Pol.Sci. 7, 635, (1951).

11. Roseveare, W.E. and Louise, P.
    J. Pol. Sci. 10, 126 (1953).

12. Flowers, A.E.
    Proc. Amer. Soc. Test. Mat. 14(ii), 565 (1914).

13. Hersey, M.D.
    J. Wash. Acad. Sci. 6, 521 (1916).

14. Sage,
   Ind. Eng. Chem. 5, 261 (1933).

15. Hubbard, R.M. and Brown. G.G.
   Ind. Eng. Chem. (Analytical Edn) 15, 212 (1943).
   Ind. Eng. Chem. 35, 1276 (1943).

16. Hersey, M.D. and Shore, H.
   Amer. Soc. Mech. Emgrs. 50, 221 (1928).

17. Dow, R.B.
   J. App. Phys. 8, 367, (1937).

18. Hoppler, Von F.
   Zeit. Tech. Phys. 14, 165, (1933).

19. Hisey and Brandon,
   Paper Tr. J. 120, 11 and 21, (1945).

20. Poirier, R.H. Kuhler, E.J. and Benington, F.
   J. Org. Chem. 17, 1437, (1952).

21. Goldschmidt, S. and Renn, K.
   Ber. 55, 628, (1922).

CHAPTER IV.

DEGRADATION OF ADDITION POLYMERS BY ULTRASONIC WAVES.

THEORETICAL

DEGRADATION OF ADDITION POLYMERS
BY ULTRASONIC WAVES.

THEORETICAL.

A. Introduction.

Most of the previous work on degradation was carried
out on samples of polymers without any attention being paid
to their initial size distribution.   Schmid, Parret and
Pfleinderer[1] considered the size distribution not from a
theoretical point of view, but to provide a further experi-
:mental proof of Schmid's picture of the mechanism of degra-
:dation of long chain polymers by ultrasonic waves.   Polymer
samples at different stages of the degradation process were
fractionated and the resulting weight distribution curves were
plotted and compared with the weight distribution curves for
the same polymer sample obtained at different stages of thermal
degradation.

Although Schmid was the first to derive a simple theory
for the kinetics of degradation of long chain polymers by
ultrasonic waves yet he did not consider, in his treatment,
the initial size distribution of the polymer sample.   Never-
:theless, he found that his experimental results can be correct-
:ly interpreted if there was a limiting chain length below
which no degradation takes place.

Jellinek and his co-workers[2] considered the size distribution during the different stages of the process of degradation by ultrasonic waves. In their work a theoretical solution by induction methods was established for an initially homogeneous polymer. Their assumptions were based upon Schmid's work and that polymers under the effect of ultrasonic waves do not degrade to the monomer but only to an intermediate (limiting) chain length.

B. Assumptions.

1. Random degradation, i.e., all linkages in a chain have the same probability for scission independent of their position in the chain.

2. The rate of degradation is dependent on the chain length decreasing progressively with decreasing chain length and reaching a zero value at a definite intermediate chain length.

3. Initial sample is heterogeneous having a known distribution:

$$N_x = N_o p^{x-1}(1 - p)^2$$

The second of these assumptions has to be modified at a later stage due to the complexity of the resulting solution.

C. General Solution.

The general rate equations at any time during the de-:gradation process are (compare Simha[3] and Jellinek[2]):

$$dN_n/dt = -k(n-y)(n-1)N_n \qquad\qquad n \longrightarrow \infty$$

$$dN_{n-1}/dt = 2k(n-y)N_n - k(n-y-1)(n-2)N_{n-1}$$

$$dN_{n-2}/dt = 2k(n-y)N_n + 2k(n-y-1)N_{n-1}$$
$$- k(n-y-2)(n-3)N_{n-2}$$

. . . .

$$dN_z/dt = 2k(n-y)N_n + 2k(n-y-1)N_{n-1} + 2k(n-y-2)N_{n-2} + \ldots$$
$$+ 2k(z-y+1)N_{z+1} - k(z-y)(z-1)N_z$$

. . . .

$$dN_{y+1}/dt = 2k(n-y)N_n + 2k(n-y-1)N_{n-1} + \ldots$$
$$+ 4kN_{y+2} - kyN_{y+1} \qquad\qquad (1)$$

$$dN_y/dt = 2k(n-y)N_n + 2k(n-y-1)N_{n-1} + \ldots$$
$$+ 4kN_{y+2} + 2kN_{y+1}$$

. . . .

$$dN_2/dt = 2k(n-y)N_n + 2k(n-y-1)N_{n-1} + \ldots$$
$$+ 4kN_{y+2} + 2kN_{y+1} \qquad\qquad (2)$$

where n, n-1, ...z,...y+1,...2 represent chain lengths in mon-
:omer units, N_n, N_{n-1},...N_z...N_{y+1}, N_y...N_2 represent the
number of molecules having chain lengths n, n-1,...z,...y+1,
y,...2.

k is constant but is related to the rate constant of
degradation by the relation:

$$K_z = k(z - y)$$

as suggested by Schmid[1].

For simplifying the mathematical treatment by matrices the rate equations (1) can be written as:

$$dX_1/dt = a_{11}X_1$$
$$dX_2/dt = a_1X_1 + a_{22}X_2$$
$$dX_3/dt = a_1X_1 + a_2X_2 + a_{33}X_3$$
$$dX_4/dt = a_1X_1 + a_2X_2 + a_3X_3 + a_{44}X_4$$

$$\cdots\cdots\cdots\cdots\cdots\cdots\cdots\cdots\cdots$$

$$dX_m/dt = a_1X_1 + a_2X_2 + \ldots + a_{m-1}X_{m-1} + a_{mm}X_m \qquad (3)$$

where the following transformations are valid:

$$X_1 = N_n \quad : \quad a_{11} = -k(n-y)(n-1) \quad :$$
$$a_1 = 2k(n-y)$$

$$X_2 = N_{n-1} \quad : \quad a_{22} = -k(n-y-1)(n-2) \quad :$$
$$a_2 = 2k(n-y-1)$$

$$X_r = N_{n-r+1} : \quad a_{rr} = -k(n-y-r+1)(n-r) \quad :$$
$$a_r = 2k(n-y-r+1) \qquad (4)$$

Equations (3) are concisely expressible as the matrix equation:

$$dX/dt = AX$$

where X is the column matrix representing the value of X at time t, i.e.,

$$X = \begin{bmatrix} X_1 \\ X_2 \\ X_3 \\ \bullet\bullet \\ \bullet\bullet \\ X_m \end{bmatrix}$$

and A is a triangular matrix given by:

$$A = \begin{bmatrix} a_{11} & & & & & \\ a_1 & a_{22} & & & & \\ a_1 & a_2 & a_{33} & & & \\ \cdots\cdots\cdots\cdots & & & & & \\ \cdots\cdots\cdots\cdots & & & & & \\ a_1 & a_2 & a_3 & \cdots & a_{m-1} & a_{mm} \end{bmatrix} \qquad (5)$$

Formally:

$$dX/dt - AX = 0$$

$$\frac{d}{dt}[e^{-At} X] = 0$$

$$\therefore X = e^{At} X_0 \qquad (6)$$

where X_0 is the column matrix representing the initial condi-
:tions of X, i.e., at $t = 0$:

$$X_0 = \begin{bmatrix} X_1^{(o)} \\ X_2^{(o)} \\ \cdot\cdot \\ X_r^{(o)} \\ \cdot\cdot \\ X_m^{(o)} \end{bmatrix}$$

for a homogeneous polymer sample:

$$X_0 = \begin{bmatrix} N_1 \\ 0 \\ \cdot\cdot \\ \cdot\cdot \\ 0 \end{bmatrix}$$

for a heterogeneous polymer (addition polymerization):

$$X_o = N_o p^n (1-p)^2 \cdot \begin{bmatrix} 1/p \\ 1/p^2 \\ 1/p^3 \\ 1/p^4 \\ \circ \circ \circ \\ 1/p^m \end{bmatrix} \tag{7}$$

The solution of the rate equations as expressed by equation (6) is an explicit solution, provided the value of e^{At} can be determined.

A triangular matrix as A in equation (5) can be expressed in terms of its eigen columns matrix and eigen rows matrix, i.e.,

$$A = P^{-1} \Lambda P$$

or:

$$= QAQ^{-1}$$

where Q is the eigen columns matrix, Q^{-1} is the reciprocal eigen columns matrix, P is the eigen rows matrix, P^{-1} is the recipro- :cal eigen rows matrix, and Λ is the diagonal matrix of the distinct eigen values of the triagonal matrix A. i.e.,

$$\Lambda = \begin{bmatrix} a_{11} & 0 & 0 & \cdots & \cdots & 0 \\ 0 & a_{22} & & & & \\ 0 & 0 & a_{33} & & & \\ \cdots & & & \cdots & & \\ \cdots & & & & \cdots & \\ 0 & 0 & \cdots & & & a_{mm} \end{bmatrix}$$

Generally speaking:

$$A^n = P^{-1} . \Lambda^n P \quad \text{(see Elementary Matrices by Fraser,}$$
$$\text{Duncan and Coller, Chapter III).}$$

or
$$= Q \Lambda^n Q^{-1}$$

and:

$$e^{At} = \sum_0^\infty (A^n t^n / n!) = P^{-1} \sum_0^\infty (\Lambda^n t^n / n!) P$$
$$= P^{-1} L P \qquad (8)$$

where

$$L = \begin{bmatrix} e^{a_{11}t} & & & & \\ & e^{a_{22}t} & & & \\ & & e^{a_{33}t} & & \\ & & & \cdots & \\ & & & & \cdots \\ & & & & e^{a_{mm}t} \end{bmatrix}$$

since:

$$PQ = K$$

where K is a unit matrix.

$$\therefore P^{-1} = K^{-1}Q = QK^{-1} \qquad (9)$$

Therefore from equations (8) and (9) we obtain the relation:

$$e^{At} = QK^{-1}LP$$
$$= QHP$$

where
$$H = K^{-1}L \qquad (10)$$

(1) <u>to find Q</u>:

For triangular matrix A (equation 5) the eigen values are obviously the diagonal elements, i.e., a_{11}, a_{22}, ... a_{mm}.

The eigen columns matrix Q for the triangular matrix A (see appendix I), worked out by conventional methods can be expressed by:

$$Q = \begin{bmatrix} 1 & & & & \\ \alpha_{21} & 1 & & & \\ \alpha_{21}\alpha_{31} & \alpha_{32} & 1 & & \\ \cdots & \cdots & \cdots & \cdots & \\ \alpha_{21}\alpha_{31}\alpha_{41} \cdots & \alpha_{32}\alpha_{42}\alpha_{52} \cdots & & \cdots & 1 \end{bmatrix} \quad (11)$$

$$\alpha_{rs} = \frac{a_{r-1,r-1} - a_{ss} - a_{r-1}}{a_{rr} - a_{ss}} \quad (12)$$

i.e., α_{rs} can be explicitly expressed in terms of any set of coefficients as given in the rate equations.

(2) <u>to find P</u>:

The eigen rows matrix P of the triangular matrix A (see appendix II) worked out in a similar way as in the case of Q can be expressed by:

$$P = \begin{bmatrix} 1 & & & & \\ \beta_{21} & 1 & & & \\ \beta_{31}\gamma_{32} & \beta_{32} & 1 & & \\ \beta_{41}\gamma_{42}\gamma_{43} & \beta_{42}\gamma_{43} & \beta_{43} & 1 & \\ \cdots & \cdots & \cdots & \cdots & \\ \cdots & \cdots & \cdots & \cdots & \\ \beta_{m1}\gamma_{m2}\cdots\gamma_{m,m-1} & \beta_{m2}\gamma_{m3}\cdots\gamma_{m,m-1} & \cdots & \cdots & 1 \end{bmatrix} \quad (13)$$

where:
$$\beta_{rs} = a_s/(a_{rr} - a_{ss}) \tag{14}$$

and:
$$\gamma_{rs} = (a_{rr} - a_{ss} + a_s)/(a_{rr} - a_{ss}) \tag{15}$$

Equation (6) can now be put as:

$$X = QLPX_o$$

where

$$QL = \begin{bmatrix} 1 & & & \\ \alpha_{21} & 1 & & \\ \alpha_{21}\alpha_{31} & \alpha_{32} & 1 & \\ \cdots & & \cdots & \\ \cdots & & \cdots & \\ \alpha_{21}\cdots\alpha_{m1} & \alpha_{32}\cdots\alpha_{m2} & \cdots & 1 \end{bmatrix} \begin{bmatrix} e^{a_{11}t} & & & \\ & e^{a_{22}t} & & \\ & & \cdots & \\ & & \cdots & \\ & & \cdots & \\ & & & e^{a_{mm}t} \end{bmatrix}$$

$$= \begin{bmatrix} e^{a_{11}t} & & & \\ \alpha_{21}e^{a_{11}t} & e^{a_{22}t} & & \\ \alpha_{21}\alpha_{32}e^{a_{11}t} & \alpha_{32}e^{a_{22}t} & e^{a_{33}t} & \\ \cdots & \cdots & \cdots & \\ \cdots & \cdots & \cdots & \\ \alpha_{21}\alpha_{31}\cdots\alpha_{m1}e^{a_{11}t} & \alpha_{32}\alpha_{42}\cdots\alpha_{m2}e^{a_{22}t} & \cdots & e^{a_{mm}t} \end{bmatrix} \tag{16}$$

Postmultiplying QL by PX_o we obtain the explicit value of X:

$$= \begin{bmatrix} e^{a_{11}t} & & & & \\ \alpha_{21}e^{a_{11}t} & e^{a_{22}t} & & & \\ \alpha_{21}\alpha_{31}e^{a_{11}t} & \alpha_{32}e^{a_{22}t} & e^{a_{33}t} & & \\ \alpha_{21}\alpha_{31}\alpha_{41}e^{a_{11}t} & \alpha_{32}\alpha_{42}e^{a_{22}t} & \alpha_{43}e^{a_{33}t} & e^{a_{44}t} & \\ \cdots & \cdots & \cdots & \cdots & \\ \alpha_{21}\cdots\alpha_{m1}e^{a_{11}t} & \alpha_{32}\cdots\alpha_{m2}e^{a_{22}t} & \cdots & \cdots & e^{a_{mm}t} \end{bmatrix} X$$

$$\begin{bmatrix} 1 & & & & & \\ \beta_{21} & & 1 & & & \\ \beta_{31}\gamma_{32} & & \beta_{32} & 1 & & \\ \cdots & & \cdots & \cdots & & \\ \cdots & & \cdots & \cdots & & \\ \beta_{m1}\gamma_{m2}\cdots\gamma_{m,m-1} & & \cdots & \cdots & 1 \end{bmatrix} x \; X_o \qquad (17)$$

where X_o is the column matrix representing the initial condit-
:ions.

The solution obtained by substituting for a_{rr} and a_r
the values given in equations (4) was found too complex to
serve any practical purpose, especially if the number of rate
equations is more than ten (for six or ten rate equations each
equation can be considered to represent a fractionated portion
of the heterogeneous polymer sample).

It was decided to make the same simplification carried
out by Jellinek and White[2], namely that all values of 'a' are
equal down to chain length y+1 and are zero for chains of length
y and smaller, i.e.,

$$a_1 = a_2 = a_3 \cdots = a_{n-y+2} = a = 2K$$

$$a_{n-y+1} = a_{n-y} \cdots = a_{n-1} = a_n = 0$$

$$a_{11} = -K(n-1) \quad a_{22} = -K(n-2) \cdots a_{rr} = -K(n-r) \qquad (18)$$

With this modification of the second assumption all
values of $\alpha_{r,r-3}$, where r is any integar greater than y+3,

are equal to zero, thus reducing the complexity of the final

solution.

To obtain an explicit value for X_r, say, from the product

matrix, we find that all values of α in the rth row of the QL

matrix vanish except the last three elements; therefore:

$$
X = \begin{bmatrix} \cdot \cdot \cdot \cdot \\ \cdot \cdot \cdot \cdot \cdot \cdot \cdot \cdot \cdot \\ 0 \cdot \cdot 0 \cdot \cdot \alpha_{r-1,r-2} \; \alpha_{r,r-2} \; e^{a_{r-2,r-2}t}, \alpha_{r,r-1} \; e^{a_{r-1,r-1}t}, e^{a_{rr}t} \end{bmatrix} x
$$

$$
\begin{bmatrix} \cdot \cdot \cdot \cdot \cdot \cdot \\ \beta_{r-2,1} \cdot \cdot \gamma_{r-2,r-3} \quad \beta_{r-2,r-3} \\ \beta_{r-1,1} \cdot \cdot \gamma_{r-1,r-2} \cdot \cdot \beta_{r-1,r-3}\gamma_{r-1,r-2}, \quad \beta_{r-1,r-2} \qquad 1 \\ \beta_{r1}\gamma_{r2} \cdot \cdot \gamma_{r,r-1} \cdot \cdot \beta_{r,r-3}\gamma_{r,r-2}\gamma_{r,r-1}, \; \beta_{r,r-2}\gamma_{r,r-1}, \; \beta_{r,r-1}, \quad 1 \end{bmatrix} x
$$

$$
\begin{bmatrix} X_1^{(o)} \\ \cdot \cdot \\ \cdot \cdot \\ X_{r-2}^{(o)} \\ X_{r-1}^{(o)} \\ X_r^{(o)} \end{bmatrix}
$$

(19)

D. Applications.

Case 1: Homogeneous Polymer Sample.

Applying this result as obtained in equation (19) to the case of an initially homogeneous polymer sample of chain length n and number of molecules $X_1^{(o)} = N_n = N_1$, we obtain:

$$X_r = [(\alpha_{r-1,r-2}\,\alpha_{r,r-2})(\beta_{r-2,1}\gamma_{r-2,2}\cdots\gamma_{r-2,r-3})\;e^{a_{r-2,r-2}t}$$
$$+ \alpha_{r,r-1}(\beta_{r-1,1}\gamma_{r-1,2}\cdots\gamma_{r-1,r-2})\;e^{a_{r-1,r-1}t}$$
$$+ \beta_{r1}\gamma_{r2}\gamma_{r3}\cdots\gamma_{r,r-1}\;e^{a_{rr}t}\;]\;X_1^{(o)}$$

Substituting the appropriate values of α, β, γ, and a, we obtain:

$$X_r = X_1^{(o)}[r-2)e^{-K(n-r+2)t} - 2(r-1)e^{-K(n-r+1)t} + re^{-K(n-r)t}]$$

Considering the transformations in Equations (4) we obtain:

$$N_{n-r+1} = X_1^{(o)}[(r-2)e^{-K(n-r+2)t} - 2(r-1)e^{-K(n-r+1)t} + re^{-K(n-r)t}]$$

if $n-r+1 = x$, we obtain a value for N_x :

$$N_x = N_1[(n-x-1)e^{-K(x+1)t} - 2(n-x)e^{-Kxt} + (n-x+1)e^{-K(x-1)t}]$$

which is the same as that developed by Jellinek and White[2], provided the following transformations hold:

$$N_{x\cdots r\cdots s} \equiv n_{x\cdots r\cdots s}$$
$$x\ldots r\ldots s \equiv P_x\cdots P_r\cdots P_s$$

Case 2: Heterogeneous Polymer Sample.

In this case a heterogeneous polymer is considered. All links are broken at random in chains whose length is greater than y, the rate constant being the same for all chains. No links at all are broken in chains of length y or less.

The initial molecule size distribution (addition poly-:merization) is given by:

$$N_x = N_o \; p^{x-1} \; (1-p)^2$$

where N_x is the number of molecules of chain length x,

N_o is the total number of monomer units,

p   is a probability factor which, for addition polymers is always less than 1 and is given by the relation:

$$\frac{1}{p} = 1 + \frac{1}{P}$$

P   being the average degree of polymerization of the sample.

a. Number and Weight Distribution Functions.

Following a treatment similar to that of a homogeneous polymer sample (see Appendix III) we find that:

$$N_x = N_o \; p^{x-1} \; e^{-K(x-1)t} [1-p \; e^{-Kt}]^2 \qquad (21)$$

In terms of the initial average degree of polymerization or the number average chain length, N_x is given by:

$$N_{x_2} = N_0 \left(\frac{P}{P+1}\right)^{x-1} e^{-K(x-1)t} \left[1 - \frac{P}{P+1} e^{-Kt}\right]^2 \qquad (22)$$

This equation gives after a time t that part of distribution which lies between the intermediate chain length y and infinity, i.e., for a chain length $y < x < \infty$.

For values of x below the intermediate chain length limit, i.e., $o < x < y$, we have from equations (1) and (2):

$$\frac{dN_x}{dt} = \frac{dN_y}{dt} = \frac{dN_{y+1}}{dt} + K(y+2) N_{y+1}$$

$$\therefore \quad N_x = N_{y+1} + K(y+2) \int N_{y+1} \cdot dt + C.$$

$$= N_0 \, p^y \, e^{-Kyt} \left[1-pe^{-Kt}\right]^2 + K(y+2) \int N_0 \, p^y \, e^{-Kyt}$$

$$\left[1 - p \, e^{-Kt}\right]^2 \cdot dt + C \qquad (23)$$

If we consider the initial value of N_x, i.e., at t=o

$$\therefore \quad N_x = N_0 \, p^{x-1} (1-p)^2 \qquad (24)$$

From equations (23) and (24) the constant of integration C can be calculated:

$$\therefore \quad C = 2N_0 \, p^y \left[\frac{1+y(1-p)}{y(y+1)}\right] + N_0 \, p^{x-1} (1-p)^2$$

Thus the part of distribution representing chain lengths less than y, i.e., $o < x < y$, can be expressed as:

$$N_{x_1} = \frac{2N_0 \, p^y}{y(y+1)} \left[1+y(1-p) - e^{-Kyt}(1+y-pye^{-Kt})\right]$$

$$+ N_0 \, p^{x-1}(1-p)^2 \qquad (25)$$

The whole of the number distribution is obtained by dividing equations (22) and (25) by pN_0 and this gives the number of

moles of any chain length when the whole polymer sample repre-
:sents one basic mole of polymer.

Hence,

$$n_{x_1} = \frac{2\ p^{y-1}}{y(y+1)}\ [1+y(1-p)\ -e^{-Kyt}(1+y-pye^{-Kt})]$$
$$+ p^{x-2}\ (1-p)^2 \tag{26}$$

for chains of length $o < x < y$

and $n_{x_2} = p^{x-2}\ e^{-K(x-1)t}\ [1-p\ e^{-Kt}]^2 \tag{27}$

for chains of length $y < x < \infty$

The weight distribution, which gives the amount of polymer in grams of a certain chain length contained in one gram of initial material is obtained by multiplying equations (26) and (27) by x; hence:

$$m_{x_1} = \frac{2x\ p^{y-1}}{y(y+1)}\ [1+y(1-p)\ -\ e^{-Kyt}\ (1+y-pye^{-Kt})]$$
$$+ xp^{x-2}\ (1-p)^2 \tag{28}$$

for $o < x < y$, and

$$m_{x_2} = x\ p^{x-2}\ e^{-K(x-1)t}\ [1-p\ e^{-Kt}]^2$$

for $y < x < \infty$. \tag{29}

The two results represented by equations (28) and (29) can be represented in terms of the initial number average chain length P, viz.,

$$m_{x_1} = \frac{2x}{y(y+1)}\ (\frac{P}{P+1})^{y-1}[1 + \frac{y}{P+1} - e^{-Kyt}(1+y-\frac{Py}{P+1}\ e^{-Kt})]$$
$$+ x\ \frac{p^{x-2}}{(P+1)^x} \tag{30}$$

for $o < x < y$, and

$$m_{x_2} = x \left(\frac{P}{P+1}\right)^{x-2} e^{-K(x-1)t} \left[1 - \frac{P}{P+1} e^{-Kt}\right]^2 \qquad (31)$$

for $y < x < \infty$.

b. Weight-Average Chain Length.

Only the weight-average chain length after a time t will be calculated here, since all average chain lengths in this work are deduced from specific viscosity measurements.

The general expression for the weight average chain length is given by:

$$P_{w_t} = \frac{{}_o\!\int^\infty x\, m_x\, dx}{{}_o\!\int^\infty m_x\, dx} = \frac{{}_o\!\int^\infty x\, m_x\, dx}{1}$$

where P_{w_t} is the weight-average chain length after time t,

and m_x is the weight fraction of chains of length x if the total initial mass of the polymer sample is 1 gm.

$$\therefore P_{w_t} = {}_o\!\int^y x_1 m_{x_1}\, dx_1 + {}_y\!\int^\infty x_2 m_{x_2}\, dx_2$$

where $o < x_1 < y$ and $y < x_2 < \infty$

Substituting the values for m_{x_1} and m_{x_2} from equations (30) and (31) and assuming that:

$$\log(1 + \tfrac{1}{P}) \cong \tfrac{1}{P}$$

since $\frac{1}{P}$ is very small, we obtain for the weight average chain length at any time t, during the process of degradation

the expression:

$$P_{w_t} = \frac{2}{3} \frac{y^2}{y+1} \left(\frac{P}{P+1}\right)^{y-1} \left[1 + \frac{y}{P+1} - e^{-Kyt}(1+y - \frac{Py}{P+1}\cdot e^{-Kt})\right]$$

$$+ 2P - \frac{P^{y-1}}{(P+1)^y} (2P^2 + y^2 + 2yP)$$

$$+ \left(\frac{P}{P+1}\right)^{y-2} \frac{P\ e^{-K(y-1)t}}{PKt+1} (1 - \frac{P\cdot e^{-Kt}}{P+1})^2 [y^2 + \frac{2yP}{PKt+1} + \frac{2P^2}{(PKt+1)^2}]$$

$$(32)$$

Introducing the relation $\alpha = 1 - e^{-Kt}$ or $e^{-Kt} = 1 - \alpha$, the weight average chain length can be explicitly expressed in its final form, viz;

$$P_{w_t} = \frac{2}{3} \frac{y^2}{(y+1)} \left(\frac{P}{P+1}\right)^{y-1} \left\{1 + \frac{y}{P+1} - (1-\alpha)^y [\frac{1+y+P(1+\alpha y)}{P+1}] \right\}$$

$$+ 2P - \frac{P^{y-1}}{(P+1)^y} (2P^2 + y^2 + 2yP)$$

$$+ \frac{P^{y-1}}{(P+1)^y}\cdot \frac{(1-\alpha)^{y-1}}{PKt+1}(1+\alpha P)^2 [y^2 + \frac{2yP}{PKt+1} + \frac{2P^2}{(PKt+1)^2}] \quad (33)$$

After an infinite time of degradation, i.e., $t = \infty$

$$P_{w_\infty} = \frac{2}{3} \frac{y^2}{y+1} \left(\frac{P}{P+1}\right)^{y-1}(1 + \frac{y}{P}) + 2P - \frac{P^{y-1}}{(P+1)^y}[2P^2+y^2+2yP] \quad (34)$$

Rearranging the terms, the equation can be put in the form:

$$P_{w_\infty} = 2P - 2P \left(\frac{P}{P+1}\right)^y [1 + \frac{2}{3}\frac{y}{P} + \frac{y^2}{6P^2}] \quad (35)$$

or $$2P - P_{w_\infty} = 2P\left(\frac{P}{P+1}\right)^y [1 + \frac{2}{3}\frac{y}{P} + \frac{y^2}{6P^2}] \quad (36)$$

Expressions (35) and (36) give the weight-average chain length at the end of degradation in terms of the initial number-average chain length P_o. The final form of this expression in terms of the initial weight-average chain length is given by:

$$P_{w_o} - P_{w_\infty} = P_{w_o} \left(\frac{P_{w_o}}{P_{w_\infty} + 2} \right)^y \left[1 + \frac{4v}{3P_{w_o}} + \frac{2}{3} \frac{y^2}{P_{w_o}^2} \right] \qquad (37)$$

where P_{w_o} is the initial weight average chain length of the polymer sample.

For an addition polymer $P_w = 2P$, a relation which can be deduced from equation (33) by considering the value of P_{w_t} at the start, i.e., at $t = o$.

E. Discussion.

The general solution given in this Chapter is hoped to be of value in solving any kinetics problem which involves similar set of rate equations. It only involves the substi-:tution of the new values of coefficients a_z, a_{zz} to determine the values of α's, β's and γ's. These values and the boundary condition at $t = o$ when substituted in the general matrix equation (19) give an explicit solution of the specific kinetics problem. This was attempted by the author to solve a few other cases which are not relevant to the work undertaken in this thesis.
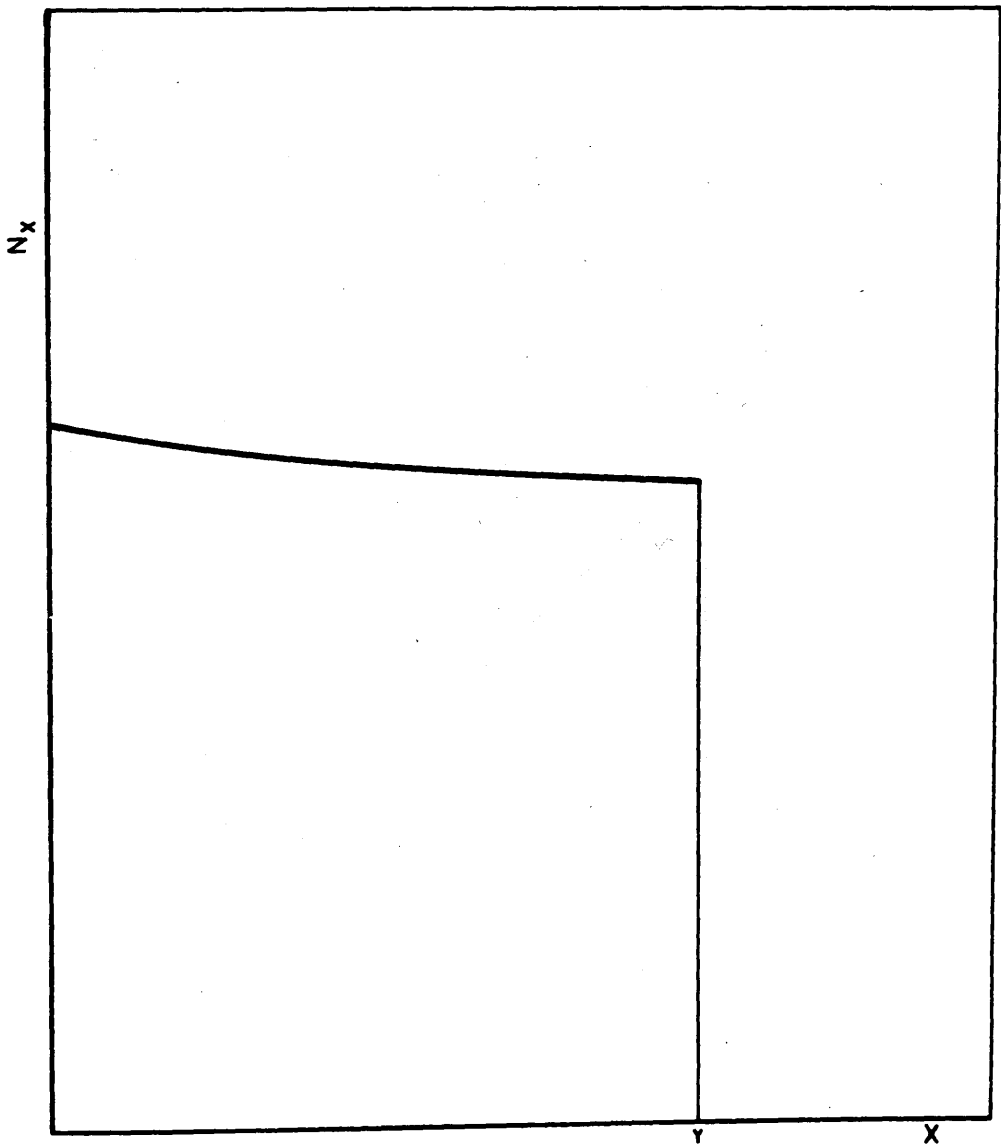
FIG. 35.   FINAL NUMBER DISTRIBUTION.
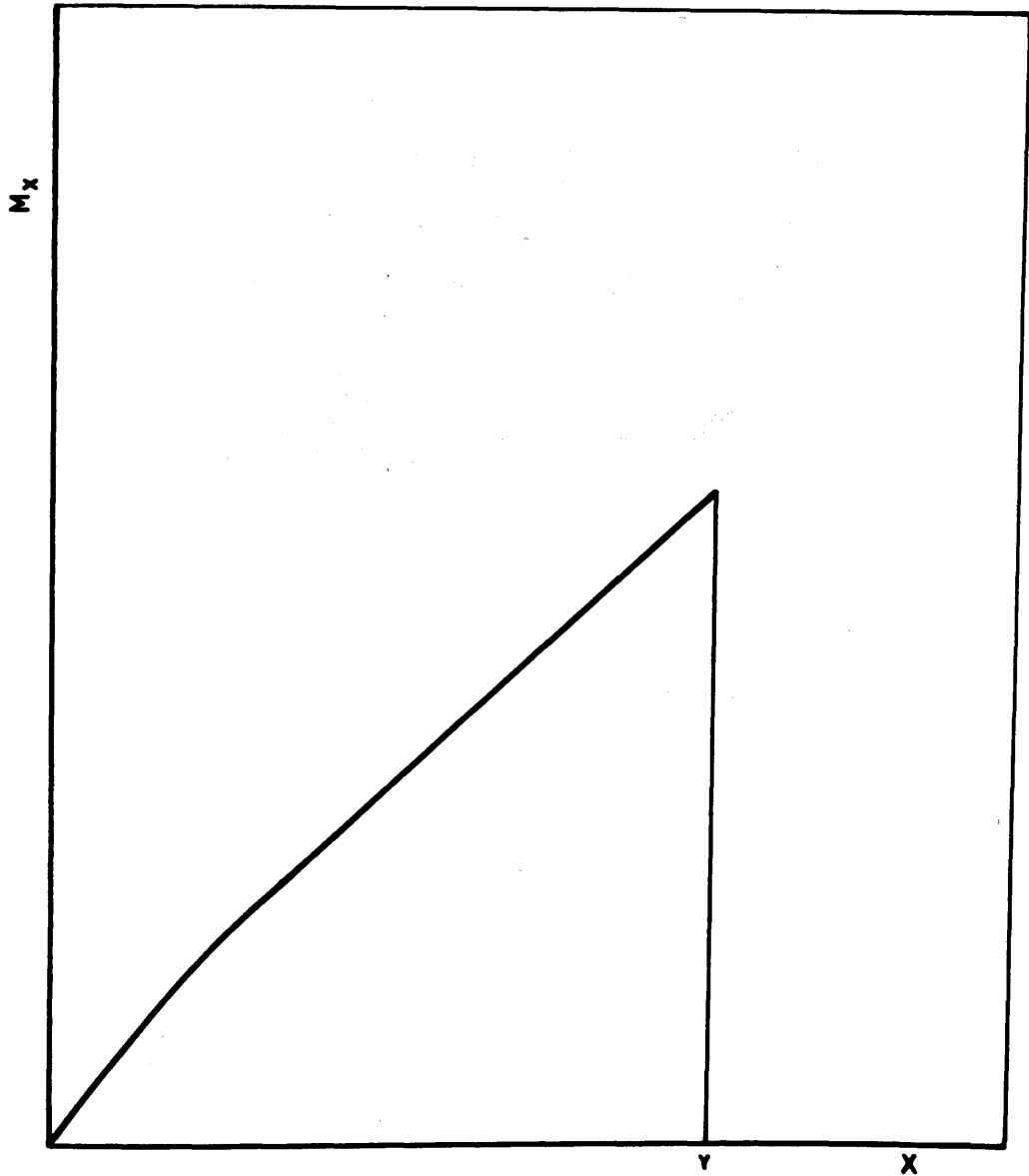
FIG. 36.   FINAL WEIGHT DISTRIBUTION.

The general solution, applied to a heterogeneous-addition-polymer sample, shows two points of interest which differ from solutions given by other authors.

(i)   The first result shows that the number of chains for chain lengths 1 to y at the end of degradation, i.e. at t=∞, is not equal but depends on the chain length, as seen from equation (26):

$$n_{x_1} = \frac{2p^{y-1}}{y(y+1)}\ [1 + y(1-p)] + p^{x-2}(1-p)^2$$
$$= A + B\ p^x$$

where A and B are constants and p is less than one.

This result gives a final number distribution as shown in Fig. 35 in which the number of chains decreases as the chain length increases from 1 to y, i.e., $1 < x < y$.

Furthermore, the final weight distribution is a curve (Fig. 36) whose shape is dependent on the initial average chain length P.   It also depends on the intensity of the ultrasonic waves since it is the main factor controlling the value of the limiting chain length 'y', below which it was assumed that no degradation takes place.

Compared with Jellinek's results[4] obtained after nine hours of degradation the shape of the curve in Fig. 36 seems a better fit to his results than his straight line representing the final weight distribution, in spite of the

fact that the polymer used in his case was a homogeneous sample (fractionated sample). The difference between the two results is mainly due to the boundary conditions considered for the determination of the constant of integration C in equation (25).

(ii)   The second result as expressed in equation (35) shows that the final weight average chain length P_{w_∞} depends mainly on the intermediate chain length y below which no degradation can take place, and to a certain extent on the initial weight average chain length P_{w_0}.   However, all previous work reported indicated that the final weight average chain length is inde-:pendent of the initial weight average chain length provided all other factors were unaltered.   The author is inclined not to disagree with this statement as it was observed that the final weight average chain length varies very slightly with changes in the initial weight average chain length of the polymer sample.

However, it is of interest to see the significance of the term P representing the initial average chain length in the formula giving the weight average chain length on the above mentioned basis.

Considering equation (35) and assuming that P_{w_∞} is independent of P, we get:

$$\frac{d\,P_{w_\infty}}{dP} = \frac{\partial\,P_{w_\infty}}{\partial P} + \frac{\partial\,P_{w_\infty}}{\partial y}\ \frac{dy}{dP} = 0$$

Working out the relevant differentiations we get:

$$\frac{dy}{dP} = -\frac{(\frac{P+1}{P})^y - \frac{y}{P+1}(1 + \frac{2y}{3P} + \frac{y^2}{6P^2}) - (1 - \frac{y^2}{6P^2})}{\frac{1}{3} + \frac{y}{3P} + \frac{y^2}{6P^2}} \qquad (38)$$

Equation (38) gives a negative value for $\frac{dy}{dP}$ and substituting

some of the experimental results obtained, we get:

for $P = 1620$ $\quad \frac{dy}{dP} = -0.0042,$ and $\left.\begin{array}{c} \\ \end{array}\right)$

for $P = 1208$ $\quad \frac{dy}{dP} = -0.012147$ $\qquad)$ $\qquad\qquad (39)$

This indicates that as the initial average chain length

decreases the value of the limiting chain length would slightly

increase.   This slight increase can be interpreted in the

light of Schmid's mechanism for the degradation of polymers

by ultrasonic waves.   In other words, as the initial average

chain length decreases the effective frictional force per

monomer unit would decrease.   Therefore, in order to break

a C-C bond by such mechanism the limiting chain length y

would have to be bigger.

However, this dependence of y on P seems qualitatively

to be consistent with Schmid's theory for the degradation of

long chain molecules by ultrasonic waves.

BIBLIOGRAPHY.

1.   Schmid, G., Paret, G. and Pfleiderer, H.
        Kolloid Z.   124, 150 (1951).

     Schmid, G.
        Z. Phys. Chem.   186A, 113 (1940).

2.   Jellinek, H.H.G. and White, G.
        J. Polymer Sci.   6, 745 (1951).

3.   Simha, R.
        J. Appl. Phys.   12, 569 (1941).

4.   Jellinek, H.H.G. and White, G.
        J. Polymer Sci.   6, 757 (1951).

N.B.   The general solution reported in this Chapter was published in the Journal of Polymer Science. Volume 22, p.p. 535 (1956).   Another paper, including the application of the theory is to appear in the same Journal soon.

CHAPTER V.

DEGRADATION OF ADDITION POLYMERS
BY ULTRASONIC WAVES.

EXPERIMENTAL.

INTRODUCTION.

The investigations reported in this chapter were carried out with two objectives in view, namely:

1. To check the validity of the theory of degradation of addition polymers by ultrasonic waves given in Chapter IV. This part of the investigations covers the following topics:

A. Analysis of samples of polystyrene in benzene solution at different stages of the degradation process.

B. Measuring the number of cuts (broken links) taking place during a specified period of degradation.

C. Application of Schmid's theory to values of chain length of the polystyrene sample during degradation.

2. To investigate the effect of different factors on the degradation parameters 'K' and 'y' as a prerequisite for a better understanding of the mechanism of ultrasonic degra-:dation. This part of the investigations covers the following points.

A. Effect of intensity of ultrasonic waves on the rate constant of degradation 'K' and limiting chain length 'y'.

B. Effect of initial value of chain length on the rate constant of degradation 'K' and limiting chain length 'y'.

C. Effect of frequency of ultrasonic waves on degra-
   :dation parameters K and y with special reference
   to cavitation.

D. Effect of suppressing cavitation on degradation
   parameters.

The role of cavitation is discussed whenever relevant
to the interpretation of results.   It should be pointed
out that a simplified solution of the rate equations has
been developed to enable the determination of the rate
constant of degradation 'K' at the beginning of degradation
without carrying complete runs (35 hours).

PART 1.

VERIFICATION OF THEORY.

A. PRELIMINARY.

(a) Sample preparation:

The polystyrene samples used in the investigations to follow were prepared in the conventional way. Styrene mon-:omer, freed from inhibitor, washed, dried, distilled under reduced pressure, was then left to polymerise under vacuum for three days in thermostatically controlled baths at temper-:atures of $120 \pm 0.5^{\circ}C$. $100 \pm 0.5^{\circ}C$. $80 \pm 0.5^{\circ}C$. and $65 \pm 0.5^{\circ}C$.

The polymer was separated from styrene monomer by pre-:paring a very dilute solution of the resulting polymer-monomer mixture in benzene and then precipitating the polymer using methyl alcohol as precipitant. The polymer extracted was then dried in an oven maintained at a temperature of $40 \pm 0.5^{\circ}C$. for 48 hours.

(b) Reproducibility of results.

The care taken in designing and constructing the push-:pull ultrasonic generator was to ensure a stable performance. Furthermore the crystal holder (Fig.17) mounted on a base of a travelling microscope and the reaction vessel (Fig.30) fitting in a platform fixed to the stand of the microscope
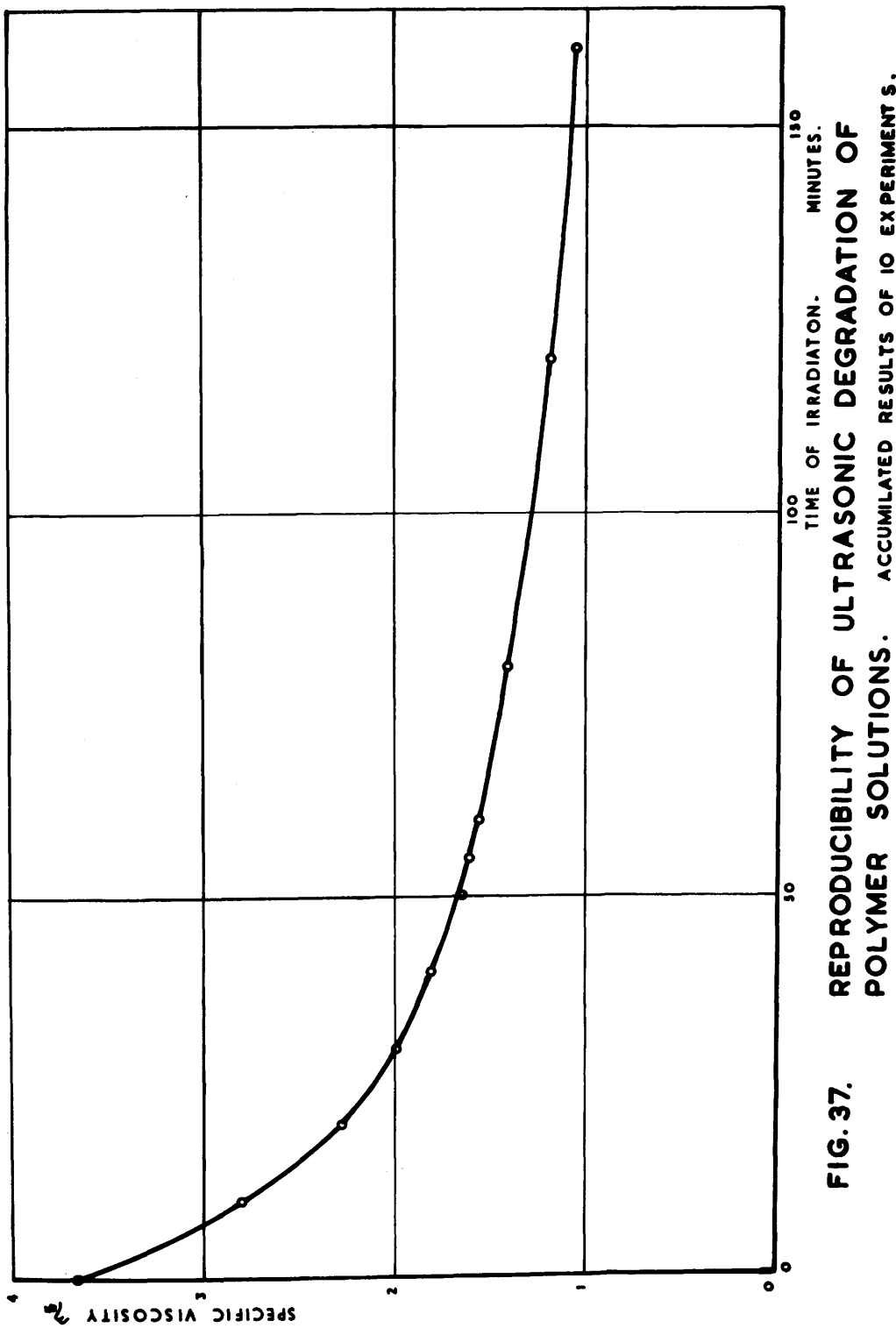
FIG. 37.   REPRODUCIBILITY OF ULTRASONIC DEGRADATION OF
POLYMER SOLUTIONS.   ACCUMILATED RESULTS OF 10 EXPERIMENT S.

made it possible to carry out any number of tests under exactly the same conditions.

In order to check experimentally the reproducibility of results under the above mentioned conditions and conse-:quently the consistency of the process of degradation ten 1% wt/vol. polystyrene in benzene samples were irradiated by the ultrasonic beam. The volume of each sample was 25 ml. and viscosity measurements were taken at various stages of degradation. The results of all the different tests are compiled and represented in Fig. 37. It is apparent from this figure that the ultrasonic generator performance is very stable and that a high degree of reproducibility has been achieved.

B. EXPERIMENTAL - DEGRADATION PARAMETERS.

25 ml. of a 1% polystyrene in benzene sample was intro-:duced in the reaction vessel of Fig. 30. The sample was then irradiated by an ultrasonic beam of frequency 0.75 Mc/sec. and intensity 12.5 watts/cm^2. in the solution proper. The degradation process was followed viscometrically by measur-:ing the specific viscosity at different stages of degradation. The corresponding weight average chain lengths were calculated from these referee viscosity measurements as mentioned in Chapter III. The weight average chain length P_{w_t} changed
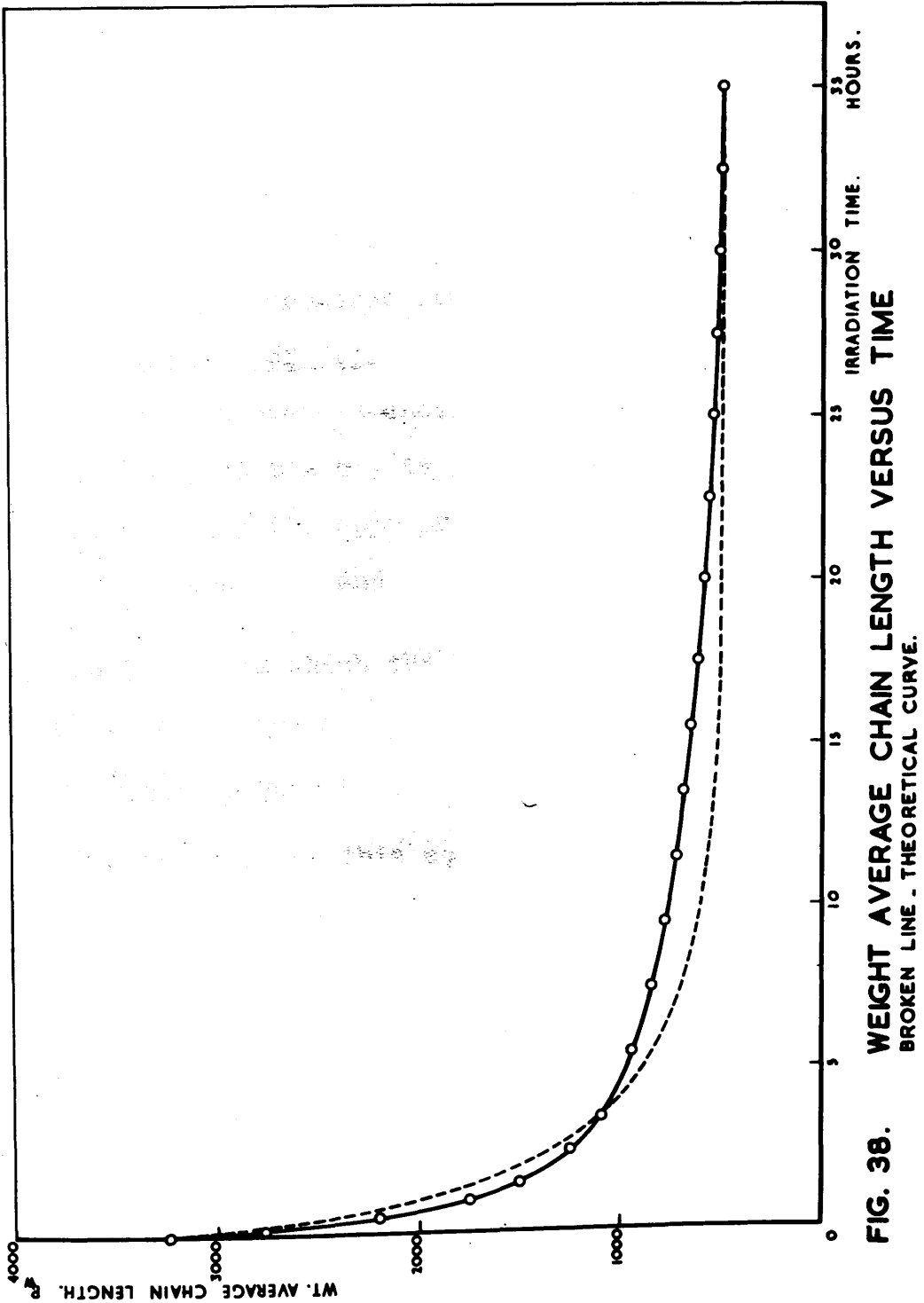
FIG. 38.   WEIGHT AVERAGE CHAIN LENGTH VERSUS TIME
BROKEN LINE - THEORETICAL CURVE.

with time of degradation in the manner shown in Fig. 38.
Details of degradation results are given in Table II.

It can be seen from Fig. 38 that the weight average
chain length 'P_w' decreases rapidly at the beginning of
degradation, consistent with a random type of degradation,
and then slowly approaches its final value of 494.

(a) Determination of 'y'.

The weight average chain length at the end of degra-
:dation, i.e., at $t = \infty$, is given by equation (37) in Chapter
IV. Introducing the appropriate values of $P_{w_\infty} \not{} P_{w_0}$, namely:

$$P_{w_\infty} = 495 \qquad \text{and} \qquad P_{w_0} = 3240$$

equation (37) from which the limiting chain length 'y' was
determined is given by:

$$2745 \left(\tfrac{1621}{1620}\right)^y = 3240 \left[1 + \tfrac{y}{2430} + \tfrac{2}{3}\left(\tfrac{y}{3240}\right)^2\right] \qquad (1)$$

The solution of this equation gave a value of 744 for
'y' the limiting chain length. It should be mentioned that
due to the nature of equation (1) and all similar equations
a seven figure logarithmic table was found necessary for
working out all calculations.

(b) Determination of K.

The value of the weight average chain length P_{w_t} at
any time 't' during the degradation process is given by
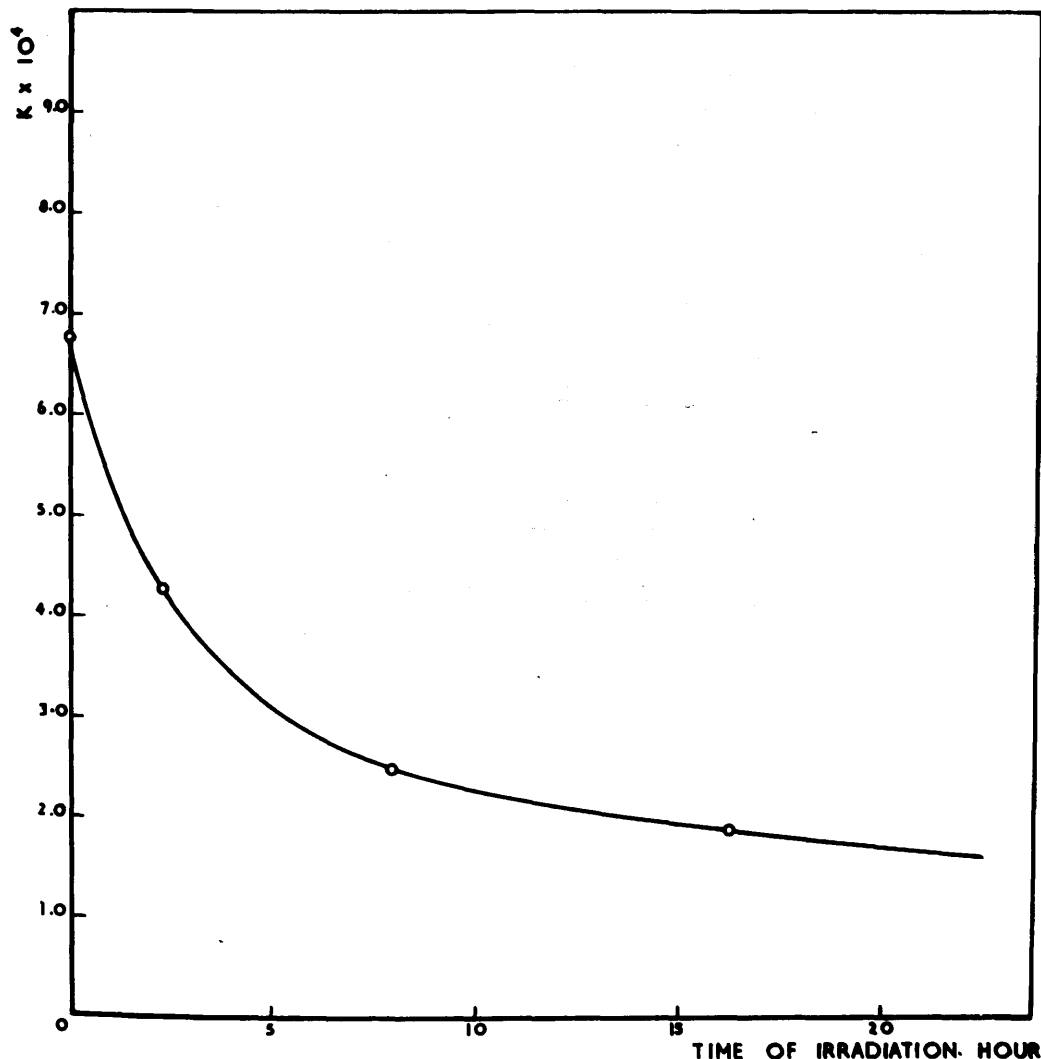
FIG. 39. RATE CONSTANT OF DEGRADATION AT DIFFERENT STAGES OF DEGRADATION.

equation (33) Chapter IV, where α is a function of time.

Values of P_{w_t} were therefore calculated from equation (33) for assumed values of α after substituting the above mentioned values of P_{w_o} and y. The times corresponding to these calculated values of P_{w_t} were then read from the degra-:dation curve in Fig. 38 and the rate constant K, at these values of P_{w_t} and t, was calculated from the relation:

$$K = \frac{1}{t} \log \frac{1}{1-\alpha} \qquad (2)$$

The results of these calculations are presented in Table III, from which it can be seen that the value of K decreases gradually, almost exponentially, as the degradation process continues, as shown in Fig. 39. The decrease in the value of 'K' confirms in a general sense that the rate constant of degradation depends on the chain length as mentioned at the beginning of Chapter IV. It also indicates, that there is a minimum chain length below which degradation ceases to take place. However, in taking an average value for K it was considered reasonable to select the value that offered the best agreement with the experimental results. The value of $K = 3.5 \times 10^{-4} (hr.^{-1})$ was therefore selected. This value of K was used for determining the theoretical values of P_{w_t} at different stages of degradation. These calculated values of P_{w_t} are plotted against time of irradiation as shown by

the dotted line in Fig.38.   The agreement with the experi-
:mental curve appears to be satisfactory.   As it was anti-
:cipated the initial part of the theoretical curve lies above
the experimental since the average value of K used in equation
(33) is less than that determined for this part of degrada-
:tion.   The actual degradation appears, for this reason, to
be more rapid at the early stages of degradation while at
the later stages it is slower than theory predicts since the
theoretical value of K is greater than the experimental.

C. WEIGHT DISTRIBUTION ANALYSIS.

25 c.c. of 1% polystyrene in benzene sample was irrad-
:iated in each run.   In order to facilitate the process of
fractionation it was decided to repeat each run twice to
provide a sufficient amount of polymer for fractionation.
Each fractionated sample was 40 ml. of 1% wt/vol. polystyrene
in benzene, i.e., 0.4 gm. of polystyrene.

The usual fractionation procedure was adopted, using
benzene as solvent and distilled methanol as precipitant, to
fractionate a 25 ml. sample after 35 hours degradation.   The
procedure proved satisfactory for the first fraction but the
other fractions gave some trouble as they showed a tendency
to gel formation.

Particulars of the first fraction were:

Weight of fraction decanted = 0.0166 gms.

η_{sp} of a 0.5% solution in benzene = 0.282

and $[\eta]$ = 5.52

The procedure of determining $[\eta]$ is discussed in Chapter III. Using Staudinger Equation $[\eta]$ = K.P. where K is a constant = $8.0x10^{-3}$ for polystyrene in benzene solution, an approximate value of P_W for the first fraction was 690. This is in agreement with the theoretical value of 744 cal-:culated for the limiting chain length below which no degra-:dation takes place. This result served as a repliminary check on the validity of the theory given in Chapter IV.

The procedure finally adopted for fractionation was as follows: 40 ml. of each sample was evaporated to dryness under vacuum, the temperature not being allowed to rise above $40^{\circ}C$ during evaporation. The solid polymer was redissolved in 100 ml. methyl ethyl ketone and fractionated using distilled methyl alcohol as precipitant. The last fraction which contains the shortest chain lengths was extracted by evapor-:ating the remaining solution under vacuum keeping the tem-:perature of the solution below $40^{\circ}C$. This method was pre-:ferred as the loss of very low molecular weight polymer from the fraction was avoided since such molecules are not usually

precipitated on adding methyl alcohol. Each fraction was carefully dried to a constant weight in an oven maintained at 40°C. Fresh 0.5% solutions in benzene were prepared from each fraction and the intrinsic viscosity determined follow-:ing the procedure explained in Chapter III, using specially designed micro-viscometer. Finally, the chain length was determined using the Staudinger formula previously mentioned.

The results of fractionation are given in Table IV.

The weight distributions of the samples have been cal-:culated by graphic differentiation of the integral weight curves ($\int$ dW) which were derived from the weight fractions (dW) by assuming that half the weight of each fraction lies above, and half below, the measured chain length. The total weight of polymer, consisting of chain lengths up to that value was obtained by summing the weights of the fractions of smaller chain lengths and adding to this sum half the weight of the fraction having the chain length under consideration. The integral weights, designated by $\int$ dW are shown in the last column of Table IV.

The theoretical weight distributions were calculated from equations (30) and (31) Chapter IV, which give the weight distribution functions m_{x_1} and m_{x_2} for chain lengths $0 < x_1 < y$, and $y < x_2 < \infty$ respectively. The results of
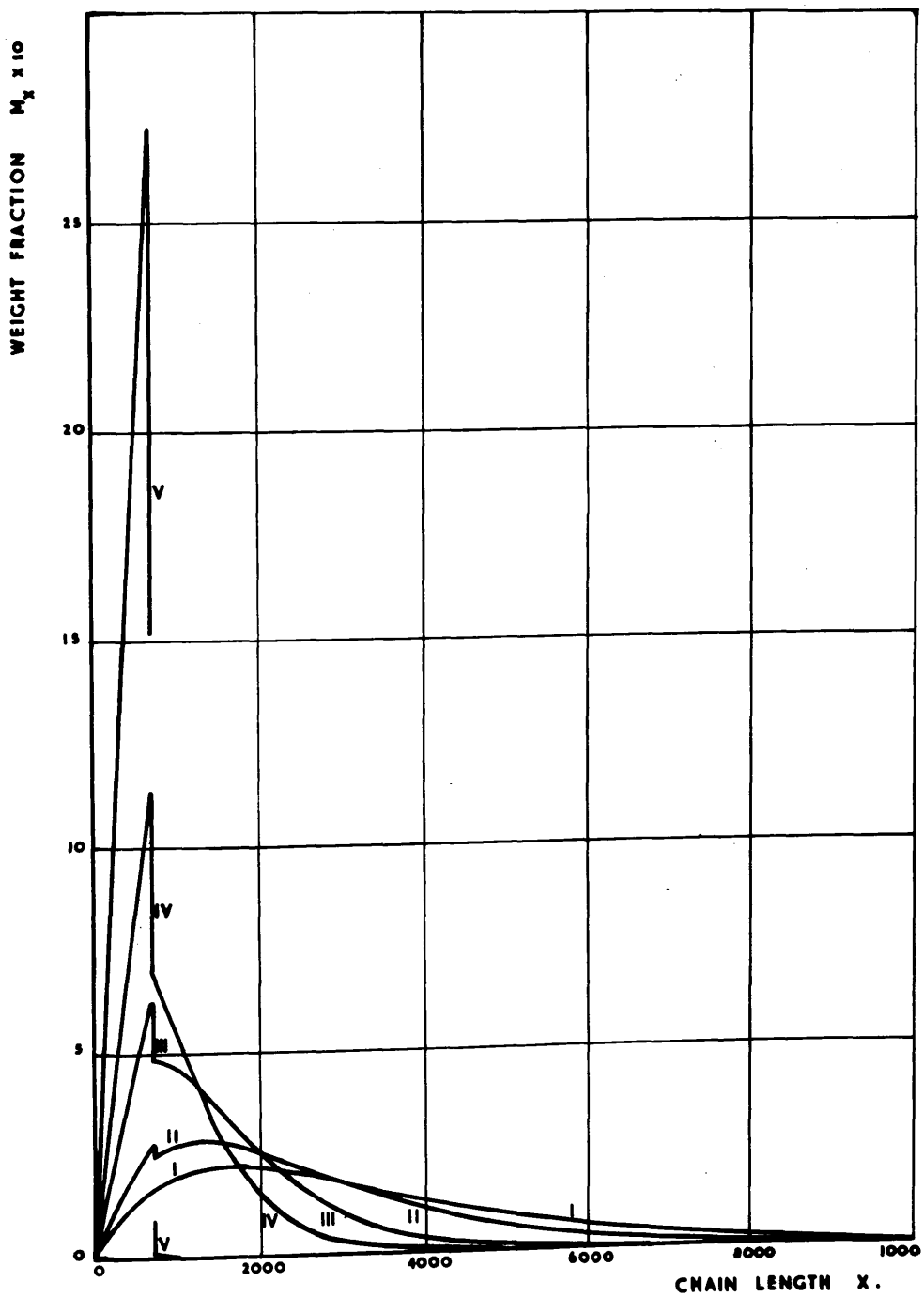
FIG. 40. THEORETICAL WEIGHT DISTRIBUTION CURVES
I. INITIAL DISTRIBUTION   II. 1/2 HOUR   III. 2 HOURS   IV. 4 HOURS
V. 35 HOURS OF IRRADIATION.
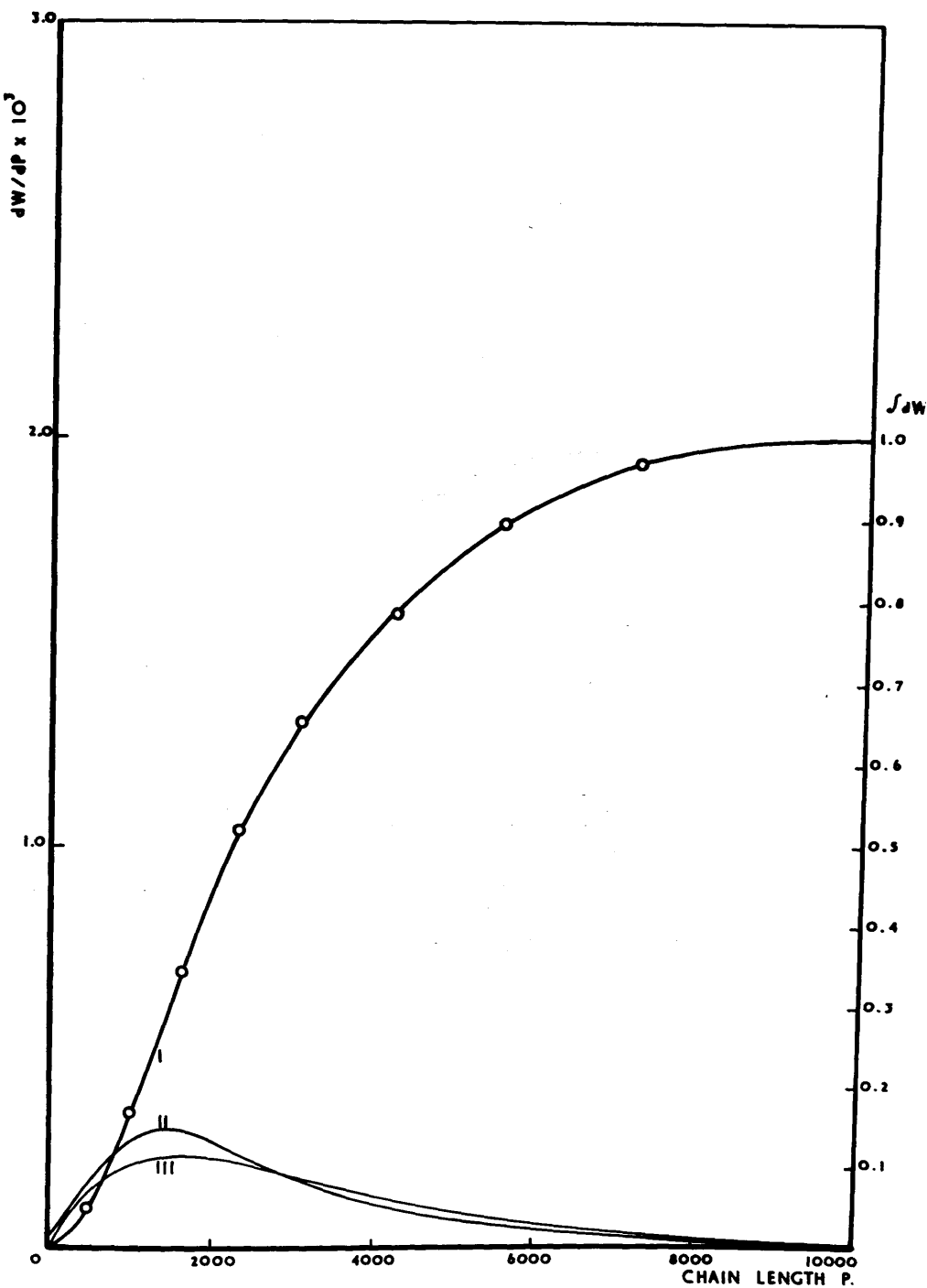
FIG.41. POLYSTYRENE SAMPLE BEFORE THE DEGRADATION. I. INTEGRAL DISTRIBUTION CURVE. II. EXPERIMENTAL DISTRIBUTION. III. THEORETICAL DISTRIBUTION
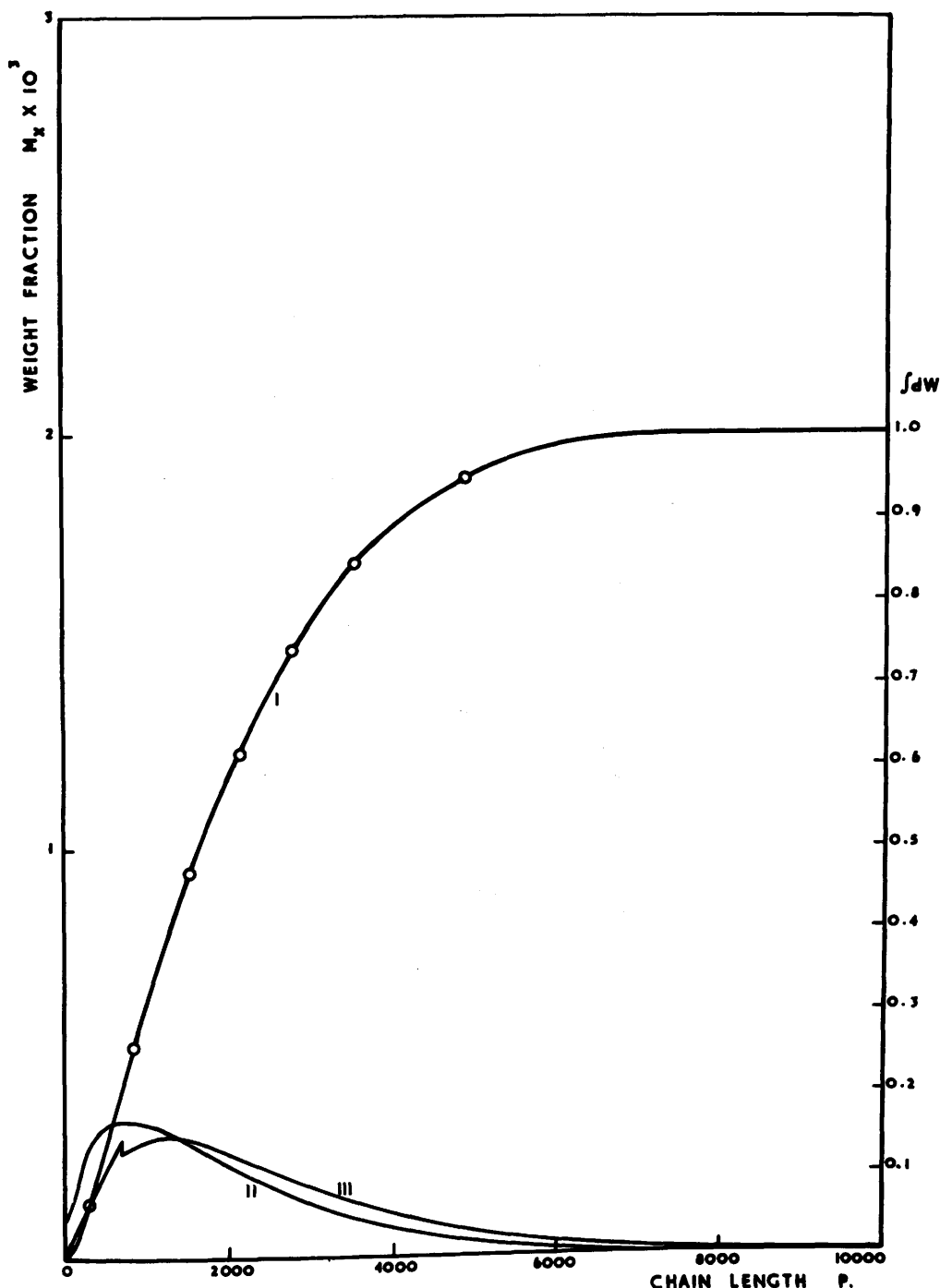
FIG. 42.   CHAIN LENGTH WEIGHT DISTRIBUTIONS AFTER HALF HOUR DEGRADATION. $P_w = 2203.$

I. INTEGRAL   II. EXPERIMENTAL   III. THEORETICAL
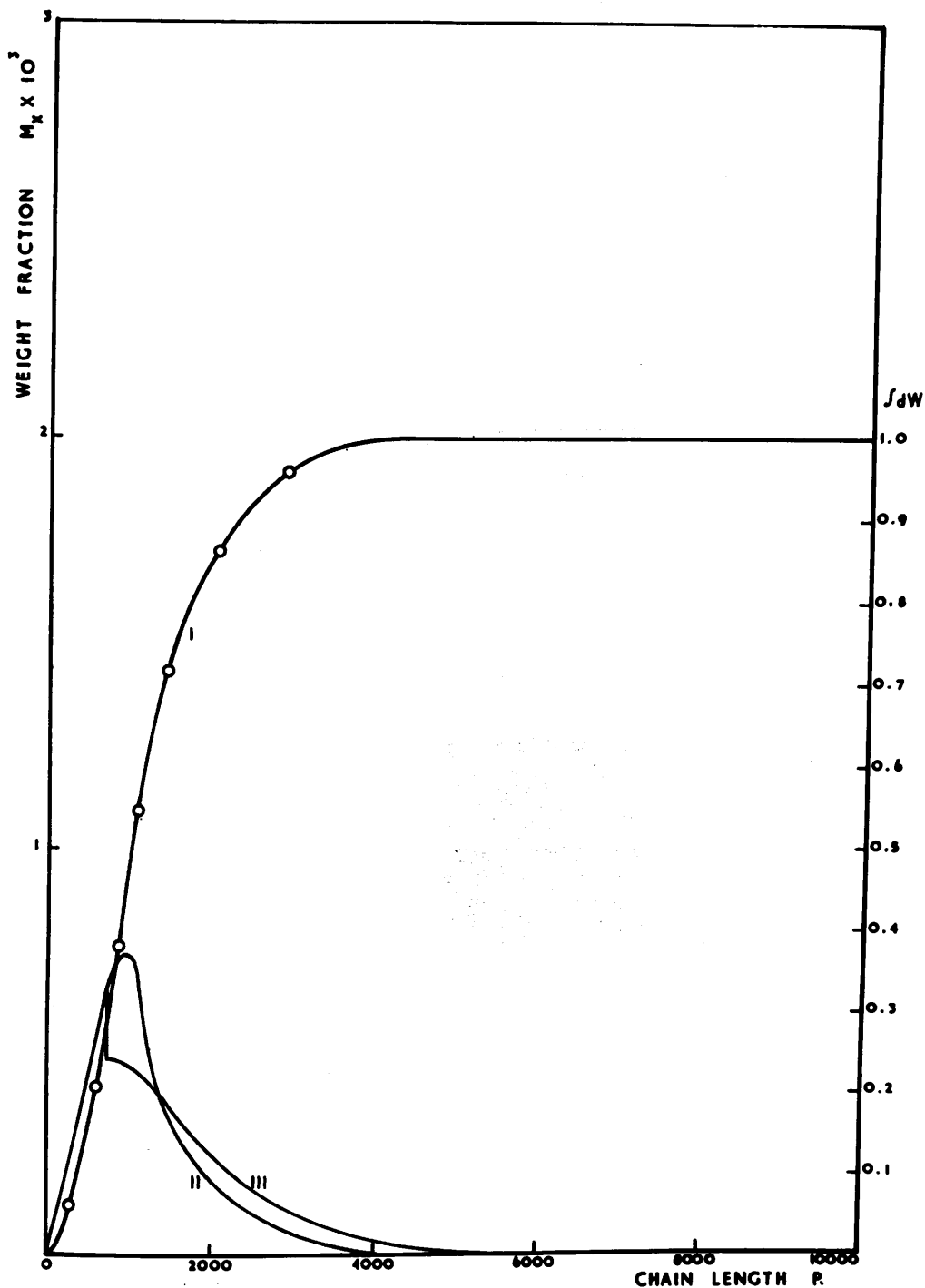
FIG. 43. CHAIN LENGTH WEIGHT DISTRIBUTIONS AFTER TWO HOURS DEGRADATION. $P_W = 1360$.
I. INTEGRAL   II. EXPERIMENTAL   III. THEORETICAL.
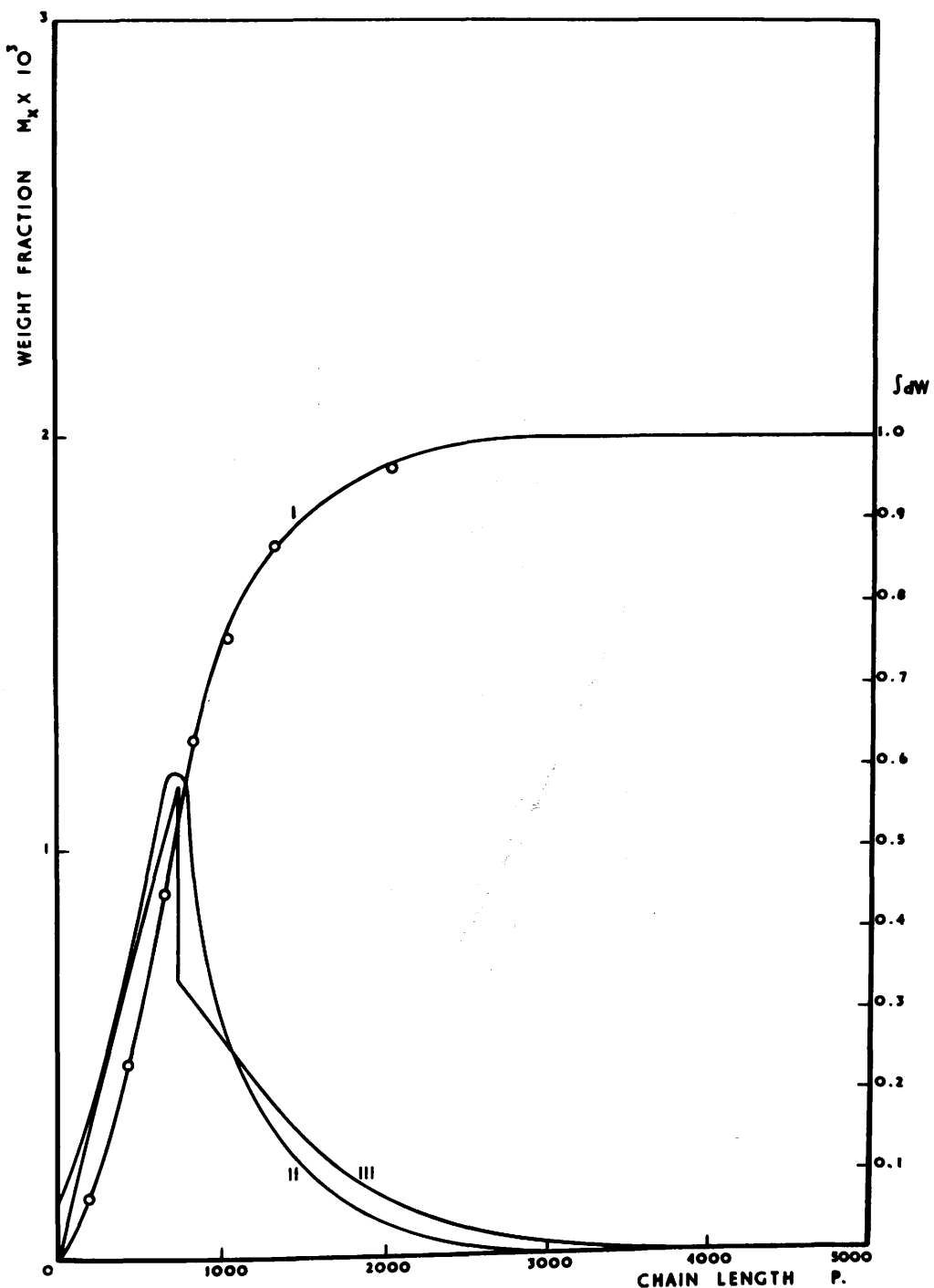
FIG. 44.　CHAIN LENGTH WEIGHT DISTRIBUTIONS AFTER FOUR HOURS DEGRADATION. $P_0 = 1044$
I. INTEGRAL　　II. EXPERIMENTAL　　III. THEORETICAL
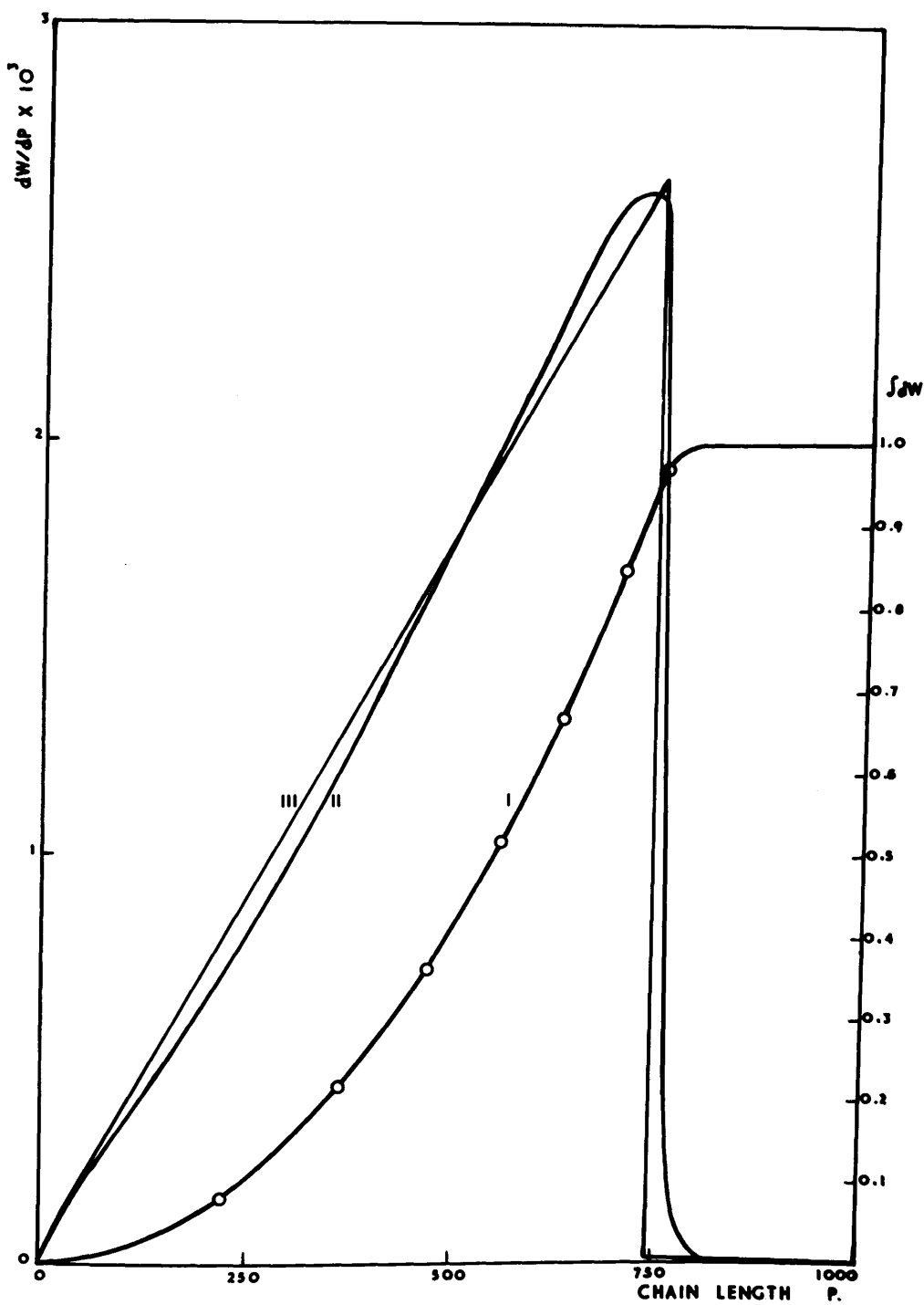
FIG. 45.   POLYSTYRENE   SAMPLE   AFTER 35 HOURS   OF   DEGRADATION.
I. INTEGRAL   DISTRIBUTION   CURVE   II. EXPERIMENTAL   DISTRIBUTION
III. THEORETICAL   DISTRIBUTION.

these calculations are shown in Table V.

The theoretical weight distributions at $t=0$, $\frac{1}{2}$, 2, 4, and 35 hours are shown in Fig.40. The figure illustrates, from theoretical considerations, the way in which the process of degradation would affect the chain length weight distri= :butions at its different stages. Figs. 41, 42, 43, 44, 45, show the theoretical weight distributions, the integral weight distribution curves and the deduced experimental weight distributions at the above mentioned stages of degradation. The area under the weight distribution curve is normalised to represent 1 gm. of polymer.

Inspection of the above figures shows that there are discrepancies between the theoretical and experimental distri= :butions. These discrepancies are thought to be due to the fact that the rate constant of degradation actually decreased in value with time while it was considered to be constant, for chain lengths between y and infinity, at all times. This may account for the smaller number of long chains in the experimental weight distribution curves at $t = \frac{1}{2}$ and 2 hours.

The sudden discontinuities at $P = 744$ in the theoretical curves are a consequence of the assumption made in the theor= :etical treatment undertaken. It was assumed that there is a discontinuity in the rate constant at the intermediate chain length y.

The experimental value of the limiting chain length y below which degradation ceases to take place is nearly the same value as that obtained from theory.   The close agreement between the theoretical and experimental distribution curves is considered to be a fair verification of the theoretical treatment undertaken in Chapter IV.

D. MEASUREMENT OF NUMBER OF CUTS.

As mentioned in Chapter III, the use of D.P.P.H. was contemplated in the hope that it would throw more light on the mechanism of degradation and termination of broken long chain molecules.   Moreover, it was hoped that further evid-:ence would be established in support of the theory developed in Chapter IV describing the kinetics of the process of degradation of addition polymers by ultrasonic waves.

The number of broken links which is the same as the number of newly created molecules is given by the relation:

Total number of broken links per unit time

$$= {_0}\!\int^{\infty} \frac{dN_x}{dt} \, dx$$

i.e. $${_0}\!\int^{y} \frac{dN_{x_1}}{dt} \, dx_1 \; + \; {_y}\!\int^{\infty} \frac{dN_{x_2}}{dt} \, dx_2$$

Equations (25) and (21), Chapter IV, give explicit values of N_{x_1} and N_{x_2} respectively.   By differentiating with respect to time the following relations are obtained, viz.,

$$\frac{dN_{x_1}}{dt} = 2 N_o K p^y e^{-Kyt}[1 - p e^{-Kt}] \ldots \ldots \text{ and}$$

$$\frac{dN_{x_2}}{dt} = N_o K p^{x-1} (1 - pe^{-Kt}) e^{-K(x-1)t}[1 + pe^{-Kt} - x(1 - pe^{-Kt})] \quad (2)$$

Introducing the 'α' transformation, the total number of broken links per unit time in chains $o < x < y$ in terms of P will be given by:

$$\int_o^y \frac{dN_{x_1}}{dt} dx_1 = \frac{2yKN_o}{P+1}(1-\alpha)^y (1+P\alpha)\left(\frac{P}{P+1}\right)^y \quad (3)$$

Similarly for $y < x < \infty$

$$\int_y^\infty \frac{dN_{x_2}}{dt} dx_2 = \frac{N_o K(1+P\alpha)}{(P+1)(PKt+1)} \left(\frac{P}{P+1}\right)^y (1-\alpha)^{y-1}[1 + 2P - P\alpha - y(1+P\alpha)$$
$$- \frac{P(1+P\alpha)}{PKt+1}] \quad (4)$$

The sum of equations (3) and (4) gives the total number of newly created molecules per unit time which is the total number of scissions per unit time. Hence the average rate of scission can be determined during any specific stage of the degradation process. Consequently the total number of cuts that took place during any of the early stages of degra-:dation can be calculated from the theory while the same number of cuts can be measured experimentally from the change in the absorption values of the D.P.P.H.

The relation between the calculated and measured

values of the number of scissions should be linear only if
the mechanism of degradation is purely mechanical. If, on
the other hand, the mechanism of degradation is complex, i.e.,
there may exist some chemical reaction - peroxidation or other-
:wise taking place - which reacts with the D.P.P.H., the linear
relation will not hold.

As mentioned earlier in this Chapter the rate constant
of degradation 'K' decreases with time in the manner shown
in Fig. 39. Because of this decrease in the value of 'K'
with time, it was decided to calculate the number of cuts by
three different methods, viz.,

(i)   Integrating equations 21 and 25 with respect to the
chain length x, between the appropriate limits, gives the
total number of molecules at any time. The difference between
the total number of molecules at any time t and the number of
molecules at t=o, gives the total number of newly created
molecules which is the same as the total number of links
broken during the same interval. The average value of K was
used in this calculation.

(ii)   Using the average value for 'K' obtained previously,
equations 3 and 4 give the total number of links broken per
unit time at any instant. An average rate of scission of
links during a specific interval can thus be obtained and
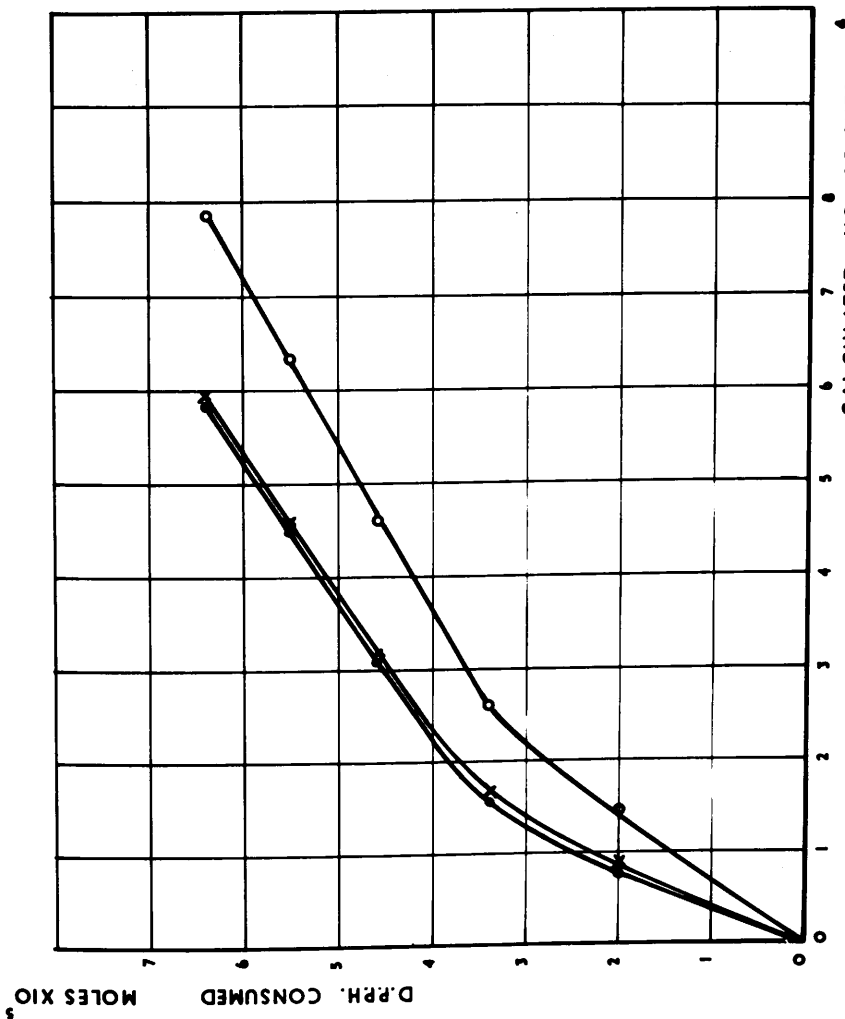
FIG. 46. THEORETICAL VERSUS EXPERIMENTAL
NUMBER OF BROKEN LINKS.

•. DIFFERENCE METHOD   x. CONSTANT K METHOD

o. VARIABLE K METHOD

and consequently the number of links broken during this period
can be calculated.

(iii)   The same as method (ii) but using the appropriate
values of K given in Fig. 39.

The results of these calculations are shown in Tables
VI, VII and VIII.

As shown in Table VI the number of cuts were calculated
over a period of two hours only.   This is due to the fact
that during two hours of irradiation most of the D.P.P.H. was
exhausted and any measurements of absorption below that low
level would be erratic. A blind run with a solution of D.P.P.H.
in sulphur and moisture free benzene was carried out.   The
solution was irradiated by 0.75 Mc/sec. ultrasonic waves of
intensity 12.5 watts/cm^2. (in the solution proper) for two
hours and the absorption was measured every half hour.

A 1% weight by volume sample of polystyrene in sulphur-
moisture-free benzene with D.P.P.H. was then irradiated by
ultrasonic waves of the same intensity, and absorption and
viscosity measurements were carried out at different stages
of degradation.   The results are shown in Table IX as well
as the accumulated calculations of number of scissions.

Fig. 46 shows the relation between the number of broken
links determined experimentally as a function of D.P.P.H.
exhausted against the corresponding number of broken links

calculated from theory as a function of the initial total number of monomer units. The three methods gave, broadly speaking, identical results. Methods (i) and (ii) gave nearly the same result since the same average value of the rate constant 'K' was used. They both differed quantitat-:ively from method (iii) in which a variable rate constant of degradation was used.

Two points of interest can be deduced from the general shape of the curves in Fig.46, namely:

1. There is a linear relationship between the theoretical and experimental values of the number of broken links after nearly half an hour of irradiation. This implies a close agreement between the number of broken links determined experimentally and that predicted from theory.

2. The change in slope of the lines and the slight curvature noticeable during the first half hour of irradiation is not easy to interpret without further experiments. However, it is safe to say that the D.P.P.H. molecules are exhausted during the first half hour at a quicker rate than the theory predicts. Phenomena, associated with cavitation, seem to be a possible cause for such behaviour. These may have a direct effect on the D.P.P.H. or may give rise to some kind
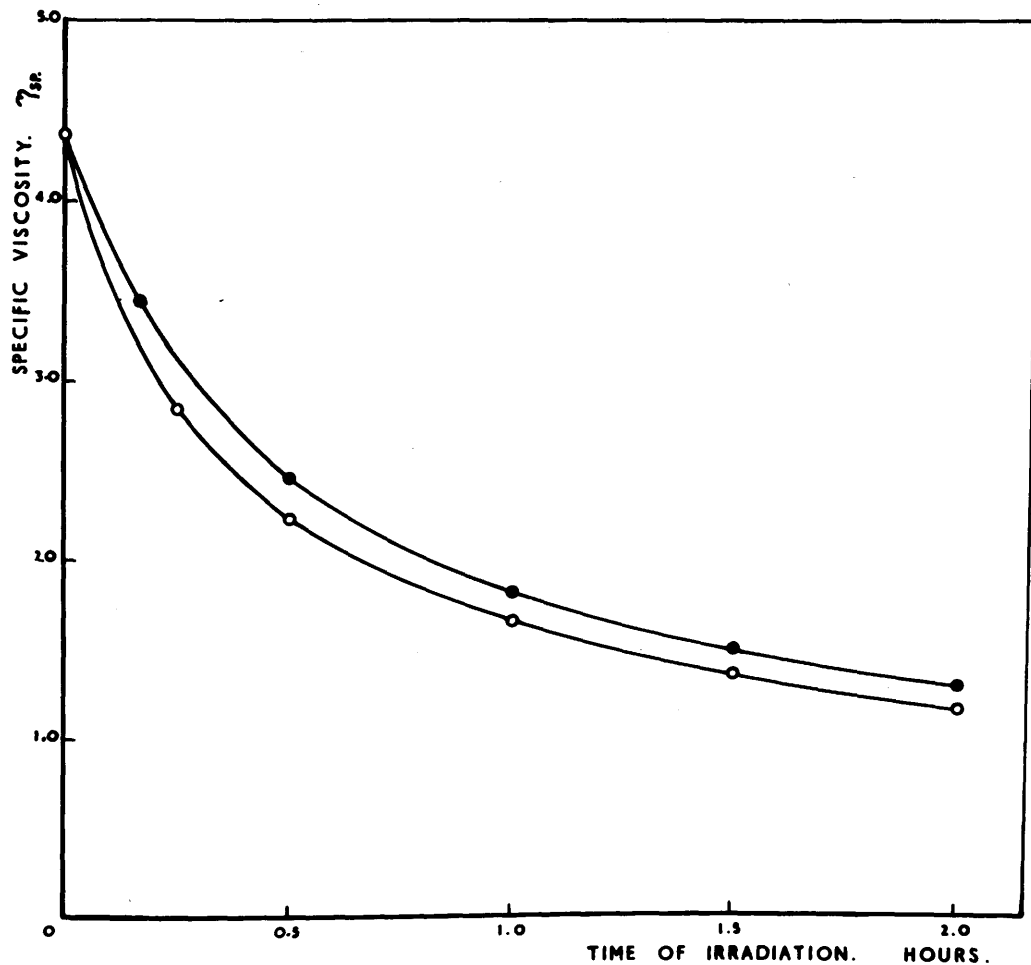
FIG. 47. EFFECT OF D.P.P.H. ON DEGRADATION OF
1% POLYSTYRENE IN BENZENE SOLUTION.
o D.P.P.H. ADDED TO SOLUTION   • NO D.P.P.H. ADDED.

of non-chain-scission reactions (peroxidation), which would consequently affect the rate of D.P.P.H. exhaustion during the initial stages of degradation. It is most unlikely, judging by the shape/ of curves, that competitive reaction between a free radical of a broken chain and a similar free radical, or between it and free radicals of the D.P.P.H. has been taking place at the later stages of degradation and consequently affecting the slope of the curves.

Fig.47 shows the effect of adding the D.P.P.H. on the specific viscosity of the polymer sample during the degrada-:tion process. It was pointed out by Grassie[1] that the termination of chains during other degradation processes is mainly by combination and disproportionation. Very little comment on this particular aspect has been mentioned in literature. Melville and Murray[2] tried to detect the production of free radicals during the degradation process but were not altogether successful . It is clear, however, from Fig.47 that the addition of D.P.P.H. to the polystyrene in benzene sample has a significant effect on its specific vis-:cosity. The apparent reduction in the specific viscosity values due to the addition of D.P.P.H. indicates that termin-:ation of chains by combin ation is substantially suppressed resulting in smaller weight average chain length. Further-:more, free radicals must have been produced in order to
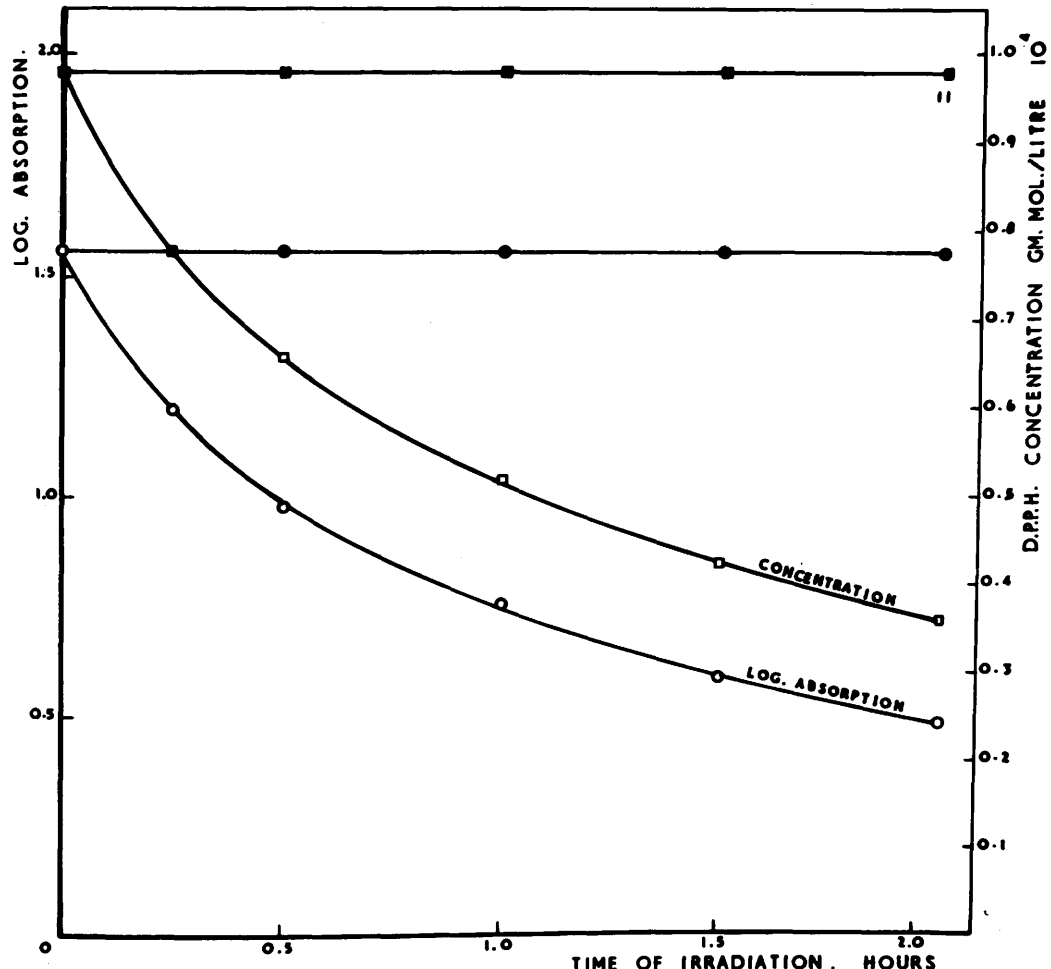
FIG. 48.   EFFECT OF DEGRADATION ON D.P.P.H.
ABSORPTION & CONCENTRATION.
● D.P.P.H. IN PURE BENZENE   ○ D.P.P.H. IN POLYSTYRENE/
■   □   BENZENE SOLUTION.

effect the observed decoloration of the D.P.P.H. - polystyrene-benzene solution, during the degradation process.

Fig.48 illustrates how the absorption of D.P.P.H. in solution decreased as degradation progressed. Similarly the deduced values of the molar concentration of the D.P.P.H. showed a similar decrease, while the pure benzene was pract-:ically unaffected.

E. INTERPRETATION OF RESULTS ALONG SCHMID'S THEORY.

Schmid[5] developed a theory to express the degradation of long chain molecules by ultrasonic waves. He assumed that the rate of breakdown is proportional to the difference (P_t-P_e) between the chain length P_t at time t, and the chain length P_e, reached at the end of degradation. However, he did not consider the size distributions obtained during the degradation process, nor did he make clear distinctions between number and weight average molecular weights. Hence a number of inconsistencies are inherent in his derivations. His initial expression is:

$$\frac{dX}{dt} = K_1 (P_t - P_e) \tag{5}$$

where X is the number of cuts per litre which is the same
    as the number of broken links per litre or the number
    of newly created molecules per litre.

and K_1 is a constant of proportionality.

Equation (5) can be put in the form:

$$\frac{1}{N} \frac{dX}{dt} = K_s (P_t - P_e) \tag{6}$$

where N is Avogadro's number;

and $\frac{1}{N} \frac{dX}{dt}$ is the average number of broken links per minute per mole.

and K_s is a rate constant of degradation.

P_t and P_e can be expressed in terms of molecular weights, i.e.,

$$P_t = \frac{M_t}{M_m} \quad \text{and} \quad P_e = \frac{M_e}{M_m} \tag{7}$$

where M_t and M_e are the respective molecular weights of the polymer and M_m is that of the monomer.

If n_o = number of molecules present at t=o,

and n_t = number of molecules present at time t from the start,

$$\therefore \quad n_t = n_o + X \tag{8}$$

but $$n_t = N. \frac{C_m}{P_t} \tag{9}$$

where C_m is the concentration of polymer in gram.mole per litre.

Therefore, from equations (8) and (9) :

$$X = N. \frac{C_m}{P_t} - n_o \tag{10}$$

and substituting for P_t from equation (7)

$$\therefore \; X = \frac{N \, C_m \, M_m}{M_t} - n_o$$

Hence $\quad \dfrac{1}{N} \dfrac{dX}{dt} = -\dfrac{C_m \, M_m}{M_t^2} \dfrac{dM_t}{dt}$ $\qquad\qquad\qquad$ (11)

From equations (6) and (11) the following relation is easily obtained:

$$- \frac{C_m \, M_m}{M_t^2} \frac{dM_t}{dt} = K_s \left(\frac{M_t}{M_m} - \frac{M_e}{M_m} \right)$$

or $\qquad \dfrac{dM_t}{dt} = -\dfrac{K_s}{C_m} \dfrac{M_t^2}{M_m^2} (M_t - M_e)$ $\qquad\qquad$ (12)

The solution of Equation (12) is given by:

$$\log \left(1 - \frac{M_e}{M_t} \right) + \frac{M_e}{M_t} = -\frac{K_s}{C_m} \left(\frac{M_e}{M_m} \right)^2 t + C$$

where C is a constant of integration to be determined from boundary conditions, i.e.,

$$\text{at} \quad t = o \quad M_t = M_o$$

and hence $\qquad C = \log \left(1 - \dfrac{M_e}{M_o} \right) + \dfrac{M_e}{M_o}$

So, according to Schmid's analysis the degradation process can be represented by the linear relation:

$$\frac{M_e}{M_t} + \log \left(1 - \frac{M_e}{M_t} \right) = -\frac{K_s}{C_m} \left(\frac{M_e}{M_m} \right)^2 t + \frac{M_e}{M_o} + \log \left(1 - \frac{M_e}{M_o} \right) \quad (13)$$

As already pointed out above, Schmid did not take account of distributions and did not distinguish between number and weight average molecular weights. Inspection of equation (7) shows, strictly speaking, that P_t and P_e are number averages ,

provided that M_t and M_e are number average molecular weights. However, Schmid's first assumption represented by Equation (5) was based on his conception that the long chain molecules are broken down by frictional forces developed from the relative motion between the solvent molecules and the solute molecules. In his conception he referred to rigidity and inertia of molecules as being responsible for this relative motion which is further affected by the entanglements of the different molecules. On this basis it seems justifiable to conclude that weight average molecular weights, as obtained from vis-:cosity measurements, would fit in equation (13) better than number average molecular weights which will not give an ade-:quate picture of the mechanism of degradation suggested by Schmid.

However, this conclusion is not far from the conclusion arrived at by Jellinek[4] as he thought that number average chain lengths should be used although weight average values were fitting Schmid's equation better than the number average chain lengths.

It is of interest to point out one limitation of Schmid's analysis, namely, that at the end of degradation, i.e., after a finite time t, M_t will be equal to M_e and the left hand side of equation (13) will have a value of $-\infty$ corresponding to a finite time. This point will not be on the straight
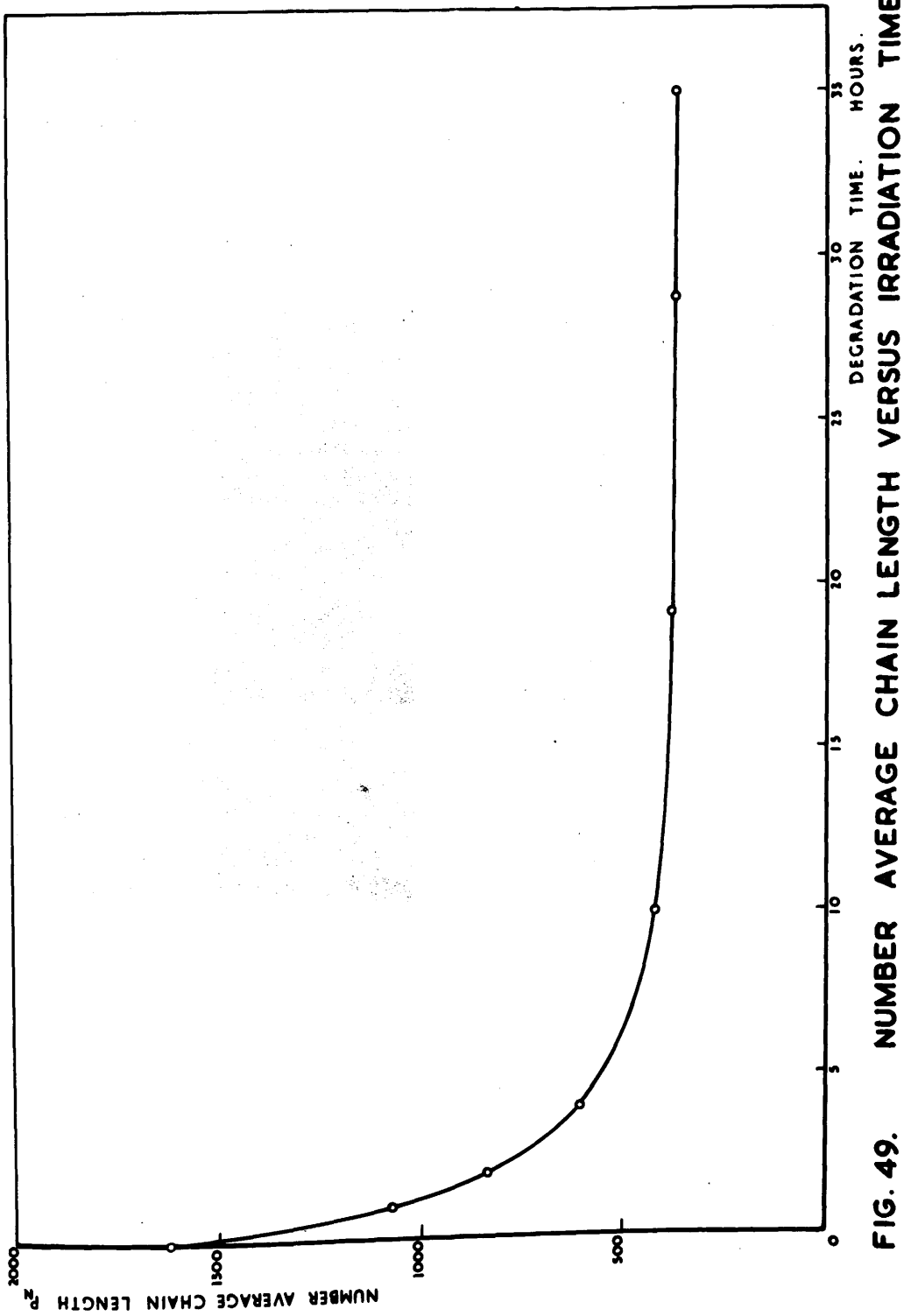
FIG. 49.   NUMBER AVERAGE CHAIN LENGTH VERSUS IRRADIATION TIME.
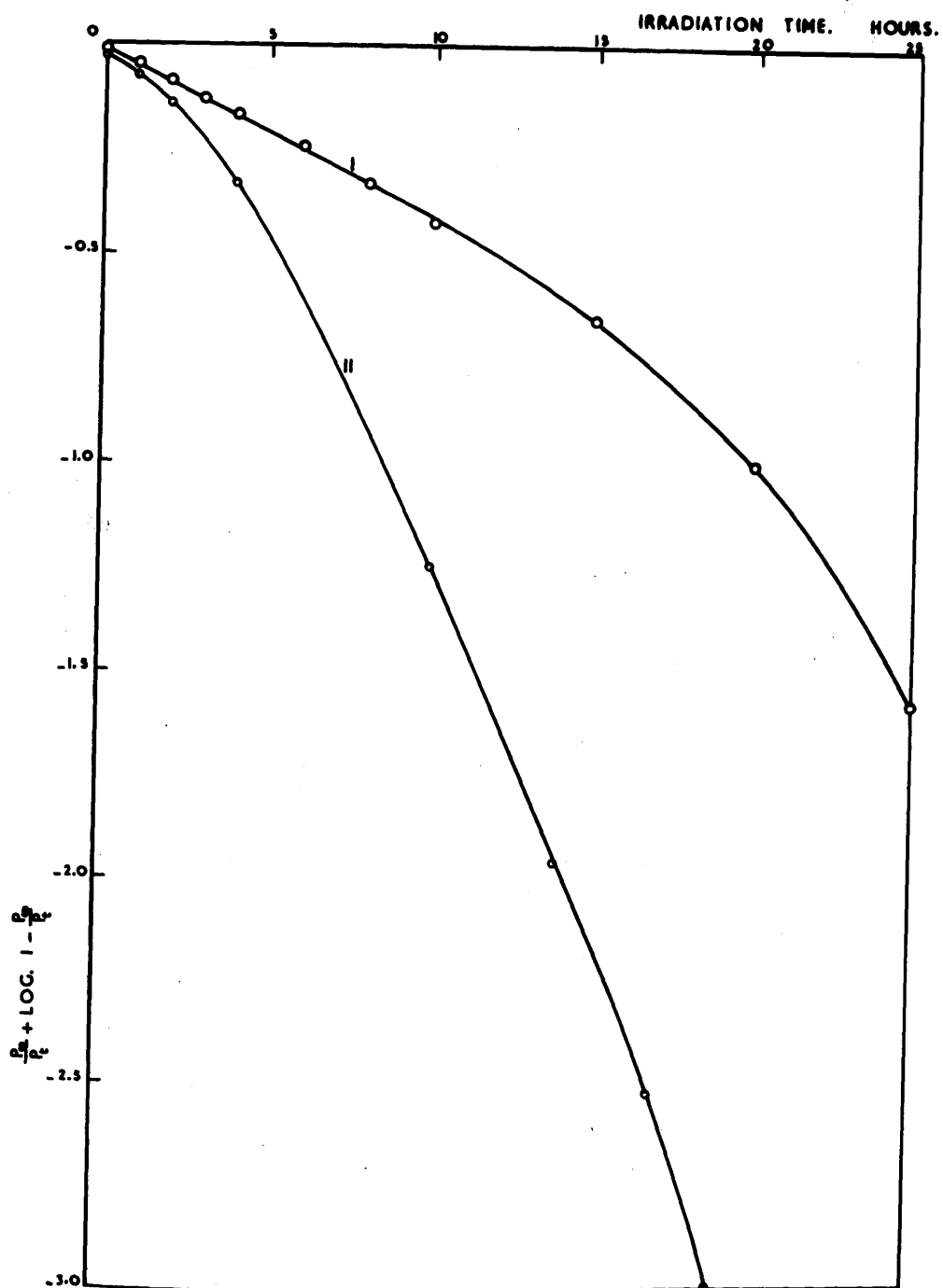
FIG. 5O.   APPLICATION OF SCHMD THEORY TO THEOR-
ETICAL P_N VALUES AND EXPERIMENTAL P_W
VALUES.   I. P_W VALUES.   II. P_N VALUES

line expressing the relation between $\frac{M_e}{M_t} + \log(1 - \frac{M_e}{M_t})$ and time 't' as given by Equation 13. Therefore, one would expect, due to the simple form of Schmid's analysis, that points representing later stages of degradation deviate from the straight line relation bending the line towards the $\frac{M_e}{M_t} + \log(1 - \frac{M_e}{M_t})$ axis.

Values of number average chain lengths 'P_{N_t}' at any time 'T' were calculated from the general relation:

$$P_{N_t} = \frac{o\int^y X_1 N_{x_1} dX_1 + y\int^\infty X_2 N_{x_2} dX_2}{o\int^y N_{x_1} dX_1 + y\int^\infty N_{x_2} dX_2}$$

The values of $\frac{P_{e_N}}{P_{t_N}} + \log(1 - \frac{P_{e_N}}{P_{t_N}})$ where the P's represent number average chain lengths, and of $\frac{P_{e_w}}{P_{t_w}} + \log(1 - \frac{P_{e_w}}{P_{t_w}})$ where the P's represent weight average chain lengths, were calculated at different stages of degradation and the results of these calculations are shown in Table X.

Fig. 49 shows the decrease in the theoretical number average chain length with time of irradiation, while the two functions mentioned above are plotted against the time of irradiation in Fig. 50. As predicted, both functions give a fairly straight line relation with time at the early stages of degradation, the weight average values being in better

agreement, and they both deviate from linearity at the later stages of degradation. The rate constant of degra-:dation 'K_s' determined from the slope of the line repre-:senting the weight average values of chain length was found to be :

$$K_s = 1.6 \times 10^{-8} \text{ mole. litre}^{-1} \text{ hr.}^{-1} .$$

PART 2.

FACTORS AFFECTING ULTRASONIC DEGRADATION.

A. INTRODUCTION.

It is generally accepted that the degradation of polymers
by ultrasonic waves is influenced by many factors. Among
those factors which have a major influence are the intensity
and frequency of ultrasonic waves. Other factors include
the initial average chain length of the polymer sample, the
concentration and the solvent used which affects the shape
of the polymer molecules and has a direct bearing on their
inertia in the solution. For a close study of the influence
of these factors on the process of degradation, i.e., on the
rate constant of degradation 'K' and the limiting chain length
'y', it was considered preferable to develop a reasonably
simplified formula on the lines followed in developing the
detailed theory reported in Chapter IV. This would make it
possible to investigate the effect of any of the above mentioned
factors on the process of degradation without carrying full
runs, each of which usually covers a period of 10 days. It
was sufficient for this purpose to follow the degradation
process for the first hour only.

B. SIMPLIFIED FORMULA.

It can be assumed for a heterogeneous (addition) poly-
:mer sample of initial number average chain length P, that
after a very short time 't' of degradation the following
relation will hold, neglecting the terms representing the
accumulation of molecules:

$$\frac{dN_{x_t}}{dt} = -K (x - 1) N_{x_t} \tag{14}$$

where 'N_{x_t}' is the number of molecules of chain length 'x'
units and 'K' is the rate constant of degradation assumed
to be independent of chain length for chains greater than
'y' and equal to zero for chains shorter than 'y'.

The solution of equation (14) is:

$$N_{x_t} = N_{x_o} \; e^{-K(x-1)t} \tag{15}$$

where 'N_{x_o}' represents the number of chains of length 'x'
at t=o, and for an addition polymer is given by:

$$N_{x_o} = N_o \, p^{x-1} \, (1-p)^2 \tag{16}$$

where 'N_o' is the total number of monomer units and 'p' is a
probability factor given by the relation:

$$p = \frac{P}{P + 1} \tag{17}$$

'P' being the initial number average chain length, as mentioned
earlier.

The weight average chain length at any time t during the degradation is given by:

$$P_{w_t} = \frac{{}_o\!\int^{\infty} x^2 N_{x_t} \, dX}{{}_o\!\int^{\infty} x \, N_{x_t} \, dX}$$

Substituting the appropriate values for 'N_{x_t}' from equations (15) and (16) and integrating we get:

$$P_{w_t} = \frac{2}{Kt - \log p} \tag{18}$$

Substituting the value of 'p' as given by equation (17) and considering $\log (1 - \frac{1}{p}) = \frac{-1}{p}$ as a first approximation, equation (18), giving the weight average chain length at time t, can be rewritten in the form:

$$P_{w_t} = \frac{2P}{PKt + 1}$$

and

$$\frac{dP_{w_t}}{dt} = - \frac{P_{w_o} \cdot PK}{(PKt+1)^2}$$

Hence

$$K = \frac{2}{P_{w_o} \cdot t} \left(\frac{P_{w_o}}{P_{w_t}} - 1 \right) \tag{19}$$

$$= - 2 \left(\frac{dP_{w_t}}{dt} \right)_{t=o} / P_{w_o}^2 \tag{20}$$

Equations (19) and (20) give explicitly the value for the rate constant of degradation 'K' at the beginning of degradation, strictly speaking at t = o. The value of 't' in equation

(19) is of the order of a few minutes. This simplified equation gave a maximum error in the values of 'K' well below 7% for the worst cases. This was considered to be a reasonable value compared to errors estimated by about 50% reported by Jellinek[5].

The exact value of the rate constant of degradation at the beginning of the process (t=o) can be obtained as a function of the limiting chain length 'y' by differentiating 'P_{w_t}', given in equation (33) Chapter IV, with respect to time. This gave the relation:

$$\left(\frac{dP_{w_t}}{dt}\right)_{t=o} = -K \left(\frac{P}{P+1}\right)^y \left[2P(P+y-1) + \frac{y^2}{P}\left(\frac{y}{3} - 1\right) + y(y-2)\right] \qquad (21)$$

Thus it is possible from a short period of degradation to determine the values of 'K' and 'y'. The procedure recommended is as follows:

1. From the value of 'P_{w_t}' after a short period of degradation, 'K' can be determined using equation (19).

2. The slope $\left(\frac{dP_{w_t}}{dt}\right)_{t=o}$ can be obtained by substituting the value of 'K' in equation (20).

3. The limiting chain length is obtained by solving equation (21) for 'y' after substituting the values of K and $\left(\frac{dP_{w_t}}{dt}\right)_{t=o}$.

However, it should be pointed out that using equation (21) is not satisfactory in determining absolute values of 'y', since a small error in $(\frac{dP_{w_t}}{dt})_{t=0}$ produces a very large error in 'y'. This can best be illustrated by calculating the change in $(\frac{dP_{w_t}}{dt})_{t=0}$ due to a small change in 'y' which, when carried out, gave:

$$\frac{d(\frac{dP_{w_t}}{dt})_{t=0}}{dy} = K \frac{y^2}{P^2} (\frac{P}{P+1})^y (\frac{y}{3} - 1)$$

$$= 0.022153 \qquad\qquad (22)$$

for $y = 744$ and $P = 1650$.

It is obvious from equation (22) that a 1% error in the value of $(\frac{dP_{w_t}}{dt})_{t=0}$ will give rise to 45.14% error in the value of y.

Although equation (21) does not give accurate absolute values of 'y', yet it can be used successfully for illustra: :ting the influence of the different factors on the limiting chain length y, provided the procedure recommended above is adopted in all the calculations for all the polymer samples used.

C. EFFECT OF INTENSITY OF ULTRASONIC WAVES.

a. Dependence of rate constant of degradation 'K' on intensity.

In attempting to explain the dependence of 'K', the rate constant of degradation, on the intensity of ultrasonic waves,

it was assumed in agreement with Jellinek[5], that the force

acting on one macro-molecule can be represented by the form:

$$f = f_o \sin (\omega t - \emptyset) \qquad\qquad (23)$$

where $\omega = \frac{2\pi}{T}$ is the angular frequency, T is the periodic

time and $\emptyset$ is a phase angle.

This is a reasonable assumption, in view of the fact

that ultrasonic waves are sinusoidal in form and travel

through solutions with constant velocity.

The two cases which are likely to represent the dynamics

of ultrasonic degradation are:

(i)   The number of molecules dN_x of length x broken in a

·time interval dt is proportional to the difference between

the force acting and the force 'γ' required to break a C-C

bond, i.e.,

$$dN_x \propto (f - \gamma) N_x dt$$

(ii) The number of molecules dN_x is independent of $(f - \gamma)$

during that part of the cycle where f is greater than γ,

i.e.,

$$dN_x \propto N_x dt$$

Case (i).

The total number of molecules broken in a time interval

dt is given by:
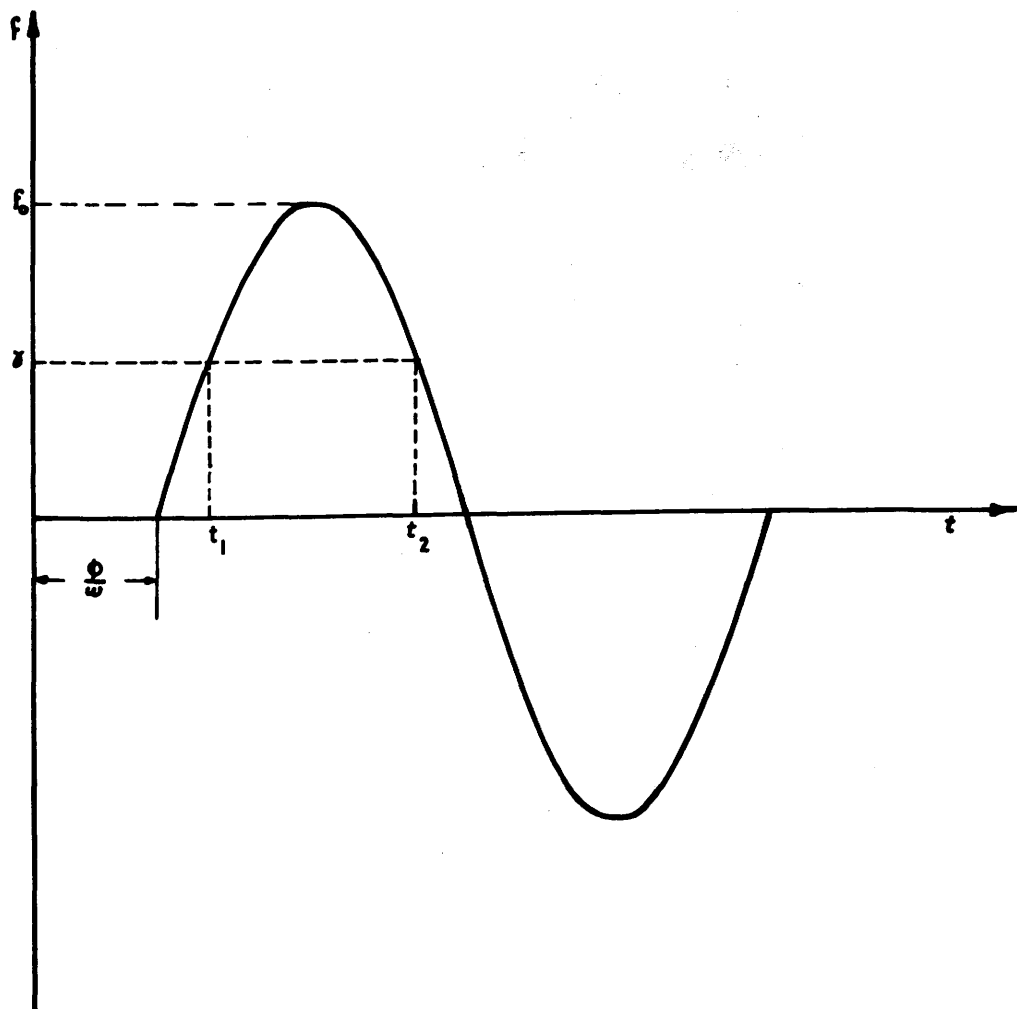
FIG. 51. FORCE EXERTED ON LONG CHAIN MOLECULE AS FUNCTION OF TIME.

$$\sum_{x=1}^{x=\infty} dN_x = \sum_{x=1}^{x=\infty} \beta_1 (f-\gamma) N_x dt$$

where β_1 is a constant of proportionality and N_x is the number of chains of length x.

From the shape of function f shown in Figure 51, the times t_1 and t_2 at which the force has a value of γ are given by the relation:

$$t = \frac{1}{\omega} \sin^{-1} \left(\frac{\gamma}{f_o}\right) + \frac{\phi}{\omega} \tag{24}$$

hence if $\sin \theta = \frac{\gamma}{f_o}$

$$\left. \begin{aligned} t_1 &= \frac{\phi + \theta}{\omega} \\ t_2 &= \frac{\phi + \pi - \theta}{\omega} \end{aligned} \right\} \tag{25}$$

The macro-molecules will only be broken during these time intervals when $f > \gamma$ and it can be shown that the total number of chains of all lengths broken per cycle is given by:

$$N_c = {}_0\!\!\int^{\infty} N_x dx = 2 \beta_1 {}_{t_1}\!\!\int^{t_2} (f-\gamma)dt \; {}_0\!\!\int^{\infty} N_x dx$$

$$= \frac{2 \beta_1 N_0}{P + 1} {}_{t_1}\!\!\int^{t_2} (f-\gamma)dt \tag{26}$$

where N_c is the total number of chains broken per cycle.

The number of chains broken per second, i.e. the rate of scission will be given by:

$$\frac{dN}{dt} = \frac{\omega N_c}{2\pi} = - \frac{\beta_1 \omega N_0}{\pi(P+1)} {}_{t_1}\!\!\int^{t_2} (f - \gamma)dt$$

Evaluating the integral, the rate of scission can be expre-
:ssed in the form:

$$\frac{dN}{dt} = - \frac{2\beta_1 N_0}{\pi(P+1)} \left[\sqrt{f_0^2 - \gamma^2} - \gamma \cos^{-1} \frac{\gamma}{f_0} \right] \qquad (27)$$

The same rate of scission can be evaluated from equations
(14), (15) and (16).   Such evaluation gave:

$$\frac{dN}{dt} = \int_0^\infty \left(\frac{dN_{xt}}{dt} \right) dx = -K N_0 \qquad (28)$$

From equations (27) and (28) and assuming that $P+1 = P$, the
value of 'K' can be expressed in the form:

$$K = \frac{2\beta_1}{\pi P} \left[\sqrt{f_0^2 - \gamma^2} - \gamma \cos^{-1} \frac{\gamma}{f_0} \right] \qquad (29)$$

Case (ii).

The number of molecules dN_x broken in a time interval
dt is independent of $(f - \gamma)$ during that part of the cycle
where 'f' is greater than 'γ'

$$i.e., \quad dN_x = \beta_2 N_x dt$$

Following a similar treatment to that carried out in Case (i)
it can be shown that the value of K at the beginning of
degradation, i.e., at $t = 0$, is given by:

$$K = \frac{2\beta_2}{\pi P} \cos^{-1} \frac{\gamma}{f_0} \qquad (30)$$

In order to find out how does 'K' depend on the intensity
of ultrasonic waves, it is necessary to know how the peak
force f_0 acting on the macro-molecules depends on the inten-
:sity.   In the light of existing theories for the mechanism
of degradation, both the frictional forces theory according
to Schmid[6], and the liquid hammer theory discussed by
Jellinek and White[5], lead to the conclusion that:

$$f_0 = \alpha V_s \qquad\qquad (31)$$

where V_s is the maximum velocity of the solvent molecules
resulting from the propagation of ultrasonic waves in the
polymer solution and 'α' is a constant, provided the same
polymer/solvent sample is used in all the degradation runs
and the ultrasonic frequency is maintained constant.

   However, for the sake of simplicity under the experi-
:mental conditions of this investigation, 'V_s' the velocity
amplitude of the solvent is proportional to the voltage
applied to the electrodes of the crystal transducer, which
is, in turn, proportional to the D.C. anode voltage V_a of
the ultrasonic generator, as can be deduced from Fig.(21).
Therefore, $f_0 = $ constant V_a $\qquad\qquad$ (32)

   For constant ultrasonic frequency and using the same
polymer solution the theoretical values of K were calculated
from equations (29) and (30) for different values of f_0.

DEGRADATION OF POLYSTYRENE AT DIFFERENT INTENSITIES.

I. INTENSITY = 4.89 WATTS/CM.²   II. I = 9.58 WATTS/CM.²   III. I = 12.5 WATTS/CM.²

IV. I = 15.8 WATTS/CM.²

$P_w = 3260$

FIG. 52.
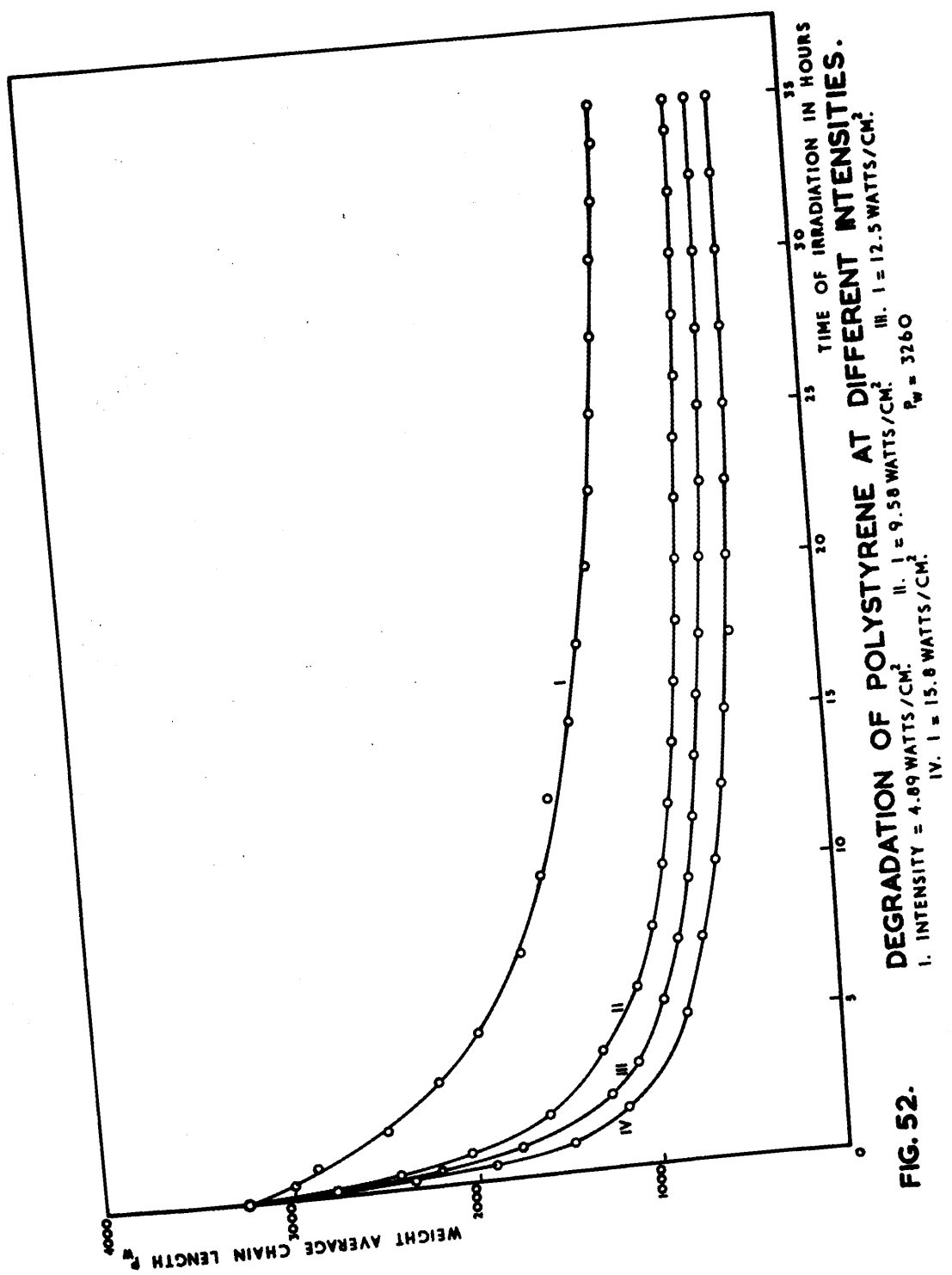
Furthermore, since 'γ', the force required to break a C—C bond, is constant, the different values of f_0 were taken as multiples of γ.

Thus equation (29) representing Case (1), can be put in the form:

$$K = \frac{2\beta_1\gamma}{\pi P} [\sqrt{(\frac{f_0}{\gamma})^2 - 1} - \cos^{-1} \frac{\gamma}{f_0}] \qquad (33)$$

and by taking $f_0 = S\gamma$, where S can take any value greater than 1,

$$\therefore K = \frac{2\beta_1\gamma}{\pi P} [\sqrt{S^2 - 1} - \cos^{-1} \frac{1}{S}] \qquad (34)$$

Similarly for Case (ii) :

$$K = \frac{2\beta_2}{\pi P} \cos^{-1} \frac{1}{S} \qquad (35)$$

Experimental.

A number of 25 mls. samples of a 1% wt./vol. polysty-:rene in benzene were irradiated by 0.75 Mc./sec. ultrasonic waves. Values of the weight average chain length during degradation by ultrasonic waves at different intensities are given in Table XI and plotted against the time of irradiation in Figure 52.

A preliminary deduction from Fig. 52 is that by increas-:ing the intensity of ultrasonic waves the rate constant of degradation 'K' increases, while the limiting chain length
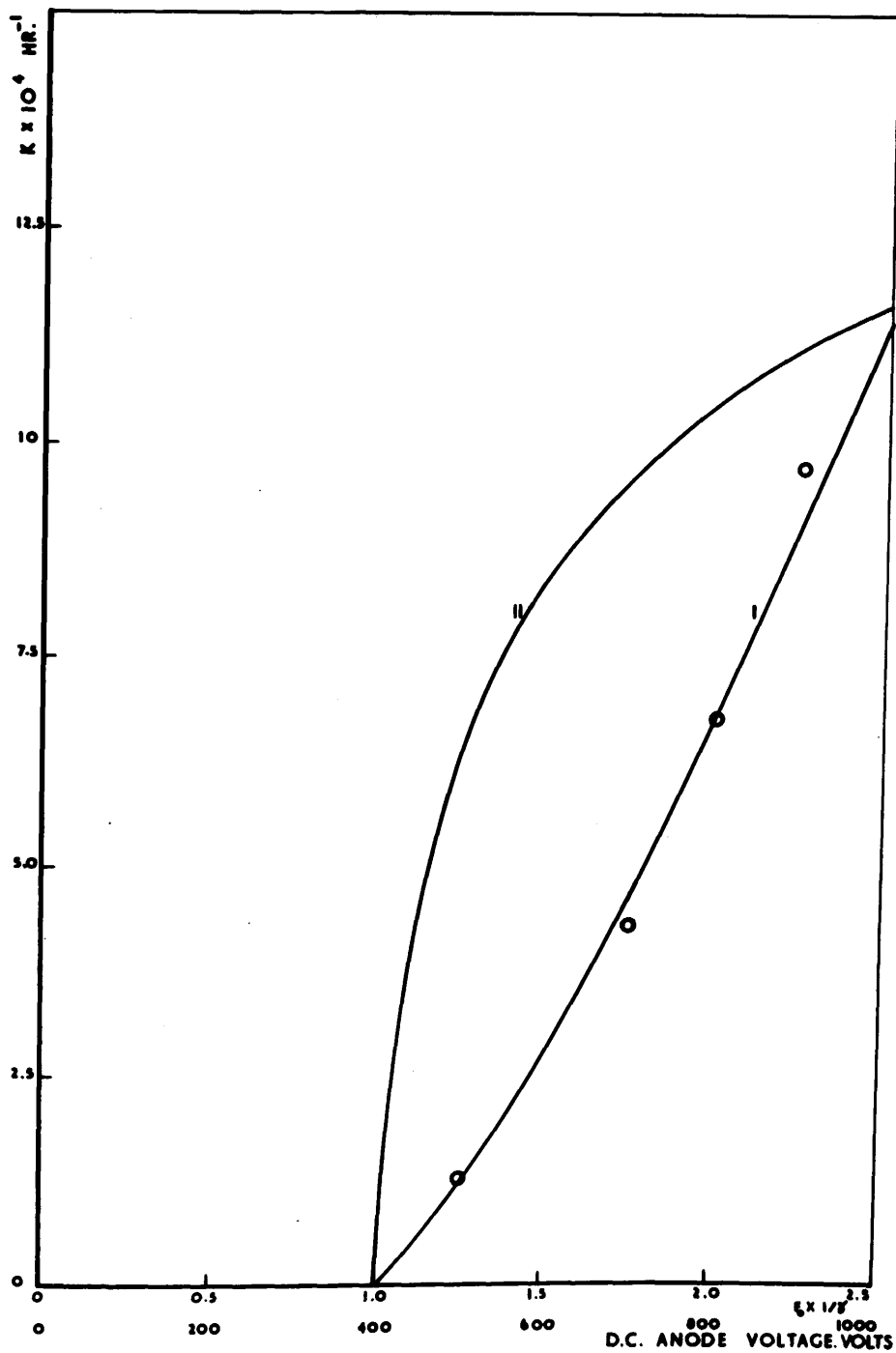
FIG. 53. VARIATION OF RATE CONSTANT WITH ULTRASONIC INTENSITY. o EXPERIMENTAL POINTS.
I. THEORETICAL CURVE CASE I   II. THEORETICAL CURVE CASE 2.

'y' decreases. However, the manner in which 'K' varies with intensity can easily be deduced by considering equations (32), (34) and (35). In Table XII theoretical values of the rate constant of degradation calculated for the two cases discussed above, are given in columns (2) and (3) while the experimental values of 'K' at different intensities, given in column (5), were calculated from equation (19).

Since the values of the constants β_1 and β_2 are arbitrary, two values were selected which gave the best agree-:ment with the experimental results. The values chosen were:

$$\beta_1 = \frac{2.545}{\Upsilon} \text{ dyne}^{-1} \text{ hr.}^{-1} \text{ for Case (i);}$$

and $\quad \beta_2 = 2.545 \text{ hr.}^{-1} \text{ for Case (ii).}$

In Figure 53, the values of 'K' are plotted against the ultrasonic force 'f$_o$'. The theoretical values of 'f$_o$' are, as mentioned earlier, given by $f_o = S\Upsilon$, where 'S' is a constant and can take any value greater than 1, while the experimental values of 'f$_o$' are substituted by the D.C. anode voltage of the ultrasonic generator.

It is quite clear from Figure (53) that the experi-:mental values of 'K' agree very closely with Case (i) in which the number of molecules dN broken during an interval of time dt is proportional to the difference between the force acting and the force 'Υ' required to break a C-C bond.

b. Dependence of Limiting Chain Length 'y' on Intensity.

The two cases which illustrate how the rate constant depends on the intensity of ultrasonic waves, were discussed briefly in the previous section.   In order to find out how the limiting chain length 'y' depends on intensity it is necessary to know how the peak force f_0' depends on 'y'. However, this knowledge should be based on a clear picture of the mechanism by which long chain molecules are likely to be broken.   Two such mechanisms were mentioned earlier.

Considering the first mechanism suggested by Schmid[6], it was assumed that the polymer molecules and the solvent molecules will respond differently to the ultrasonic waves. This will result in a relative velocity between the solvent and the long chain molecules.   This relative velocity can reach its maximum value if the polymer molecule can be considered as rigidly fixed, either due to its own inertia or as a result of entanglements with other molecules.   However, if the polymer molecule is replaced by a frictionless thread, having spheres at regular intervals along its axis repre-
:senting the benzene rings (radius 3 A.U.), the total frict-
:ional force can be calculated from Stoke's formula:

$$f_0 = P. 6\pi\eta r V_s \qquad\qquad (36)$$

where η is the viscosity of solvent,

r is the radius of benzene ring,

P is the average chain length of polymer molecule,

and V_s is the maximum velocity of solvent molecules.

Under experimental conditions $6\pi\eta r$ is constant and therefore:

$$f_o = \alpha_1 PV_s \qquad (37)$$

'α_1' being a constant.

Again, if we consider the second mechanism for the breakdown of long chain molecules, discussed by Jellinek[5], the polymer molecules are broken by a liquid hammer result-:ing from the impact forces set up when the solvent mole-:cules collide with them. From dynamical considerations the force acting during collision on the polymer molecule, which is assumed fixed at both ends, is given by the relation:

$$f_o = \frac{\rho \, \delta \, Pd \, (\frac{\lambda}{4})(\frac{2}{\pi}) \, V_s}{\pi/2\omega} \qquad (38)$$

where ρ is the density of solvent in gm./c.c.;

δ is the spacing between monomer units in cm.;

d is the diameter of benzene rings in cm.;

λ is the wavelength of ultrasonic waves in cm.

As in the case of equation (36), the value for 'f_o' given by equation (38) can be put in the simple form:

$$f_o = \alpha_2 PV_s \qquad (39)$$

'α_2' being a constant.

The two mechanisms, virtually, give similar dependence of the peak force 'f_0' on the initial average chain length and the maximum solvent velocity 'V_s', as expressed in equations (37) and (39). It is safe, therefore, to consider the general expression for 'f_0' to be of the form:

$$f_0 = \alpha \; PV_s \qquad\qquad (40)$$

where 'α' is a constant of proportionality.

Furthermore, since 'γ' is the force required to break a C-C bond, it is justifiable to assume that the rate constant of degradation 'K' has a zero value when $f_0 = \gamma$. Under this condition 'P' will have the limiting value of chain length, i.e., $P = y$.

Therefore, $\gamma = \alpha \; yV_s \qquad\qquad (41)$

Equation (41) indicates that as the intensity of ultrasonic waves is increased, 'V_s' will increase and, consequently, 'y' must decrease since 'γ', the force required to break a C-C bond, is constant.

From equations (40) and (41) we get the simple relation:

$$\frac{f_0}{\gamma} = \frac{P}{y} \qquad\qquad (42)$$

Introducing this value of $\frac{f_0}{\gamma}$, equations (33) and (30) can be written in the form:

$$K = \frac{2\beta_1 \gamma}{\pi P} \; \left[\sqrt{\left(\frac{P}{y}\right)^2 - 1} - \cos^{-1} \frac{y}{P} \; \right] \qquad\qquad (43)$$

for Case (1);
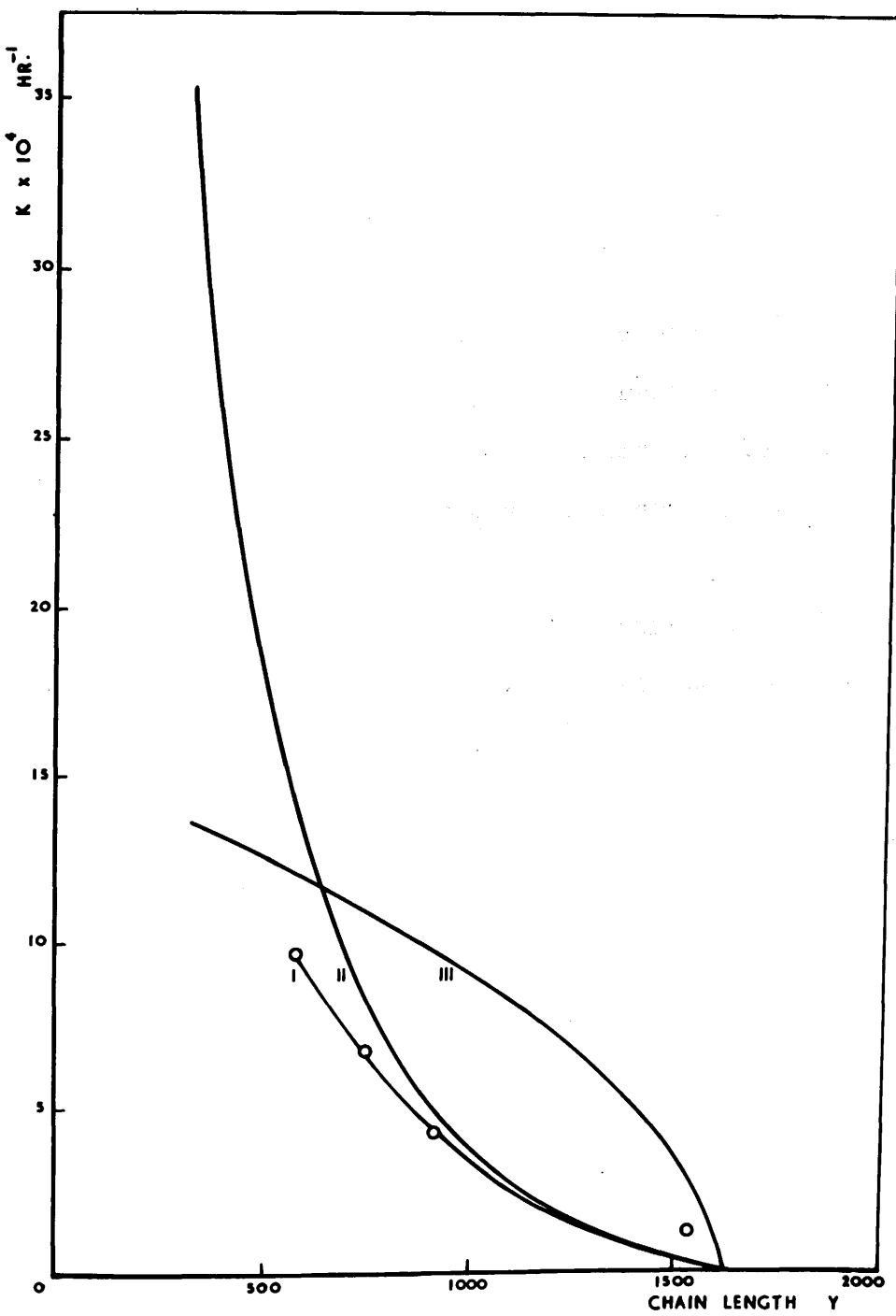
FIG. 54. VARIATION OF LIMITING CHAIN LENGTH Y
WITH INTENSITY   I. EXPERIMENTAL CURVE.
II. THEORETICAL CURVE CASE I   III. THEORETICAL CURVE CASE 2

and
$$K = \frac{2\beta_2}{\pi P} \cos^{-1} \left(\frac{y}{P}\right) \tag{44}$$

for Case (ii).

'P' the initial number average chain length in both equations (43) and (44) is constant and for the polymer sample used P = 1650. Theoretical values of 'K' for both cases were calculated by giving different values of 'y' as a fraction of 'P', i.e., y = m P, where 'm' is a fraction which can take any value between zero and 1, i.e.,

$o < m \leqslant 1.$

Thus equations (43) and (44) giving the theoretical values of 'K' for Case (i) and Case (ii) can be put in their final forms:

$$K = \frac{2\beta_1 Y}{\pi P} \left[\sqrt{\frac{1 - m^2}{m^2}} - \cos^{-1} m \right] \tag{45}$$

for Case (i), and

$$K = \frac{2\beta_2}{\pi P} \cos^{-1} m \tag{46}$$

for Case (ii)

In figure (54) the theoretical values of 'K' cal-
:culated from equations (45) and (46) are plotted against 'y' and compared with the corresponding experimental values. The values of 'K' are given in Table XIII.
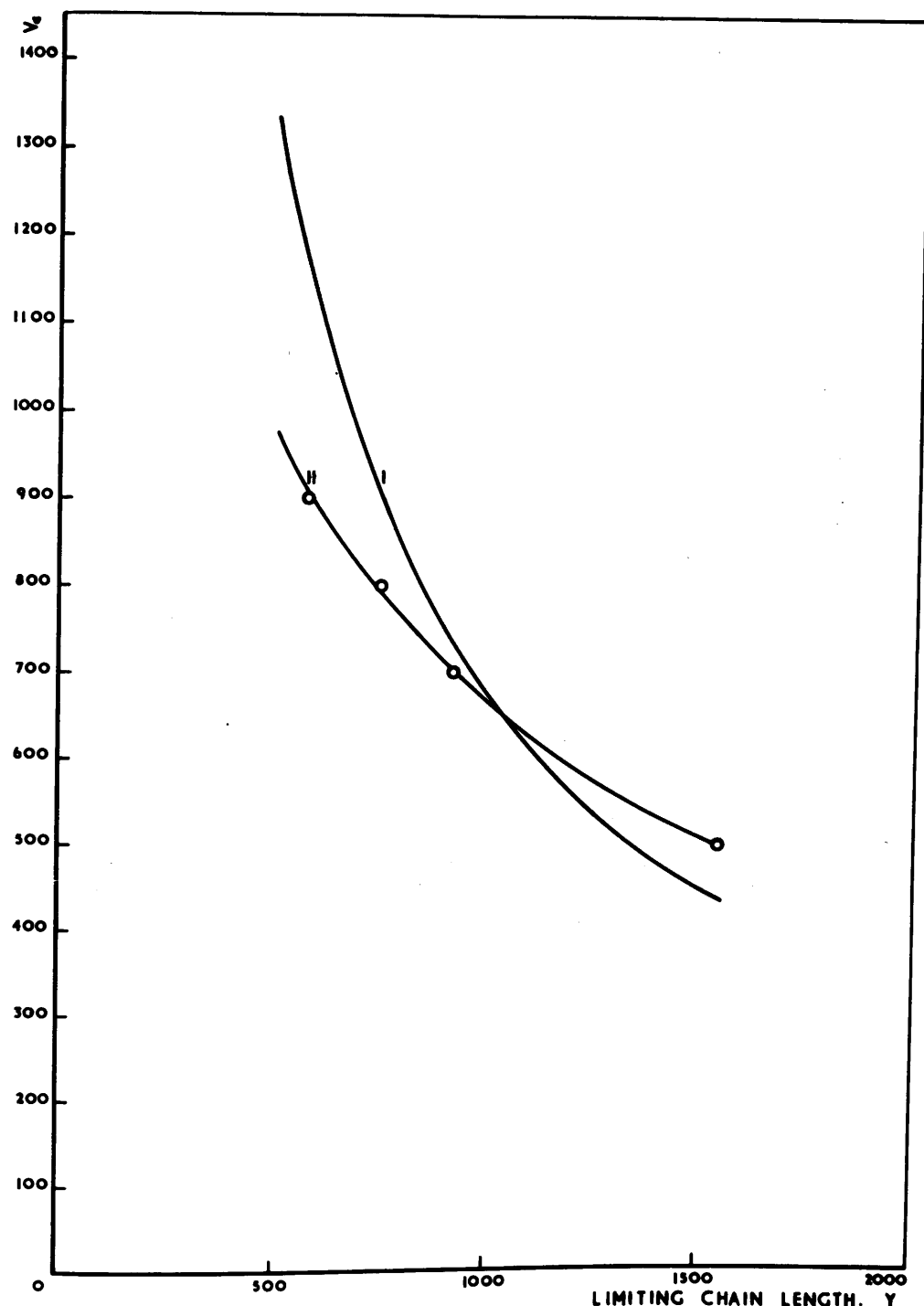
FIG. 55.　ULTRAONIC FORCE (V$_d$) VERSUS LIMITING
CHAIN LENGTH y.　I. THEORETICAL　II. EXPERIMENTAL.

Inspection of Figure 54 shows that the experimental values of the rate constant of degradation are in reasonable agreement with Case (i).

Considering equation (37), the product 'y V_s' is known to be constant. Furthermore, since 'V_s', the ultrasonic velocity amplitude of solvent molecules, is proportional to 'V_a' the D.C. anode voltage, therefore $y V_a$ = constant, i.e., the relation between limiting chain length 'y' and the D.C. anode voltage 'V_a' can be represented by a rectangular hyperbola.

Theoretical and experimental values of 'y' plotted against 'V_a' in Figure 55 show a reasonable qualitative agreement.

c. Discussion.

It should be pointed out at this stage that the discussion to follow is basically qualitative. Any attempt to draw a quantitative conclusion is bound to be misleading in view of the fact that the degradation of polymer solutions is affected by two distinct types of forces, namely:

(1) forces due to ultrasonic waves proper, and

(2) forces due to cavitation which may result in
     shock waves or liquid hammer or otherwise.

Consequently, since existing theories on cavitation produced by ultrasonics, its inception, and particularly the factors controlling its effect, are by no means complete, it will be difficult to analyse its effects, let alone its exact role and contribution to the process of degradation. Further-:more, the mechanism of degradation by ultrasonic waves alone is still a matter of conjecture if not of controversy.

However, it is reasonably clear from the experimental results that the ultrasonic intensity has a marked effect on the degradation. The experimental values of the degradation parameters 'K' and 'y' seem to agree qualitatively with Case (i).

For quantitative study of the influence of intensity on the degradation parameters 'K' and 'y', the constants β_1 and β_2 should be, strictly speaking, constants of propor-:tionality between degradation parameters and the ultrasonic force 'f_o', where 'f_o' can be substituted either by the D.C. anode voltage of the driving oscillator or by the pressure amplitude of the ultrasonic wave 'p_o'. However, in assign-:ing values for β_1 and β_2 to fit the experimental results, the effect of cavitation was included. Furthermore, it was implied that cavitation intensity (severity) increases linearly with the increase of 'f_o' or 'V_a'.

That the severity of cavitation increases linearly with the increase of 'f_o' cannot be assumed without reser:vation. The only available information on this subject was reported by Noltingk and Neppiras[7] who studied the cavitation produced by ultrasonic waves.

Unfortunately, the differential equations expressing the growth and collapse of cavities are insoluble mathemat:ically and, consequently, any quantitative interpretation of the results reported in this section along that theory[7] is, at the moment, out of the question. However, on the assumption that <u>cavities maintain their spherical shape during collapse</u>, Noltingk and Neppiras, from a number of solutions of their equation on a differential analyser, predicted the manner in which cavitation intensity (severity) would be affected when the pressure amplitude of the ultrasonic waves is increased.

For a constant frequency of ultrasonic waves and con:stant hydrostatic pressure in the liquid irradiated and fixed size of nuclei present in the solution, it follows according to Noltingk and Neppiras that there exists a lower threshold of ultrasonic intensity or, more precisely, ultrasonic pressure amplitude 'p_o' below which cavitation can never occur. Further:-more, an upper threshold in 'p_o' appears to exist, above which cavitation would be suppressed.

Considering the polymer solution used in this investi-
:gation, it will be assumed that the size of nuclei necessary
for cavitation inception depends on the initial length and
shape of polymer molecules in solution. Consequently, the
initial sizes of nuclei (R_o) are independent of intensity
and can be considered constant.

A qualitative picture for the effect of ultrasonic
intensity on cavitation severity can thus be predicted. The
cavitation intensity (severity) increases rapidly, as the
ultrasonic intensity is increased, until it reaches a peak
value. Any further increase in ultrasonic intensity will
result in a diminishing cavitation intensity until the upper
threshold is reached and destructive cavitation would event-
:ually cease to occur. Noltingk and Neppiras gave $p_o = 6.5$
atm. as an upper threshold above which destructive cavitation
will be highly suppressed due to incomplete collapse of
cavities.

Although the value of $p_o = 6.5$ atm. was predicted for
a hydrostatic pressure in the liquid $P_A = 10^6$ dynes/cm.^{2}
angular frequency $\omega = 9 \times 10^4$ rad./sec. and initial nucleus
size $R_o = 3.2$ microns (see Fig. 12), yet according to theory
they claimed thatthe threshold value of 'p_o' is independent
of frequency and not very dependent on 'R_o' provided that

'R_o' is well inside the cavitation range of nuclei sizes.

It should be pointed out that the prediction of thresh-:olds in 'p_o' from the theory was based on the assumption that cavities maintain their spherical shape during collapse. This assumption is not by any means always valid[8]. Kornfeld and Suvorov[9] found polygonal shapes of cavities at lower acoustic intensities when their bubbles were presumably not cavitating. However, since this assumption is not completely beyond dispute, it is sensible to accept the predictions of the theory with reservations. For example, the upper threshold of 'p_o' may not be independent of frequency or its value may be more than that predicted by theory.

However, it is safe to conclude that cavitation inten-:sity (severity) does not increase linearly with the increase in ultrasonic pressure amplitude (considered proportional to D.C. anode voltage of oscillator). If this conclusion is accepted, the deviation of the experimental values of 'k' in Figure 54 from their theoretical values of Case (i) can therefore be anticipated. In addition, it can be deduced from the same figure that the upper threshold of 'p_o' is greater than 7.5 atm. which is roughly the maximum ultra-:sonic pressure amplitude used in this investigation.

d. Conclusions.

The following conclusions can be derived from the exper-
:imental results and theoretical considerations:

1. There is a minimum ultrasonic intensity below which no
degradation takes place. This threshold of intensity is
approximately 3.125 watts/cm^2. when the weight average chain
length of the undegraded polymer sample is 3260.

2. The assumption made in developing the theory of degra-
:dation of addition polymers by ultrasonic waves, that the
rate constant 'K' is independent of chain length above a
limiting value, seems to be valid. However, this validity
can be obscured under certain experimental conditions by
factors like initial average chain length, frequency of
ultrasonic waves↓cavitation inception.

3. The experimental rate constant curves appear to agree
closely with Case (i). It is the author's opinion that
neither of the two theoretical mechanisms mentioned in
this work gives a complete and satisfactory picture of the
dynamics of the degradation of long chain molecules, and
furthermore, that the true mechanism is not likely to make
the results obtained less valid.

4.   Considering the existing means of producing intense
ultrasonic waves in practice, it seems unlikely that degra-
:dation of polymer samples down to monomer can be expected.

D.   EFFECT OF INITIAL CHAIN LENGTH.

a.   Dependence of y on the initial chain length.

The dependence of the limiting chain 'y' on the initial
average chain length was mentioned briefly at the end of
Chapter IV.   Based on the experimental observation, that
the weight average chain length at the end of degradation
is almost independent of its value before degradation, it
was shown by equation (38), Chapter IV, that as the initial
average chain length 'P' decreases, the limiting chain length
'y' increases.   This behaviour was considered to be consis-
:tent with the physical picture of the degradation mechanism
suggested by Schmid.

However, this change in 'y' for a change in 'P' is very
small indeed, as illustrated by equation (39), Chapter IV.

b.   Dependence of K on the initial chain length.

In order to investigate theoretically the dependence
of the rate constant 'K' on the initial average chain length
'P' it is assumed that the limiting chain length y is inde-
:pendent of P.   This assumption is justifiable since the

changes in y due to a change in 'P' are so small. The error that may arise from this simplifying assumption cannot exceed 5% and consequently is unlikely to invalidate any conclusions derived from the following analysis.

Equations (43) and (44) gave the theoretical dependence that would exist between K, P and y for cases (i) and (ii) respectively. As mentioned above y is considered constant and P for simplicity will be considered as a multiple of y, i.e., P = ny, where n can take any value greater than one, i.e., n > 1.

With this simplification equations (43) and (44) can be put in the form:

$$K = \frac{2\beta_1 \gamma}{n\pi y} \left[\sqrt{n^2 - 1} - \cos^{-1} \frac{1}{n} \right] \qquad (47)$$

for Case (i);

and
$$K = \frac{2\beta_2}{n\pi y} \cdot \cos^{-1} \frac{1}{n} \qquad (48)$$
for Case (ii).

c. Experimental.

Four samples of 1% polystyrene in benzene of different initial average chain length were irradiated by 0.75 Mc. per sec. ultrasonic waves of intensity 12.5 watts/cm^2. in the solution proper. The degradation process for three samples was followed for 35 hours to confirm the fact that the chain
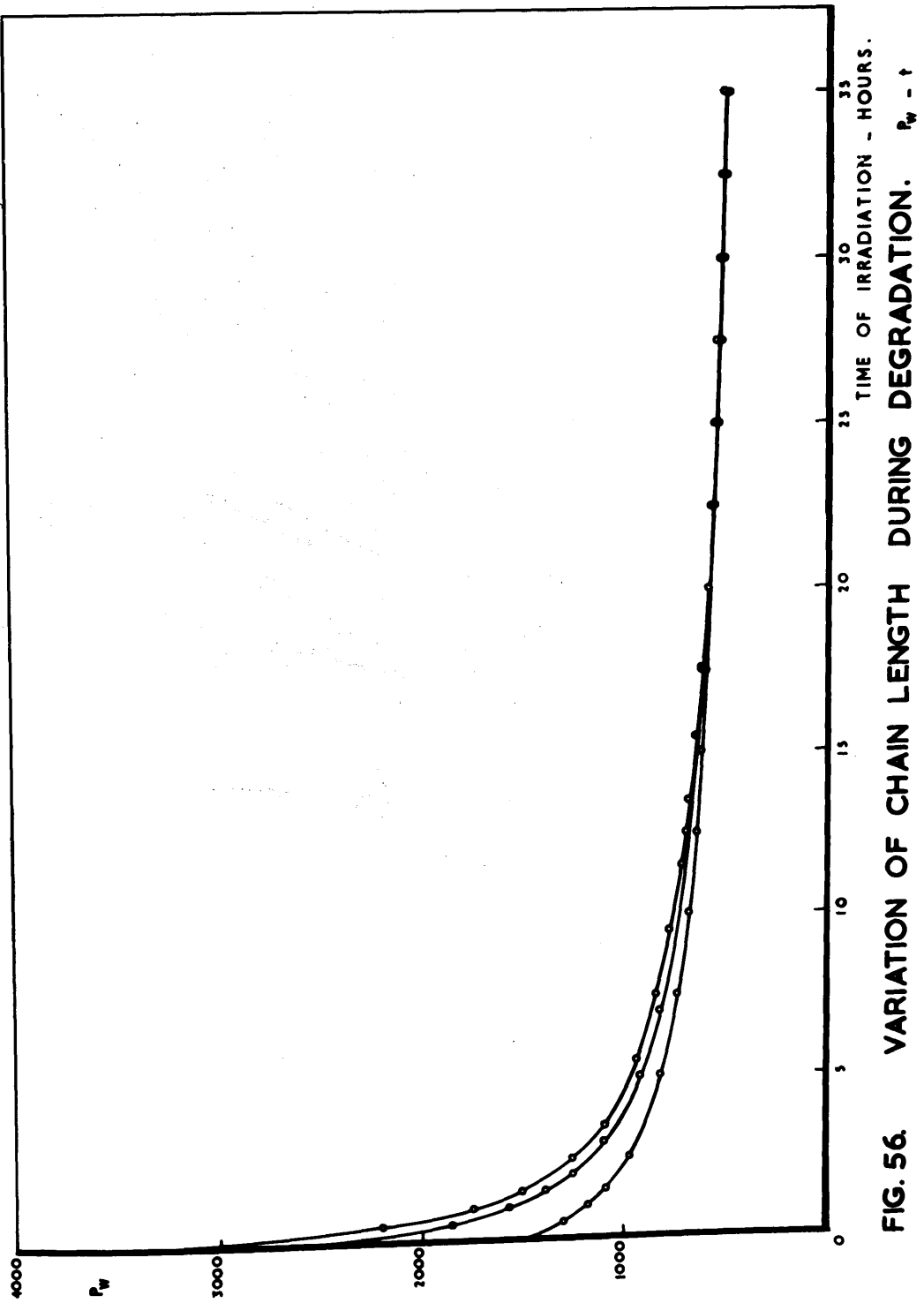
FIG. 56.   VARIATION OF CHAIN LENGTH DURING DEGRADATION. $P_W - t$
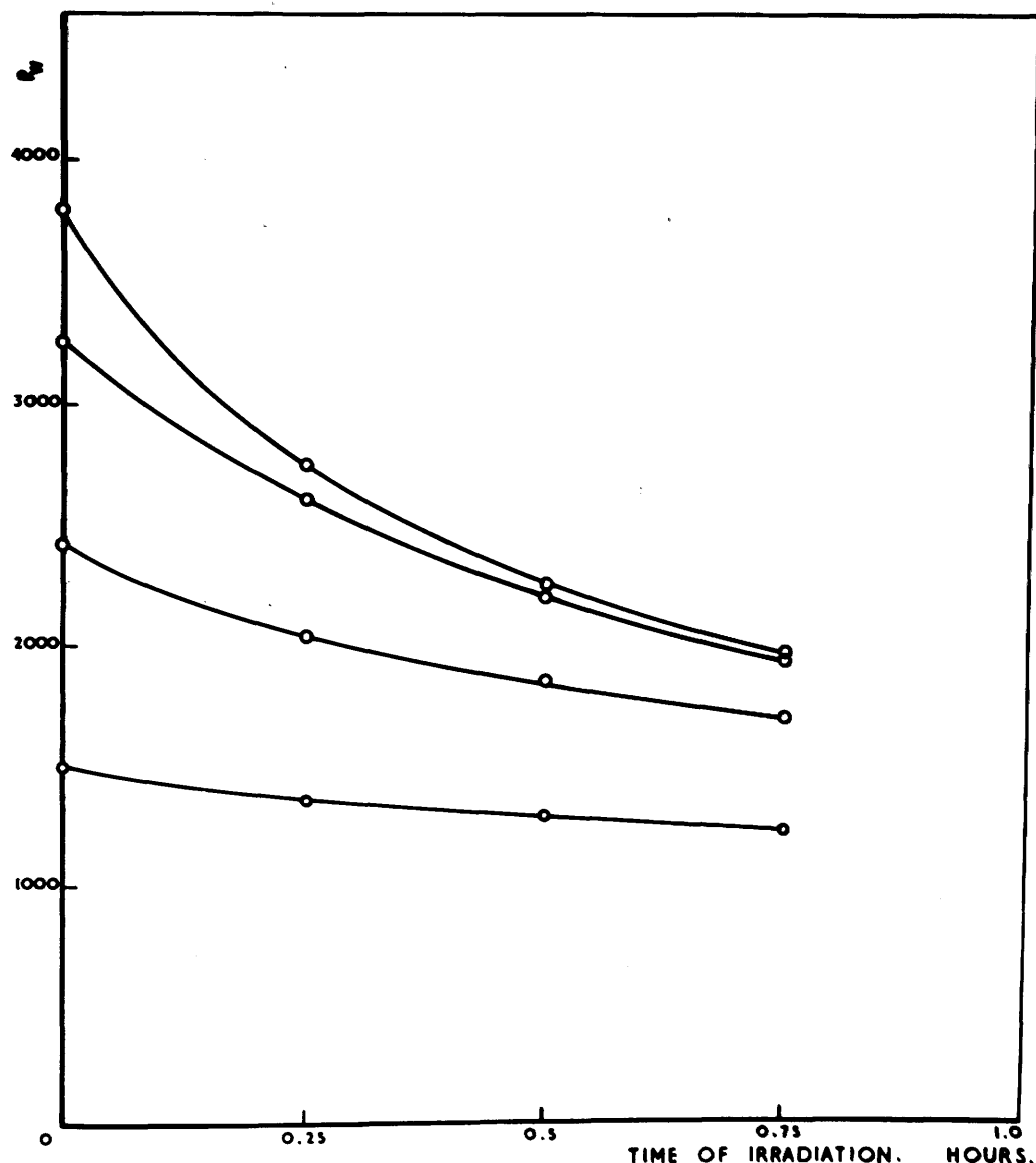
FIG. 57.   DEGRADATION OF 1% POLYSTYRENE IN BENZENE SOLUTIONS.   FREQUENCY 0.75 MC./SEC.
ACOUSTIC INTENSITY 12.5 WATTS/CM²

length at the end of degradation is almost independent of
the initial chain length values, while the degradation of the
4th sample was followed for one hour only. The results of
the four degradation runs are given in Table XIV. The
weight average chain length of the first three samples
decreases with the time of irradiation in the manner shown
in Fig. 56, while the early stages of degradation of the four
samples are presented in Fig. 57.

d. Discussion.

The degradation curves shown in Fig. 56 confirm obser-
:vations by previous investigators who reported that the chain
length at the end of degradation is almost independent of
initial chain length of polymer samples. However, calcula-
:tion of the limiting chain length 'y' for the different
samples showed that it can be represented by:

$$y = 750 \pm 4\%$$

This value justifies the assumption that y is constant in
equations (47) and (48).

The experimental values of the rate constant 'K' at the
beginning of degradation of the different samples were cal-
:culated from equation (19). The theoretical values of K
were calculated from equations (47) for Case (i) and (48) for
Case (ii), with $\beta_1 = \dfrac{1.475}{Y}$ dyne^{-1} hr.$^{-1}$ and $\beta_2 = 1.475$ hr.$^{-1}$
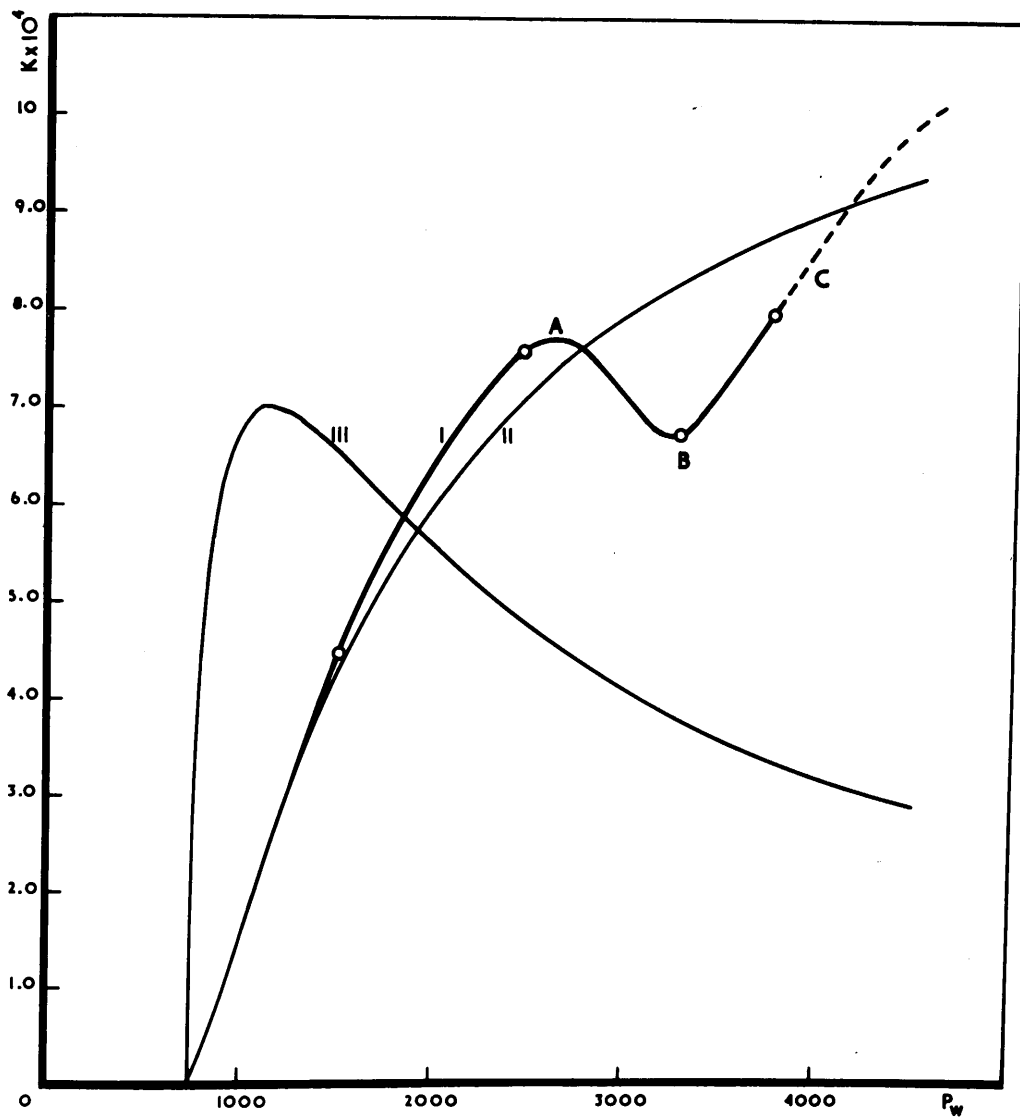
FIG. 58.   RATE CONSTANT OF DEGRADATION VERSUS
CHAIN LENGTH.   I. EXRIMENTAL CURVE.
II. THEORETICAL CASE I.   III. THEORETICAL CASE 2.

as the best values to fit the experimental results.   Both
experimental and theoretical values of K are given in Table
XV and plotted against chain length P in Fig.58.

Fig.58 shows that the experimental values agree closely
with Case (i) up to point A.   The rest of the experimental
curve, i.e., ABC shows an anomolous behaviour.   Similar
behaviour has been observed by Jellinek and White[5] who did
not give any explanation for the observed rise at point A.
A detailed study of Fig.58 and the similar curve reported by
Jellinek and White[5] showed that a certain relation exists
between the two curves.   In both curves the following re-
-lation holds reasonably well:

Frequency of ultrasonic waves 'f' x chain length P_w
corresponding to point A = constant.

Numerically the product fP_w = 4300 x 0.5 x 10^6 = 2.15 x 10^6
deduced from Jellinek's curve,

and = 2650 x 0.75 x 10^6 = 2.0 x 10^9
deduced from Figure 58.

Considering that Jellinek's investigation was carried out
on a homogeneous sample of polystyrene in benzene while this
investigation was carried out on a heterogeneous sample, the
constancy of the product fP_w in both cases was considered
to be significant of a frequency effect.   If one assumes
that some sort of resonance takes place whenever the product

$fP_W = 2 \times 10^9$ or its multiples, therefore the anomolous behaviour shown by the part ABC of the curve can be easily explained. Approaching resonance the rate constant of degradation will gradually increase until point A is reached, and immediately after the rate constant will decrease because of the antiresonance. The increase in rate constant at A is not peaky as was the case with the homogeneous sample of Jellinek. This was considered to be due to the heterogeneous nature of the polystyrene sample giving a broader response to resonance.

Furthermore, the postulation of the existence of a resonance effect implies that there will be a second peak at a chain length of 5320 and a third at $P_W = 7980$ and so on. According to this picture it can be concluded that the occur-
:rence of resonance has to satisfy the condition:

$$P_W f = 2 \times 10^9 C \qquad\qquad (49)$$

where C = 1 for the fundamental;

C = 2 for the second harmonic, and

C = 3 for the third harmonic and so on.

In addition to this resonance effect there is again the effect of cavitation. Under the conditions of this experiment, the frequency and intensity of ultrasonic waves were kept constant. The only variable parameter which may have some

bearing on the intensity of cavitation is the initial chain length. Horton[10] investigated the effect of intermolecular bond strength on the onset of cavitation. He concluded from his experiments on bacterial cells, that cavitation occurs most readily when the interfacial linkages between the cell and the surrounding liquid are weakest. The inference from his conclusion/is that it may not be too erratic to consider, by similarity, that cavitation occurs most easily when the linkage between polymer molecule and solvent molecules is weakest. Amplifying this inference it may be said that the polymer molecules appear to be potential nuclei for the onset of cavitation, i.e., the chain length is related to R_o in Noltingk's theory mentioned earlier. Furthermore, this point of view coincides with Frenkel's statement [11] that in high polymer solutions molecules of the solvent stick to the dissolved polymer molecules in the same way as to the walls of the vessel containing the liquid, or to the surface of macroscopic solid bodies immersed in it. The latter cases are considered as potential nuclei for cavitation.

The conception of cavitation nuclei, presented above, may have a certain effect on the cavitation intensity and consequently on the rate constant of degradation. Parallel to that, the selected numerical values of β_1 and β_2 would be affected.

e. <u>Conclusion.</u>

The following conclusions can be drawn up pending
further experimental confirmation.

1.   Degradation of addition polymers by ultrasonic waves
is frequency dependent.   Consequently <u>degradation can be</u>
<u>effected by ultrasonic waves alone in the absence of cavitation.</u>

2.   Some resonance effect takes place whenever the product
of fP_w is equal to or multiple of 2.0×10^9.

Pending further evidence it is possible that the length
of the polymer chain affects the size of nuclei in the polymer
solution.

E.   <u>EFFECT OF FREQUENCY OF ULTRASONIC WAVES.</u>

a.   <u>Introduction.</u>

A complete study of the dependence of degradation of
long chain molecules on frequency of ultrasonic waves should
cover two main aspects; namely;
(i)   the effect of frequency on cavitation intensity (severity)
which <u>plays the major role</u> in the process of degradation, and
(ii) the effect of frequency on the degradation parameters
K and y.

Considering the first effect, it was mentioned in Chapter
I that there exists an upper threshold of frequency beyond

which no cavitation occurs. This threshold depends mainly on (1) the initial size (radius R_0) of the nuclei present in the liquid, and on (2) the pressure amplitude 'P_0' of the ultrasonic waves. Unfortunately the cavitation nuclei cannot be controlled neither in size nor in nature. Conse-:quently, any detailed study of this aspect is limited by the incomplete knowledge of the nature and dimensions of nuclei in high polymer solutions.

Gaertner[12] suggested the existence of an optimum frequency at which cavitation intensity reaches a maximum. He expected this optimum frequency to be below 2 or 1 Mc. per sec. Furthermore he predicted, from a simplified theory, that cavitation will almost be suppressed when the frequency exceeds 2 Mc. per sec. On the other hand N_0ltingk and Neppiras[7] predicted a higher frequency threshold of 10 Mc. per sec. (under specific conditions) beyond which cavitation will not occur.

Reverting to the effect of frequency on K and y, investigations on the degradation of long chain molecules with different initial average chain length should provide more evidence about the occurrence of resonance. Schmid and Poppe[13] investigated the frequency dependence of ultrasonic degradation of long chain molecules using three different frequencies. The three frequencies were 284 Kc/sec.

from a piezoelectric transducer and 10 Kc. and 175 Kc/sec.
from a magnetostriction transducer. They found that the
rate of depolymerisation of polymethylmethacrylate in ben-
:zene is nearly independent of frequency in that range.
However, it is safe to say that their analysis was not com-
:plete, and it is quite likely that their sample was in fact
affected by the 284 Kc/sec. frequency. That this may be
the case can be roughly verified from the product Pf_w for
their sample.

$$fP_w \;=\; 7000 \times 284 \times 10^3 \;=\; 2 \times 10^9$$

This value is the same as that deduced in the previous section.
Inspection of Fig. 3, after Schmid and Poppe, shows that the
polymethylmethacrylate sample irradiated at 300 Kc/sec.
(284 Kc/sec.) responded somehow differently. Mark[14] and
Crawford[15] remarked that this sample is very susceptible
to degradation without giving any reason for their remark.
Could this behaviour be interpreted as a frequency effect?

b. Experimental.

The frequency of the ultrasonic waves was changed by
changing the tank circuit coil of the oscillator. Two coils
were used; the first coil gave a frequency range 0.5 - 1.25
Mc/sec. while the second made it possible to cover a range
of 0.75 - 2.0 Mc. per sec. Thus it was possible to apply
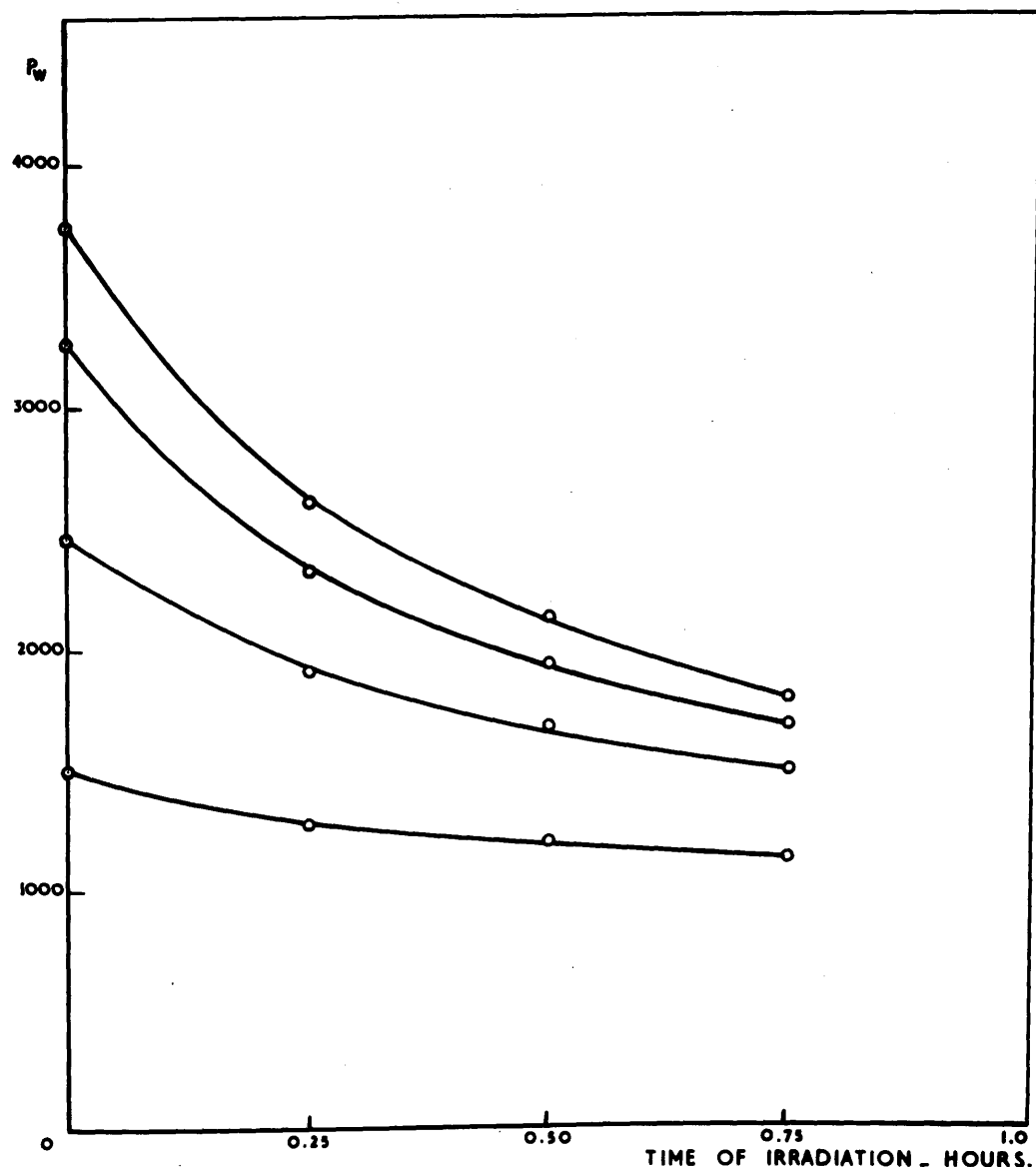
FIG. 59.   DEGRADATION OF 1% POLYSTYRENE IN
BENZENE SOLUTIONS.   FREQUENCY - 1.0 MC./SEC.
ACOUSTIC INTENSITY - 12.5 WATTS/ CM.²
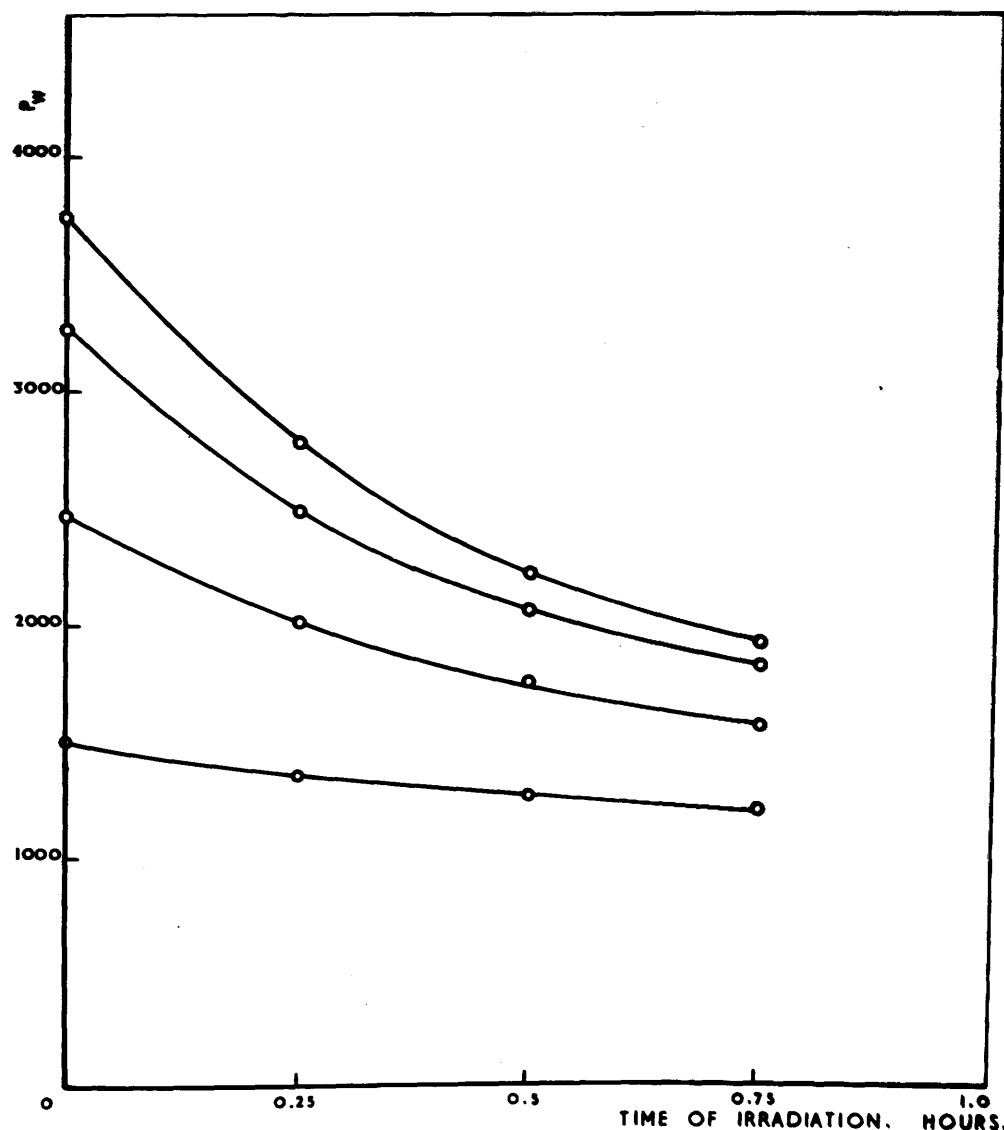
FIG. 6O.   DEGRADATION OF 1% POLYSTYRENE IN BENZENE SOLUTIONS.   FREQUENCY 1.25 MC./SEC.
ACOUSTIC INTENSITY   12.5 WATTS/CM.²
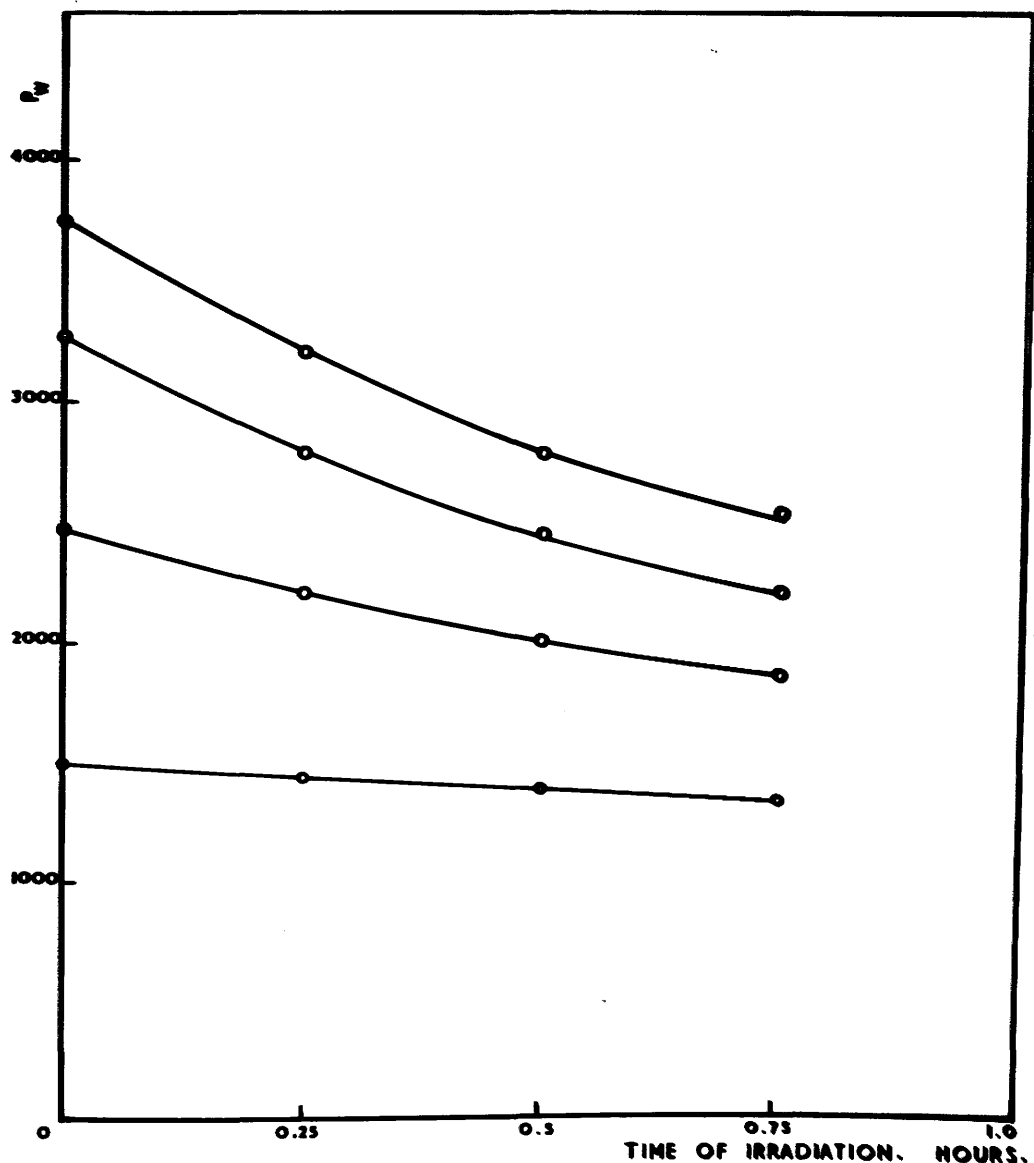
FIG. 61.   DEGRADATION OF 1% POLYSTYRENE IN
BENZENE SOLUTIONS.   FREQUENCY 1.5 MC./SEC.
ACOUSTIC INTENSITY 12.5 WATTS/CM²
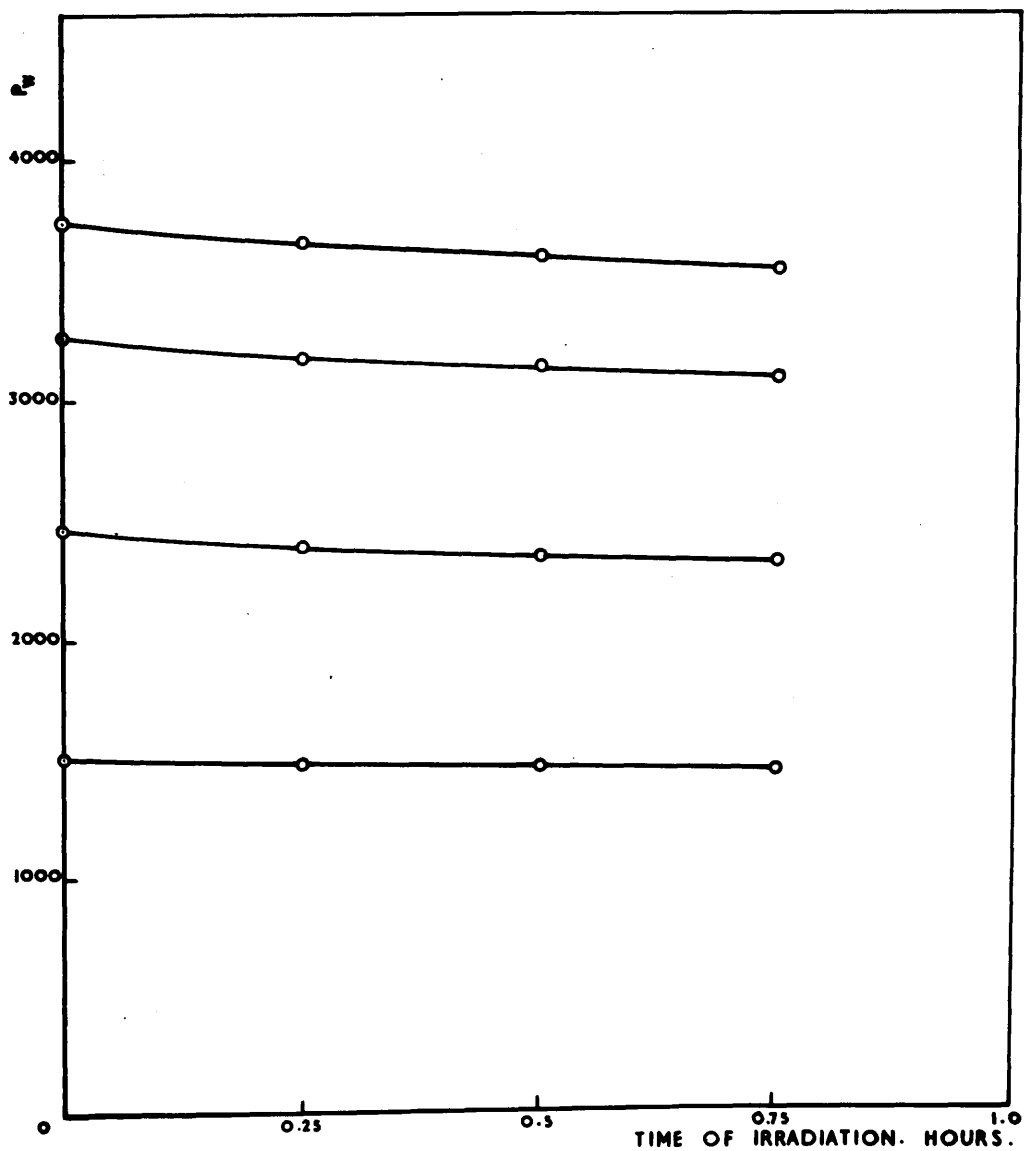
FIG. 62. DEGRADATION OF 1% POLYSTYRENE IN BENZENE SOLUTIONS. FREQUENCY 2.0 MC./S. ACOUSTIC INTENSITY 12.5 WATTS/CM.

ultrasonic waves, of constant intensity, having different frequencies to the high polymer solutions.

Samples of 25 mls. of 1% polystyrene in benzene having different initial average chain length were irradiated by ultrasonic waves of intensity 12.5 watts/cm^2 having a fre-:quency of 0.75 Mc/sec.

This process was repeated with frequencies of 1.0, 1.25, 1.5 and 2 Mc. per sec. Results of these irradiations are shown in Table XVI and represented graphically in Figures 59, 60. 61 and 62, from which values of K were deduced using equation (19).

c. <u>Discussion</u>.

It was convenient for easier interpretation to represent the results in the form given in Figs. 63, 64, 65 and 66. Each of these figures illustrates clearly the effect of increasing the frequency on the degradation of polystyrene in benzene samples.

All figures have the following features in common:

(i) Irradiation by 2 Mc/sec. ultrasonic waves resulted in a very slight degradation taking place.

(ii) Increasing the frequency of the applied ultrasonic waves from 0.75 Mc. per sec. caused an increase in
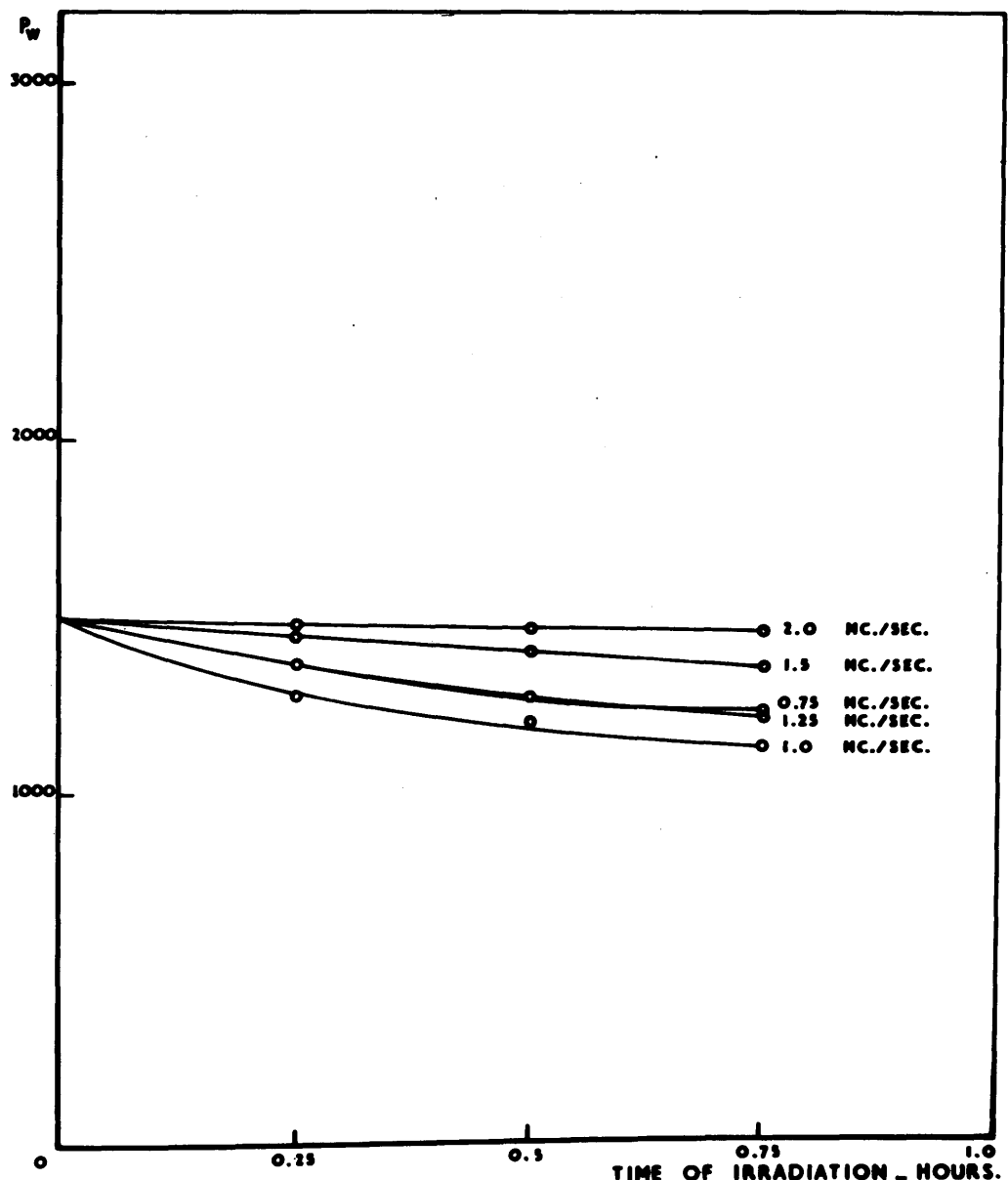
FIG. 63. DEGRADATION OF POLYSTYRENE/BENZENE AT DIFFERENT ULTRASONIC FREQUENCIES.

INTENSITY = 12.5 WATTS/CM². P_W = 1505
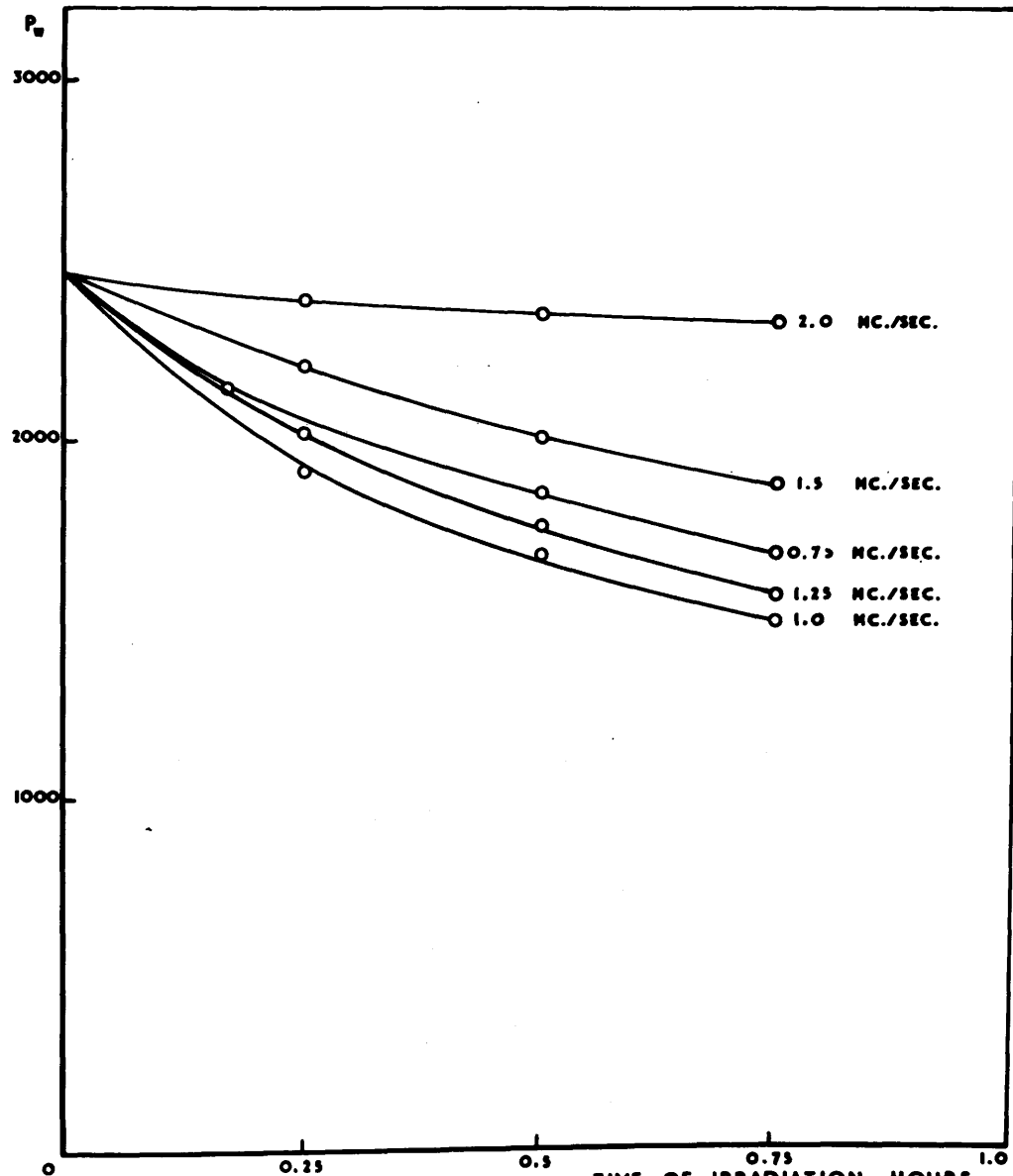
FIG. 64. DEGRADATION OF POLYSTYRENE/BENZENE AT DIFFERENT ULTRASONIC FREQUENCIES.
INTENSITY = 12.5 WATTS/CM^2. P_0 = 2460.

FIG. 65. DEGRADATION OF POLYSTYRENE/BENZENE AT DIFFERENT ULTRASONIC FREQUENCIES. INTENSITY = 12.5 WATTS/CM². P₀ = 3260.
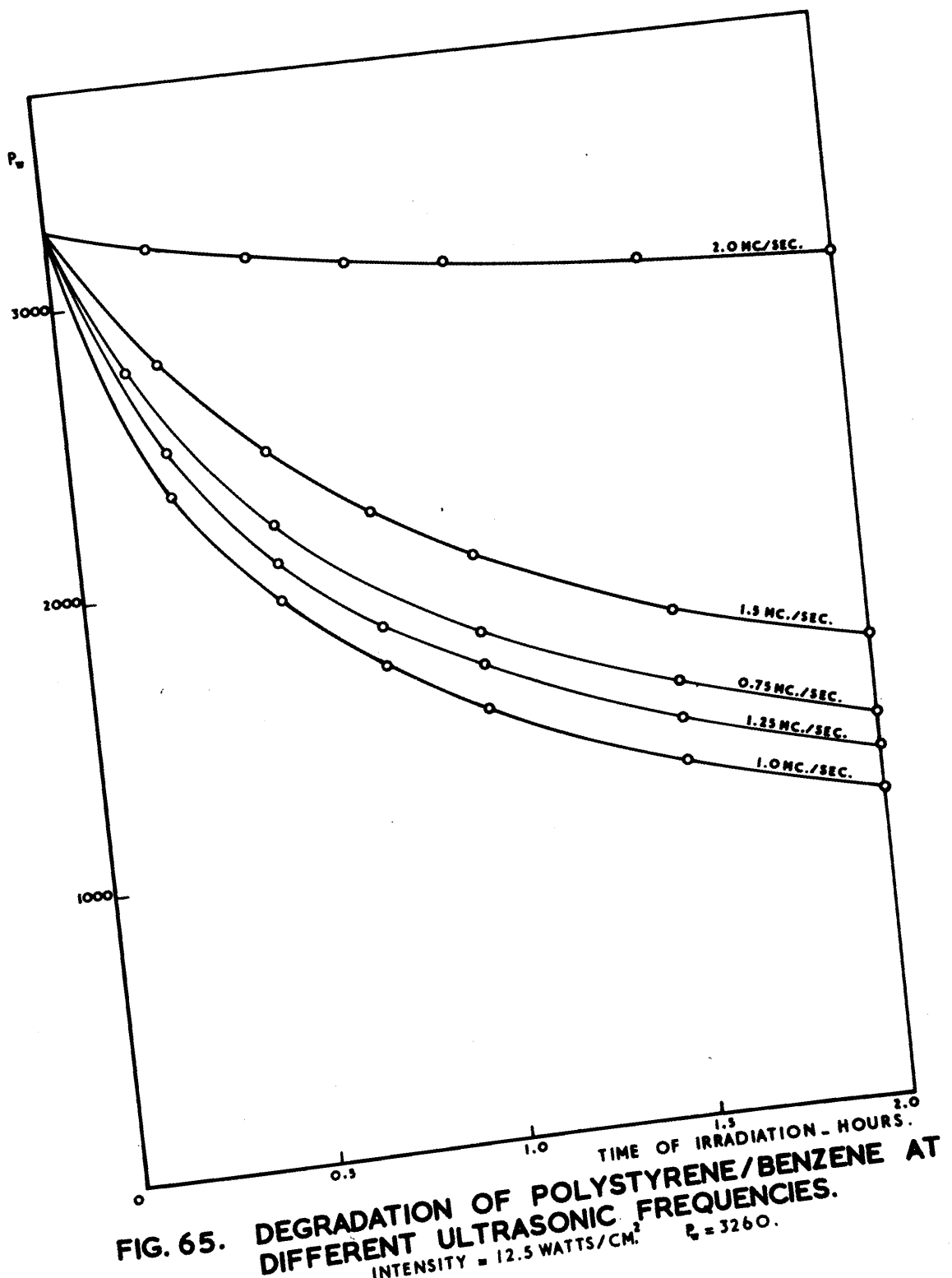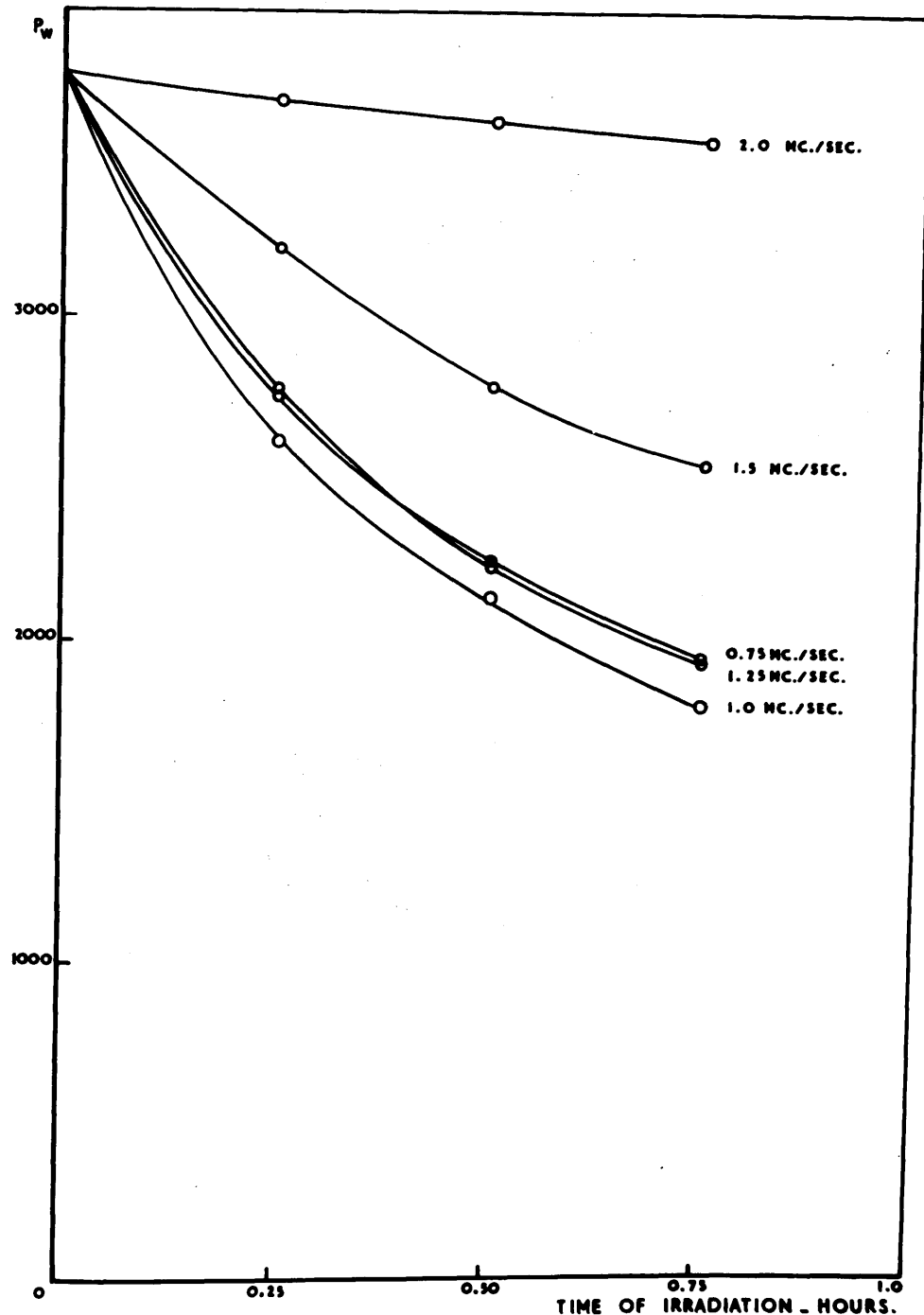
FIG. 66. DEGRADATION OF POLYSTYRENE/BENZENE AT
DIFFERENT ULTRASONIC FREQUENCIES.
INTENSITY = 12.5 WATTS/CM². P_w = 3744

resulting degradation.   Maximum degradation seems to

take place at a frequency of 1 Mc. per sec.   A fur-

:ther increase in frequency caused a reduction in

degradation.

However, it can be easily deduced that the optimum fre-

:quency at which the cavitation intensity reached its maximum

and consequently produced maximum degradation is about 1 Mc.

per sec.   This result agrees with the predictions of Gaertner

and differs quantitatively from thepredictions of Noltingk

and Neppiras.

The rate constant of degradation K in each of the above

mentioned degradation runs was calculated from equation (19).

Calculated values of K are shown in Table XVII in a conven-

:ient way for their interpretation.

Hypothetical values of P_W which satisfy the condition,

$$f \, P_W \; = \; 2 \times 10^9 \; C$$

were entered in red print in the table, while the mode of

vibration is given in blue type.   The values of 'K' shown

in the Table are plotted against chain length in Fig.67.

However, the curves in Fig.67 are conjectural and are drawn

to fit the experimental results and at the same time to

satisfy the above condition for the occurrence of resonance.

The experimental values of K seem to fit in the curves quite

reasonably.
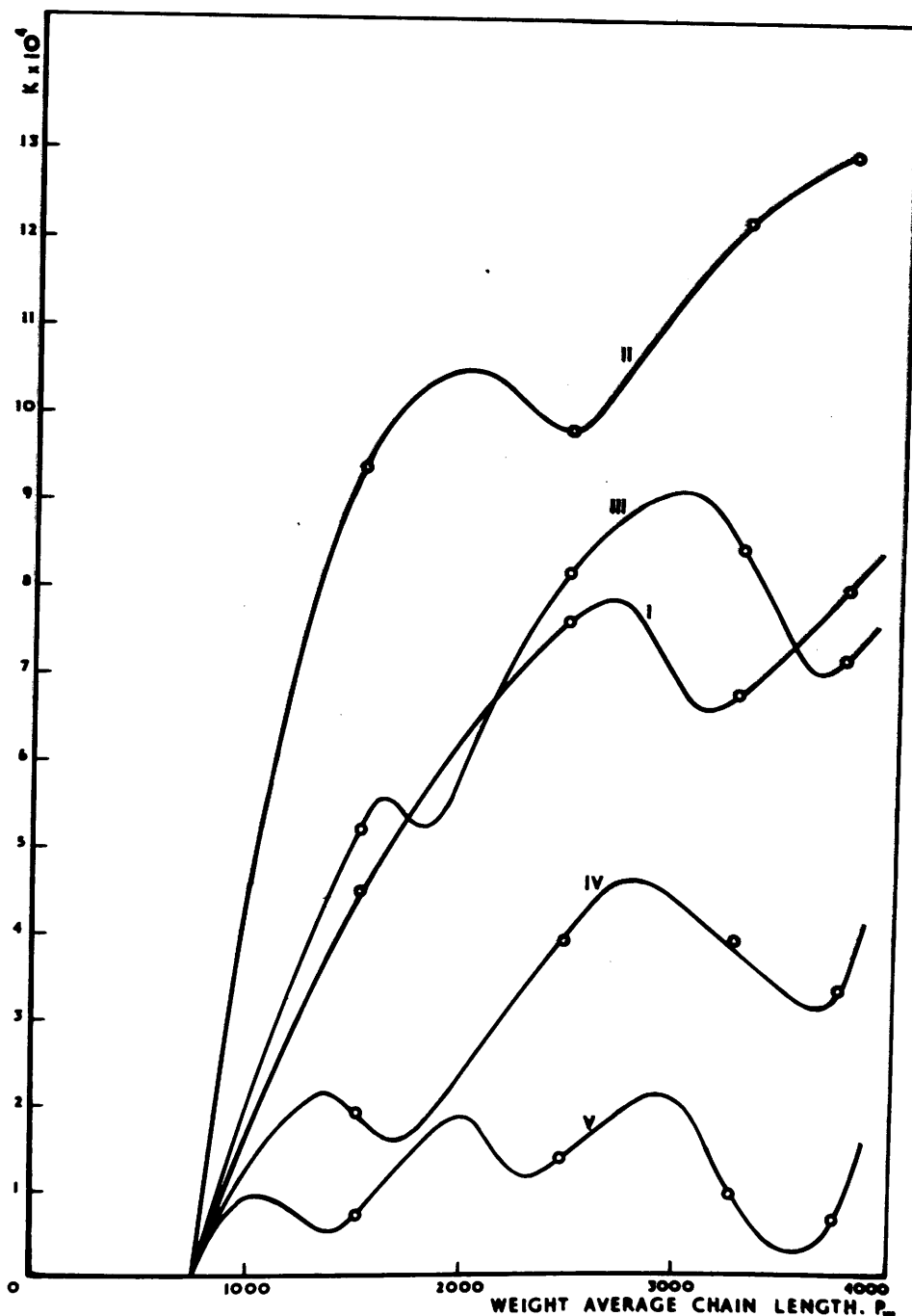
FIG. 67.　K VERSUS P_w　FOR DIFFERENT FREQUENCIES

I. 0.75 MC.　　II. 1.0 MC.　　III. 1.25 MC.　　IV. 1.5 MC.　　V. 2.0 MC.

Comparing the different curves in Fig.67 which includes the experimental curve in Fig. 58, it can be easily observed that the relative values of the rate constant of degradation for different initial average chain lengths were not maintain-:ed when different frequencies were used.   <u>This observation is not affected by the conjectural way in which the different curves are drawn.</u>

However, this observation was the main experimental feature which gave rise to many speculations regarding an alternative mechanism by which long chain molecules could be ruptured when irradiated by ultrasonic waves, and which is frequency dependent.

In attempting to outline such a mechanism which may account for the dependence of degradation on frequency and chain length the following assumptions were made:

1.   The long chain molecule is to be represented by a frictionless thread having spheres of radius 3 A.U., represenging the benzene rings, attached to its axis at equal distances of 3.00 A.U., the distance between two successive benzene rings.

2.   The chain is fixed at both ends, and for simplicity has its length at right angles to the direction of propa-:gation of plane ultrasonic waves.   This assumption differs
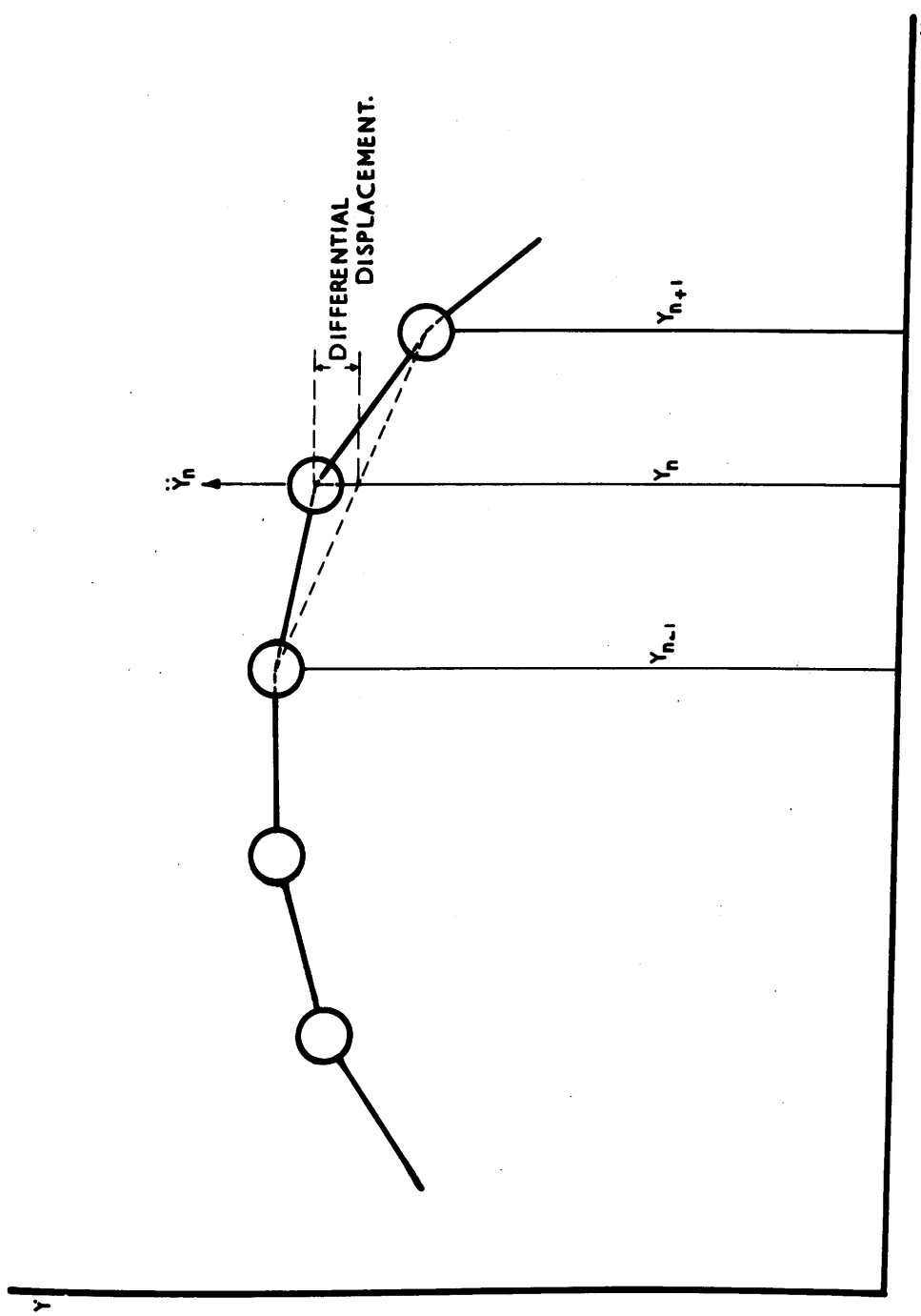
FIG. 68.   ILLUSTRATIVE MODEL OF A LONG CHAIN MOLECULE.

from the assumption made by Schmid[6] in which the chain was considered to have one end fixed while the other is free to follow the ultrasonic waves. Furthermore, this assumption is justified by the fact that the probability for one end of the chain to be fixed is the same as the probability of the other end.

3. There will be no tension along the axis of the C-C bond during the motion of the chain.

4. The effect of side groups and hindered rotation is neglected.

5. The bond angle is taken as 180° instead of 109° 26' for geometrical simplicity.

With these assumptions in mind the long chain molecule is represented in Fig.68. The small circles represent the benzene rings. The forces causing the motion are frictional forces resulting from the motion of solvent past the benzene rings. Both solvent and solute molecules will follow the wave motion differently giving rise to a relative velocity between the two. When the chain molecule is set in motion the bond angles will change, increasing and decreasing in quick succession. Since about 1000 cal. per mole is the energy required to cause a change of 10° in the bond angle from its minimum energy value, therefore a restoring force will come into action to maintain the minimum energy configuration of the chain molecule.

Assuming that oscillation of the long chain is poss-

:ible, resonance will take place when the mode of vibration of the long chain molecule has its natural undamped frequency the same as that of the acting external force and their ampli:tudes are in phase. Under these conditions the equation of the undamped motion of the nth benzene ring will be given by:

$$m \ddot{y}_n + \alpha(y_n - \frac{y_{n+1} + y_{n-1}}{2}) = 0 \qquad (50)$$

where m is the mass of the benzene ring or mass of monomer unit; y_{n+1}, y_n, y_{n-1}, are the displacements of the n+1, n, and n-1 spheres from the equilibrium position at any time t.

α is a restoring force per unit differential dis:placement (deformation constant) which can be calculated from energy considerations.

$$\therefore \quad \frac{2m}{\alpha} \ddot{y}_n + 2y_n - y_{n+1} - y_{n-1} = 0$$

$$\text{if} \quad y_n = A_n e^{i\omega t} \qquad (51)$$

$$\therefore \quad A_{n-1} + \gamma A_n + A_{n+1} = 0 \qquad (52)$$

$$\text{where} \quad \gamma = \frac{2 m \omega^2}{\alpha} - 2 \qquad (53)$$

If there are P units in the chain, P such equations are needed and since the chain is assumed to be fixed at both ends, therefore:

$$A_0 = A_{P+1} = 0$$

The following set of equations will therefore represent the motion of the long chain molecule:

$$\Upsilon A_1 + A_2 \quad \ldots\ldots\ldots\ldots\ldots\ldots\ldots = 0$$
$$A_1 + \Upsilon A_2 + A_3 \ldots\ldots\ldots\ldots\ldots = 0$$
$$A_2 + \Upsilon A_3 + A_4 \ldots\ldots = 0 \qquad (54)$$
$$\ldots\ldots\ldots\ldots\ldots\ldots\ldots\ldots\ldots$$
$$\ldots\ldots\ldots\ldots\ldots\ldots\ldots\ldots\ldots$$
$$A_{P-1} + \Upsilon A_P \qquad = 0$$

Equation (54) represents P homogeneous linear equations for A_1, A_2 ... A_P, and in order that they may have a solution, Υ must be a root of:

$$D_P = \begin{vmatrix} \Upsilon & 1 & 0 & 0 & 0 & \ldots\ldots & 0 \\ 1 & \Upsilon & 1 & 0 & 0 & \ldots\ldots & 0 \\ 0 & 1 & \Upsilon & 1 & 0 & \ldots\ldots & 0 \\ \ldots\ldots\ldots\ldots\ldots\ldots\ldots & 1 \\ \ldots\ldots\ldots\ldots\ldots\ldots 1 & \Upsilon \end{vmatrix} = 0 \qquad (55)$$

which is the frequency equation.

Expanding the determinant we get:

$$D_P = D_{P-1} - D_{P-2} \qquad = 0$$

Such recurrence relation has the solution:

$$D_P = \frac{\sin(P+1)\theta}{\sin\theta}$$

where $\Upsilon = 2\cos\theta$ $\qquad (56)$

Therefore:

$$D_P = 0 \quad \text{if} \quad \sin(P+1)\theta = 0$$

i.e. $(P+1)\theta = C\pi$

or $\theta = \dfrac{C\pi}{P+1}$ $\qquad (57)$

where C is an integer that can take any value between 0 and P.

From equations (53), (56) and (57)

$$\therefore \quad \frac{2\,m\,\omega^2}{\alpha} - 2 = 2\,\text{Cos}\,\frac{C\pi}{P+1}$$

The lowest natural frequency of vibration is given by:

$$C = P,$$

i.e.,
$$\frac{2\,m\,\omega^2}{\alpha} - 2 = 2\,\text{Cos}\,\frac{P\pi}{P+1} = 2\,\text{Cos}\,(\pi - \frac{\pi}{P+1})$$

$$= -2\,\text{Cos}\,\frac{\pi}{P+1} \qquad (58)$$

since P is large, by expanding in power series, we get:

$$\text{Cos}\,\frac{\pi}{P+1} = 1 - \frac{\pi^2}{2(P+1)^2} \quad \text{as a first approximation.}$$

Therefore equation (58) can be written in the form:

$$\frac{m\,\omega^2}{\alpha} = \frac{\pi^2}{2(P+1)^2}$$

or
$$\omega = \pm \frac{\pi}{(P+1)} \sqrt{\frac{\alpha}{2\,m}}$$

Considering P+1 = P for P large, the natural frequency of vibration is given by:

$$f = \frac{1}{2\,P} \sqrt{\frac{\alpha}{2\,m}}$$

i.e.,
$$fP = \frac{1}{2}\sqrt{\frac{\alpha}{2\,m}} \qquad (59)$$

Similarly for the next mode of vibration, C will have a value of P-1, and following the same treatment we get the frequency of the second mode of vibration as :

$$f = \frac{1}{P}\sqrt{\frac{\alpha}{2\,m}}$$

or
$$fP = \sqrt{\frac{\alpha}{2\,m}} \qquad\qquad (60)$$

Hence, the frequency of vibration of the undamped long chain molecule is given by the general expression:

$$fP = \frac{C}{2}\sqrt{\frac{\alpha}{2\,m}} \qquad\qquad (61)$$

where C is an integer which can take any value between

1 and P depending on the mode of vibration;

and $\frac{1}{2}\sqrt{\frac{\alpha}{2\,m}}$ is a constant that can be evaluated.

Comparing the theoretical condition for the occurrence of resonance given by equation (61) with the deduced condition from experiment, i.e., $fP_w = C \times 2 \times 10^9$, it seems that the similarity between the two conditions is unlikely to be a mere coincidence.   However, for numerical evaluation of the theoretical value of the product fP, we consider the value of 'm' and 'α'.

$m = 1.7 \times 10^{-22}$ gms. for a benzene ring.

The value of the deformation constant 'α' varies considerably and it depends on the type of molecules whether triangular, pyramidal, tetrahedral or symmetrical chain molecules.   For an energy of about 1000 cal./mole required to cause a deformation of 10^0, the calculated value of $\alpha = 10^4$ dyne/cm.

For the fundamental mode of vibration of a long chain molecule, the theoretical value of the product fP is given by:

$$fP = \frac{1}{2}\sqrt{\frac{10^4}{2 \times 1.7 \times 10^{-22}}} = 2.71 \times 10^{12} \qquad (62)$$

compared with 2×10^9 as determined from experiment. Obviously the theoretical value of 'fP' is far greater than the experi-:mental. However, this big difference should not invalidate the close similarity between the theoretically derived and experimentally deduced forms of 'fP'.

A brief review of the possible degradation mechanisms suggested by previous workers in this field is of paramount importance in illustrating the intricate nature of this pro-:blem. Moreover this review should account for the discrep-:ancy between the two values of 'fP' and the assumption that the chain length is fixed at both ends.

Szalay[16], from a comparison between colloidal particle velocities due to thermal agitation (causing degra-:dation) and particle velocities due to ultrasonic waves - derived from intensity measurements - considered the increase in the velocity of colloidal particles, due to ultrasonic waves, as the cause of degradation. According to his con-:ception macromolecules having greater velocities than solvent molecules will have greater kinetic energies. He believed in the transformation of this vibrational energy,

by unknown methods, into the activation energy of depolymer-
:isation.

Thieme[17] in another attempt to explain the mechanism
of degradation, suggested that collisions between macromole-
:cules are strong enough, due to their increased kinetic
energies in the presence of ultrasonic waves, to cause degra-
:dation.   Comparing the length of a macromolecule
(6 x 10^{-5} cms.) with the wave length of ultrasonic waves
(4 x 10^{-1} cms.), collisions between macromolecules seem
unlikely to take place.   If the macromolecules are free to
move they will follow the wave motion without collision.
On the other hand, if they are constrained from motion their
response will depend on the way they are constrained, and yet
in no case will there be a possibility of collisions, which
can cause degradation.

Schmid[6] suggested a third mechanism for the degra-
:dation.   In view of the fact that it is accepted as a
possible mechanism by which long chain molecules can be rupt-
:ured, it is relevant to discuss his suggested mechanism in
detail especially if it is likely to elucidate the discrep-
:ancy between the two values of 'fP'.

Basically, Schmid analysed two extreme cases repre-
:senting the behaviour of a long chain molecule in an ultra-
:sonic field.

Case (1).

In his first hypothetical case, he represented the long chain polystyrene molecule (D.P. = 1000) with one benzene ring associated to every second carbon atom by a frictionless thread with spheres representing the benzene rings (radius = 3 A.U.) attached to its axis at equal intervals of 3.0 A.U. (distance between two successive benzene rings). He then considered one end of the molecule fixed and the other end free to follow the ultrasonic vibrations. The total friction coeff-:icient is the sum of the Stoke's friction coefficients of the single spheres, which will be $6\pi\eta r$ x 1000 = 6 x 10^{-6} gm. sec.$^{-1}$, for 1000 spheres, and $\eta = 10^{-2}$ gm. cm.$^{-1}$ sec.$^{-1}$. Considering the maximum relative velocity between solvent and spheres to be equal to the velocity of solvent particles (spheres fixed) = 4 0 cm. sec.$^{-1}$, the maximum frictional force will be 2.4 x 10^{-4} dynes, which is of the same order of magnitude as that required to break a C-C bond.

Case (ii).

In this case he considered the macromolecule free at both ends with no entanglements to constrain its response to the ultrasonic waves. Considering the whole molecule as one mass m_K, its motion was represented by the equation:

$$m_K \cdot \frac{dV_K}{dt} + \beta\, V_r = 0 \qquad\qquad (63)$$

where

β is the total Stoke's friction coefficient $= 6\pi\eta r.P$, P being the D.P. of the chain;

V_K is the velocity of the long chain molecule; and

V_r is the relative velocity of the molecule with respect to the solvent molecules, i.e., $V_r = (V_K - V)$, where V is the velocity of solvent given by $V = V_o e^{i\omega t}$.

The solution of equation (63) is given by:

$$V_r = \frac{\dfrac{\omega m_K}{\beta}}{\sqrt{1 + \dfrac{\omega^2 m_K^2}{\beta^2}}} \cdot V_o e^{i(\omega t - \phi)} \qquad (64)$$

where ϕ, the angle of lag $= \tan^{-1} \dfrac{\beta}{\omega\, m_K}$

Substituting the numerical values, Schmid found that:

$\dfrac{\omega m_K}{\beta} = \underline{5 \times 10^{-8}}$ which can be neglected compared to 1.

Therefore, $V_r = \dfrac{\omega m_K}{\beta} \cdot V_o e^{i(\omega t - \phi)}$ \qquad (65)

The inference from equation (65) is that for a mobile molecule, free from entanglements, the relative velocity 'V_r' will be equal to $5 \times 10^{-8} V_o$ for a frequency of 284 Kc./sec. and consequently the frictional force developed will be about 5×10^{-8} times that required to break a C-C bond.

However, Schmid discussed the effect of entanglements and aggregation in the light of modern theories of high poly-
:mer solutions. Changing the effective length of the chain by entanglements will have no effect on the ratio $\frac{m_K}{\beta}$ and consequently the value of $\frac{\omega m_K}{\beta}$ will remain unaffected. Hence it was concluded that the entanglements and aggregation will cause an effective increase in the mass of the spheres. Other molecules entangled with the spheres and the trapped and immobilised solvent will effectively cause an increase in its effective mass proportional to the $(\text{radius})^3$ while the increase in the friction coefficient will be proportional to the radius only and therefore $\frac{m_K}{\beta}$ will increase as the square of the radius of the sphere.

In conclusion he visualised that the value of $\frac{\omega m_K}{\beta}$ would eventually increase from 5×10^{-8} to more than 10 so that the quantity $\frac{\omega m_K}{\beta} / \sqrt{1 + \frac{\omega^2 m_K^2}{\beta^2}}$ will be approximately = 1. Concurrently the free mobile molecule will become entang-
:led enough to justify his hypothetical case with the macro-
:molecule fixed at one end only. (Why one end only? Why not the two ends?).

Reverting to the discrepancy between the experimental value of 2×10^9 and the theoretical value of 2.71×10^{12} for fP, it is obvious that the discrepancy in this case, which is of the order of 10^3, is far less than the discrepancy

in Schmid's case which is of the order of 10^8.

Following Schmid's reasoning it seems equally logical to consider that the entanglements and aggregation of macro-:molecules may modify the macromolecule's response to ultra-:sonic waves, so that it can be simulated by a chain fixed at both ends with effectively greater mass per sphere.

This conclusion can be further confirmed by a process of successive elimination of the factors involved in equation (59) in the light of the known and observed facts about high polymers and their degradation.

The value of the deformation constant 'α' may change slightly if the effect of the hindered rotation and the com-:ponent of whatever tension that my develop along the length of the C-C bond in the direction of deformation, are taken into consideration. However, the resulting slight increase in the value of 'α' will have practically no effect on the theoretical value of fP.

If the effect of entanglements and aggregation is to increase the effective length of the chain P by 1000 times, to bring the value of 'fP' to about 2×10^9, then the effective chain length will be comparable to the wave length of ultra-:sonic waves. Obviously, the effect of ultrasonic waves would be to allign all such entangled molecules with their

lengths parallel to the wave fronts of the pressure wave, with the consequent dissociation of the entangled ends, with-:out rupturing any C-C bond.

If, on the other hand, the length of chain is highly increased by the addition of other chains of different lengths, via end to end entanglements, to bring 'Pf' to experimental value, then it will be difficult to see why any particular chain length should have a direct effect on the rate of degradation, as was observed by Jellinek[5] and as shown in Fig. 58.

Furthermore, the conception of an increase in the effective chain length will not justify the assumption that the chain is fixed at both ends. Hence, it seems unlikely that a change in the effective value of 'P' will yield a theoretical picture which can illustrate the experimental results observed.

Finally, confirming that an increase in the value of 'm' in equation (59) is the outcome of the entanglements and aggregation in the polymer solution, it should be emphasised that an increase in 'm' is the only logical modification that will render the macromolecule dynamically liable to be ruptured by ultrasonic waves, yielding results in agreement with experimental observations. Further discussions of this

mechanism are given in Chapter VI, where in some calculations the effective mass of the sphere is considered for comparison.

An obvious deduction from the above analysis is that at very low concentrations, when no entanglements of chains are likely to take place, the ends of the chain molecule will be free to move and the chain, as a whole, will oscillate and consequently rupture of bonds will cease. No degradation will take place. On the other hand at high concentrations entanglements will be excessive and the long chain molecule will be highly constrained. The polymer chains will behave as a scaffolding resulting again in an appreciable decrease in degradation. Thus one would expect an optimum concentra-:tion at which degradation will be maximum. This picture agrees with results of degradation of long chain molecules reported by different investigators.

However, for a complete analysis of the problem, the effect of phase difference and damping has to be considered. In attempting to solve this part of the problem, the mathe-:matics became so complex that it was very difficult to handle. Further comment on this aspect will be made in the following Chapter.

Summing up, it can be stated that long chain molecules can be ruptured by ultrasonic waves alone. The mechanism by which C-C bonds can be broken involves frictional forces

which cause alternate changes in the bond angles, which
ultimately result in scission of the most vulnerable link[18].

Furthermore, considering the degradation curves, Figs. 63, 64,
65 and 66 it is obvious that frequency has a definite effect
on the final weight average chain length.   Consequently it
can be stated that the limiting chain length y, below which
degradation will not take place is dependent on the frequency
of ultrasonic waves in the range 0.5 - 2 Mc. per second.
Increasing the frequency beyond 0.5 Mc. the limiting chain
length y will decrease and will reach its minimum value at the
optimum frequency, at which cavitation intensity is maximum.
Beyond the optimum value any further increase in frequency
will result in an increase in the limiting chain length.
Thus the limiting chain length 'y' below which degradation will
not occur is dependent on the frequency of the ultrasonic
waves; a fact which was ignored by most previous investi-
:gators.

d. Conclusions.

The following conclusions can be drawn out of the above
discussion:

1.   The degradation parameters K and y are dependent on the
ultrasonic frequency in the range 0.75 - 2 Mc. per sec. as a
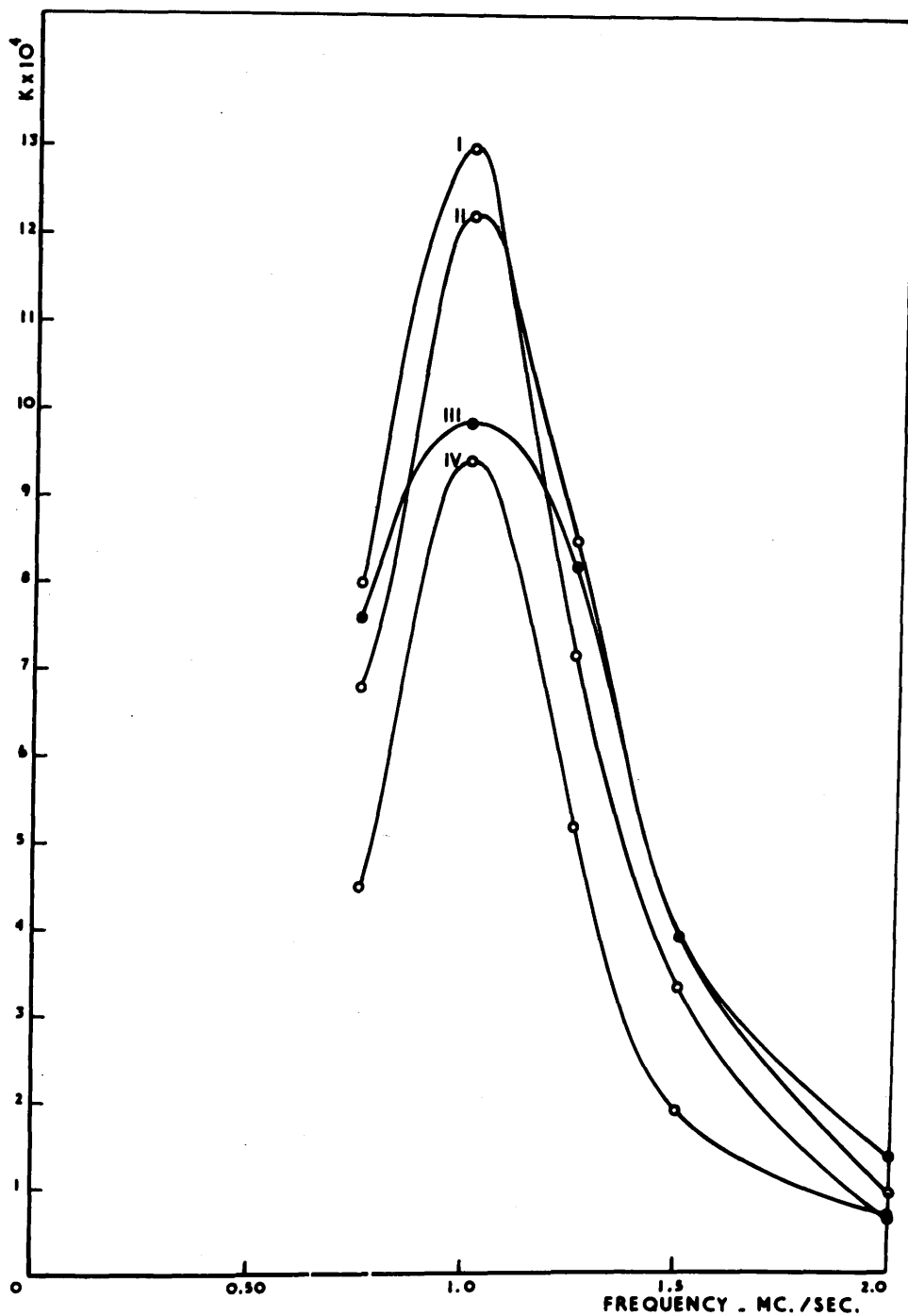
FIG. 69.   RATE CONSTANT OF DEGRADATION VERSUS
FREQUENCY.   INTENSITY = 12.5 WATTS/CM.²
I. P_W = 3744   II. P_W = 3260   III. P_W = 2460   IV. P_W = 1505.

consequence of cavitation intensity. K increases up till the optimum frequency is reached and then decreases, as shown in Fig.69, while y decreases reaching a minimum at the optimum frequency and then increases.

2. Superimposed on the continuous change in the value of K is/cyclic change corresponding to resonance effects. A similar cyclic variation in the value of y should be expected purely on a theoretical basis.

3. Resonance phenomenon occurs whenever the condition $fP_w = 2 \times 10^9 . C.$

4. The optimum ultrasonic frequency at which cavitation intensity (severity) reaches a maximum is about 1 Mc. per second.

5. Degradation of long chain molecules decreased markedly as the frequency was increased beyond its optimum value, 1 Mc. per second. This is mainly due to the reduction in cavitation intensity.

6. Cavitation produced by ultrasonic waves ceases at a frequency of 2 Mc. per second or more.

COMMENT.

It is the author's hope that the outcome of the above investigation of the effect of frequency of ultrasonic waves on the degradation of long chain molecules will be considered more informative as pointed out in Chapter II.

F. EFFECT OF CAVITATION.

a. Introduction.

As mentioned in Chapter III the reaction vessel was designed so that reflection of ultrasonic waves from its bottom would be virtually eliminated. The fixing of the 0.0005" terylene membrane at the bottom of the reaction vessel was therefore to ensure that the ultrasonic energy would be transmitted through the polymer solution without any loss.

Degradation of high polymers by ultrasonic waves alone without cavitation proved to be possible, following discussion in the previous section. Only the amount of degradation caused by cavitation at different frequencies of ultrasonic waves remains to be estimated.

However, in order to confirm that cavitation would be completely suppressed when the frequency of ultrasonic waves is 2 Mc./sec. or more, degradation of polystyrene in benzene solution was carried out under vacuo. The optimum frequency for cavitation intensity was chosen for the ultrasonic waves
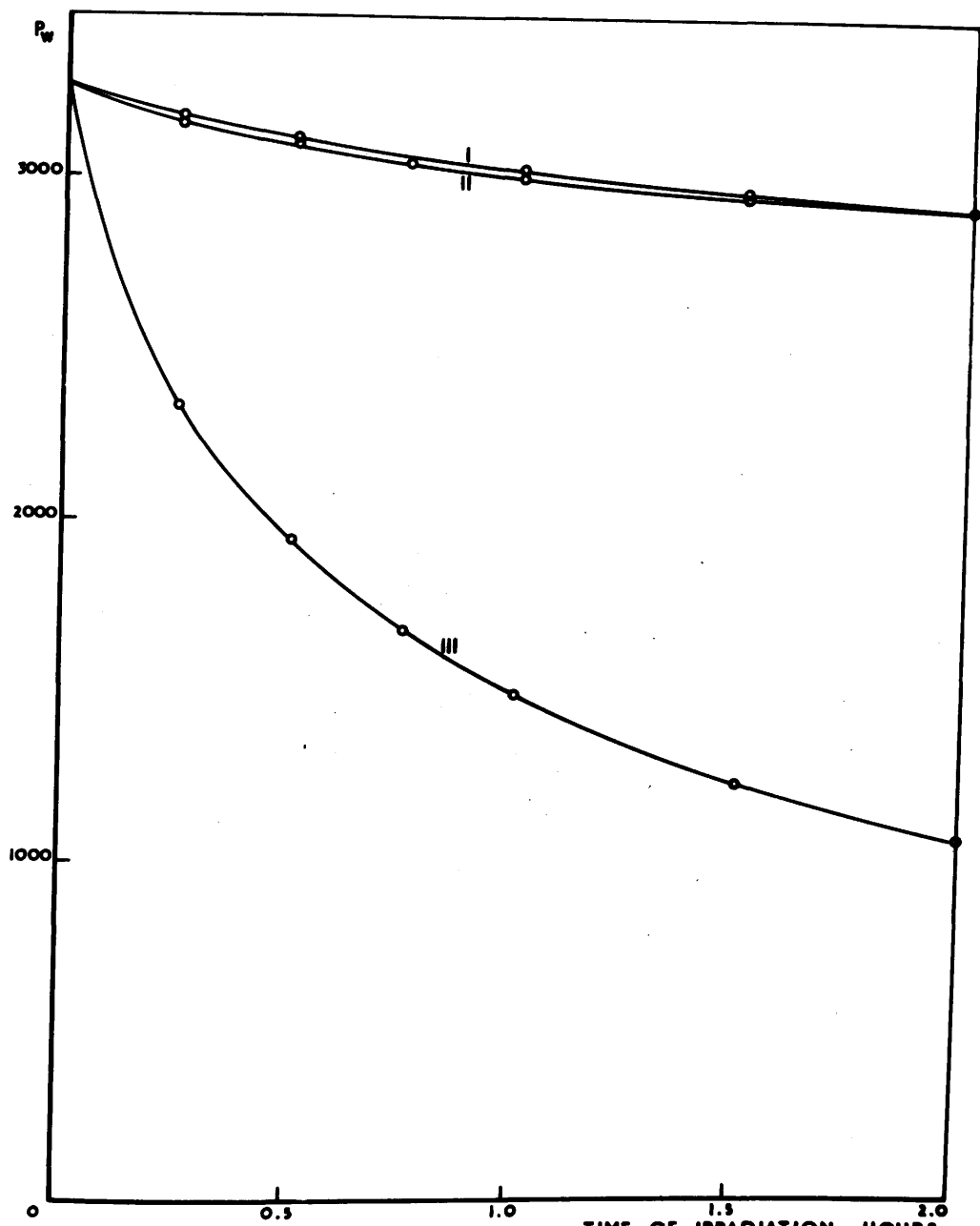
FIG. 7O.   DEGRADATION OF POLYSTYRENE IN VACUO.

I. 2 MC./SEC._ATMOSPHERIC PRESSURE   II. IMC./SEC _ VACUUM.
III. IMC./SEC._ATMOSPHERIC PRESSURE   INTENSITY = 12.5 WATTS/CM.^{2}

P_W = 3260.

used in this investigation in order to provide the most informative experimental conditions.

b. Experimental.

25 mls. of a 1% polystyrene in benzene solution of initial weight average chain P_w = 3260 were introduced in the reaction vessel. Fig.17, and its B10 quick fit cone was fitted to the two stage vacuum line. The sample was thoroughly degassed and the reaction vessel was then sealed at the neck (using a flame master), maintaining vacuum inside the vessel.

The reaction vessel was then mounted on the platform and the polystyrene sample was irradiated by 1 Mc. ultrasonic waves of intensity 12.5 watts/cm^2. Viscosity measurements were carried out at different stages of the ultrasonic irradiation which continued for 2 hours, without disturbing the vacuum.

Results of the irradiation process which are given in Table XVIII show how the weight average chain length 'P_w' decreases during irradiation.

In Fig.70, the weight average chain length is plotted against time of irradiation. Two more curves are included in the figure for comparison. The intensity of ultrasonic waves in the three cases was the same, i.e., 12.5 watts/cm^2,

It is of interest to mention that the bubbles which
used to appear in practically all the previous experiments
did not appear at all in the bulk of the polymer sample when
irradiated in vacuo.

c. **Discussion.**

Full mathematical treatment of cavitation, i.e., cavity
growth and collapse, was always complicated by the many factors
involved; surface tension, liquid compressibility, thermal
transfer, gas and vapour transfer and diffusion, etc., which
have to be considered. However, only the aspect of supp-
:ressing cavitation is of interest in connection with this
work. It is an established fact that destructive cavitation
can be suppressed either by applying, directly to the liquid,
an external pressure greater than the pressure amplitude of
the ultrasonic waves or by thoroughly degassing the liquid
and maintaining vacuum on top of its free surface. Both
methods were adopted by previous research workers to investi-
:gate the degradation of high polymers by ultrasonic waves in
the absence of cavitation. Their results were not always
in agreement as is discussed in the critical survey, Chapter I.

Fig.70 shows clearly that high polymers can be degraded
by ultrasonic waves alone in the absence of cavitation. The

role of cavitation in the degradation process is clearly
demonstrated by the marked difference between curve II which
represents the effect of ultrasonic waves alone, and curve
III representing the combined effect of ultrasonic waves and

associated cavitation. Quantitatively the rate constant of
degradation, calculated from equation (19) was found to be
1.008 hr.$^{-1}$ in the absence of cavitation, compared to 12.22
hr.$^{-1}$ when cavitation intensity (severity) is at its maximum.
In other words the rate constant of degradation due to ultra-
:sonic waves alone is only 8.23% of its total value when
cavitation is in action. Obviously cavitation inception
has a marked effect on the value of the limiting chain length y.

It is of interest to compare the results of degradation
represented by curves 1 and 11. Curve 1 shows the change
in the weight average chain length P_w of the polystyrene
sample when irradiated by 2 Mc./sec. ultrasonic waves of
intensity 12.5 watts/cm^2. at atmospheric pressure, while
Curve 11 shows the change in P_w when treated by 1 Mc.sec.
ultrasonic waves of the same intensity but in vacuo. The
degradation in both cases is almost of the same order of
magnitude, with the rate constant of degradation
$K = 0.952 \times 10^{-4}$ hr.$^{-1}$ calculated from curve I, against

1.008×10^{-4} hr.$^{-1}$ for curve 11.   The small difference between the two values of 'K' is attributed to the effect of frequency on the attenuation of sound energy transmitted in the polymer solution.

The pressure amplitude of plane ultrasonic waves at a distance x from the source along the direction of propaga-:tion is generally given by the expression:

$$p = p_o e^{-ax}$$

where p_o is the pressure amplitude at the surface of
                the source, and

       a   is a combined attenuation constant representing
                the effect of viscosity and heat conduction.

The attenuation constant 'a' is dependent on the wave length of ultrasonic waves.   Under the experimental conditions mentioned above, it is simply proportional to the square of frequency.   Hence, although the ultrasonic intensity which was always measured at a plane 1 cm. above the terylene membrane, was the same, yet its overall average value will be slightly different in both cases due to the different frequencies used and their consequent effect on attenuation.

Therefore, in the absence of cavitation and maintaining the same intensity, it is to be expected that the degradation produced by 2.0 Mc/sec. ultrasonic waves would be slightly

less than that produced when a frequency of 1 Mc/sec. is used.

The experimental results obtained were, in fact, in agreement with the theoretical result anticipated.

Reverting to the conclusions arrived at in Section E, it can be emphasised that cavitation is completely suppressed in liquids under normal atmospheric conditions, when the frequency of applied ultrasonic waves is 2 Mc./sec. or more. In other words, in the absence of cavitation degradation of high polymers will be effected by ultrasonic waves alone when the frequency is 2 Mc./sec. or more.

d.   Conclusions.

1.   Below 1.5 Mc/sec. high polymers are degraded by the combined action of cavitation and ultrasonic waves, with cavitation playing the main role.

2.   At a frequency of 2 Mc./sec. or more, cavitation is suppressed and degradation is effected by ultrasonic waves alone.

3.   Cavitation is suppressed when degradation is carried in vacuo.   The resulting degradation is about 10% of the degradation produced in presence of cavitation at a frequency of 1 Mc./sec.

TABLE II.

Variation of chain length "P_w" with time of irradiation "t".

Time of irradiation (hrs.)	η_{sp}	P_w
0	4.36	3240
0.1667	3.45	2771
0.5	2.465	2203
1.0	1.834	1755
1.5	1.505	1509
2.5	1.186	1253
3.5	1.0152	1096
5.5	0.8461	941
7.5	0.7477	843
9.5	0.6862	780
11.5	0.621	717
13.5	0.5866	688
15.5	0.5606	654
17.5	0.5255	617
20.0	0.5014	585
22.5	0.472	556
25.0	0.455	539
27.5	0.446	522
30.0	0.432	512
32.5	0.422	499
35.0	0.420	494

TABLE III.

Rate constant of degradation at different stages of degradation.

α	P_w	t(hours)	K(hr.$^{-1}$).
0.0001	2887	0.15	6.6×10^{-4}
0.001	1280	2.34	4.2735×10^{-4}
0.002	811	8.00	2.5×10^{-4}
0.003	643	16.00	1.8778×10^{-4}

TABLE IV.

Fractionation of Polystyrene Samples.

Time of irradiation (hours).	Fraction	Chain length P_W	Weight Fraction dW	Integral weight $\int dW$
0	1	7198	0.0624	0.9688
	2	5505	0.082	0.8966
	3	4210	0.138	0.7866
	4	3051	0.126	0.6546
	5	2302	0.1416	0.5208
	6	1621	0.2094	0.3453
	7	992	0.1426	0.1693
	8	472	0.098	0.049
0.5	1	4828	0.1050	0.9475
	2	3530	0.0951	0.84745
	3	2781	0.1151	0.74235
	4	2149	0.1348	0.6174
	5	1537	0.1549	0.47255
	6	848	0.2599	0.26515
	7	300	0.1352	0.0676
2	1	2870	0.0852	0.9574
	2	2032	0.1049	0.86235
	3	1440	0.1851	0.71735
	4	1100	0.1548	0.5474
	5	874	0.1799	0.38005
	6	615	0.1652	0.2075
	7	280	0.1249	0.06245
4	1	2035	0.0750	0.9625
	2	1300	0.1098	0.8701
	3	951	0.1152	0.7576
	4	715	0.1301	0.63495
	5	523	0.2449	0.44745
	6	320	0.1748	0.2376
	7	150	0.1502	0.0751
35	1	751	0.0596	0.9684
	2	705	0.1888	0.8460
	3	632	0.1696	0.6668
	4	558	0.1300	0.5170
	5	468	0.1804	0.3618
	6	352	0.1104	0.2164
	7	222	0.1612	0.0806

TABLE V.

Theoretical Weight Distributions.

Time of irradiation hours.	Chain length.	$m_x \times 10^4$	Remarks.
0	500	1.399	$y = 744$
	1000	2.053	
	1620	2.271	
	2000	2.218	
	4000	1.292	
	6000	0.563	
	8000	0.2188	
	10000	0.0795	
0.5	500	2.1285	$0 < x < 744$
	744	2.8765	
	744	2.5911	
	1000	2.8434	$744 < x < \infty$
	2000	2.5755	
	4000	1.0566	
	6000	0.32507	
	8000	0.088902	
	10000	0.022795	
2	500	4.63	$<$ $<$
	744	6.599	
	744	4.848555	$744 < x < \infty$
	1000	4.65138	
	2000	2.4918	
	4000	0.35753	
	6000	0.038478	
	8000	0.00368085	
4	500	7.9842541	0 x 744
	744	11.5891	
	744	6.75415	
	1000	5.4155	744 x ∞
	2000	1.43969	
	4000	0.0508744	
	6000	0.00134831	
35	500	17.908	0 x 744
	744	26.35646	
	744	0.0857625	744 x ∞
	1000	0.004277663	

TABLE VI.

Theoretical number of cuts at different stages of
degradation calculated by method (1).

Time of irradiation hours.	$\int_0^y N_{z_1} \, dz_1 \times 10^4/N_o$	$\int_y^\infty N_{z_2} \, dz_2 \times 10^4/N_o$	Total number of molecules $\times 10^4/N_o$.	Number of cuts. $\times 10^4/N_o$
0	2.788846	4.170243	6.16903	0
0.25	3.34625	4.39294	6.959089	0.790059
0.50	4.5331	4.70932	7.73919	1.57016
1	5.83134	4.8833	9.24242	3.07339
1.5	7.0649	4.94393	10.71464	4.53561
2			12.00883	5.83980

TABLE VII.

Theoretical number of cuts at different stages of degradation
calculated by method (11)

$$K = 3.5 \times 10^{-4} \text{ hr.}^{-1}$$

Time of irradiation hours.	Number of broken links per hour x $10^4/N_0$			Average rate of scission x $10^4/N_0$	Number of cuts at stages of degradation x $10^4/N_0$	Total number of cuts x $10^4/N_0$
	$0 < x < y$	$y < x < \infty$	Total			
0	2.03005	1.939455	3.969505	3.563688865	0	0
0.25	2.17173723	0.9861355	3.1578727'9	3.121393965	0.890922216	0.890922216
0.50	2.28735445	0.79756075	3.0849152.	3.007387	0.78048491	1.671407126
1	2.4517	0.4781588	2.9298588	2.8485987	1.5036935	3.175100626
1.5	2.541898	0.2254406	2.7673386		1.42429935	4.599999976
2	2.57286	0.0260854	2.5989454	2.683142	1.341571	5.940970976

TABLE VII.

Theoretical number of cuts at different stages of degradation calculated by method (iii)

Variable K.

Time of Irradia-tion hours.	Number of broken links per hour 0 < x < y x 10⁴/N₀	y < x < ∞	Total	Average rate of scission x 10⁴/N₀	Number of cuts at stages of degradation x 10⁴/N₀	Total number of cuts x 10⁴/N₀
0	3.567	3.4079	6.9749	5.89345	0	0
0.25	3.4524	1.3596	4.8120	4.562935	1.47336	1.47336
0.5	3.3828	0.93107	4.31387	4.015585	1.140734	2.614094
1.0	3.22818	0.489123	3.7173	3.45835	2.0077925	4.6218865
1.5	3.0798	0.1196	3.1994	3.0175025	1.729175	6.3510615
2.0	2.90104	-0.065435	2.835605		1.50875	7.8598

TABLE IX.

Theoretical and Experimental number of cuts and Effect of D.P.P.H.

Time of Irrad-iation hours.	$?sp$		log absorp-tion.	D.P.P.H. Measurements.		Number of cuts x $10^x/N_0$		
	Without D.P.P.H.	With D.P.P.H.		D.P.P.H. concn. moles/litre.	D.P.P.H. exhausted moles/litre.	method (1)	method (11)	method (111)
0	4.36	4.36	1.56	9.8×10^{-5}	0	0	0	0
0.25	3.22	2.85	1.202	7.8×10^{-5}	2.0×10^{-5}	0.79	0.8909	1.47336
0.5	2.465	2.24	0.98	6.4×10^{-5}	3.4×10^{-5}	1.57	1.6714	2.6141
1.0	1.834	1.665	0.756	5.2×10^{-5}	4.6×10^{-5}	3.0734	3.1751	4.6219
1.5	1.505	1.377	0.588	4.26×10^{-5}	5.54×10^{-5}	4.5456	4.5994	6.351
2.0	1.29	1.166	0.486	3.4×10^{-5}	6.40×10^{-5}	5.8398	5.94097	7.8598

TABLE X.

Application to Schmid's Theory.

Number Average		Weight Average.	
Time of irradiation hours.	$\dfrac{P_{N_\infty}}{P_{N_t}} + \log(1 - \dfrac{P_{N_\infty}}{P_{N_t}})$	Time of irradiation hours.	$\dfrac{P_{W_\infty}}{P_{W_t}} + \log(1 - \dfrac{P_{W_\infty}}{P_{W_t}})$
0	-0.03071	0	0.01302
0.25	-0.03803	0.5	-0.031
0.5	-0.050715	1.0	-0.0486
1	-0.07754	1.5	-0.0693
2	-0.1426	2.0	-0.0885
4	-0.33307	2.5	-0.1095
10	-1.245205	3.0	-0.1302
20	-2.3275	3.5	-0.1477
28.7	-4.9182	4.0	-0.1675
35	$-\infty$	6	-0.2412
		8	-0.331
		10	-0.4255
		15	-0.6555
		20	-1.033
		25	-1.583
		30	2.5692
		35	$-\infty$

TABLE XI.

Degradation of polystyrene at different intensities.

$I = 4.89$ watts/cm^2.		$I = 9.53$ watts/cm^2.	
Time of irradiation hours.	P_w	Time of irradiation hours.	P_w
0	3260	0	3260
0.5	2987	0.5	2420
1	2867	1	2030
2	2474	2	1590
3.5	2181	4	1293
5	1944	6	1079
7.5	1687	8	971
10	1553	10	895
12.5	1480	12	843
15	1336	14	797
17.5	1273	16	768
20	1198	18	736
22.5	1147	20	717
25.0	1114	22	694
27.5	1084	24	684
30	1061	26	654
32.5	1033	28	643
35	1004	30	635
		32	616
		34	605
		35	603

TABLE XI. (Continued).

I = 12.5 watts/cm^2		I = 15.8 watts/cm^2	
Time of irradiation hours.	P$_w$	Time of irradiation hours.	P$_w$
0	3260	0	3260
10 min.	2771	0.25	2350
0.5	2203	0.5	1900
1	1755	1	1469
1.5	1509	2	1164
2.5	1253	5	825
3.5	1096	7.5	711
5.5	941	10	608
7.5	843	12.5	549
9.5	780	15	511
11.5	717	17.5	459
13.5	688	20	447
15.5	654	22.5	422
17.5	617	25	402
20	585	27.5	394
22.5	556	30	388
25	539	32.5	383
27.5	522	35	380
30	512		
32.5	499		
35	494		

TABLE XII.

Effect of Intensity on Rate Constant 'K'.

P = 1630 $\qquad$ $\beta_1 = \dfrac{2.545}{\gamma}$ dyne^{-1} hr.$^{-1}$ $\qquad$ $\beta_2 = 2.545$ hr.$^{-1}$

	Theoretical		Experimental	
S	K Case (i) x 10^4 hr.$^{-1}$	K Case (ii) x 10^4 hr.$^{-1}$	V_a volts.	K x 10^4
1.25	1.1	6.45	500	1.286
1.5	2.79	8.41	700	4.30
2.0	6.85	10.47	800	6.768
2.25	9.08	11.1	900	9.731
2.5	11.4	11.6		

TABLE XIII.

Dependence of limiting chain length 'y' on intensity.

$$P = 1630 \qquad \beta_1 = \frac{2.545}{\gamma} \text{ dyne}^{-1} \text{ hr.}^{-1} \qquad \beta_2 = 2.545 \text{ hr.}^{-1}$$

$\underline{m}$	Theoretical.		Experimental	
	$K \times 10^4$ (Case i)hr^{-1}	$K \times 10^4$ (Case ii)hr^{-1}	y	$k \times 10^4$ hr^{-1}
0.2	35.315	13.685	1539	1.286
0.3	19.02	12.78	912	4.30
0.5	6.854	10.466	744	6.768
0.7	2.243	7.972	572	9.731
1.0	0	0		

Effect of Initial Average Chain Length.

Variation of Chain Length with time of Irradiation.

TABLE XIV.

Time of Irradiation hours.	P_w	Time of Irradiation hours.	P_w	Time of Irradiation hours	P_w	Time of Irradiation hours.	P_w
0	3260	0	2460	0	1505	0	3744
0.1667	2771	0.1667	2131	0.5	1302	0.25	2757
0.5	2203	0.5	1856	1.0	1180	0.5	2249
1.0	1755	1.0	1575	1.5	1093	1.0	1726
1.5	1509	1.50	1392	2.5	968		
2.5	1253	2.0	1254	5.0	819		
3.5	1096	3.0	1105	7.5	739		
5.5	941	5.0	921	10.0	685		
7.5	843	7.0	825	12.5	643		
9.5	780	10.0	749	15.0	620		
11.5	717	12.5	699	17.5	598		
13.5	688	15.0	682	20.0	590		
15.5	654	17.5	624	22.5	570		
17.5	617	20.0	596	25.0	550		
20	585	22.5	578	27.5	538		
22.5	556	22.5	578	30.0	529		
25	539	25	562	32.5	519		
27.5	522	27.5	550	35.0	509		
30	512	30.0	533				
32.5	499	32.5	521				
35	494	35	518				

TABLE XV.

Effect of Initial Weight Average Chain Length.
on Rate Constant "K".

$$y = 750 \qquad \beta_1 = \frac{1.475}{\gamma} \text{ dyne}^{-1} \text{ hr.}^{-1} \qquad \beta_2 = 1.475 \text{ hr.}^{-1}$$

	Theoretical.		Experimental.	
n	K Case (i) x 10^4 hr.$^{-1}$	K Case (ii) x 10^4 hr.$^{-1}$	P_{W_0}	K x 10^4 hr.$^{-1}$
1	0	0	750	0
1.2	0.80	6.10	1505	4.49
1.5	2.31	7.00	2460	7.59
1.7	3.20	6.90	3260	6.768
2.0	4.29	6.55	3744	7.97
2.5	5.67	5.8		
3.0	6.67	5.14		
3.5	7.40	4.57		
4.0	8.00	4.12		
5.0	8.82	3.42		
6.0	9.38	2.92		

TABLE XVI.

Degradation of Different Polystyrene Samples
at Different Frequencies.

Frequency Mc/sec.	Time of Irradiation hours.	Polystyrene Samples.			
		P_w	P_w	P_w	P_w
1.0	0	1505	2460	3260	3744
	0.25	1268	1912	2332	2683
	0.50	1198	1678	1947	2160
	0.75	1123	1485	1680	1865
	1.00			1496	
	1.50			1248	
	2.00			1080	
1.25	0	1505	2460	3260	3744
	0.25	1362	2018	2486	2783
	0.50	1270	1758	2069	2222
	0.75	1204	1560	1825	1931
	1.00			1642	
	1.50			1380	
	2.00			1216	

TABLE XVI (Continued).

Frequency Mc./sec.	Time of Irradiation hours.	Polystyrene Samples.				
		P_w	P_w	P_w	P_w	P_w
1.5	0	1505	2460	3260	3744	
	0.25	1448	2208	2788	3202	
	0.50	1398	2006	2445	2780	
	0.75	1343	1863	2204	2538	
	1.00			2020		
	1.50			1748		
	2.00			1600		
2.0	0	1505	2460	3260	3744	
	0.25	1483	2391	3180	3658	
	0.50	1462	2345	3140	3600	
	0.75	1446	2320	3083	3540	
	1.00			3027		
	1.50			1964		
	2.00			1920		

TABLE XVII.

Rate Constant of degradation of polystyrene samples with different initial average chain lengths at different frequencies.

Intensity 12.5 watts/cm.³

Initial chain length of Polymer P_w	"K" at different Frequencies of Ultrasonic Waves.				
	0.75 Mc.	1.00 Mc.	1.25 Mc.	1.50 Mc.	2.00 Mc.
3744	7.97	12.98 / 4000 (1st)	7.196 / 4800 (2nd)	3.356 / 4000 (2nd)	0.65 / 4000 (3rd)
3260	6.768 / 2667(f)	12.22	8.49 / 3200 (1st)	3.922 / 2667 (1st)	0.952 / 3000 (2nd)
2460	7.59	9.82 / 2000(f)	8.18 / 1600(f)	3.942	1.382 / 3000 (1st)
1505	4.49	9.40	5.22	1.926 / 1334(f)	0.722 / 1000 (f)

TABLE XVIII.

Effect of Cavitation on the Degradation of Polystyrene.

Frequency Kc/sec.	Time of Irradiation hours.	P_v	Remarks.
1	0	3260	Degradation at atmospheric pressure.
	0.25	2332	
	0.50	1947	
	0.75	1680	
	1.00	1496	
	1.50	1248	
	2.00	1080	
1	0	3260	Degradation in vacuo.
	0.25	3155	
	0.50	3093	
	0.75	3041	
	1.00	2998	
	1.5	2945	
	2.0	2921	
2	0	3260	Degradation at atmospheric pressure.
	0.25	3180	
	0.50	3140	
	0.75	3083	
	1.00	3033	
	1.50	2964	
	2.00	2920	

BIBLIOGRAPHY.

1. Grassie, N.
   'Chemistry of High Polymer Degradation Processes'
   Chapters I and II.   Butterworths Scientific
   Publications, London 1956.

2. Melville, H.W. and Murray, A.J.R.
   Trans. Farad. Soc.   46, 996 (1950).

3. Schmid, G.
   Z. Physik. Chem.   186A, 113 (1940).

4. Jellinek, H.H.G. and White, G.
   J. Pol. Sci.   6, 757 (1951).

5. Jellinek, H.H.G. and White, G.
   J. Pol. Sci.   7, 21 (1951).

6. Schmid, G.
   Physik. Zeit.   41, 326 (1940).

   Schmid, G. and Beuttenmüller, E.
   Z. Elektrochem. 49, 325 (1943).

7. Noltingk, B.E. and Neppiras, E.A.
   Proc. Phys. Soc.   B.64, 1032 (1951).

8. Taylor, Sir Geoffrey,
   Proc. Roy. Soc. Lond.   A 201, 192 (1950).

9. Kornfeld, M. and Suvlrov, L.
   J. App. Phys.   15, 495 (1944).

10. Horton, J.P.
    J. Acoust. Soc. Amer.   25, 480 (1953).

11. Frenkel, J.
    'Kinetic Theory of Liquids' Chapter VIII, p.p.448
    Clarendon Press, Oxford.

12. Gaertner, W.

J. Acoust. Soc. Amer. 25, 977 (1953).

13. Schmid, G. and Poppe, W.

Z. Elektrochem. 53, 28 (1949).

14. Mark, H.

J. Acoust. Soc. Amer. 16, 183 (1945).

15. Crawford, A.E.

'Ultrasonic Engineering' Chapter 9,
Butterworths Scientific Publications, London 1955.

16. Szalay, A.

Z. Physik. Chem. 164 A, 234 (1933).
Physik. Z. 35, 293, 639 (1934).

17. Thieme, A.

Physik. Z. 39, 384 (1938).

18. Mark, H. and Tobolsky, A.V.

'Physical Chemistry of High Polymeric Systems'
Chapters I, II and III. Interscience Publishers
Ltd., London 1950.

CHAPTER VI.

COMMENTS.

COMMENTS.

In the preceding Chapter a few conclusions were drawn out regarding different aspects of the degradation of long chain molecules by ultrasonic waves.

It became clear that although degradation can be effected by ultrasonics alone, yet within a certain frequency range (0.5 - 1.5 Mc/sec.) as much as 90% of degradation is caused by cavitation. There is also a periodical increase in the rate of degradation whenever the product of frequency and weight average chain length reaches a value of 2×10^9 or its multiples, i.e.,

$$f \; P_w \; = \; 2 \times 10^9 \times C$$

where C is an integer.

In the light of the conclusions reached a brief comment on the theoretical and experimental aspects of the problem seems to be relevant.

It should be emphasised from the start that there are two main factors which have a direct influence on degradation and which are beyond control. viz:

(1) the size and nature of nuclei present in the polymer solution, essential for the inception of cavitation, which plays an important role in degradation.

(2)   The entanglements and aggregation in the high polymer

solution without which long chain molecules will

follow the ultrasonic waves and consequently no

degradation will take place.

1. Kinetics of Degradation.

Reverting to the kinetics of degradation of long chain

molecules by ultrasonic waves, it should be pointed out that

the rate equations (1) Chapter IV, do not precisely represent

the degradation produced by ultrasonic waves.   This is due

to the term (Z - 1) in the general equation for $\frac{dN_z}{dt}$. This

term implies that each bond in a long chain molecule has the

same probability for rupture under random degradation condit-

:ions.   This, with reasonable approximation, may be the case

when cavitation is the main factor controlling degradation.

Under conditions of cavitation a bubble will grow whenever

there is a nucleus.   It is most likely that nuclei are

distributed at random in the solution, and consequently

intense pressure waves, resulting from the collapse of bubbles,

can break any bond irrespective of its position in the long

chain molecule, provided the chains are sufficiently entangled.

However, the rate equations would have to be modified

if a precise and accurate study of the kinetics of degradation

by ultrasonic waves is to be followed.

According to the mechanism of degradation suggested in Section E, Chapter V, it follows that when a long chain is fixed at both ends there will be a length ℓ from each end where the forces developed at any of its bonds are not suff-:icient to effect a scission. Consequently, the rate of degradation of a chain of length Z will be proportional to $(Z - 2\ell)$, where $(Z - 2\ell)$ represents the central length of the chain which could be ruptured. Hence the general term in equation (1), modified to express the degradation caused by ultrasonic waves alone, would be :

$$\frac{dN_z}{dt} = \sum_{R=Z+\ell+1}^{R=\infty} 2(R-Z-\ell) \, N_r - K(Z - 2\ell)N_z \quad \ldots\ldots\ldots(1)$$

It can be deduced from this modification that $y = 2\ell$ since no degradation will take place if the length of the chain is 2ℓ or y (the limiting chain length). The terms representing the cumulation of molecules have to be modified and they are represented by the sum:

$$\sum_{R=Z+\ell+1}^{R=\infty} 2(R-Z-\ell) \qquad \text{where } Z > \ell$$

Obviously, as represented by Equation (1) the degradation of long chain molecules by ultrasonic waves in the absence of cavitation will not be a process of true random degradation.

There is no intention in this comment to elaborate on a solution of the new rate equations, as this proved to be mathematically intractable in explicit terms.

2. Factors affecting Degradation.

The effect of a few factors on the degradation of polystyrene by ultrasonic waves has been studied and the results obtained discussed in Chapter V. The analysis of the results was based on two postulates, namely:

A. The force acting on a long chain molecule is periodic, having the same frequency as that of the ultrasonic waves, and represented by $f = f_o \sin(\omega t - \emptyset)$.

B. Whether due to frictional forces or impact forces, the mechanism of rupturing the long chain molecule can be represented by the general relation:

$$f_o = \alpha V_s \qquad \text{[Equation (31); Chapter V.]}$$

The first postulate is valid for degradation by ultra-:sonic waves in the absence of cavitation, where the frictional forces developed can be represented by $f = f_o \sin (\omega t - \emptyset)$. However, it should be pointed out that in the frequency range where degradation is mainly caused by cavitation, there will be two forces acting; (a) frictional or impact force

represented by $f_0 \sin(\omega t - \emptyset)$;   and (b) impact force due to bubble collapse which cannot be represented by a simple contin:uous periodic function and more specifically by a trigno:metrical function.

Moreover, inspection of Figs. 10, 11 and 12, which illustrate the effect of different factors on the growth of bubbles and intensity of cavitation, indicates that the bubble will grow up to its maximum size (R_m), after a time t_m from the beginning of the negative half cycle of the ultrasonic pressure wave[1]. The value of t_m depends on the values of the controlling factors, namely, R_o, p_o, p_A and ω.   Consider:ing the period of ultrasonic waves T to be $\frac{2\pi}{\omega}$, therefore:

$$t_m = \frac{1.3\pi}{\omega}$$

for R_o = 1 to 3μ; p_o = 4 x 10^6; p_A = 10^6; and ω = 9 x 10^4, and t_m varies from $\frac{\pi}{2\omega}$ to slightly less than $\frac{3\pi}{2\omega}$, when p_o varies from 1 atm. to 8 atmosphere, for R_o = 3.2μ, P_A = 1 atm. and ω = 9 x 10^4.

Using a differential analyser to solve their differ:ential equations Noltingk and Neppiras[2] represented graph:ically the growth and collapse of a gas-filled bubble when p_o = 4 atm., ω = 3 x 10^6, and R_o = 3.2 x 10^{-4}cm. The radius-time curve showed that the time taken by the bubble to grow to its maximum size before collapse was about 0.7 of a period,

while the collapse was almost completed before the end of the period.   Hence, strictly speaking, neither the cavitation pressures nor the high radial liquid velocities developed during the collapse of bubbles can be represented by a simple continuous periodic function.   Consequently, the second postulate which leads to the relation $f_o = \alpha\, V_s$ would have to be modified.   Such a modification cannot be envisaged without a complete theoretical study of cavitation.   However, although the force acting on a long chain molecule cannot be truly represented by $f = f_o \sin(\omega t - \emptyset)$, yet this assumption offers the best possible approximation when the cavitation effect is taken into consideration.   Hence, the results obtained in Chapter V, Section C, D, and E, would still be significant, notwithstanding the limitations of the aforementioned postulates.

The effect of intensity on the degradation parameters K and y was discussed in Section C, Chapter V.   It was shown from the discussion of results, that the number of chains broken per unit time is proportional to the difference between the force acting and the force γ required to break a C-C bond.

However, some discrepancy between experimental and theoretical results was found.   As can be seen from Fig. 54, the discrepancy is more obvious at low intensities, i.e., high values of y. This discrepancy should be expected as a

consequence of cavitation inception. That this is the case
can be shown by considering Fig.12.   Cavitation does not
occur for values of p_0 below 1 atmosphere which is the value
of p_A.   When the value of p_0 just exceeds that of p_A incept-
:ion of cavitation takes place associated with a sudden
increase in the bubble radius, and consequently, a sudden
increase in cavitation intensity.   This sudden increase in
cavitation intensity will result in a greater rate of degra-
:dation K as was found experimentally to be the case in the
low intensity region, as shown in Fig.54.

3. Mechanism of Degradation.

It was mentioned in Section D, Chapter V, that the
anomolous dip A-B-C in Fig.58, which illustrates the effect
of initial chain length on the rate constant of degradation
'K', may be attributed to a frequency effect.   Further, it
was shown in Table XVII that changing the frequency of ultra-
:sonic waves affects the relative values of 'K'.   Thereafter,
a theoretical analysis was attempted to study the dynamical
behaviour of long chain molecules in an ultrasonic field, in
order to account for the frequency dependence of ultrasonic
degradation and the possibility of resonance taking place.
It was concluded, however, that the effect of entanglements
and aggregation is to increase the effective mass of monomer

units, and that with such proviso degradation as well as resonance vibrations can occur.

In section E, Chapter V, the condition for resonant vibrations of a long chain molecule was found to be :

$$fP \; = \; \frac{C}{2} \, . \, [\alpha/m]^{1/2}$$

where C is an integer. The effect of viscous damping on the forced oscillations of macromolecules in an ultrasonic field was studied in order to see if the energy of oscillation is sufficient to break a C-C bond. An exact solution was first attempted (see Appendix IV), but it was found later that it became too complex to serve any useful purpose at that stage. An approximate solution was then attempted and a few conclus-:ions were reached.

In addition to the assumptions made in Section E, Chapter V, it is further assumed that the force acting on each sphere (representing a benzene ring) is given by $\beta(V - \overset{\circ}{y})$, where:

   β is Stoke's friction coefficient and is given by
      $6\pi\eta r$, as mentioned earlier, and

   V is the particle velocity of the solvent and is given
      by $V = V_o \sin \omega t$.

Reverting to Fig. 68, the equation representing the motion of the <u>nth</u> sphere is given by:

$$m \ddot{y}_n = -\alpha(y_n - \frac{y_{n+1} + y}{2}) + \beta(V - \dot{y}_n) \ , \quad \text{or}$$

$$2m \ddot{y}_n + \alpha(2y_n - y_{n+1} - y_{n-1}) + 2\beta \dot{y}_n = 2\beta V$$
$$= 2\beta V_0 \sin \omega t \qquad (2)$$

It is easier to find the solution for a particular integral

of the form $2\beta V_0 e^{i\omega t}$ and then to pick out its imaginary

part. Hence equation (1) can be put in the form:

$$2m \ddot{y}_n + \alpha(2y_n - y_{n+1} - y_{n-1}) + 2\beta \dot{y}_n = 2\beta V_0 e^{i\omega t} \qquad (3)$$

Putting $y_n = Y_n e^{i\omega t}$ where Y_n is a complex quantity, there-

:fore:

$$(- \frac{2m\omega^2}{\alpha} + \frac{2i\omega\beta}{\alpha}) Y_n - (Y_{n+1} - 2Y_n + Y_{n-1}) = \frac{2\beta V_0}{\alpha} \qquad (4)$$

If the distance between each two successive spheres in

Fig. 68 is equal to δx, then the length of the chain 'ℓ' = $P_0 \delta x$,

where P is the chain length in monomer units. Dividing both

sides of equation (4) by $(\delta x)^2$, it can be put in the form:

$$K^2 Y_n + \frac{Y_{n+1} - 2Y_n + Y_{n-1}}{(\delta x)^2} = -M \qquad (5)$$

where $K^2 \equiv \frac{2m\omega^2 - 2i\omega\beta}{\alpha(\delta x)^2} \qquad (6)$

and $M \equiv \frac{2\beta V_0}{\alpha(\delta x)^2} \qquad (7)$

If the fundamental mode of vibration of the long chain is

considered, the spheres in any displaced position can be

imagined to lie on a parabolic curve and the following approx=
:imation will hold; viz;

$$\frac{y_{n+1} - 2Y_n + Y_{n-1}}{(\delta x)^2} = \frac{d^2 Y_n}{dx^2} \qquad (8)$$

Hence equation (4) can be transformed to the new differential
equation given by:

$$\frac{d^2 Y_n}{dx^2} + K^2 Y_n = -M \qquad (9)$$

The solution of equation (9) is given by:

$$Y_n = -\frac{M}{K^2} + A \sin K x + B \cos K x \qquad (10)$$

where A and B are constants to be determined from boundary
conditions, and x is the distance of the **nth** sphere from the
fixed end of the molecule and is given by $X = n\delta x$.

Since the long chain is assumed to be fixed at both
ends, it follows that:

$$Y = 0 \quad \text{at } x = 0 \quad \text{and } x = \ell = P\delta x$$

Therefore,

$$B = \frac{M}{K^2}$$

and

$$A = \frac{M}{K^2} \left(\frac{1 - \cos K\ell}{\sin K\ell} \right)$$

$$= \frac{M}{K^2} \tan \frac{K\ell}{2}$$

Substituting the values of A and B in equation (10), the value of Y_n is given by:

$$Y_n = \frac{M}{K^2} \left[\cos Kx - 1 + \tan \frac{K\ell}{2} \sin Kx \right] \qquad (11)$$

Equation (11) gives the value of the amplitude of vibration of the nth sphere in the chain. For the fundamental mode of vibration, the sphere at the centre of the chain will have the largest amplitude of vibration. For the sake of simplicity the amplitude of the central sphere only will be considered.

Hence for the sphere at the middle of the chain:

$$Y_n = Y_{centre} = Y_c \qquad \text{at } x = \frac{\ell}{2}$$

Therefore:

$$Y_c = \frac{M}{K^2} \left[\cos \frac{K\ell}{2} - 1 + \tan \frac{K\ell}{2} \sin \frac{K\ell}{2} \right]$$

$$= \frac{M}{K^2} \left[\frac{1 - \cos \frac{K\ell}{2}}{\cos \frac{K\ell}{2}} \right] \qquad (12)$$

From equation (6), the value of K is given by:

$$K = \frac{\omega}{\delta x} \left(\frac{2m}{\alpha} \right)^{1/2} \left(1 - i \frac{\beta}{m\omega} \right)^{1/2}$$

Taking into consideration the relative values of β, m and ω, it can be shown that:

$$K = \frac{1}{\delta x} \left[\left(\frac{\beta\omega}{\alpha} \right)^{1/2} - i \left(\frac{\beta\omega}{\alpha} \right)^{1/2} \right] \qquad (13)$$

Hence,

$$\text{Cos } \frac{K\ell}{2} = \text{Cos } \frac{P\delta x}{2\delta x} \left[\left(\frac{\beta\omega}{\alpha}\right)^{1/2} - i\left(\frac{\beta\omega}{\alpha}\right)^{1/2} \right]$$

$$= \text{Cos } \left[\frac{P}{2} \left(\frac{\beta\omega}{\alpha}\right)^{1/2} - i \frac{P}{2} \left(\frac{\beta\omega}{\alpha}\right)^{1/2} \right]$$

and considering $\frac{P}{2} \left(\frac{\beta\omega}{\alpha}\right)^{1/2} = \gamma$

Therefore:

$$\text{Cos } \frac{K\ell}{2} = \text{Cos } \gamma \text{ Cosh } \gamma + i \sin \gamma \sinh \gamma \qquad (14)$$

Further, from equations (6) and (7), it follows that:

$$\frac{M}{K^2} = \frac{\beta V_o}{m\omega^2 - i\omega\beta} \qquad (15)$$

Hence from equations (12), (14) and (15), the value of 'Y_c'
is given by:

$$Y_c = \frac{\beta V_o}{m\omega^2 - i\omega\beta} \left[\frac{1 - \text{Cos } \gamma \text{ Cosh } \gamma - i \sin \gamma \sinh \gamma}{\text{Cos } \gamma \text{ Cosh } \gamma + i \sin \gamma \sinh \gamma} \right] \qquad (16)$$

Rationalising equation (16) once gives:

$$Y_c = \frac{\beta V_o}{m\omega^2 - i\omega\beta} \left[\frac{\text{Cos } \gamma \text{ Cosh } \gamma + \sin^2\gamma - \text{Cosh}^2\gamma - i \sin \gamma \sinh \gamma}{\text{Cosh}^2\gamma - \sin^2\gamma} \right]$$
$$.. (17)$$

Rationalising equation (17) once gives:

$$Y_c = \frac{\beta V_o}{(\text{Cosh}^2\gamma - \sin^2\gamma)(m^2\omega^4 + \omega^2\beta^2)} \text{ x}$$

$$\left\{ m\omega^2(\text{Cos } \gamma \text{ Cosh } \gamma + \sin^2\gamma - \text{Cosh}^2\gamma) + \omega\beta \sin \gamma \sinh \gamma + \right.$$

$$\left. i\left[\omega\beta(\cos \gamma \cosh \gamma + \sin^2\gamma - \cosh^2\gamma) - m\omega^2 \sin \gamma \sinh \gamma \right] \right\}$$

$$.. (18)$$

Rationalising equation (18) once gives:

$$Y_c = \beta V_0 \left[\frac{(\cos\gamma\cosh\gamma + \sin^2\gamma - \cosh^2\gamma)^2 + \sin^2\gamma\sinh^2\gamma}{(m^2\omega^4 + \omega^2\beta^2)(\cosh^2\gamma - \sin^2\gamma)^2}\right]^{\frac{1}{2}} e^{i\phi}$$

$$..(19)$$

where ϕ is a phase angle, and is given by:

$$\phi = \tan^{-1}\frac{\omega\beta(\cos\gamma\cosh\gamma + \sin^2\gamma - \cosh^2\gamma) - m\omega^2\sin\gamma\sinh\gamma}{m\omega^2(\cos\gamma\cosh\gamma + \sin^2\gamma - \cosh^2\gamma) + \omega\beta\sin\gamma\sinh\gamma} \quad (20)$$

Hence the displacement of the middle sphere in the chain is given by:

$$y_c = Y_c\, e^{i\omega t} \quad \text{where } Y_c \text{ is given by equation (19).}$$

Considering only the imaginary part of y_c, therefore the displacement produced at the centre by a force $[\beta V_0 \sin\omega t]$ acting on the long chain molecule is given by:

$$y_c = \beta V_0 \left[\frac{(\cos\gamma\cosh\gamma + \sin^2\gamma - \cosh^2\gamma)^2 + \sin^2\gamma\sinh^2\gamma}{(m^2\omega^4 + \omega^2\beta^2)(\cosh^2\gamma - \sin^2\gamma)^2}\right]^{\frac{1}{2}}.$$

$$:\sin(\omega t + \phi) \quad (21)$$

which can be put in the form:

$$y_c = \beta V_0\, R\, \sin(\omega t + \phi) \quad (22)$$

where

$$R = \left[\frac{(\cos\gamma\cosh\gamma + \sin^2\gamma - \cosh^2\gamma)^2 + \sin^2\gamma\sinh^2\gamma}{(m^2\omega^4 + \omega^2\beta^2)(\cosh^2\gamma - \sin^2\gamma)^2}\right]^{\frac{1}{2}} \quad (23)$$

The work done by the force $\beta V_0 \sin\omega t$ in producing a dis-
:placement 'y_c' at the centre of the long chain molecule is given by:

$$W.D. = \int_0^{Y_c} \beta V_0 \sin\omega t\; dy_c \quad (24)$$

where 'dy_c' can be obtained from equation (22) and is given
by:

$$dy_c = \omega \beta V_o R \cos (\omega t + \phi) \, dt.$$

Hence:

$$W.D. = \int_o^{\frac{\pi}{2\omega}} \omega R \, \beta^2 V_o^2 \cos (\omega t + \phi) \sin \omega t \, dt.$$

Integrating between o and $\frac{\pi}{2\omega}$, the work done is given by:

$$W.D. = \frac{\beta^2 V_o^2 R}{4} (2 \cos \phi - \pi \sin \phi) \tag{25}$$

Hence the input energy for producing the maximum displacement
of the sphere at the centre of the long chain molecule can
be evaluated and compared with the energy required to break
a C-C bond.

In order to illustrate that the above mentioned energy
is sufficient to break a C-C bond, the values of γ, ϕ, R and
the kinetic energy of oscillation were calculated for three
different chain lengths. These calculations were carried
out for two values of m and β, i.e.,

(i)   the true mass of a benzene ring and the Stoke's
        friction coefficient acting on it;   and

(ii)   the effective mass, calculated from experimental
        values, and the corresponding friction coefficient.

Results of these calculations are shown in Table XIX
from which the following general principles can be deduced.

a. The phase angle 'ϕ' varies with chain length. It has a zero value at a certain chain length, depending on the mass of each sphere and the friction coefficient. It is of interest to notice that for case (i) the displacement leads the acting force for small chain lengths and lags behind it when the chain length is increased beyond its critical (resonant) value, while the reverse applies to case (ii).

b. The kinetic energy of oscillation increases steadily as the chain length increases until an upper chain length limit is reached, beyond which the energy of oscillation remains practically the same.

c. The kinetic energy of oscillation varies inversely with the frequency of ultrasonic waves.

Concurrent with these deductions, it is obvious from rows 8 and 9, that in case (i) the energy of oscillation is of the same order of magnitude as the energy required to break a C-C bond[3]. In case (ii) the energy of oscillation is greater than that required to break a C-C bond.

It is important to point out, however, the common ground between case (i) and case (ii), and to emphasise the important role of entanglements and aggregation in the degradation of high polymer solutions.

As ultrasonic waves can effect degradation of long chain molecules in the absence of cavitation, it follows that they should be capable of rupturing at least one C-C bond in the chain. Without entanglements and aggregation, long chain molecules will be swept away and follow the ultrasonic oscill-:ations whatever the length of molecules. Consequently, degradation will not take place. Further, as was shown earlier the quantity $\frac{\omega m_K}{\beta}$ must be at least 10^8 times greater than its theoretical value, implying that the long chain should be rigid enough to be considered fixed, either at one end or at both ends. Hence, unless a chain is rigid enough (i.e., its effective mass is increased) it cannot be assumed fixed at both ends. This rigidity cannot be presupposed unless the molecules are reasonably entangled. Even in dilute solutions entanglements and aggregation of polymer molecules do occur, so that frictional forces are acting on large masses. Thus the assumption that the macromolecule is fixed at both ends, seems justified provided an appropriate modification in the values of 'm' and 'β' is considered.

From the above it is obvious that case (ii) simulates conditions which can be realised physically and chemically, while case (i) is purely hypothetical, since 'm' and 'β' are not modified. However, the figures in Table XIX show that

in case (1) the kinetic energy of oscillation can still reach the order of magnitude required to break a C-C bond.

It is essential to correlate the theoretical treatment carried out in this Chapter with that given in Chapter V, Section E, so that a complete qualitative picture of ultra- :sonic degradation (in the absence of cavitation) can be drawn. This picture has to be qualitative, since the quantitative effect of entanglements and aggregation on 'm' and 'β' cannot be easily predicted.

At reasonable polymer concentrations, the long chain molecules will be sufficiently entangled, with a consequent effect on their rigidity so that they will vibrate in the ultra- :sonic field, as if the molecules have fixed ends and effect- :ively greater mass per monomer unit. For a constant ultra- :sonic frequency, the kinetic energy of vibration increases with the chain length of the macromolecule. When the chain length reaches a limiting value, the kinetic energy of vibra- :tion will be sufficient to break a C-C bond, and rupture will be effected. A further increase in chain length results in a greater energy of oscillation and consequently a greater rate of degradation. Approaching a length of chains which resonates with the applied frequency, the energy of oscillation and consequently the rate of degradation will increase steeply[4]

for a homogeneous polymer sample, and gradually for a hetero-
:geneous sample (Fig.58; point A), until a peak is reached
when resonance occurs and the chains are vibrating at their
fundamental mode.

A further increase in chain length beyond this value
results in a drop in the rate of degradation due to anti-
resonance. The rate of degradation reaches a minimum and
then increases again when the chain length is further increased.
Concurrent with this change there is a transition from the
fundamental to the second mode of vibration (second harmonic).
The rate of degradation will reach its second peak when the
second resonance occurs where the chains vibrate at their
second mode of vibration. The kinetic energy of oscillation
and consequently the rate of degradation reach constant values
when the length of chains exceeds a certain value. There
will only be a cyclic change whenever the condition for
resonance is satisfied, i.e., $fP_w = 2 \times 10^9$ C.

From the above picture it is clear that the force act-
:ing on the macromolecule can be represented by:

$$f = f_o \sin (\omega t - \emptyset) = \beta V_o \sin (\omega t - \emptyset)$$

as mentioned in Chapter V, Sections C and D.

Further, the energies in case (ii) are greater than the
energy required to break a C-C bond. In practice the molecules
are not exactly fixed at both ends, nor are they orientated

specifically at right angles to the direction of propagation of ultrasonic waves.   Furthermore, the bond angle is 109° 26' and not 180°.   All these considerations will modify the resulting kinetic energy of oscillation and consequently effect a rate of degradation which is of the same order as that realised in practice.

Finally it is relevant to mention that all the features of ultrasonic degradation can be explained by this suggested mechanism, and in particular:

(i)   the anomolous behaviour illustrated in Fig. 58 (resonance).

(ii)   the lower rate of degradation at 2 Mc/sec. compared to that at 1 Mc/sec. in the absence of cavitation, (K.E. α $\frac{1}{\omega}$ for constant P).

(iii)   the optimum concentration for degradation (entangle-:ments).

TABLE XIX.

Calculation of Kinetic Energy of Oscillation of the central unit in a long chain molecule.

Case.	Chain length "p" units.	(i)			(ii)		
		100	500	1000	100	500	1000
1	$m \times 10^{22}$ in gms.	1.7	1.7	1.7	3.13×10^{6}	3.13×10^{6}	3.13×10^{6}
2	$\beta \times 10$ in gm.sec.	5.6	5.6	5.6	690	690	690
3	$\gamma = \frac{P}{2}\left[\beta\omega/\alpha\right]^{\frac{1}{2}}$	0.094	0.47	0.94	1.04	5.2	10.4
4	ϕ	$-0°\ 30'$	$-10°\ 37'$	$-36°\ 48'$	$-41°\ 46'$	$+89°\ 17'$	$+90°$
5	$R \times \omega\beta$	8.82×10^{-3}	0.208	0.715	0.83	1	1
6	V_o cms./sec.	50	50	50	50	50	50
7	$\omega/2\pi$ (c.p.s.)	10^{8}	10^{6}	10^{6}	10^{6}	10^{6}	10^{6}
8	Energy per bond (ergs).	9.84×10^{-15}	2.94×10^{-13}	1.39×10^{-12}	2.04×10^{-10}	2.16×10^{-10}	2.16×10^{-10}
9	Energy required to break a C-C bond (ergs.)	4.1×10^{-12}	4.1×10^{-12}	4.1×10^{-12}	4.1×10^{-12}	4.1×10^{-12}	4.1×10^{-12}

BIBLIOGRAPHY.

1. Noltingk, B.E. and Neppiras. E.A.
     Proc. Phys. Soc.   B.64, 1032 (1951).

2. Noltingk, B.E. and Neppiras. E.A.
     Proc. Phys. Soc.   B.63, 674 (1950).

3. Pauling, L.
     'The Nature of the Chemical Bond'
     Chapter II-10, p.p.53.

     Cornell University Press, New York.

4. Jellinek, H.H.G. and White, G.
     J. Pol.Sci.   7, 21 (1951).

APPENDIX I.

APPENDIX I.

$$A = \begin{bmatrix} a_{11} & 0 & 0 & 0 & & 0 \\ a_1 & a_{22} & 0 & & & 0 \\ a_1 & a_2 & a_{33} & & & 0 \\ & & & a_{n-1,n-1} & \\ a_1 & a_2 & a_3 & & a_{n-1} & a_{n,n} \end{bmatrix}$$

The eigen values are defined by the equation

$$[A - \lambda I] X = 0$$

where I is a unit matrix of the same order.

Obviously the eigen values are simply the diagonal elements,

i.e., $\lambda_1 = a_{11}$, $\lambda_2 = a_{22}$, $\lambda_n = a_{nn}$

To find q_1 in the eigen columns matrix Q:

let $q_1 = \{ x_1^{(1)} \quad x_2^{(1)} \text{------} x_n^{(1)} \}$

$\therefore$ $[A - \lambda_1 I] q_1 = 0$

$\therefore$ $$\begin{bmatrix} 0 & 0 & & & \\ a_1 & a_{22}-a_{11} & & & \\ a_1 & a_2 & a_{33}-a_{11} & & \\ & & & & \\ a_1 & a_2 & a_3 & & a_{nn}-a_{11} \end{bmatrix} \begin{bmatrix} x_1^{(1)} \\ x_2^{(1)} \\ x_3^{(1)} \\ \\ x_n^{(1)} \end{bmatrix} = 0$$

$x_1^{(1)}$ can be chosen arbitrarily .. say $x_1^{(1)} = 1$

then:

$$(a_{22}-a_{11})\ x_2^{(1)} = -a_1$$

$$a_2 \quad x_2^{(1)} + (a_{33}-a_{11})\ x_3^{(1)} = -a_1$$

$$a_2 \quad x_2^{(1)} + a_3 \quad x_3^{(1)} + (a_{44}-a_{11})\ x_4^{(1)} = -a_1$$

$$-- \quad -- \quad -- \quad -- \quad -- \quad -- \quad -- \quad -- \quad --$$

$$a_2 \quad x_2^{(1)} + a_3\ x_3^{(1)} + \ldots + a_{n-1}\ x_{n-1}^{(1)} + (a_{nn}-a_{11})\ x_n^{(1)} = -a_1$$

$$\therefore \quad x_2^{(1)} = -\frac{a_1}{a_{22}-a_{11}} \tag{1}$$

By subtracting the rth equation from the (r+1)th we obtain the relations:

$$(a_{22}-a_{11}-a_2)\ x_2^{(1)} = (a_{33}-a_{11})\ x_3^{(1)} \tag{2}$$

$$(a_{33}-a_{11}-a_3)\ x_3^{(1)} = (a_{44}-a_{11})\ x_4^{(1)} \quad \text{etc....} \tag{3}$$

If the following definitions are applied, viz.,

$$\alpha_{21} = -\frac{a_1}{a_{22}-a_{11}} \tag{4}$$

$$\alpha_{r1} = -\frac{a_{r-1,r-1} - a_{11} - a_{r-1}}{a_{rr} - a_{11}} \tag{5}$$

Therefore equations (1) and (4) give

$$x_2^{(1)} = \alpha_{21} \tag{6}$$

Similarly equations (2), (5) and (6) give

$$x_3^{(1)} = \alpha_{21}\cdot\alpha_{31} \tag{7}$$

and equations (3), (5) and (7) give:

$$x_4^{(1)} = \alpha_{21} \cdot \alpha_{31} \cdot \alpha_{41} \tag{8}$$

The same procedure applies to the other eigen columns

$$q_2, \quad q_3, \quad \ldots q_s, \quad \ldots q_n$$

In general, considering the s th eigen column

i.e., $\quad q_s = \left\{ \; x_1^{(s)}, \quad x_2^{(s)}, \quad \ldots \ldots x_r^{(s)}, \quad \ldots \ldots x_n^{(s)} \; \right\}$

it is easy to find out from the relation $[A - \lambda_s I]q_s = 0$,

that:

$$x_1^{(s)} = x_2^{(s)} = \ldots \ldots = x_{s-1} = 0$$

and $(a_{ss} - a_{ss}) \; x_s^{(s)} = 0$,

i.e. $\quad 0 \cdot x_s^{(s)} = 0$

$x_s^{(s)}$ similar to $x_1^{(1)}$ can be arbitrarily chosen and is taken to be unity, i.e., $\quad x_s^{(s)} = 1$.

Following a similar analysis used in determining $x_2^{(1)}$, $x_3^{(1)}$

$\ldots x_n^{(1)}$ we obtain relations of the form, viz:

$$(a_{s+1,s+1} - a_{ss}) \; x_{s+1} = -a_s , \qquad \text{or}$$

$$x_{s+1} = \frac{-a_s}{a_{s+1,s+1} - a_{ss}} \tag{9}$$

The general term for such relations is therefore:

$$x_r = \frac{a_{r-1,r-1} - a_{ss} - a_{r-1}}{a_{rr} - a_{ss}} \tag{10}$$

of which equation (9) is a special case.

Following the same notation as before, we get that

$$\alpha_{s+1,s} = \frac{-a_s}{a_{s+1,s+1} - a_{ss}} \qquad (11)$$

and $\quad \alpha_{rs} = \dfrac{a_{r-1,r-1} - a_{ss} - a_{r-1}}{a_{rr} - a_{ss}} \qquad (12)$

To sum up it is clear from equations (6), (7) and (8) that:

$$x_r^{(1)} = \alpha_{21} \ \alpha_{31} \ \alpha_{41} \ \cdots\cdots\cdots\cdots \alpha_{r1}$$

Applying the same treatment to any other element in the eigen columns matrix we obtain the general term for the element of the (r)th row and (s)th column

as $\qquad x_r^{(s)} = \alpha_{s+1,s} \cdot \ \alpha_{s+2,s} \cdot \ \alpha_{s+3,s} \cdots\cdots\cdots \alpha_{rs}$

APPENDIX II.

The eigen rows of the triangular matrix A are defined by the relation:

$$p_s [A - \lambda_s I] = 0$$

I being a unit matrix of the same order as A.

As in Appendix I the eigen values are the diagonal elements.

1. Consider the first eigen row:

$$p_1 = [y_1^{(1)}, \; y_2^{(1)}, \; \ldots \ldots y_n^{(1)}]$$

$$\therefore \; [y_1^{(1)} \quad y_2^{(1)} \quad \ldots y_n^{(1)}] \begin{bmatrix} 0 & 0 & 0 & 0 \\ a_1 & a_{22}\text{-}a_{11} & 0 & 0 \\ a_1 & a_2 & a_{33}\text{-}a_{11} & 0 \\ a_1 & a_2 & a_3 & \\ & & & \\ a_1 & a_2 & a_3 & a_{nn}\text{-}a_{11} \end{bmatrix}$$

i.e., $y_1^{(1)}.0 + (y_2^{(1)} + y_3^{(1)} + \ldots \ldots + y_n^{(1)}) \; a_1 \qquad = 0$

since $a_1 \neq 0$

$$\therefore \; y_2^{(1)} + y_3^{(1)} + \ldots \ldots + y_n^{(1)} = 0$$

$\therefore \; y_1^{(1)}$ can be arbitrarily chosen

$$y_1^{(1)} = 1$$

and $\qquad y_n^{(1)} = y_{n-1}^{(1)} = \ldots \ldots \ldots = y_2^{(1)} \qquad = 0$

2. Consider the second eigen row:

$$p_2 = [\; y_1^{(2)}, \; y_2^{(2)}. \; \ldots \ldots y_n^{(2)} \;]$$

$$\therefore \; [y_1^{(2)} \; y_2^{(2)} \; \ldots y_n^{(2)}] \begin{bmatrix} a_{11}-a_{22} & 0 & 0 & & 0 \\ a_1 & 0 & 0 & & \\ a_1 & a_2 & a_{33}-a_{22} & & \\ a_1 & a_2 & a_3 & & \\ & & & & \\ a_1 & a_2 & a_3 & & a_{nn}-a_{22} \end{bmatrix} = 0$$

$$\therefore \; y_n^{(2)} = y_{n-1}^{(2)} = \ldots\ldots\ldots\ldots = y_3^{(2)} = 0$$

and $\; y_2^{(1)} \cdot 0 \; = \; 0$

and $\; y_2^{(1)} \quad = \; 1 \;$ arbitrarily chosen.

and $\; y_1^{(2)}(a_{11}-a_{22}) + y_2^{(2)} \; a_1 \; = \; 0$

$$\therefore \; y_1^2 = \frac{-a_1}{a_{11}-a_{22}} \; = \; \frac{a_1}{a_{22}-a_{11}} \; = \; \beta_{21}$$

where the relation $\beta_{rs} = \dfrac{a_s}{a_{rr}-a_{ss}} \;$ is generally maintained.

3. Consider the third eigen row:

$$p_3 = [y_1^{(3)}, \; y_2^{(3)}, \; \ldots\ldots\ldots y_n^{(3)} \quad]$$

$$\therefore \; [y_1^{(3)} \; y_2^{(3)} \ldots y_n^{(3)}] \begin{bmatrix} a_{11}-a_{33} & 0 & & 0 \\ a_1 & a_{22}-a_{33} & & 0 \\ a_1 & a_2 & & 0 \\ a_1 & a_2 & & a_3 \\ a_1 & a_2 & & a_3 & a_{nn}-a_{33} \end{bmatrix} = 0$$

giving $y_n^{(3)} = y_{n-1}^{(3)} = \ldots\ldots\ldots = y_4^{(3)} = 0$

and $y_3^{(3)}$ is arbitrarily chosen, i.e. $y_3^{(3)} = 1$

and $y_2^{(3)}(a_{22}-a_{33}) + a_2 = 0$

i.e. $y_2^{(3)} = \dfrac{-a_2}{a_{22}-a_{33}} = \dfrac{a_2}{a_{33}-a_{22}} = \beta_{32}$ (1)

and $(a_{22}-a_{33})\, y_2^{(3)} + a_2\, y_3^{(3)} = 0$ (2)

$y_1^{(3)}(a_{11}-a_{33}) + a_1\, y_2^{(3)} + a_1\, y_3^{(3)} = 0$ (3)

Multiplying equation (3) by $\dfrac{a_2}{a_1}$ and then subtracting from equation (2) we obtain:

$(a_{22}-a_{33}-a_2)\, y_2^{(3)} - \dfrac{a_2}{a_1}\,(a_{11}-a_{33})\, y_1^{(3)} = 0$

$\therefore y_1^{(3)} = \dfrac{a_1}{a_2}\; \dfrac{a_{22}-a_{33}-a_2}{a_{11}-a_{33}}\; y_2^{(3)}$

substituting for $y_2^{(3)}$ from equation (1) and rearranging the terms we obtain that:

$y_1^{(3)} = \dfrac{a_1}{a_{33}-a_{11}} \cdot \dfrac{a_{33}-a_{22}+a_2}{a_{33}-a_{22}}$

$= \beta_{31} \cdot \gamma_{32}$ (4)

where in general $\gamma_{rs} = \dfrac{a_{rr}-a_{ss}+a_s}{a_{rr}-a_{ss}}$

4. Consider the fourth eigen row:

$$P_4 = [y_1^{(4)},\ y_2^{(4)},\ \ldots\ldots\ldots y_n^{(4)}]$$

$$\therefore [y_1^{(4)} \ y_2^{(4)} \ \dots y_n^{(4)}] \begin{bmatrix} a_{11}-a_{44} & 0 & 0 & 0 & 0 \\ a_1 & a_{22}-a_{44} & 0 & 0 & \\ a_1 & a_2 & a_{33}-a_{44} & 0 & \\ a_1 & a_2 & a_2 & 0 & \\ a_1 & a_2 & a_3 & a_4 & \\ & & & & \\ a_1 & a_2 & a_3 & a_4 & a_{nn}-a_{44} \end{bmatrix} = 0$$

giving:

$$y_n^{(4)} = y_{n-1}^{(4)} = \dots = y_5^{(4)} = 0$$

$$y_3^{(4)} = \frac{-a_3}{a_{33}-a_{44}} = \frac{a_3}{a_{44}-a_{33}} = \beta_{45} \qquad (5)$$

$y_4^{(4)} = 1$ arbitrarily chosen.

$$y_3^{(4)}(a_{33}-a_{44}) + a_3 = 0 \qquad (6)$$

$$y_2^{(4)}(a_{22}-a_{44}) + y_3^{(4)} \quad a_2 \quad + a_2 = 0 \qquad (7)$$

$$y_1^{(4)}(a_{11}-a_{44}) + y_2^{(4)} \quad a_1 \quad + y_3^{(4)} \quad a_1 \quad + a_1 = 0 \qquad (8)$$

From equations (6) and (7) the following relation is obtained:

$$y_2^{(4)}(a_{22}-a_{44}) \frac{a_3}{a_2} - y_3^{(4)}(a_{33}-a_{44}-a_3) = 0$$

$$\therefore y_2^{(4)} = y_3^{(4)} \frac{a_2}{a_3} \frac{a_{33}-a_{44}-a_3}{a_{22}-a_{44}}$$

Substituting for $y_3^{(4)}$ and rearranging the terms we get:

$$y_2^{(4)} = \frac{a_2}{a_{44}-a_{22}} \cdot \frac{a_{44}-a_{33}+a_3}{a_{44}-a_{33}} = \beta_{42} \cdot \gamma_{43}. \tag{9}$$

The following relation can also be obtained from equations (7) and (8).

$$y_1^{(4)} = y_2^{(4)} \cdot \frac{a_1}{a_2} \frac{a_{22}-a_{44}-a_2}{a_{11}-a_{44}}$$

$$= \frac{a_1}{a_{44}-a_{11}} \cdot \frac{a_{44}-a_{22}+a_2}{a_{44}-a_{22}} \cdot \frac{a_{44}-a_{33}+a_3}{a_{44}-a_{33}}$$

$$= \beta_{41} \cdot \gamma_{42} \cdot \gamma_{43} \tag{10}$$

Hence the general element in the eigen rows matrix can be deduced by inspecting equations (4), (9) and (10).

The general expression is:

$$y_r^{(s)} = \beta_{sr} \cdot \gamma_{s,r+1} \cdot \gamma_{s,r+2} \cdots\cdots\cdots\gamma_{s,s-1}.$$

APPENDIX III.

Consider the case of a heterogeneous (addition)
polymer with an initial distribution

$$N_x = N_0 \, p^{x-1} \, (1-p)^2$$

The value of the rth row of matrix equation (19) arranged
in a series form is given by:

$$X_r = N_0 \, p^n(1-p)^2 \sum_{s=1}^{s=r-1} \frac{1}{p^s}[\,(r-s-1)e^{a_{r-2,r-2}t}$$

$$- 2(r-s)e^{a_{r-1,r-1}t} + (r-s+1)e^{a_{rr}t}\,] + N_0 \, p^{n-r}(1-p)^2 \, e^{a_{rr}t} \quad (1)$$

where

$$\sum_{s=1}^{s=r-1} \frac{r-s-1}{p^s} = \frac{(r-2)(1-p^{r-1})}{p^{r-1}(1-p)} + \frac{(2-p)-r(1-p)-p^{r-1}}{p^{r-1}(1-p)^2} \quad , \text{ and}$$

$$\sum_{s=1}^{s=r-1} \frac{2(r-s)}{p^s} = \frac{2(r-1)(1-p^{r-1})}{p^{r-1}(1-p)} + 2\frac{(2-p)-r(1-p)-p^{r-1}}{p^{r-1}(1-p)^2} \quad , \text{ and}$$

$$\sum_{s=1}^{s=r-1} \frac{r-s+1}{p^s} = \frac{r(1-p^{r-1})}{p^{r-1}(1-p)} + \frac{(2-p)-r(1-p)-p^{r-1}}{p^{r-1}(1-p)^2}$$

$$\therefore X_r = N_{n-r+1} = N_0 \, p^n(1-p)^2 \, [\frac{1-p^{r-1}}{p^{r-1}(1-p)}\left\{(r-2)e^{a_{r-2,r-2}t}\right.$$

$$- 2(r-1)e^{a_{r-1,r-1}t} + r \, e^{a_{rr}t}\right\}$$

$$+ \frac{(2-p)-r(1-p)-p^{r-1}}{p^{r-1}(1-p)^2}\left\{e^{a_{r-2,r-2}t} - 2e^{a_{r-1,r-1}t}\right.$$

$$\left. + e^{a_{rr}t}\right\}\,] + N_0 \, p^n(1-p)^2 \, e^{a_{rr}t} \quad (2)$$

Substituting in equation (2) the appropriate values for
a_{ss} and applying the transformation $n-r+1 = x$, the value
of N_x can be:

$$N_x = N_0 \; p^n(1-p)^2 \; [\frac{1-p^{n-x}}{p^{n-x}(1-p)} \{(n-x-1)e^{-K(x+1)t} - 2(n-x)e^{-Kxt}$$

$$+ (n-x+1)e^{-K(x-1)t} \} + \frac{(2-p)-(1-p)(n-x+1)-p^{n-x}}{p^{n-x}(1-p)^2} \} \; e^{-K(x+1)t}$$

$$- 2e^{-Kxt} + e^{-K(x-1)t} \}] + N_0 \; p^n(1-p)^2 \; e^{-K(x-1)t} \qquad (3)$$

Since p is less than unity and n tends to infinity, therefore p^n can be taken as zero, and equation (3) rearranged can be put in the form:

$$N_x = N_0 \; p^{x-1}[p^2 \; e^{-K(x+1)t} - 2 \; p \; e^{-Kxt} + e^{-K(x-1)t}]$$

$$\therefore \; N_x = N_0 \; p^{x-1} \; e^{-K(x-1)t} \; [1 - p \; e^{-Kt}]^2 \qquad (4)$$

APPENDIX IV.

The motion of the n<u>th</u> sphere in the long chain mole-:cule is given by:

$$2m\ddot{y}_n + \alpha(2y_n - y_{n+1} - y_{n-1}) + 2\beta\dot{y}_n = 2\beta V$$

$$= 2\beta V_0 \, e^{i\omega t} \qquad (1)$$

Considering $y_n = Y_n \, e^{i\omega t}$ where Y_n is complex.

Therefore equation (1) can be put in the form:

$$Y_{n-1} + \left(\frac{2\omega^2 m}{\alpha} - \frac{2i\omega\beta}{\alpha} - 2\right)Y_n + Y_{n+1} = \frac{2\beta V_0}{\alpha}$$

If the length of the chain is P units, then there will be P such equation to express the motion of the chain. Further $Y_0 = Y_{P+1} = 0$, since the chain is assumed fixed at both ends.

Putting $\dfrac{2\omega^2 m}{\alpha} - \dfrac{2i\omega\beta}{\alpha} - 2 = \delta$,   and

$$\frac{2\beta V_0}{\alpha} = \Upsilon$$

the motion of the chain can be represented by the following set of linear algebraic equations, viz:

$$
\left.
\begin{aligned}
\delta Y_1 + Y_2 &= \Upsilon \\
Y_1 + \delta Y_2 + Y_3 &= \Upsilon \\
Y_2 + \delta Y_3 + Y_4 &= \Upsilon \\
\cdots\cdots\cdots\cdots\cdots\cdots\cdots & \\
Y_{n-1} + \delta Y_n + Y_{n+1} &= \Upsilon \\
\cdots\cdots\cdots\cdots\cdots\cdots\cdots & \\
Y_{P-1} + \delta Y_P &= \Upsilon
\end{aligned}
\right\} \quad (2)
$$

Equations (2) can be put in the matrix form:

$$MY = \Upsilon \qquad\qquad (3)$$

where Y and Υ are column matrices and M is a symmetrical matrix of order P, given by:

$$M_P = \begin{bmatrix} \delta & 1 & 0 & 0 & \cdots & 0 \\ 1 & \delta & 1 & & & \\ 0 & 1 & \delta & 1 & & \\ \cdots\cdots\cdots\cdots\cdots\cdots & & & & 1 \\ 0 & \cdots\cdots\cdots\cdots & & & 1 & \delta \end{bmatrix}$$

and its determinant is given by:

$$D_P = \frac{\sin(P+1)\theta}{\sin\theta} \qquad\qquad (4)$$

where:

$$\delta = 2\cos\theta \qquad\qquad (5)$$

Premultiplying both sides of equation (3) by the reciprocal matrix M_s^{-1} we get:

$$Y = M^{-1}\Upsilon \qquad\qquad (6)$$

where M_P^{-1} is a symmetrical matrix given by:

$$M_P^{-1} = \frac{1}{S_1 S_{P+1}} \begin{bmatrix} S_1 S_P & -S_1 S_{P-1} & S_1 S_{P-2} & \cdots\cdots & \pm S_1 S_1 \\ -S_1 S_{P-1} & S_2 S_{P-1} & -S_2 S_{P-2} & \cdots\cdots & \pm S_2 S_1 \\ S_1 S_{P-2} & -S_2 S_{P-2} & S_3 S_{P-2} & \cdots\cdots & \pm S_3 S_1 \\ \cdots\cdots\cdots\cdots\cdots\cdots\cdots\cdots\cdots\cdots\cdots & & & & \\ \cdots\cdots\cdots\cdots\cdots\cdots\cdots\cdots\cdots\cdots & & & & \pm S_P S_1 \end{bmatrix} \qquad (7)$$

where $\qquad S_r = \sin r\,\theta$ $\qquad\qquad\qquad\qquad$ (8)

Hence equation (6) can be put in the form:

$$
\begin{bmatrix} Y_1 \\ Y_2 \\ \circ \\ \bullet \\ \bullet \\ \circ \\ Y_P \end{bmatrix} = \frac{1}{S_1 S_{P+1}}
\begin{bmatrix}
S_1 S_P & -S_1 S_{P-1} & \cdots\cdots\cdots\cdots & \pm S_1 S_1 \\
-S_1 S_{P-1} & S_2 S_{P-1} & -S_2 S_{P-2} \cdots\cdots & \pm S_2 S_1 \\
\cdots\cdots & \cdots\cdots & \cdots\cdots\cdots & \cdots \\
S_1 S_{P-r+1} & -S_2 S_{P-r+1} & \cdots S_r S_{P-r+1} \cdots & \pm S_r S_1 \\
\cdots\cdots & \cdots\cdots & \cdots\cdots\cdots & \cdots \\
\pm S_1 S_1 & \pm S_2 S_1 & S_3 S_1 \cdots\cdots & \pm S_p S_1
\end{bmatrix}
$$

$$
\begin{bmatrix} Y \\ Y \\ \circ \\ \bullet \\ \bullet \\ Y \end{bmatrix} \qquad\qquad\qquad (9)
$$

The general term of equation (9) is given by:

$$
Y_r = \frac{Y}{S_1 S_{P+1}}\left[S_{P-r+1}(S_1 - S_2 + S_3 \cdots \pm S_r) \pm S_r(S_1 - S_2 + S_3 \cdots \pm S_{P-r})\right] \quad (10)
$$

Substituting the value of S_r given by equation (8), we get:

$$
{}^{\Sigma}S_1 - S_2 + S_3 \cdots \pm S_r = \sin\left[\theta + \frac{(r-1)(\theta+\pi)}{2}\right]\sin\left[\frac{r(\theta+\pi)}{2}\right]/\cos\frac{\theta}{2} \quad (11)
$$

and

$$
{}^{\Sigma}S_1 - S_2 + S_3 \cdots \pm S_{P-r} = \sin\left[\theta + \frac{(P-r-1)(\theta+\pi)}{2}\right]
$$

$$
\sin\left[\frac{(P-r)(\theta+\pi)}{2}\right] / \cos\frac{\theta}{2} \qquad\qquad (12)
$$

Hence from equations (10), (11) and (12) the amplitude of
vibration of the r$\underline{th}$ sphere in the chain is given by:

$$Y_r = \frac{\Upsilon \sin(P-r+1)\theta}{\sin \theta \sin(P+1)\theta} \times \sin[\theta + \frac{(r-1)(\theta+\pi)}{2}]\sin[\frac{r(\theta+\pi)}{2}]/\cos \frac{\theta}{2}$$

$$\pm \frac{\Upsilon \sin r\theta}{\sin \theta \sin(P+1)\theta} \times \sin[\theta + \frac{(P-r-1)(\theta+\pi)}{2}]$$

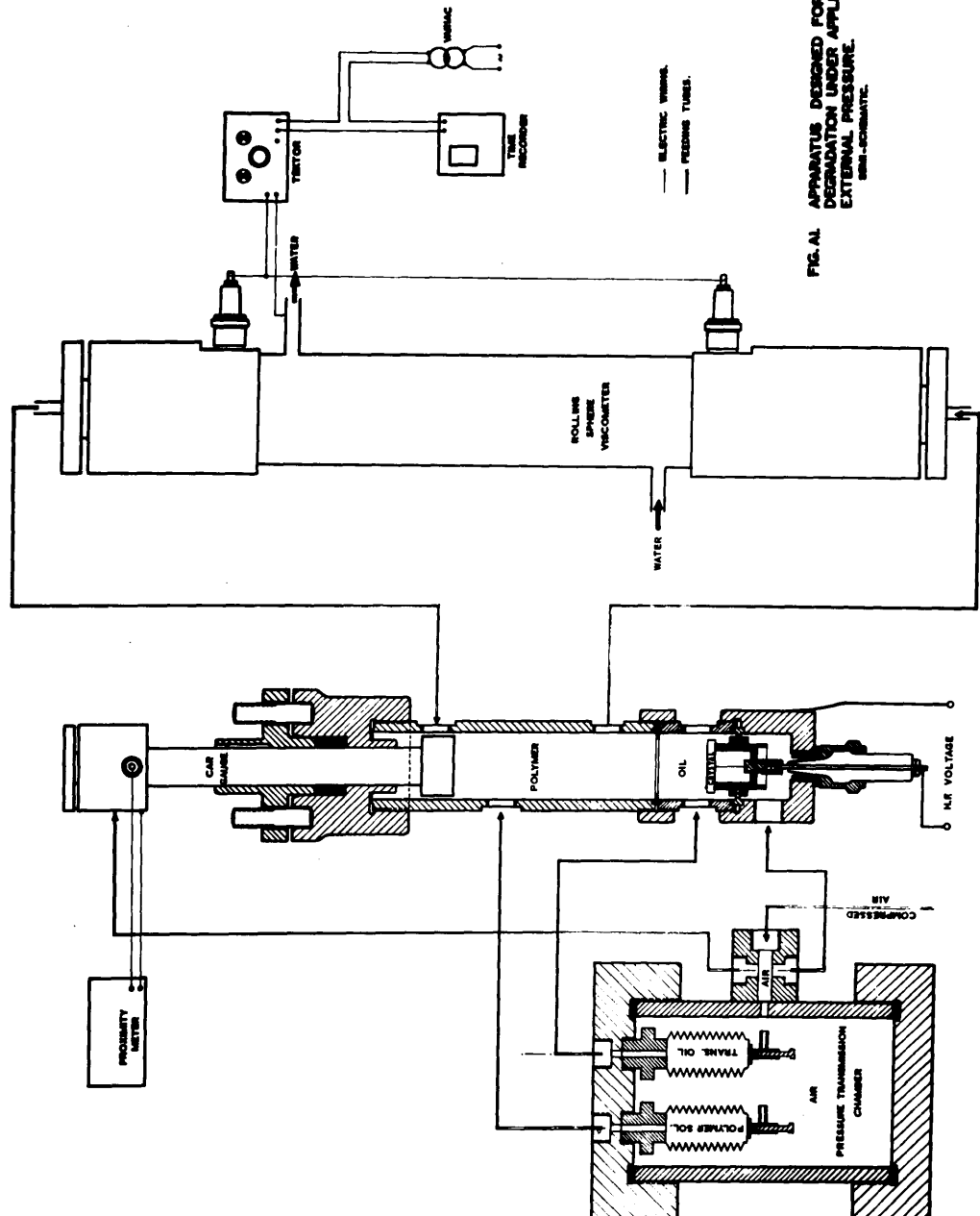$$\sin [\frac{(P-r)(\theta+\pi)}{2}] / \cos \frac{\theta}{2} \qquad\qquad (13)$$

where $\theta = \cos^{-1} [\frac{\omega^2 m}{\alpha} - \frac{i\omega\beta}{\alpha} - 1]$

and $\Upsilon = \frac{2\beta V_0}{\alpha}$

and $y_r = Y_r e^{i\omega t}$

APPENDIX V.

FIG. A1 APPARATUS DESIGNED FOR DEGRADATION UNDER APPLIED EXTERNAL PRESSURE.

The apparatus designed for studying degradation of polymers under applied external pressure includes, as illus-:trated semi-schematically in Fig.A1, the following components:

1. A pressure chamber incorporating the capacity gauge for measuring the ultrasonic intensity with the aid of a proximity meter unit (P.M.4).

2. A crystal mounting inside the pressure chamber.

3. A rolling sphere viscometer and the associated tektor and multi-speed recorder.

4. A pressure transmitting chamber.

1. PRESSURE CHAMBER.

The pressure chamber is a steel tube designed to stand a pressure of 1000 atmospheres. The inside of the whole chamber is chromium plated against any possible effect of free radicals. A sparking plug fitted in the bottom of the chamber serves as a H.T. lead. The chamber is divided into three compartments.

Polymer solution is separated from transformer oil by an 0.0005" terylene membrane which is transparent to ultra-:sonic waves. A liquid tight seal makes it possible to have an air space at the back of the crystal. A chevron

packing between the top cover of the chamber and the capacity gauge provides an efficient seal without restricting the move- :ment of the latter when required. Brass tubes with simplifix fittings connect the different compartments of the chamber to the other components of the apparatus, including the rolling sphere viscometers.

2. CRYSTAL MOUNTING.

The crystal mounting is another version of Stumpf's crystal holder. The lower face of the crystal is fixed with araldite type 101 to a perspex cylindrical base. A high tension electrode, which is a soft thin copper wire, is soft soldered to the lower face of the crystal and then secured in a screw head by a fixing screw. The screw head is soldered to a spring. A small perspex tube acts as a guide for the central electrode of a sparking plug and serves to secure a proper contact between the spring and the central electrode leading the H.T. from the oscillator to the crystal. The earthed electrode is soft soldered at one end to the upper face of the crystal, while the other end is soldered to a brass collar on top of which rests a brass ring with a terylene mem- :brane (0.0005" thick) affixed to it by araldite 101. The quartz crystal assembly is supported in position by means of

an adjustable liquid tight joint incorporating a steel flange, two threaded brass plates to squeeze a leather gasket which seals off the transformer oil from the pressurised air at the back of the crystal.

It is worth mentioning that by using an electrode in the form of a spring, in direct contact with the face of the crystal, sparking always took place between the spring tip and the face of the crystal. This is due to the fact that the vibration of the crystal and that of the spring are bound to come out of phase with each other at some instant, creating an air gap, resulting in a spark-over. To avoid such sparking taking place, a soft thin copper wire was soldered to the face of the crystal and used as an intermediate connection between the crystal face and the spring.

3. ROLLING SPHERE VISCOMETER.

See Chapter III, Section 2.

4. PRESSURE TRANSMITTING COMPARTMENT.

An air cylinder fitted with a regulating valve provides the external pressure to be applied to the polymer solution. Pressure is transmitted to the polymer solution and transformer oil via two very flexible bellows, while air at the controlled pressure is applied directly to the back of the crystal and

to the back of the nilo 36 diaphragm in the capacity gauge.
By such an arrangement the pressure in all parts of the chamber
will be the same, and damage to any of the internal components
will be avoided.

Other components of this apparatus have been discussed
in previous Chapters.